2016-06-01

Human Herpesvirus 6A Infection and Immunopathogenesis in Humanized Rag2$^{-/-}\gamma c^{-/-}$ Mice and Relevance to HIV/AIDS and Autoimmunity

Anne Tanner
Brigham Young University

Human Herpesvirus 6A Infection and Immunopathogenesis in Humanized $Rag2^{-/-}\gamma c^{-/-}$ Mice and Relevance to HIV/AIDS and Autoimmunity

Anne Tanner

A dissertation submitted to the faculty of
Brigham Young University
in partial fulfillment of the degree of

Doctor of Philosophy

Bradford K. Berges, Chair
Kim L. O'Neill
Sandra Hope
Brian D. Poole
Jeffery R. Barrow

Department of Microbiology and Molecular Biology

Brigham Young University

June 2016

ABSTRACT

Human Herpesvirus 6A Infection and Immunopathogenesis in Humanized $Rag2^{-/-}\gamma c^{-/-}$ Mice and Relevance to HIV/AIDS and Autoimmunity

Anne Tanner
Department of Microbiology and Molecular Biology, BYU
Doctor of Philosophy

Human herpesvirus 6A (HHV-6A) has yet to be definitively linked to a specific disease. This is due in part to the ubiquitous nature of the virus. Humanized $Rag2^{-/-}\gamma c^{-/-}$ (Rag-hu) mice were tested to determine if these were a suitable animal model to study the virus. Both cell-free and cell-associated virus was used for infection and both were found to be efficient at infecting the mice. Viral DNA was found in the plasma and cellular blood fractions, bone marrow, lymph node, and thymus, indicating successful infection and propagation of the virus *in vivo*. The $CD3^+CD4^-$ population was depleted, while the $CD3^-CD4^+$ was increased in infected animals. The $CD3^-CD4^+CD8^-$ and $CD3^+CD4^+CD8^-$ populations were depleted and the $CD3^+CD4^+CD8^+$ population increased when analysis was gated upon $CD4^+$ cells. The $CD3^-CD4^+CD8^+$ population expanded and the $CD3^-CD4^+CD8^-$ population was reduced when analysis was gated on the $CD3^-$ population. Additional flow cytometry analysis revealed increases in $CD4^+CD8^+$ double positive cells in the peripheral blood of cell-free infected mice, which could indicate improper T cell selection and a premature departure of these cells from the thymus, possibly contributing to autoimmunity. Previous research has shown that HIV and HHV-6A may have a synergistic effect on one another and that HHV-6A may act as a cofactor in the progression to AIDS. After determining the Rag-hu mouse model was suitable for studying HHV-6A infection, a coinfection of HHV-6A and HIV-1 was performed. Coinfected mice had fewer thymocytes when compared with the HIV-1 only, mock-infected, and to a lesser extent HHV-6A only groups which could indicate increased cell death in the coinfected group as well as possible disruptions in migration of cells, possibly causing cells to be sequestered in the bone marrow and unable to migrate to the thymus, which would explain the smaller cellular populations found in the coinfected mouse thymi. The potential for HHV-6A to induce premature egress of the cells in the thymus due in part to premature upregulation of sphingosine-1 phosphate receptor (S1P1) was also investigated. Additional studies were performed to determine if a preferential targeting existed between HHV-6A and HIV-1 as these viruses are found simultaneously coinfecting the same cell. Preferential targeting was not observed by cell-associated migration assay, but increased migration of HHV-6A-infected cells was observed in a CCL21 dependent manner. These studies have provided useful information about HHV-6A and its relevance to HIV/AIDS as well as a possible mechanism of the involvement of HHV-6A in multiple sclerosis (MS) and other autoimmune diseases.

Keywords: HHV-6A, Humanized $Rag2^{-/-}\gamma c^{-/-}$ (Rag-hu) mice, HIV, animal model, AIDS, autoimmunity

ACKNOWLEDGMENTS

I thank my parents for their countless hours of listening to ideas and for providing encouragement, love, and support throughout this entire process. I'm grateful to my siblings and their spouses who have also been great sounding blocks and incredibly supportive and encouraging. Special thanks go to Dr. Brittany Needham for serving as somewhat of a second mentor throughout my graduate studies and for always freely offering her time and expertise to provide invaluable help, advice, and encouragement on publications and research. I'm grateful to the members of my committee: Drs. Sandra Hope, Brian Poole, Kim O'Neill, and Jeff Barrow for willingly giving of their time to provide insight and perspective on my projects and for taking time to counsel with me personally. Their mentorship has made a huge difference in my education and research and their willingness to counsel with me one-on-one and their timely encouragement have impacted me in my studies as well as personally. I would like to thank Dr. Eric Wilson, who did not formally serve on my committee but who has been a great mentor and friend throughout my studies and who consulted with me on more than one of my projects. I would like to thank Dr. Brad Berges for giving me this opportunity and for serving as my advisor, mentor, and friend throughout this entire process. I cannot remember a single time that he did not stop what he was doing in order to answer a question or listen to a new idea or hash out details of a project. He freely shared his time, knowledge, and expertise with me and also allowed me room to experiment on my own, for which I am extremely grateful. I could not have done it without my friends both in and out of the department who have gone above and beyond to provide encouragement, love, and support. And finally I would like to thank God, who has been with me every step of the way and given me the strength and capacity to do what He wanted me to do.

Table of Contents

List of Tables

List of Figures

I. Introduction

Portions from the following publications, of which I was an author, were used throughout the introduction section: “Piracy on the molecular level: human herpesviruses manipulate cellular chemotaxis”(1), “Modeling of human herpesvirus infections in humanized mice”(2), “Humanized Mice as a Model to Study Human Hematopoietic Stem Cell Transplantation”(3).

A. Human herpesvirus 6 overview

Human herpesvirus 6 (HHV-6) is an enveloped, linear dsDNA virus that belongs to the *Herpesviridae* family and *Betaherpesvirinae* subfamily of viruses, which consists of HHV-6A and HHV-6B, Human cytomegalovirus (HCMV), and Human herpesvirus 7 (HHV-7). The virus was discovered in 1986 and was originally called human B-lymphotropic virus (HBLV) (4). Previously HHV-6A and HHV-6B were classified as subtypes of the same virus with an overall nucleotide sequence identity of 90%, but they are now classified as two distinct viruses (5-9). This distinction is due in part to the differences in cellular tropism and variations in DNA sequences that are conserved between the two viruses (10). The lack of knowledge of these being two distinct viruses in the early studies and literature makes it difficult to determine which virus was used in a particular study, as in the early literature the viruses were often referred to simply as HHV-6. Therefore, HHV-6 will be used when specification between HHV-6A and HHV-6B is not supplied in the literature being cited or when the information applies to both viruses. Primary focus will be on HHV-6A as this is the virus of interest in this body of research.

Human Herpesvirus 6 (HHV-6) has recently emerged as a potentially clinically important virus. It is estimated that ~90% of the population is infected with Human Herpesvirus 6 before the age of two and it remains in the body for the life of the individual, as more than 90% of adults have antibody against the virus (11). HHV-6 persists in a latent form but, like other herpes

viruses, can be reactivated (12). The mature virion of HHV-6A (strain U1102, a strain used in these studies) consists of a genome of 159,322 bp (13) and has an icosahedral nucleocapsid that is ~200 nm in diameter in mature virions (14-16). HHV-6A has primary tropism for $CD4^+$ T cells and can also infect $CD8^+$ T cells, natural killer (NK) cells, gamma/delta T cells, human neural stem cells, human progenitor-derived astrocytes, and oligodendrocyte progenitor cells (10, 17-19). It has also been shown to lytically infect B cells that have been immortalized with EBV (20). Many of these cell types play important roles in immune system defense and their infection could be detrimental to the host and its ability to mount an effective immune response.

HHV-6 can integrate into the subtelomeric region of cell chromosomes leading to chromosomally integrated or ciHHV-6 and can then be passed to offspring, which causes inherited chromosomally integrated or iciHHV-6. This condition results in the presence of the viral genome in every cell of the body. The condition is diagnosed by comparing DNA copies per number of cells in the peripheral blood where 60-80 viral DNA copies per cell are expected in non iciHHV-6 individuals. It is estimated that 40-70 million individuals currently have iciHHV-6. The integrated virus can be reactivated and preliminary analysis indicates that individuals with iciHHV-6 are ~3 times more likely to develop angina pectoris (21).

It is thought that one of the main routes of viral transmission of HHV-6 is through saliva (22) and seroconversion for the virus has been reported to peak at 13 months (23). HHV-6B is usually the first of the two variants to infect the individual, but coinfection with HHV-6B and A is commonly seen (24, 25). The immune system mounts a response with specific IgM antibodies followed by long lived specific IgG antibodies to the virus (26). Cellular immunity plays an important role in the control of HHV-6 infections and is apparent with reactivation of the virus in immunosuppressed individuals (27).

B. Human herpesvirus 6 disease implications

It is known that HHV-6B causes *exanthum subitum,* also known as roseola or sixths disease. This presents as a rash and fever typically seen in infants before the age of two and usually resolves without complication. HHV-6A has not been proven as the causative agent of any disease, this is in part due to the lack of a viable animal model for the virus and is part of the reason we have undertaken these projects in order to help determine the causative roles the virus plays in disease. The virus has been implicated in diseases including: multiple sclerosis (MS)(28), mesial temporal lobe epilepsy, encephalitis, graft-versus-host disease (29), other clinical complications of solid organ transplant and hematopoietic stem-cell transplants, chronic fatigue syndrome (30), drug induced hypersensitivity syndrome, malignancies, myocarditis, cardiomyopathy (31, 32), Hashimoto's thyroiditis (33) and it has been suggested as a cofactor in acquired immunodeficiency syndrome (AIDS)(34-36). There is evidence that HHV-6 causes some forms of cancer such as cervical cancer (HHV-6 may act as a co-factor with HPV)(37), primary cutaneous diffuse large B-cell lymphoma (38), nodular sclerosis Hodgkin's lymphoma (39), angioimmunoblastic lymphadenopathy with dysproteinemia (40), and hepatocellular carcinoma (41). There is also evidence that the HHV-6 genome may have some oncogenes (42, 43).

Multiple studies have been done on the association with HHV-6 and multiple sclerosis. A review of evidence linking HHV-6 with multiple sclerosis has recently been written (44). Studies have shown HHV-6 DNA present in both brain (45) and CSF (46) and that the demyelinating plaques found in the brain of MS patients had higher levels of viral DNA (47, 48).

C. Current animal models to study HHV-6 infection

The limited host-species range of HHV-6 contributes to the difficulty of creating a widely used animal model. The HHV-6 animal models being used prior to our research were the SCID-hu thy/liv mouse model, CD46 transgenic mice (49), the macaque model, the chimpanzee model, and most recently the marmoset (50). These models have been reviewed here (51). While valuable information has been obtained from these models, limitations to them still obstruct further progress. An animal model that is susceptible to infection with the human homologue of the virus and that has similar immunologic effects from infection is desirable for further study and elucidation of the role HHV-6 plays in human disease. Researchers studying HHV-6 will acquire knowledge more readily with an animal model that not only could be used effectively to reproduce the observed effects of the virus seen in humans, but could also be widely used by other researchers to determine possible involvement of HHV-6 in the diseases they study. It should be noted that there are *in vitro* models being used to study HHV-6 (52) that provide important information about the virus and the potential connections to disease, but again lack the ability to sufficiently simulate the human infection.

SCID-hu thy/liv mouse model

The SCID-hu *thy/liv* mice are a well-established model for studying human viruses. SCID mice are unable to produce B or T lymphocytes due to a gene mutation that prevents DNA rearrangement steps required to generate the genes encoding B and T cell receptors. However, these mice do go on to produce a limited repertoire of mature B and T cells as they age (53) and thus different/additional genes involved in lymphocyte development are now commonly targeted. These mice are created by taking a small piece of human fetal liver and thymus and co-implanting them into the kidney capsule of immunodeficient SCID mice. These tissues fuse and

grow into a single organ that is morphologically and functionally equivalent to a human thymus and can be infected by direct injection with human virus. The implanted *thy/liv* organ is composed of five main thymocyte subpopulations; triple-negative phenotype ($CD3^{-}CD4^{-}CD8^{-}$), intrathymic T progenitor cells ($CD3^{-}CD4^{+}CD8^{-}$), double-positive thymocytes ($CD3^{-}CD4^{+}CD8^{+}$ and $CD3^{+}CD4^{+}CD8^{+}$), and single-positive 4 thymocytes ($CD3^{+}CD4^{+}CD8^{-}$) and single-positive 8 thymocytes ($CD3^{+}$ $CD4^{-}CD8^{+}$) (54).

The SCID-hu *thy/liv* mice are susceptible to infection with HHV-6. In one study, the implanted thy/liv organ of SCID-hu *thy/liv* mice was surgically exposed and injected with HHV-6 strain GS and the thy/liv organs were harvested at 4, 7, 11, and 27 days post inoculation. The study showed efficient HHV-6A replication in the thy/liv organs and showed that the amount of HHV-6A DNA peaked 14 days after inoculation. The virus also induced severe depletion of thymocytes, especially the intrathymic T progenitor cells (34). A coinfection study of HHV-6 and HIV was performed with these mice showing no evidence that either of the two viruses act to drive replication of the other, thus negating the implication that HHV-6 is acting as a cofactor with HIV to cause AIDS. The author points out that this result may be because this particular animal model may not accurately reflect the infection pattern in humans and further studies to determine causation are necessary (55).

The SCID-hu *thy/liv* mouse was the first small animal model for HHV-6 (34) and important information has been obtained from its use, but there are limitations to its effectiveness as a model for this virus. In this model the effects of HHV-6 can only be studied on the thymus, which is limited to the five main thymocyte subpopulations of cells, thus preventing study of key cells involved in viral replication and infection. lack of distribution of human cells in the mouse (thy/liv model), and inability to generate primary human immune responses (PBL and thy/liv

models)It does not allow for study of what the virus does to the body as a whole, what specific organs it infects, or the effect it may have on other disease-causing agents. Also, the actual creation of SCID-hu *thy/liv* mice is somewhat technical and labor intensive.

CD46 transgenic mouse model

CD46 transgenic mice have also been shown to be susceptible to HHV-6 infection (56). These mice were injected intracranially with HHV-6A and HHV-6B. Although HHV-6B DNA levels rapidly decreased after infections, HHV-6A DNA was detectable in the brain for up to 9 months post infection. Primary brain glial cultures from the transgenic mice that were infected with HHV-6A showed production of proinflammatory cytokines CCL2, CCL5, and CXCL10. This represents the first murine model to study HHV-6A infection in the brain.

Macaque model

Three species of macaques are susceptible to HHV-6 infection: Pigtail macaques (*Macaca nemestrina*), Cynomolgus monkeys (*Macaca fascicularis)*, and Rhesus macaques (Macaca mulatta) (57, 58). Macaques represent the major non-human primate resource for biomedical research with over 73 infectious diseases and agents having been studied using the macaque as a model (59). There are 16 species of macaques which are found mainly in southern Asia. The species most commonly used in biomedical research are rhesus macaques (*M. mulatta;* from India, but no longer imported); cynomolgus, long-tailed, or crab-eating macaques (*M. fascicularis;* from southern Asia); and pigtail macaques (*M. nemestrina;* from Southeast Asia)(59).

Pigtail macaques have been used to study the possible relationship between HIV and HHV-6A. One study used twelve pig tailed macaques between 6 and 7 years old and that had all

tested negative against SIV and HHV-6 infection prior to the study. These were divided into three groups where group 1 and 3 were inoculated intravenously with SIV and group 2 was inoculated intravenously with HHV-6A. After 14 days, group 3 was inoculated with HHV-6A and group 1 was inoculated with a mock HHV-6A inoculum. Importantly, this study showed that in the presence of SIV, HHV-6A appeared to accelerate AIDS progression and was asymptomatic alone (57).

Lusso et al. tested uninoculated pigtail macaques peripheral blood mononuclear cells (PBMCs) by PCR to see if HHV-6 was present. No virus was detected, suggesting that unlike humans, these animals are not commonly naturally infected with HHV-6 and therefore could make a good model for studying the virus (60). In another study, HHV-6 was detected in the peripheral blood of the Cynomolgus monkeys (*Macaca fascicularis)* and African green monkeys (*Cercopithecus aethiops*) after inoculation and the virus was also found in the animals' spleen and lymph nodes. However, the results in this study show that these two species may only be susceptible to certain strains of HHV-6 and not others which limits their usefulness as models (58).

Chimpanzee model

Chimpanzees represent one of the few species tested that are susceptible to HHV-6 infection. Chimpanzee T lymphocytes can be coinfected by HIV-1 as well, which is necessary in order to study the implication that HHV-6 and HIV act as cofactors in AIDS. Serological testing shows that like the macaque model, chimpanzees do not have a high rate of natural infection of HHV-6, which is a necessary feature of an animal model used to study the virus (61). PanHV6, a chimpanzee herpesvirus that is very closely related to HHV-6, has been discovered (from *P.*

troglodytes verus). This could potentially take the place of the human herpesvirus in chimpanzee studies and make them a more plausible animal model (62). However, as with any animal virus that is not genetically identical to the human homologue, different results and responses could be observed and such variation is not ideal.

As with the other animal models previously discussed, the chimpanzee model has limitations. It is well known that the cost of chimpanzees is very high compared to that of a murine model. Because the average cost per chimpanzee used for research is substantially higher than the cost for a murine model, many laboratories are unable to use non-human primates in research. A lack of facility space and expertise also limit the widespread use of this model, and even though they do sustain infection with HHV-6, a small animal model would still be highly utilized by those who are unable to use the non-human primate model.

Humanized mice

Immunodeficient mice can be engrafted with various types of human cells to produce what are referred to as "humanized mice". These have been used in research since their creation in the 1980s (63, 64) and were used in this project because of their potential as a suitable model for HHV-6A. They have gone through multiple improvements, starting with the human peripheral blood cell mice (hu-PBL-SCID) and the SCID-hu *thy/liv* mice (63, 64), up to the humanized Rag2−/−γc−/− and NOD-*scid IL2R*γ_c^{null} mice and the BLT (bone marrow-liver-thymus) mice. A number of diseases have been studied using humanized mice as a model, including the following: Human immunodeficiency virus type 1 (HIV-1), Human T-lymphotropic virus (HTLV), Epstein-Barr virus (EBV), Kaposi's sarcoma-associated herpesvirus (KSHV), herpes simplex 2 virus (HSV-2), dengue virus (65), and human cytomegalovirus

(hCMV)(66). Notably, there are also human cancers that have already been shown to be induced in humanized mice by EBV and HTLV such as diffuse large B cell lymphomas (67) and adult T-cell leukemia/lymphomas (68) respectively.

As our understanding of hematopoietic stem cells (HSCs) has grown, new humanized mouse models have been sought that can recapitulate the human immune system more faithfully. A groundbreaking study was published in 2004 when Traggiai et al. showed that highly immunodeficient Rag2$^{-/-}$ γc $^{-/-}$ mice (C.129-Rag2^{tm1Fwa}Il2rg^{tm1Sug} strain) can be engrafted intrahepatically with human HSCs (CD34^{+} cells) isolated from umbilical cord blood. They demonstrated multi-lineage hematopoiesis, a broad distribution of human immune cells, and functional human antibody and CD8^{+} T cell responses (69). Many other studies have been published using similar protocols, and a wide variety of human hematopoietic cell types have been detected in these models including strong production of B and T lymphocytes, monocytes/macrophages, dendritic cells, and typically a weak production of granulocytes, erythrocytes, and platelets (69-73). The precursor cells for production of granulocytes, erythrocytes, and platelets are detectable in the bone marrow of humanized mice, but murine macrophages appear to prevent proper development of erythrocytes and platelets as evidenced by increased detection following murine macrophage depletion (74, 75). These human cells are in many cases widely dispersed throughout the lymphoid organs (bone marrow, thymus, lymph nodes, and spleen) as well as other organs (brain, lungs, gut mucosa, reproductive tracts, etc.) (69, 71, 76-79).

We determined humanized mice would be susceptible to infection with HHV-6 because other herpesviruses (EBV, KSHV, hCMV, HSV-2) have been successfully studied in humanized mouse models (2). The humanized mouse models address the limitations of the current HHV-6

models such as: the SCID-hu *thy/liv* model and it's limited cell types and lack of distribution of cells, the high cost and need for specialized facilities of both the macaque and chimpanzee models, and the need to use an animal homologue such as SIV or PanHV6 rather than human herpesvirus 6, which make it a suitable animal model for this virus.

A broad diversity of humanized mouse models is currently in use. Models differ based upon many variables, but successful engraftment of human HSCs has been detected under many different experimental conditions. These differing conditions include the mouse strain used as a recipient, the conditioning protocol used to prepare mice for transplantation, the source of human HSCs used for engraftment, the phenotypes of HSCs used for engraftment, the culture and/or expansion of HSCs with various cytokines or no culturing at all, the number of cells used for engraftment, the use of fresh or frozen cells, the use of co-injected non-HSC support cells, and the method or site of inoculation of cells into the host. Although the vast array of conditions used to make humanized mice make it difficult to directly compare the results of these various studies in order to determine which method is most effective, they also indicate that a wide variety of engraftment protocols can be successfully carried out in immunodeficient mice.

Thus, factors which influence the efficacy of HSCT can be compared to discover methods which are more effective and carry fewer risks. The use of well-controlled experiments to compare single variables and their individual effects on the efficacy of HSCT is an area which is still underdeveloped in the humanized mouse field.

The definition of the phenotype of a true HSC is currently not well defined, but nearly always includes the CD34 marker. A review of the capacity of $CD34^-$ cells to act as HSCs is available (80). Interestingly, one common way to define HSC populations is actually in terms of

their ability to engraft immunodeficient mice; in this case the HSCs are referred to as SCID-repopulating cells. As mentioned previously, Traggiai et al. showed that intrahepatic injection of UCB $CD34^+$ cells into $Rag2^{-/-}\gamma c^{-/-}$ mice resulted in the development of human B, T, and dendritic cells (69). Since then experiments have been performed with various types of cellular populations that revolved around the CD34 marker. Results of these various studies are summarized in Table 2 as a function of the cellular phenotype and the source of HSCs. Notta et al. recently showed that a single purified human HSC is capable of producing detectable engraftment in highly immunodeficient mice, and their work sheds further light on the phenotype of true HSCs (81). There are several methods of isolating human HSCs in order to engraft humanized mice, including from UCB, fetal liver, mobilized peripheral blood, and from adult human bone marrow. UCB is a common source of HSC because it is readily available and has a high concentration of HSCs. Mononuclear cells from human UCB are isolated by Ficoll separation and then enriched using $CD34^+$ specific magnetic beads. The cells can either be used immediately for engrafting or they can be cultured. Culturing these cells requires specific cytokines in order to stimulate growth/expansion without differentiation.

Fetal liver is another source of the HSCs for engraftment. Tissues are minced and a single cell suspension is created, then $CD34^+$ cells are isolated as above. These samples are more difficult to obtain, but contain much higher numbers of $CD34^+$ cells as compared to UCB (71). HSCs can also be obtained by direct extraction from bone marrow, followed by similar methods to obtain the $CD34^+$ fraction (82).

Murine engraftment can also be accomplished using human mobilized peripheral blood as a source of cells. A human patient is injected with cytokines such as granulocyte-colony stimulating factor (G-CSF) which increases the number of circulating HSCs. A blood sample is

drawn and leukapheresis is performed. $CD34^+$ cells are then purified out of the sample (83). It has been reported that 50-fold more cells are required to achieve the same level of mouse engraftment when comparing hMPB cells to UCB cells (84) but it is unclear why these cells require a higher dose.

Human embryonic stem cells (hESC) or induced pluripotent stem cells (IPSCs) can also be used to obtain $CD34^+$ cells for engraftment and multiple types of human blood cells have successfully been produced from these sources (85, 86). One way to do this is to culture the hESCs with irradiated murine cell lines. This co-culture allows hESCs to differentiate into HSCs without additional cytokines (87). These differentiated cells are injected into irradiated mice to produce human immune cell engraftment. Since samples containing primary HSCs can be difficult to obtain due to scarcity, the ability to derive HSCs from a replenishable source is highly desirable. In addition, cells from a replenishable source can be better characterized as compared to those obtained from cord blood or fetal liver where each donor is unique. hESCs can be maintained in their undifferentiated state indefinitely if they are passaged regularly (87) and this suggests their utility as a HSC source. Human HSCs themselves cannot currently be expanded indefinitely in culture without losing their potency for long-term engraftment and multi-lineage hematopoiesis. Tian et al. demonstrated successful murine engraftment when hESC-derived HSCs were injected into the bone marrow or intravenously (88).

Highly immunodeficient mice are critical for success in the engraftment of human HSCs, and many such mouse strains are currently in use. Common strains include NOD-SCID (non-obese diabetic/severe combined immunodeficient mice), NOD-SCID $\gamma c^{-/-}$ (NSG or NOG; see Table 1), $Rag2^{-/-}\gamma c^{-/-}$, $Rag1^{-/-}\gamma c^{-/-}$, among others and have all been used to make humanized mice and study HSC transplantation (71, 89-92). These mutations impair the ability to produce

functional T and B lymphocytes (SCID, Rag1, Rag2) or mature NK cells (γc). γc is the signaling subunit of both the IL-2 and IL-15 receptors, thus preventing expansion/maturation of T cells and NK cells, respectively. When HSC donor and recipient MHCs do not match then myeloablative conditioning and use of highly immunodeficient mice is required for effective engraftment (93). For the above mouse strains, conditioning is always required in order to achieve human engraftment levels higher than a low fraction (1-5%) of chimerism in peripheral blood. Waskow et al. created a mouse model that they termed a "universal" HSC recipient because it can accept allogeneic grafts without prior conditioning. The mouse strain used ($Rag2^{-/-}\gamma c^{-/-}Kit^{W/Wv}$) was generated in a $Rag2^{-/-}\gamma c^{-/-}$ background and additionally has a *Kit* knockout which prevents sustained self-renewal of HSCs (93). Excellent reviews of the types of immunodeficient mouse strains currently in use to make humanized mice are available (94-96).

There is another type of humanized mouse model, referred to as the BLT (bone marrow, liver, and thymus) mouse, that utilizes these immunodeficient mouse strains to make an effective model of HSC engraftment. In this model, immunodeficient mice (NOD/SCID, NSG, or $Rag2^{-/-}\gamma c^{-/-}$) are sublethally irradiated and the following day 1 mm^3 human fetal liver and thymus tissue fragments are inserted under the kidney capsule of the mouse. These tissues develop into a human thymic organoid. After the thymic organoid develops, the mice are then injected intravenously with autologous human fetal liver-derived $CD34^+$ cells in order to create the BLT model. This model also shows good engraftment and has the added advantage of the selection of human T cells on human MHC-I-expressing stromal cells in the thymic graft, which leads to better human T cell responses *in vivo* (97-99).

HSC homing to the bone marrow in humanized mice occurs rapidly and engraftment can be a long-lasting and stable phenomenon. Human HSC homing to the murine bone marrow has

been seen in as little as 20 hours following intravenous injection of $CD34^+$ HSCs into NOD/SCID mice (100, 101). Humanized $Rag2^{-/-}\gamma c^{-/-}$ mice injected with human fetal liver $CD34^+$ cells showed evidence of human cell engraftment up to 63 weeks later (102). Various other studies have shown engraftment lasting for at least 6 months (71, 91, 103-105). Takahashi et al. showed that $CD34^+$ cells were present in NOG mice at a statistically constant level over four months (101).

The two most common methods for engraftment of human HSCs into immunodeficient mice are intrahepatic (i.h.) injection and intravenous (i.v.) injection. Other methods of injection include intraperitoneal, intracardial, intrasplenic, or directly into the bone marrow. It is currently unknown if one of these methods is significantly better than the others because of multiple variables across the various studies. However, a comparison of i.h. and i.v. injection showed an insignificant difference in the effectiveness of human HSC engraftment (106). I.h. injection of cells is commonly used in newborn mice; this method may be effective because HSCs are primarily located in the liver of newborn mice and traffic to the bone marrow within the first weeks after birth. It is possible that human HSCs respond to the same trafficking signals as murine HSCs, thus explaining the effectiveness of this method. However, i.v. injection is also successfully used in newborn mice, and it is clear that a variety of injection routes are successful in both newborn and adult mice. In the literature, $Rag2^{-/-}\gamma c^{-/-}$ mice are commonly engrafted as newborns (71, 106, 107) while mice on the NOD/SCID background are commonly engrafted as adults (100, 101), although animals with the NOD/SCID background can be engrafted as newborns as well (72, 108).

The humanized $Rag2^{-/-}\gamma c^{-/-}$ mice can be engrafted to be genetically identical or genetically divergent, thus allowing the researcher to decide what is best for the specific

experiment and reduce problems from intra-species variation. These mice express all of the cell types that are believed to be infected by HHV-6, which are: human $CD4^+$ T cells, $CD8^+$ T cells, monocytes and macrophages, natural killer cells, hematopoietic stem cells, dendritic cells, epithelial cells, and brain-derived cells (109, 110). The humanized Rag2−/−γc−/− mice would provide a way that the affected human cells could be studied *in vivo*. In order to better understand this model and its uses, examples of the humanized mouse model for other *Herpesviridae* family viruses are given below. A review of the topic can be found here (2).

Human Cytomegalovirus (HCMV) Humanized Mouse Model

huCD34$^+$ engrafted NOD-*scid IL2R*γ_c^{null} humanized mice have been used to study Human Cytomegalovirus (HCMV). HCMV is a cause of morbidity and mortality in organ transplant recipients (66). It can also cause congenital CMV which causes mental retardation and sensorineural hearing loss (111). Because this virus only infects human cells, the creation of an animal model has been difficult. In a review of non-primate models of congenital CMV published in 2006, Mark Schleiss reported that it would be better to test vaccines in animal models prior to human trials, but unfortunately laboratory animals could not be infected with human CMV (111). Since this review, a suitable humanized mouse model, huCD34$^+$ engrafted NOD-*scid IL2R*γ_c^{null} mice, has been used to study HCMV. These mice show sustainable infection with HCMV and serve as the first humanized mouse model where latency and reactivation can be studied in this virus (66). This model is now a valuable tool for studying HCMV and potential anti-viral treatments (66). Prior to this model, other mouse models were used to study HCMV that are similar to those used for HHV-6, where a certain engrafted tissue can be infected, but a systemic infection is unattainable. The successful infection of HCMV in

humanized mice was part of the rationale behind the hypothesis that humanized mice could also sustain infection with HHV-6 and provide a better model to study the virus.

Epstein-Barr Virus (EBV) Humanized Mouse Model

EBV and HHV-6 are members of the *Herpesviridae* family of viruses and have similarities in structure and infection. EBV is similar to HHV-6 in that it is ubiquitous in the population. Although it is known that EBV is the causative agent of infectious mononucleosis and post-transplant lymphoproliferative disorder, the almost universal presence of the virus in the human population has made the virus difficult to study and has made it hard to define a causative role between the virus and disease (112).

The main target cells of EBV *in vivo* are epithelial cells and B lymphocytes, although there is also evidence for infection of T lymphocytes and NK cells. Latency is established in B lymphocytes or epithelial cells (113). EBV infection is strongly correlated to a number of human cancers including Burkitt's lymphoma, nasopharyngeal carcinoma, Hodgkin's lymphoma and gastric carcinoma; in addition EBV infection is associated with autoimmune diseases such as multiple sclerosis, systemic lupus erythematosus, and rheumatoid arthritis (114).

Most of the early work on EBV in humanized mice used the SCID-hu-PBL model, and since human blood donors have a high frequency of persistent EBV infection researchers were able to characterize the effects of transplantation of EBV^+ blood into immunodeficient mice (115, 116) and lymphoproliferation was noted in many cases. Since these reports constitute transfer of virus-infected cells rather than *in vivo* transmission of cell-free virus, we will focus on the latter. Humanized mice can be successfully infected with EBV by several injection mechanisms, including intrasplenic (117, 118), intraperitoneal (119-121), and intravenous

inoculation (122-124). Exposure of HSC-humanized mice to EBV results in detectable viral DNA by 2-4 weeks post-inoculation in the spleen, blood, bone marrow, liver, kidneys, adrenal gland, lungs, and lymph node (69, 117, 122). Blood viral load typically peaked in the range of 10^4 to 10^5 genome copies (117).

One of the achievements with human HSC-transplanted mice is the ability to detect and characterize de novo human adaptive immune responses in response to viral antigens. Both T cell and antibody responses have been detected in humanized mice towards EBV antigens, and it is thought that the inability of the virus to cause tumors after low-dose exposure may be due to control of the virus by the human immune response (69). T cell expansion and an inversion of the normal CD4:CD8 ratio have been reported (69, 122), along with EBV-specific T cells responses which are commonly measured by ELISPOT assay to detect IFN-γ production after exposure to EBV antigen or by a cell killing assay (69, 122, 125, 126). Further evidence of the protective effects of human T cell responses was gained by depleting either all human T cells or just the $CD8^+$ fraction; these experiments showed a higher viral load and a reduced lifespan in EBV-infected humanized mice (121, 125). Lytic antigens are targeted more frequently by T cells than latent antigens, and the response is also stronger to these antigens (121). Human antibody responses to EBV have also been detected in these models (122). The success of the humanized mouse model in studying EBV along with the similarities between EBV and HHV-6 provides further rationale to support the use of a humanized mouse model to study infection with HHV-6.

Human Immunodeficiency Virus (HIV) Humanized Mouse Model

Although HIV is not a herpesvirus, HIV humanized mouse animal models are of interest to discuss because of the previously mentioned implication that HHV-6 acts as a cofactor in AIDS. HIV-1 has been studied using humanized mice as a model since the late 1990's (127) . The (hu)-Rag2$^{-/-}$yc$^{-/-}$ humanized mice display long-term chronic infection with HIV-1 and have replication and CD4^{+} T cell depletion after infection with both CCR5 and CXCR4 tropic HIV-1 (128-131). The BLT (bone marrow-liver-thymus) humanized mice have also been used to study HIV. The BLT humanized mice have human immune cells that are present in the thy/liv implant, as well as peripheral blood, lymph nodes, gut, lungs, bone marrow, and liver (132). Because humanized mouse models already exist for HIV-1, experiments to test the validity of the implication of HHV-6 as a cofactor in AIDS can commence immediately following successful infection of one of these humanized mouse models with HHV-6.

The potential impact a suitable animal model for HHV-6 could have in HHV-6 research as well as other disease research is clear: Because over 90% of the population is infected with the virus, there is no natural negative control for experimental comparison. This makes it nearly impossible to make conclusions about any disease associations by studying it in humans alone. Once experiments with animals can be performed where conclusive data can be produced, the research about HHV-6 can be sharpened and focus can be placed on known interactions and diseases rather than on suspected interactions and implicated diseases. This will allow researchers to focus their efforts in the most important areas and terminate research on areas where HHV-6 proves not to be involved. If the virus proves to play a role in even one of the diseases in which it is implicated, an effective small animal model that recapitulates infection and disease will be beneficial in investigating the pathology and discovering the exact involvement of it in the disease as well as testing drugs against the virus. There are currently no

approved drugs for the treatment of HHV-6 infection (133) so anti-cytomegalovirus (CMV) agents ganciclovir (Cytovene® IV), cidofovir (Vistide® IV), and foscarnet (Foscavir® IV) are used for clinical treatment.

D. HHV-6 modulations on cellular migration

Thymocyte development

As CD4+ T cells are a primary target of HHV-6, it is important to understand their development. The thymus is located just above the heart in the thoracic cavity and is where T cell development occurs. The organ consists of two distinct but identical lobes which are comprised of the cortex and medulla regions. CCR7 synergizes with CCR9 and CXCR4 to induce migration of precursor cells from the bone marrow to the thymus. This is where T cell development occurs, including positive and negative selection. The $CD4^{+}CD8^{+}$ double positive (DP) cells that successfully pass through positive selection in the cortex become single positive (SP) CD4 or CD8 cells, depending on whether they interact well with MHC II or MHC I respectively, at which point CCR7 is upregulated causing the cells to migrate to the medulla to undergo negative selection. A majority of thymocytes die in the thymus, not having received the necessary survival signals during the development process because of too strong or too weak affinity to MHC or interacting too strongly with self-antigen. Cells that have successfully developed and received the necessary survival signals exit the thymus into the periphery. T cell egress is induced by upregulation of the sphingosine-1 phosphate receptor 1 (S1P1) which counteracts the retention signal of CCR7 (134).

HHV-6A

HHV-6A can alter the expression of different cellular markers involved in cellular homing and trafficking, which causes significant disruption to immune cell function and viability. HHV-6 has one functional chemokine-like protein, U83 (see Table 3). The viral chemokine U83A from HHV-6A is involved in chemoattraction and has selective specificity for receptors CCR1, CCR4, CCR5, CCR6 and CCR8. These are found on T cells, monocytes/macrophages and activated T lymphocytes (CCR1, CCR5, CCR8), skin-homing T lymphocytes (CCR4, CCR8), immature dendritic cells (CCR1, CCR6) and NK cells (CCR8) (10, 135, 136). The difference in specificity of U83A (from HHV-6A) and U83B (from HHV-6B) to attract diverse cell types (see Table 3) could account for the variable tropism of the two viruses (137). U83A is found in a full-length form as well as a truncated splice variant (138). It is thought that, because of the different forms of the peptide, U83A could block both innate and adaptive immune responses, as well as attract the cells involved in these responses for further infection (136). U83A induces chemotaxis and morphological changes in cells expressing CCR5 in a manner similar to CCL4, but with a significantly delayed internalization of CCR5 compared with CCL4. Interestingly, binding of U83A to CCR5 has been shown to inhibit CCR5 tropic HIV-1 infection (139).

HHV-6 has two GPCRs, U12 and U51, which encode chemokine receptors (see Table 2). U51, known to affect migration in HHV-6A infected cells, is expressed at early time points post-infection, whereas U12 is expressed late and influences chemotaxis of HHV-6B-infected cells. HHV-6A U51A has novel specificity for CCL5 and can also bind CCL2, CCL11, CCL7 and CCL13. This makes U51A unique among viral and cellular receptors in that it overlaps activity with CCR1, CCR2, CCR3 and CCR5 in the binding of CCL5 (135). There is also overlap with CCR2, CCR4, US28, UL12, D6 and Duffy in the binding of CCL2; CCR3 and E1 in the binding

of CCL11; CCR1, CCR3, US28 and D6 in the binding of CCL7; and CCR2 and CCR3 in the binding of CCL13. Unlike many viral GPCRs that have constitutive signaling, U51A has been shown to perform both inducible and constitutive signaling (135, 140).

U51A expression has been shown to cause a reduction of CCL5 expression using the Hut78 human $CD4^+$ T lymphocyte cell line. U51A has high relative affinity for XCL1, which normally binds human receptor XCR1 found on NK cells and T lymphocytes. This binding could have a number of effects, including: preventing infected cells from interacting with NK cells; inducing chemotaxis to T lymphocytes, which could spread infection; and preventing apoptotic signals within infected cells (141). CCL19, normally bound by human receptor CCR7, can also be bound by U51A. This could cause infected cells to migrate to the T cell-rich lymph node, promoting viral spread. HHV-6A U83A chemokine does not bind U51A. Expression of U51A ligands in the brain could also allow migration of infected cells into the central nervous system. Damaged epithelial lung cells and airway parasympathetic nerves express CCL2 and CCL11, which both bind U51A, and could promote migration of the infected cells to these areas to be transmitted to new hosts.

CCR7, which is expressed in various lymphoid tissues, is another receptor that is modulated by herpesviruses (see Table 4). HHV-6A and HHV-6B upregulate CCR7 expression in $CD4^+$ T cells (142). CCR7 is specific for CCL19 and CCL21 and plays roles in cell migration and proliferation (143). This upregulation of CCR7 could be an important aspect of HHV-6 pathogenesis as upregulation of CCR7 promotes migration of T cells and dendritic cells to the paracortex in lymph nodes (where T cell priming occurs) and the periarteriolar lymphoid sheath in the spleen, both of which are T cell-rich (134).

As mentioned previously, HHV-6A can also downregulate cellular receptors. Along with downregulation of CD46 (its entry receptor) and CD3 (144), CXCR4 is downregulated by HHV-6A in primary $CD4^+$ T lymphocytes and the JJhan T cell line, which affect the chemotactic response of the cells to CXCL12, the natural ligand of CXCR4 (145). The disruption of CXCR4/CXCL12 signaling by downregulation of CXCR4 by HHV-6A could prevent the retention of hematopoietic stem/progenitor cells (HSPCs) and more mature leukocytes in the bone marrow, allowing these cells to be mobilized and enter into circulation (146). The migration of CXCR4-expressing thymocytes out of the thymus was shown to occur in a CXCL12-dependent manner (147, 148); so the downregulation of CXCR4 by HHV-6A could be another way the virus prevents migration away from areas where target cells are present. Additionally, the downregulation of CXCR4 by HHV-6A could prevent homing of bone marrow-derived precursor cells to the thymus (149), possibly preventing positive and negative selection from occurring in these cells.

HHV-6 has been shown to cause modulations to CCL5 expression. This chemokine has selective chemoattractive activity on resting $CD4^+$ memory T cells (142) and has been shown to be upregulated by HHV-6 in an ex vivo study where human tonsil blocks were infected with both HHV-6 and HIV-1. This upregulation of CCL5 was shown to suppress HIV-1 CCR5-tropic variants and possibly to stimulate replication of CXCR4- utilizing variants, which gives evidence that HHV-6 may play a role in HIV pathogenesis by promoting the switch between CCR5-tropic to CXCR4-tropic HIV-1 (150). In contrast, CCL5 expression in epithelial cells is downregulated by U51A from HHV-6A (151). Epithelial cells expressing U51A also had morphological changes and exhibited increased spreading and flattening, which could increase the ability of HHV-6 to spread to uninfected cells as it is primarily spread by cell-to-cell contact (151). As has

been observed with other viral chemokines and chemokine receptors, their functions could be multipurpose in attracting cells to the area of infection, and also in evading the immune cells of the host so replication and latency can take place.

As described above, HHV-6A alters the expression of different cellular markers. Many of these markers are involved in cellular homing and tracking to specific areas of the body, and when altered can cause significant disruption to immune cell function and viability. Further research into HHV-6A effects on cellular trafficking could serve as a critical guide for developing new treatments to prevent these disease-causing disruptions.

HHV-6B

HHV-6B causes exanthem subitum (roseola) (152) and is found in approximately 95–100% of adults worldwide. Unlike HHV-6A, HHV-6B has very little to no ability to infect $CD8^+$ T cells, NK cells and gamma/delta T cells (144, 153). The cellular receptor for HHV-6B is CD134 which, like the cellular receptor for HHV-6A, CD46, is expressed on almost all human cells (154), indicating that other factors are required for effective viral replication.

The HHV-6B viral chemokine U83B is specific for CCR2 and can cause chemoattraction of CCR2-expressing cells (classical and intermediate monocytes) for infection (10, 137, 155) (see Table 3). U83 from HHV-6B induced transient calcium mobilization and efficient migration in THP-1 cells (a monocyte cell line derived from monocytic leukemia) (156). U83B has been shown to have a different specificity from U83A as U83B chemoattracts CCR2-expressing monocytes, whereas U83A has a broader but still selective specificity as mentioned previously (135, 136). The specificity of U83B for CCR2 appears to be due to its N-terminal region. Human chemokines can induce rapid internalization of CCR2 upon binding, whereas *in vitro*

experiments show U83B does not cause CCR2 internalization. This finding is similar to the delayed internalization of CCR5 observed with U83A. CCR2 expression is induced in pro-inflammatory conditions and, interestingly, HHV-6B is associated with inflammatory diseases such as encephalitis and myocarditis (137).

The HHV-6B GPCR U12 efficiently binds CCL2, CCL5 and CCL4, so it has overlapping activity with the receptors for CCL2 and CCL5 as in HHV-6A, but also has overlapping activity with the receptors for CCL4 (157, 158) (see Table 2). The exact role of chemokine receptors with these viruses is still unknown, but they could be multipurpose, in that they could have been developed for immune evasion to intercept chemokines that would otherwise be attracting immune cells to the area of infection, to attract uninfected cells that could then be infected, to induce latency, or to transition from latency to active replication.

Similar to HHV-6A, HHV-6B was shown to downregulate CXCR4 in $CD4^+$ T lymphocytes as well as MT-4 cells. This downregulation impaired the chemotactic response of the cells to the natural ligand, CXCL12 (145). Similar to HHV-6A, this could induce mobilization of HSPCs into the circulation as well as prevent migration of cells out of the thymus, both of which aid in the propagation and survival of the virus.

E. Human Immunodeficiency virus

HIV was discovered as the causative agent for acquired immunodeficiency syndrome (AIDS) in 1984 (159) and has since become one of the most extensively studied viruses worldwide. Since its discovery, it is estimated that 70 million people have been infected with HIV and about 35 million people have died due to AIDS. As of 2011 it is estimated that 34 million people are infected with HIV with 1.7 million AIDS-related deaths in 2011 (Global

Health Observatory, HIV/AIDS. World Health Organization. Web. 19 June 2013). HIV consists of two copies of a positive single stranded RNA genome and is an enveloped spherical virus particle with a diameter of about 120 nm. CD4 is the primary receptor for HIV with CCR5 and CXCR4 acting as coreceptors for viral entry. Once inside, HIV integrates into the host cell genome, becoming proviral ds DNA. The virus preferentially infects $CD4^+$ T cells, and the depletion of these cells below 200 $CD4^+$ cells/µl blood is what constitutes AIDS. Currently the most common form of treatment for HIV/AIDS is highly active antiretroviral therapy (HAART)(160) but the use of antiviral drugs only delays the onset of AIDS and does not represent a cure. A vast amount of knowledge has been gained with the extensive amounts of money and resources used for HIV research but it continues to be a problem worldwide and may require different approaches than have already been considered to combat the disease.

There is experimental evidence that indicates that HHV-6A and HIV have a synergistic effect on one another and that HHV-6A can act as a co-factor with HIV to cause more rapid progression to AIDS than HIV alone (57). Both HIV and HHV-6A have tropism for $CD4^+$ T cells and it has been shown that these viruses can coinfect the same cell (161), which may be relevant in disease development. This study showed that the majority of cells that were infected with HIV-1 were simultaneously expressing antigens from HHV-6 and that reverse transcriptase activity was detected earlier in the coinfected cultures as compared to the HIV only infected cultures. Additionally, HHV-6A causes CD4 upregulation in cells that do not typically express CD4 (such as $CD8^+$ T cells) by the IE1 and IE2 proteins (162) causing them to be susceptible to HIV infection (17). HHV-6A has also been shown to transactivate the HIV-1 long terminal repeat (LTR) promoter causing increased HIV-1 replication (163, 164). These studies indicate that further research on the interaction between HIV and HHV-6A would be beneficial in order

to determine effects of the viruses *in vivo* and possible new drug targets. Because of previous studies showing that RAG-hu mice can be infected with HIV-1 and that they develop CD4 T cell depletion as in AIDS, we believe they will be a good model to study the interactions between HHV-6A and HIV.

F. HIV research in humanized mice

As advancements in humanized mouse models have occurred, the use of these animal models to study HIV has increased. Multiple strains of humanized mice have been successfully developed and infected with HIV-1 including Balb/c Rag2$^{-/-}\gamma c^{-/-}$, Balb/c Rag1$^{-/-}\gamma c^{-/-}$, NOD/SCID $\gamma c^{-/-}$, NOD/SCID BLT, and hNSG BLT (bone marrow-liver-thymus). Multiple isolates of HIV-1 have also been used in these humanized mice including CCR5 tropic JR-CSF, BaL-1, YU-2, ADA, NFN-SX (SL9), 1157, and CXCR4 tropic NL4-3, LAI, and MNp. These models allow researchers to study HIV as opposed to the related but genetically different SIV, and to observe the effects HIV has on human cells *in vivo* rather than on non-human primate cells (65, 165).

Humanized mice infected with HIV-1 exhibit similar characteristics to human infection. HIV-1 infected mice exhibit $CD4^+$ T cell loss in blood as well as in organs as is seen in human AIDS patients. High levels of viral replication are seen in the spleen, thymus, and lymph nodes of humanized mice which is where high levels of replication occur in HIV-1 infected humans. Virus is also detected in humanized mouse bone marrow, lungs, small and large intestine, and male and female reproductive tracts. Viremia is typically observed at 1 week post infection in humanized mice and they have been shown to sustain infection for up to 67 weeks, indicating that infection is lifelong (129). CXCR4 tropic HIV has a higher peak viremia, ~10^7 viral genomes per ml, compared to CCR5 tropic HIV that has a peak viremia of ~10^6 viral genomes per ml. Different pathogenesis is also seen between the two with CXCR4 tropic HIV causing a

more severe depletion of CD4+ T cells in the blood. The Rag-hu mouse model is susceptible to infection through both vaginal and rectal transmission routes (76, 166). Because our Rag-hu mice are already a well-established model for HIV research, we believe that with the development of our Rag-hu HHV-6A model we will have the ability to effectively study these viruses together *in vivo*.

II. Materials and Methods

A. Production and Characterization of Humanized Rag2 −/−γc −/− Mice

This section describes the generation of humanized mice through purification of human HSCs, intrahepatic transplantation into newborn BALB/c $Rag2^{-/-}\gamma c^{-/-}$ mice, and verification of successful engraftment through FACS analysis of peripheral blood samples. This section is adapted from "Production and characterization of humanized $Rag2^{-/-}$ $\gamma c^{-/-}$ mice" by Freddy M. Sanchez, German I. Cuadra, Stanton J. Nielsen, Anne Tanner, and Bradford K. Berges (167).

1. Materials

1.1 Purification and culture of human hematopoietic stem cells (HSCs)

1. Human $CD34^{+}$ Selection Kit (Miltenyi Biotec, Auburn, CA, USA or Stem Cell Technologies, Vancouver, BC, Canada). We have successfully used both kits.
2. Iscove's Modified Dulbecco's Medium supplemented with 10% fetal calf serum, 2% penicillin-streptomycin, and 10 ng/ml each of SCF, IL-3, and IL-6. Filter-sterilize the medium and store at 4°C.

1.2 Transplantation of BALB/c $Rag2^{-/-}$ $\gamma c^{-/-}$ mice with human HSCs

1. BALB/c $Rag2^{-/-}$ $\gamma c^{-/-}$ mice (*see* **Note 1**)

2. 28 gauge insulin syringes

3. Cultured human HSCs

4. Iscove's Modified Dulbecco's Medium

1.3 Bleeding mice to screen for human cell engraftment

1. Heating pad

2. Mouse restraint apparatus (Model TV-150; Braintree scientific Inc., Braintree, MA, USA). This device has a groove across the top. Pull the mouse tail through the groove and the mouse enters the apparatus backwards. A plunger prevents the mouse from escaping.
3. Scalpel blade (surgical blade stainless steel No. 11; Feather, Kita-ku, Osaka, Japan)
4. Gauze pads
5. Styptic powder (Kwik-Stop Styptic Powder with Benzocaine; ARC Laboratories)
6. Heparinized microcapillary tubes (Heparinized Micro-hematocrit capillary tubes; Thermo Fisher Scientific Inc., Waltham, MA, USA).
7. Micropipettor with tips.

1.4 FACS analysis to detect and quantify human cell engraftment

1. Antibodies: hCD45-PE and mCD45-PE-Cy7 (eBioscience, San Diego, CA, USA).
2. 10x ammonium chloride erythrocyte lysing solution: Dissolve 89.9 g NH_4Cl, 10.0 g $KHCO_3$, and 370.0 mg tetrasodium EDTA in 1 liter of ddH_2O. Adjust pH to 7.3. Store at 4°C in full, tightly closed 50 ml tubes. Dilute to 1x with ddH_2O and use immediately.
3. FACS Stain Buffer: 1x PBS + 0.1% BSA + 0.1% azide. Store at 4°C.
4. Block Buffer: Human Gamma Globulin (Jackson Immunoresearch Labs, West Grove, PA, USA), Normal Mouse Serum (Jackson Immunoresearch Labs), 2.4G2 monoclonal antibody to murine CD16/CD32 (BD, Franklin Lakes, NJ, USA). Reconstitute Normal Mouse Serum with 5.0 ml of ddH20. Add 2 ml of Human Gamma Globulin. Add 200 µl of 2.4G2 anti-mouse CD16/CD32. Store at 4°C.

5. 1% paraformaldehyde in 1x PBS: Paraformaldehyde does not dissolve effectively in PBS. Prepare a stock of 2% paraformaldehyde in ddH2O and a stock of 2x PBS in ddH2O. Mix these solutions together in equal parts and store at 4°C.
6. Flow cytometer
7. FACS tubes

2. Methods

2.1 Preparation of human HSCs for transplantation

1. $CD34^+$ human HSCs are purified from human umbilical cord blood or other sources (*see* **Note 2**) using magnetically-labeled antibodies according to the manufacturer's protocol. $CD34^+$ cells are cultured for 40-48 hours (*see* **Note 3**) post-extraction in IMDM supplemented with 10% FCS, 1x penicillin/streptomycin, and 10 ng/ml each of IL-3, IL-6, and SCF.
2. Re-suspend cells by repeated pipetting, since many cells will be semi-adherent. Count cells using a hemocytometer. Samples used for engrafting mice may be divided to engraft multiple mice.
3. Centrifuge samples for 3 minutes at 3000 rpm and discard the supernatant. Re-suspend the cell pellet in serum-free IMDM. Approximately 30-50 µl of re-suspended cells is best for an individual mouse injection. Divide the solution into different samples equal to the number of pups that will be engrafted. We use a minimal dose of 250,000 cells per mouse in order to achieve consistent, high-level engraftment (*see* **Note 4**).

2.2 Conditioning pups for transplantation

1. 1 to 5-day-old pups (*see* **Note 5**) are conditioned by gamma irradiation at a dose of 350 rads. Wait at least 1 hour between irradiation and cell injection. Care must be taken to

prevent animals from being exposed to mouse pathogens during transportation and cell injection (*see* **Note 6**).

2.3 Transplantation of pups with human HSCs

1. Add 30-50 µl of $CD34^+$ cells in solution into each syringe. The exact volume depends upon the age and size of the pups (*see* **Note 7**). 30 µl is best for 1-day-old pups. Since some volume is retained in the needle after injection, larger volumes are preferable for older pups in order to prevent loss of cells due to retention of liquid in the syringe.

2. Place pups on their backs and stretch out their bodies to allow visualization of the liver. Since pups are albino, the liver is readily visible. Pups are injected with cells in the liver at a depth of 1-2 mm. Greater depths can result in bleeding from the injection site. Following injection keep the syringe inserted for 20 seconds to prevent cells from being expelled after needle withdrawal. Upon completion of the injection, place the pups back with their mother.

2.4 Bleeding mice for FACS analysis

1. Eight weeks post-reconstitution, mice should be screened for human cell engraftment. Warm up the mice by placing them in an empty plastic cage on top of a heating pad. Allow at least 5 minutes for the mice to sufficiently heat up. The mice are warm enough when their movements are rapid and they are breathing fast.
2. Remove a mouse from the heating cage and place it in the restraint apparatus. Holding the mouse by the tail, gently pull the mouse (tail first) into the apparatus. Pull the tail along the grove in the top of the apparatus, thus pulling the mouse into the apparatus. Push the plunger into the front of the apparatus so the mouse is held inside (*see* **Note 8**).

3. Locate the veins on the tail and choose one for tail nick bleeding. Using the scalpel, make a small transverse cut across the selected vein. After the mouse begins to bleed, hold the capillary tube horizontally (to avoid forming air bubbles that can lead to clotting) at the cut site and begin collecting blood. When the capillary is full (reaches the red line) withdraw it (keeping it horizontal) and place the blood sample into an appropriately labeled microfuge tube.
4. Pinch the tail above the cut site to stop the blood flow and wipe away any excess blood. Scoop out a small amount of styptic powder and apply it to the cut site. Allow enough time for clotting to occur. Place the mouse back into its original cage.
5. Eject the blood from the capillary tube using the micropipettor and by drawing the capillary tube up and out of the microfuge tube as you eject the blood. This technique will prevent the blood from coming back up into the capillary.

2.5 Preparing Blood Samples for FACS Analysis

1. Lyse red blood cells by adding 1.4 ml erythrocyte lysing solution per 100 µl of blood. Incubate at room temperature for 5-10 minutes. Centrifuge samples at 3,000 rpm for 3 minutes. Discard the supernatant and re-suspend the cell pellet in 100 µl of FACS stain buffer.
2. Add 3 µl of Fc Block and place samples at 4°C for 15 minutes (*see* **Note 9**). Add 3 µl of both mCD45-PE and hCD45-PE-Cy7 to each sample and incubate at 4°C for 30 minutes. Keep light exposure to a minimum.
3. Add 900 µl of 1% paraformaldehyde in 1x PBS to each sample. Spin samples at 3,000 rpm for 3 minutes. Dispose of the supernatant and re-suspend the pellet in 150 µl of 1x PBS solution. Transfer samples into FACS tubes and analyze by FACS.

3. Notes

1. There are multiple types of immunodeficient mouse strains that support engraftment of human hematopoietic stem cells and multi-lineage hematopoiesis. The original SCID mouse retains natural killer (NK) cell activity and the SCID mutation can result in leaky production of lymphocytes in older mice; both NK cells and T lymphocytes recognize and reject foreign cells. As a result, strains with greater defects in NK and T cell development are now typically used, including $Rag2^{-/-}\gamma c^{-/-}$ mice, NOD/SCID mice, NOD/SCID $\gamma c^{-/-}$ mice, and $Rag1^{-/-}$ $\gamma c^{-/-}$ mice. $Rag2^{-/-}$ $\gamma c^{-/-}$ mice are commercially available on a C57BL/6 background, but for unknown reasons these animals cannot be effectively engrafted (BALB/c $Rag2^{-/-}$ $\gamma c^{-/-}$ mice work effectively). Excellent reviews are available that explain the phenotype of each mutation, as well as the history of using these strains to produce humanized mice (168, 169).

2. Three main sources are currently employed to obtain human hematopoietic stem cells: umbilical cord blood, fetal liver, and mobilized peripheral blood. Magnetic separation techniques are commonly employed to purify $CD34^+$ cells. Umbilical cord blood is most readily available, but this source yields low numbers of cells, at most $1x10^6$. Relatively fewer mice can be engrafted per sample due to lower yields. Fetal liver samples have ethical constraints and few suppliers exist, but these samples yield more cells. Fetal liver samples commonly yield greater than 20×10^6 cells. We have no experience using mobilized peripheral blood and this source is rarely used to produce humanized mice (170, 171).

3. $CD34^+$ cells are cultured for 40-48 hours in order to obtain maximum expansion of the hematopoietic stem cell population, while preventing differentiation of the stem cells.

There is no method currently available to culture hematopoietic stem cells without eventual differentiation and loss of potency for engraftment. Density of cells is critical for expansion during culture. Denser cell cultures grow more efficiently than cultures that are less dense. We culture cells in 48-well plates since that provides the appropriate cell density for most umbilical cord blood-derived samples.

4. The number of $CD34^+$ HSCs to inject varies considerably in the literature. In the original paper by Traggiai et al showing HSC engraftment in $Rag2^{-/-}$ $\gamma c^{-/-}$ mice, they found engraftment with as few as $3.8x10^4$ $CD34^+$ HSCs (110). We typically use at least $2.5x10^5$ cells per mouse to achieve consistent, high-level engraftment. Some researchers use up to $1\text{-}2x10^6$ cells per mouse (172).

5. Several experiments have shown that age of mice at the time of engraftment has an impact on the level of engraftment achieved. We have found that engraftment levels are superior when $Rag2^{-/-}$ $\gamma c^{-/-}$ pups are less than 5 days of age at the time of irradiation and transplantation. Attempts to engraft older $Rag2^{-/-}\gamma c^{-/-}$ mice result in lower levels of engraftment. Different mouse strains can show effective engraftment with older mice (e.g., NOD/SCID $\gamma c^{-/-}$), but in some cases different conditioning techniques were used (171, 173-175).

6. Immunodeficient mice are housed in specific-pathogen free facilities because they are unable to defend against various types of infections. They are often given antibiotics in their drinking water in order to prevent bacterial infection. When preparing mice for irradiation, they often have to leave the animal facility; therefore, great care must be

taken to keep the animals pathogen-free while in transit so as to avoid contaminating the colony.

7. Intrahepatic injection into newborn mice can be technically challenging. BALB/c mice are albino and hence the liver is readily visible. We typically inject a volume of 30-50 µl of cells per mouse. However, we find that the volume used for cell injection must be smaller for 1-day-old pups; if not the inoculated cells can exit the injection site after withdrawing the needle due to pressure accumulated during injection. For smaller pups, we use an injection volume of 30 µl. Allow the needle to remain in place for 20 seconds to ensure that the cells will not be expelled from the mouse.

8. Be careful not to catch the mouse's feet between the plunger and the wall of the apparatus. Do not let go of the tail or the mouse may pull the tail inside. Animals can sometimes bury their heads underneath their bodies and suffocate, so make sure that the head stays up for access to fresh air.

9. FACS analysis using cells from chimeric animals is more complicated than using cells from a single organism due to the requirement to block non-specific antibody binding to both human and mouse cells. We perform initial work-up experiments with FACS antibodies on pure mouse blood or pure human blood to verify the accuracy of the staining. We block non-specific staining by using a combination mouse/human Fc block consisting of anti-mouse CD16/CD32, human gamma globulin, and normal mouse serum (*see* **Materials**). We typically use mouse monoclonal antibodies for FACS staining and we rarely detect background or cross-species staining.

B. Cells and viruses

1. Cells used for engraftment

Human cord blood samples were obtained with permission from the University of Colorado Cord Blood Bank. The Institutional Review Board does not require a protocol for human cord blood because samples are shipped without patient identifiers. HSCs were purified from human cord blood based upon the CD34 marker using the EasySep Human Cord Blood CD34 positive selection kit (StemCell Technologies, Vancouver, British Columbia, Canada). Cells were cultured for ~48 hours in IMDM (Invitrogen) supplemented with 10% FCS and 10 ng/ml each of human IL-3, IL-6, and SCF (R&D Systems, Minneapolis, MN, USA). Cells were suspended and counted at ~44 hours post extraction to determine number of mice to be irradiated and engrafted. Mice were irradiated and returned to their cages for 3 to 5 hours and then they were engrafted with the $CD34^+$ cells in IMDM only.

2. Virus propagation

HHV-6A U1102

BAC-derived HHV-6A, strain U1102, was previously engineered to express GFP (176). BAC-derived HHV-6A DNA was isolated from overnight *E. coli* cultures grown at 32°C in LB containing chloramphenicol (15 µg/ml) and purified using NucleoBond PC 100 columns (Clontech) per the manufacturer's protocols. HHV-6A BAC DNA (5 µg) and 1 µg of the human cytomegalovirus pp71-expressing plasmid pCGN1-pp71 (177) were transfected into 5×10^6 Jjhan cells with transfection reagent "V" utilizing a Nucleofector, (Lonza AG) per the manufacturer's protocols. After transfection the cells were maintained in 3 mL RMPI media containing 8% Fetal Bovine Serum (Sigma) and supplemented with 100 U/ml each of penicillin and streptomycin. After 5-7 days the media was changed and supplemented with 20ng/mL TPA (Sigma) and 3 mM

Na-butyrate (Sigma) for 24 hours. Cells were washed 3x with PBS to remove the TPA and Na-butyrate and co-cultured with an equal number of HSB-2 cells that were pre-stimulated for 24 hours with 2pg/ml IL-2 (Sigma) and 5ng/ml PHA (Sigma). Fresh pre-stimulated HSB2 cells are added every 4-6 days to allow accumulation of the virus by cell-to-cell spread.

To isolate virus, the cultures were pelleted by low-speed centrifugation and the supernatant was reserved. Infected cells were resuspended in 10 ml of media and sonicated to release virus from infected cells. The media was then cleared of cellular debris, and the supernatant was added to the reserved media. Virus was then purified by ultracentrifugation through a 20% sorbitol cushion in a SW28 rotor for 90 minutes at 53,000 x *g*. The resulting pellet was resuspended in media supplemented with 1.5% BSA and aliquots were stored at –80°C following snap-freeze in liquid nitrogen.

HHV-6A GS

HHV-6A strain GS was used in the migration assay experiments. Viral propagation was performed in the JJhan T cell line or primary $CD34^-$ cord blood cells that had been stimulated with 20 µg/ml PHA for 48 hours followed by 100 units/ml IL-2. Cells were spun down and resuspended in viral media (typically in a microcentrifuge tube with 500-1000 µl) with 5 µg/ml polybrene (to assist in infection) at an MOI of ~0.02 and infected for ~2 hours at 37 ºC and 5% CO2, flicking tube by hand to resuspend cells every 30 min. After 2 hour infection, cells were spun down and viral media removed. Cells were then resuspended in RPMI 1640 + 10% FBS + 1x Penicillin/Streptomycin and plated in appropriate size flask for amount of cells infected. Of the methods attempted, harvesting the virus 8 days post infection yielded the highest titers of virus. When collecting virus, all virally infected cells were pelleted at low speed and supernatant

was removed to a separate conical tube. Cellular pellets were then resuspended in ~2 ml FBS and underwent 3-4 freeze/thaw cycles, flash freezing in liquid nitrogen and thawing in a 37 ºC water bath, to lyse and release cell-associated virus. Cellular debris was then pelleted and supernatant removed and added to previously collected supernatant. Aliquots were frozen in RPMI with 1.5% BSA (bovine serum albumin) at -80 ºC. Typically infections were done on a relatively small number of cells (~3 x 10^5) due to the low titers usually achieved in viral propagation. It should be noted that Herpes 6 is somewhat more difficult to achieve high titers as other viruses. Ultracentrifugation was performed to achieve a higher titer of HHV-6A, however, the freeze/thaw method described above yielded higher titers than the ultracentrifuge method.

HIV strain JRCSF

HIV strain JRCSF (CCR5 topic) was transfected into HEK 293 T cells using lipofectamine 2000. Incubated 24 µg of JRCSF plasmid in 1.5 ml OPTI-MEM 5 min. Incubated 60 µl Lipofectamine 2000 in 1.5 ml OPTI-MEM for 5 min. The two solutions were gently mixed after incubation and incubated an additional 20 min at room temperature. Added final solution (3 ml) to ~70% confluent tissue culture dish (100 mm x 20 mm) containing HEK 293T cells and incubated at 37 °C and 5% CO_2. Virus was collected and frozen at -80 °C.

HIV strain NL4-3

HIV-1 strain NL4-3 (CXCR4 tropic) was propagated in JJhan cells in RPMI 1640 + 10% FBS + 1x Penicillin/Streptomycin media. Cells were spun down and resuspended in viral media (typically in a microcentrifuge tube with 200-500 µl virus) with 5 µg/ml polybrene (to assist in infection) at an MOI of ~0.01 and infected for ~2 hours at 37 ºC and 5% CO2, flicking tube by hand to resuspend cells every 30 min. After 2 hour infection, cells were spun down and viral

media removed. Cells were then resuspended in RPMI 1640 + 10% FBS + 1x Penicillin/Streptomycin and plated in appropriate size well for amount of cells infected. At ~9 days post infection, cells were spun down and supernatant was collected and frozen at -80 °C as cell-free virus stock.

3. Titering of Virus

Determination of HHV-6A-GFP titers

Titers of HHV-6A U1102 were calculated using standard 50% tissue culture infective doses ($TCID_{50}$) assays (178). Briefly, Jjhan cells were plated into a 96-well plate at 1×10^5 cells per well and incubated overnight at 37°C. Aliquots of HHV-6A were thawed on ice and briefly sonicated or vortexed. The stock was serially diluted in 10-fold increments and used to inoculate JJhan cells. 5 µg/ml polybrene was used to support infection. The cultures were incubated in a 37°C incubator with 5% CO_2 for 10-14 days. GFP positive wells were scored to determine the titer of the stock. GFP signal is present within 24-48 hours post-infection and determination of viral presence or absence can be determined within that time if an exact titer is unnecessary.

Determination of HHV-6A strain GS titers

Titers of HHV-6A strain GS were performed according to the protocol for HHV-6A-GFP U1102 except this strain contains no GFP and therefore it cannot be used for titering purposes. A number of papers suggest titering of HHV-6A can be done according to number of enlarged cells present in the culture, a common cytopathic effect of the virus. However, this method proved unreliable when using JJhan cells as even uninfected cells vary in cell size and can be enlarged, depending on how long they have been culturing *in vitro*. Therefore, the titer of this strain was determined by quantitative polymerase chain reaction (Q-PCR).

Determination of HIV-1 JRCSF titers

Titers of HIV-1 JRCSF (CCR5 tropic) were calculated by using standard $TCID_{50}$ assay. Ghost Hi-5 cells were initially grown in High glucose DMEM with 10% FBS, 500 μg/ml G418, 100 μg/ml hygromycin, 1x pen/strep, and 1 μg/ml puromycin (179) and were then spun down and resuspended in DMEM +10% FBS + 1x pen/strep and plated in 12 well plate at 2.5 x 10^4 cells/well 24 hours prior to infection with HIV. 1:10 serial dilutions were made with 20 μg/ml polybrene per well. Ghost Hi-5 cells turn green when infected with HIV and were then run on the flow cytometer at least 48 hours post infection (BD Attune) to determine exact titer.

Determination of HIV-1 NL4-3 titers

Titers of HIV-1 NL4-3 stocks (CXCR4 tropic) were calculated using $TCID_{50}$ assays using the reporter cell line, CEM GFP cells. 5 x 10^4 CEM GFP cells/well were grown in selectable media (RPMI 1640 medium with 10% fetal bovine serum, 1% penicillin/streptomycin, 1% 200 mM L-glutamine, and 500 μg/ml G418) and plated in 96 well plate 24 hours prior to infection with HIV. Prior to plating for TCID50 assay, cells were spun down, supernatant removed, and resuspended in RPMI 1640 + 10% FBS + 1x L-glutamine. Cells were infected with 1:10 serial dilutions of HIV-1 NL4-3 in RPMI + 5 μg/ml polybrene for at least 48 hours prior to titering. Viral medium was not removed after infection but was just allowed to incubate with cells. CEM GFP cells turn green upon infection with HIV and are then run on the flow cytometer to quantify percentage of green cells to calculate viral titer.

4. Animals

Balb/c-Rag2$^{-/-}$γc$^{-/-}$ mice were humanized by engraftment with CD34$^+$ human HSCs purified from human umbilical cord blood as described previously (69). Mice were maintained in

the specific pathogen-free room at the Brigham Young University Central Animal Care Facility. These studies have been reviewed and approved by the Institutional Animal Use and Care Committee (Protocol 120101 and 150108). Briefly, 1-5 day old mice were conditioned by irradiating with 350 rads and then injected intrahepatically with 2-5×10^5 human $CD34^+$ cells per mouse. Both male and female mice were used for engraftment and infection experiments. Mice were screened for human cell engraftment at 8 weeks post-engraftment. Peripheral blood was collected by tail bleed and stained with antibodies specific to either human or mouse CD45 (the pan-leukocyte marker). FACS analysis was performed to determine percent peripheral blood engraftment of human cells (89, 180). For a detailed description and materials see (167).

5. Preparation of carrier cells for viral transmission to humanized mice

1×10^6 fresh CD34 depleted cord blood mononuclear cells were cultured in basal medium (RPMI 1640 + 10% FCS + 1x Pen/Strep) and were stimulated with PHA (20 µg/ml) for 48 hours followed by IL-2 (100 units/ml) for 10 days. We chose to use these cells because 1) they are routinely used for HHV-6A infections and 2) they are readily available in our lab. DNA extraction and Q-PCR were performed on a portion of cells to verify lack of endogenous HHV-6A. 1.7×10^6 cells were infected with 3.3×10^5 infectious units (i.u.) of a recombinant strain of HHV-6A expressing GFP under the CMV IE promoter, and in the U1102 strain background (176) (hereafter referred to as HHV-6A-GFP) + 5 µg/ml polybrene (Sigma) and mock-infected cells were re-suspended in basal medium with polybrene. Samples were infected at 37 °C and 5% CO_2 for 2 hours, and cells were resuspended by hand every 30 min. Final MOI was 0.02. After incubation, cells were resuspended in 3 ml basal medium and plated in a 6-well plate. IL-2 was added and cells were incubated at 37 °C and 5% CO_2 for 48 hours. FACS analysis was performed on infected and mock-infected cells to detect and quantify HHV-6A-infected cells

prior to mouse infection. GFP was used to identify infected cells, and samples were stained with anti-human CD3, CD4, and CD8 antibodies (see below) to characterize infected cell types.

6. HHV-6A transmission to humanized mice

In the cell-associated viral transmission study, 1×10^5 cells (of which ~20% were GFP^+) in 100 µl serum-free RPMI 1640 were injected intraperitoneally (i.p) into mice. Uninfected mice were injected similarly with uninfected cells in the same medium as infected mice. In the cell-free viral transmission study, cell-free HHV-6A-GFP was thawed and immediately diluted in RPMI 1640 (no serum or antibiotics). 100 µl of cell-free virus (4.3×10^5 i.u./mouse) was injected i.p. into mice.

7. HIV transmission to humanized mice

HIV strain JRCSF (CCR5 tropic) was used in the coinfection study. 200 µl of cell-free virus in serum-free RPMI 1640 was injected i.p. into mice in the HIV only and coinfected groups. The titer of this stock was ~1 x 10^4 so the mice were injected with ~2,000 infectious units each. HIV injections were done 14 days post infection with HHV-6A to attempt to replicate infection in the human population with infection with HHV-6 usually coming prior to infection with HIV. Verification of infection was performed by RT-PCR.

C. Viral load

1. Measurement of blood viral load in HHV-6A Rag-hu mouse study

Blood was collected by tail bleed for 6 weeks in cell-associated HHV-6A infected mice. 70 µl of whole blood was collected per time point in heparin free micro-hematocrit capillary tubes (Fisherbrand) and blood was placed in microcentrifuge tubes containing ~0.5 mg/ml EDTA which was usually centrifuged to separate cellular and plasma fractions. DNA was then

extracted with the QIAamp DNA Blood Mini Kit (Qiagen). Q-PCR was performed using an Applied Biosystems StepOne machine to detect and quantify presence of viral genomes using a published assay (181). 10-fold serial dilutions of a plasmid containing the target HHV-6A sequence were used as copy number standards, and the sensitivity of the assay was previously reported to be 10 DNA copies (181). The limit of detection of the assay was 1,000 normalized copies in plasma/ml or 400 copies in bone marrow, thymus, and spleen.

2. Measurement of blood viral load in HIV-1/HHV-6A Rag-hu mouse coinfection study

Blood was collected by tail bleed for 12 weeks. About 140 microliters of whole blood was collected (2 capillaries) per time point, and the blood was centrifuged to separate cellular and plasma fractions. DNA and RNA were then simultaneously extracted with a QIAamp MinElute Virus Spin kit (Qiagen, Cat. #57704) using purification of viral nucleic acids from plasma or serum protocol from said Qiagen kit. DNA/RNA was eluted in 50 µl Buffer AVE. Q-PCR was performed using an Applied Biosystems StepOne and StepOne Plus machine to detect and quantify the presence of HHV-6A genomes using a published assay (181). Serial dilutions (10-fold) of a plasmid containing the target HHV-6A sequence were used as copy number standards; the sensitivity of the assay was previously reported to be 10 DNA copies (181). Reverse transcriptase-polymerase chain reaction (RT-PCR) was performed using 5 µl RNA. HIV primers used for first strand synthesis were HIV-1 LTR forward (IDT #44095175) and HIV-1 LTR reverse (IDT #44095176) and HIV-Q probe (IDT #46308067) was used for Q-PCR of cDNA. The "High capacity cDNA Reverse Transcription Kit" (Applied Biosystems, cat. #4368814) was used.

<u>Primer dilutions:</u>

Primer stocks are 50 µM. Need to perform a 1:25 dilution to make primers for first strand synthesis (2 µM stock). Need to perform a 1:10 dilution of primers for Q-PCR of cDNA (5 µM stock).

Probe dilution:

Probe stock is 25 µM. Need to perform the following dilution to get a 2 µM stock: add 16 µl to 184 µl ddH2O.

First strand synthesis (making cDNA from RNA)

For LTR primer (2 µM):	1 µl
Rev LTR primer (2 µM):	1 µl
dNTPs (10 mM):	1 µl
RNA	5 µl
RNase-free ddH2O (in kit)	2 µl
Total	10 µl

Reaction conditions: 65 °C for 5 min., then ice (or 4 °C) for >1 min.

Make a master mix of additional reagents (all of these are in kit):

10X RT buffer	2 µl
25mM MgCl2	4 µl
0.1M DTT	2 µl
RNaseOUT	1 µl
Superscript III Reverse Transcriptase	1 µl
Total	10 µl

--Add 10 µl of this mix per tube

Reaction conditions: 50 min. at 50 °C, 85 °C for 5 min., then 4 °C.

cDNA synthesis is now complete.

Q-PCR of cDNA

For LTR primer (5 µM stock)	2.5 µl
Rev LTR primer (5 µM stock)	2.5 µl
LTR probe (2 µM stock)	1 µl
Q-PCR master mix	12.5 µl
ddH20	1.5 µl
cDNA	5 µl
Total	25 µl

Reaction conditions: 50 cycles of 95 °C for 15 sec., 60 °C for 1 min.

3. Organ collection and measurement of viral load in HHV-6A Rag-hu mouse study

In the HHV-6A cell-associated study, mice were sacrificed by CO_2 asphyxiation (time points ranging from 6.5 to 9.5 weeks post-infection, see Table 1) and lymphoid organs collected (thymus, bone marrow, lymph nodes, and spleen). Bone marrow was extracted from both femurs. The thymus was divided in half for Q-PCR or FACS analysis in one infected and one mock-infected animal. Subsequently, single cell suspensions were made using a 70 µm cell strainer and divided in half in order to perform both FACS and Q-PCR analysis. For Q-PCR, DNA was extracted using the QIAamp DNA blood mini kit and analyzed by Q-PCR as described above. Similar methods were used for organ collection in the cell-free HHV-6A viral transmission study except mice were sacrificed at 1 week p.i.

4. Organ collection and measurement of viral load in HIV-1/HHV-6A Rag-hu mouse coinfection study

Mice were sacrificed by CO2 asphyxiation at 12 weeks p.i. with HHV-6A (10 weeks post-infection with HIV) and lymphoid organs (thymus, bone marrow, lymph nodes, and spleen) were collected. Bone marrow was extracted from both femurs. The thymi were divided in half and single cell suspensions made so both Q-PCR and FACS analysis could be performed. For Q-PCR and RT-PCR, DNA and RNA were extracted simultaneously using a QIAamp MinElute virus spin kit (Qiagen) and analyzed by Q-PCR and RT-PCR as described above.

D. Migration Assays

Migration assays were performed differently, depending upon the specific experiment. Listed here are the parameters that remained standard throughout all migration assays. For a description of individual experiments, see specific sub sections below. Migration assays were performed using 24-well Corning transwells with 5 μm pore polycarbonate inserts (Sigma # CLS3421). PHA and IL-2 stimulated $CD34^-$ cells or JJhan cells (unstimulated) were infected as described previously in "Viral propagation" section of this document. 100 μl media + cells (anywhere from $1x10^5$ to 1×10^6 depending on the experiment) was carefully added to transwell prior to moving it onto the 600 μl media in bottom of well. Plates were then incubated at 37 ºC and 5% CO2 for varying amounts of time, depending on the specific experiment. Transwells were carefully removed from wells and cells and media in the lower well were collected and stained for HHV-6A and HIV-1 (where applicable) as well as CD3, CD4, CD8, CCR7, CXCR4, and S1P1 (see "flow cytometry analysis of migration assays" section for additional details). CCL21 (Peprotech catalogue #300-35), which attracts CCR7, was used as a positive control.

1. Time course of HHV-6A towards CCL21

CD34$^-$ human umbilical cord blood cells that were stimulated for 48 hours with 20 µg/ml PHA followed with 100 units/ml IL-2 for an additional 72 hours were then infected with HHV-6A wt strain GS at an MOI of 11. It should be noted that this MOI is based off of DNA copies of HHV-6A as determined by Q-PCR and not by infectious particles and that this virus has a relatively high amount of defective viral particles and the MOI of infectious particles would be lower.

2. Cell-free viral migration assays

Cell-free virus was used in these experiments along with 24-well Corning transwells. Although virus can freely pass through the 5 µm pore polycarbonate inserts they were used as a method to separate the media and attempt to observe any viral movement. HHV-6A wild type strain GS with a titer of 3.325 x 10^6 genome copies/ml and HIV-1 NL4-3 with a titer of ~3.2 x 10^4 were used. Viruses were thawed on ice and briefly vortexed prior to use. Four separate wells were run with HIV over RPMI, HHV-6A over RPMI, HIV over HHV-6A, and HHV-6A over HIV. 100 µl of virus was placed in transwell in the same media it had been frozen in prior to moving transwell on top of lower well containing 600 µl virus or RPMI only, according to the well. Assay was incubated for 70 min. at 37 C and 5% CO2. As additional controls, 50 µl HIV and 50 µl HHV-6A were incubated in separate 1.5 ml microcentrifuge tubes and incubated the same as the migration assays. Also as controls, freshly thawed HIV and HHV-6A were immediately loaded onto electron microscopy grid and stained with phosphotungstic acid (PTA) for imaging with electron microscope. After incubation, 100 µl was collected from the center of bottom wells, 50 µl of which was used to load on electron microscopy grids and stained as outlined in the “Electron Microscopy” section of this document.

E. Electron Microscopy

Electron microscopy was performed on the FEI Helios NanoLab 600 DualBeam FIB/SEM and the FEI Tecnai F20 TEM/STEM/AEM microscopes. Support films carbon type B, 200 mesh, Cu (Prod. # 01810, Ted Pella Inc.) grids were used. 50 µl of viral containing media was placed onto parafilm wax, EM grid was placed on top of viral drop with copper side facing up for 1.5 min., at which point the grid was removed with tweezers and the edge of grid was carefully touched to a kim wipe to remove liquid from grid and allowed to partially dry, grid was then placed on a drop of 10 µl of 2% PTA and allowed to sit for 1.5 min. and liquid was carefully removed as before. Grids were placed on 1% paraformaldehyde to inactivate virus and liquid removed and grids were then imaged.

F. Flow cytometry

1. Flow cytometry analysis of mice

Anti-human CD45 (eBioscience, Cat. No. 25-0459-42) and anti-mouse CD45 (eBioscience, Cat. No. 12-0451-83) were used for screening mice pre-infection to determine percent engraftment. Anti-human CD3 (BioLegend, Cat. No. 300310), anti-human CD4 (eBioscience, Cat. No. 25-0049-42), anti-human CD8 (eBioscience, Cat. No. 47-0088-42) and anti-human CD46 (eBioscience, Cat. No. 12-0469-42) were used in FACS analysis of regular tail bleeds and on the harvested organs. Anti-human S1P1 (CD363)(eBioscience, Cat. #50-3639-41), anti-human CCR7 (CD197)(eBioscience, Cat. #12-1979-42), anti-human CXCR4 (CD184)(eBioscience, Cat. #17-9999-42), HHV-6A (unconjugated primary antibody gp116/64/54 and CF750 Goat Anti-Mouse IgG2b as the secondary antibody, Biotium, Cat. #20430) and HIV (anti-HIV-1 Core Antigen, Clone: KC57, Beckman Coulter, Cat. #CO6604665) were stained for in HIV/HHV-6A coinfection study. Samples were run on a BD

FACSCanto flow cytometer and analyzed with Summit v4.3 software for the study entitled, "*Human herpesvirus 6A infection and immunopathogenesis in humanized Rag2$^{-/-}$γc$^{-/-}$ Mice"* and samples were run on an Attune Acoustic Focusing Cytometer and analyzed with Attune Cytometric software version 2.1.0 for the study entitled, "*Coinfection with human herpesvirus 6A and HIV and immunopathogenesis in humanized Rag2$^{-/-}$γc$^{-/-}$ Mice and relevance to HIV/AIDS."*

2. Flow cytometry analysis of B cells

70 µL of whole blood was obtained through tail bleed and treated with a mouse red blood cell lysis buffer for 15 min. Following this treatment the cells were centrifuged at 3300 rpm for 3 min and the supernatant was discarded. The pellet was then resuspended in 100 µL FACS staining buffer. 3 µL blocking buffer was then added and allowed to incubate in the dark at 4°C for 15 min. This was followed by the addition of 3 µL of the desired conjugated antibodies and incubated in the dark at 4°C for a period of 30 min. To determine percent human peripheral blood engraftment, peripheral blood was stained with human CD45 PECy-7 and mouse CD45 PE antibodies and FACS analysis was performed (71). Antibodies used for B cell characterization were: hCD45 PECy-7, hCD19 APC eFluor 780 (eBioscience), hCD3 PE, hCD138 PECy5.5 (Invitrogen), and hIgM FITC (BioLegend). Immediately following this 30 min step, 900 µL of 1% paraformaldehyde in 1x PBS was added to fix samples. Samples were then centrifuged at 3300 rpm for 3 min and the supernatant was discarded. The pellet was then resuspended in 150 µL 1x PBS and submitted for FACS analysis. An Attune Acoustic Focusing Cytometer (Applied Biosystems) was used to run samples, and Attune software v2.1 was used to analyze the results. All antibodies used in these studies do not cross-react with murine antigens, as assessed by staining of unengrafted Rag2$^{-/-}$γc$^{-/-}$ blood and lymphoid organs.

3. Flow cytometry analysis of migration assays

The flow cytometry for the migration assays consisted of both intracellular and extracellular surface staining. HHV-6A (Primary antibody: NIH Aids Reagent Program, Anti-HHV6 gp116/64/54 monoclonal (6A5G3). Secondary antibody: Biotium, CF750 Goat Anti-Mouse IgG2b) and HIV FITC conjugated anti-HIV-1 Core Antigen, Clone: KC57 (Beckman Coulter) as well as CD3 PE-Cy5 (eBioscience), CD4 PE-Cy7 (eBioscience), CD8 APC eflour 780 (eBioscience), CCR7 PE (eBioscience), CXCR4 APC (eBioscience), and S1PR1 Anti-Human CD363 (S1PR1) eFluor 660 (eBioscience). After cellular migration assay, cells were collected and spun down at 3,400 rpm for 3 min. and supernatant removed. Samples were resuspended in 100 µl FACS stain buffer (1X PBS +.1% BSA + .1% sodium azide) and blocked with FC block for 15 min at 4 °C, then spun down and 50 µl supernatant removed and added 100 µl "A" from fix and perm kit (Fix&Perm Cell permeabilization kit, Nordic MUbio, Cat. # GAS-002) and incubated 15 min. at room temperature, then washed with 5 ml PBS and spun down at 300 g for 5 min., removed supernatant and added 3 µl primary antibody for HHV-6A (gp116/64/54) and 3 µl anti-HIV-1 core antigen and 100 µl "B" from fix and perm kit , briefly vortexed, and let sit at room temperature for 30 min. Samples were then washed with 1 ml PBS, spun down and removed all but 100 µl of supernatant and added secondary antibody for HHV-6A (Goat Anti-Mouse IgG2b) and let sit at room temperature for 30 min., then washed with 5 ml PBS, spun down and removed supernatant and added 900 µl 1% paraformaldehyde and let sit for 30 min., then spun down and resuspended in ~250 µl 1X PBS to run on the flow cytometer. The samples that only had surface stains were just blocked for 15 min. with FC block and then stained with the appropriate antibody for 30 min. and then inactivated in 1% paraformaldehyde and resuspended in PBS to run on flow cytometer.

4. S1P1 expression time course

Anti-Human CD363 (S1PR1) eFluor 660 antibody (eBioscience) was used in this study. 3 x 10^5 JJhan cells were infected with 1 ml of 3.325 x 10^6 genome copies/ml HHV-6A GS wild type and for HIV-1 NL4-3 the MOI was .05. Cells were infected as described previously in "Virus propagation" section under subsection "HHV-6A strain GS" and subsection "HIV NL4-3". A small amount of cells were removed from the cultures at specific time points and stained with anti-human CD363 conjugated antibody with the same method as described in "Flow cytometry analysis of B cells" section of this document, excluding the red blood cell lysis step. Cells were then run on the Attune Acoustic Focusing Cytometer (Applied Biosystems) and Attune software v2.1 was used to analyze the results.

G. Antibody Concentrations

Mouse plasma samples were obtained by centrifuging whole blood at 3300 rpm for 3 min and then collecting the supernatant. ELISA tests were run using the Total Human IgM, Total Human IgG, and Total Human IgA kits (ALerCHEK) according to the manufacturer's instructions. Since human antibody concentrations are typically low in humanized mice, plasma was diluted 1:100 for IgM and IgG assays and 1:20 for IgA assays in order to obtain results in the linear range of the assay.

H. Statistics

Human T and B cell development in mouse peripheral blood was analyzed by Welch's ANOVA test (with Games-Howell *post hoc* test when applicable). To compare B cell levels in bone marrow, spleen, and blood, an ANOVA with Tukey-Kramer *post hoc* test was performed. For comparison of the different time points of plasma antibody concentrations an ANOVA with Tukey-Kramer post hoc test (where applicable) were performed. Standard Error (SE) was

calculated and indicated in all bar graphs. R^2 values were calculated to determine if a correlation exists between total antibody concentrations and peripheral blood engraftment levels in the humanized mice.

III. Results/Research Chapters

A. HHV-6A infection in humanized mice

Human herpesvirus 6A infection and immunopathogenesis in humanized Rag2-/-γc-/- Mice

Running title: HHV-6A infection in humanized mice

Anne Tanner[1], Stephanie A. Carlson[1], Masatoshi Nukui[2], Eain A. Murphy[2], and Bradford K. Berges[1]

Abstract

Although serious human diseases have been correlated to human herpesvirus 6A (HHV-6A) and human herpesvirus 6B (HHV-6B), the lack of animal models has prevented studies which would more definitively link these viral infections to disease. HHV-6A and HHV-6B have recently been classified as two distinct viruses and in this study we focus specifically on developing an *in vivo* model for HHV-6A. Here we show that $Rag2^{-/-}\gamma c^{-/-}$ mice humanized with cord blood-derived human hematopoietic stem cells produce human T cells that express the major HHV-6A receptor, CD46. Both cell-associated and cell-free viral transmission of HHV-6A into the peritoneal cavity resulted in detectable viral DNA in at least one of the samples (blood, bone marrow, etc.) analyzed in nearly all engrafted mice. Organs and cells positive for HHV-6A DNA were the plasma and cellular blood fractions, bone marrow, lymph node, and thymic samples whereas control mice had undetectable viral DNA. We also noted viral pathogenic effects on certain T cell populations. Specific thymocyte populations were significantly modified in cell-associated infected humanized mice, including $CD3^{-}CD4^{+}CD8^{-}$ and $CD3^{+}CD4^{-}$ cells. In addition, we detected significantly increased proportions of $CD4^{+}CD8^{+}$ cells in the blood of cell-free infected animals. These findings provide additional evidence that

HHV-6A may play a role in human immunodeficiencies. These results indicate that humanized mice can be used to study *in vivo* infection and replication of HHV-6A, including aspects of viral pathogenesis.

Introduction

Human herpesvirus 6 (HHV-6) is a member of the β-herpesvirus subfamily and was identified in 1986 (182). Recently this virus has been reclassified as two distinct variants, HHV-6A and HHV-6B based upon differences in tropism, disease, and epidemiology. These two variants have an overall nucleotide identity of 90% (9, 183) and serological assays to differentiate the variants are in development (184). The main cellular receptor for HHV-6A is CD46, which is expressed on all nucleated cells (185). CD134 has recently been identified as a cellular receptor for HHV-6B (154). While HHV-6B infection is ubiquitous in humans and is known to cause roseola infantum (186), the prevalence of HHV-6A and its role in human disease is poorly understood. HHV-6 has been implicated in diseases including multiple sclerosis (28, 187, 188), encephalitis, graft-versus-host disease (29, 189), other clinical complications of solid organ transplant and hematopoietic stem-cell transplants (190, 191), drug induced hypersensitivity syndrome (192, 193), malignancies, myocarditis, and cardiomyopathy (32, 194). HHV-6A has an impact upon human T cell populations (195), and can enhance HIV-1 replication (196). HHV-6A infects helper T cells as does HIV-1, and HHV-6A has been suggested as a potential co-factor in AIDS progression (194, 196-198).

A variety of animals models have been explored for HHV-6 studies, but with limited success. Early reports indicated that HHV-6A was able to replicate in T cells isolated from

chimpanzees (199) and pigtailed macaques (200). More recent reports have shown that non-human primate (NHP) models exhibit signs of disease following infection with HHV-6. Leibovitch et al. recently showed that common marmosets can be infected with HHV-6A, accompanied by neurological symptoms (201). Lusso et al. demonstrated that HHV-6A replicates *in vivo* in pigtailed macaques, and that coinfection of macaques with HHV-6A and Simian Immunodeficiency Virus resulted in faster depletion of $CD4^+$ T cells (198). The requirement for specialized facilities and the expenses involved in NHP research have been detrimental to further studies.

A small animal model of HHV-6 infection would allow for further investigation of viral pathogenesis without the costs and facilities required for NHP research. The viral target cells in humanized mice are human immune cells and hence viral infection in humanized mice may be more reflective of human infection due to differences in human and NHP genetics. Additionally, humanized mice can be infected with HIV-1 as opposed to the genetically distinct SIV isolates used in NHP models. Humanized mice infected with HIV-1 manifest symptoms of AIDS (166) for studies of HHV-6A as a co-factor in AIDS progression.

Here we report on the use of a newer generation of humanized mice to study HHV-6A replication and pathogenesis *in vivo*. $Rag2^{-/-}\gamma c^{-/-}$ mice (RAG-hu mice) are engrafted with human HSCs and undergo multi-lineage hematopoiesis to produce a variety of human blood cell types which are dispersed throughout the lymphoid and non-lymphoid organs. These mice (and other similar HSC-humanized mouse models) have been shown to support replication and viral pathogenesis after challenge with the herpesviruses EBV (119, 121, 122, 126), KSHV (202, 203), and hCMV (204). Here, RAG-hu mice were challenged with either cell-free or cell-associated recombinant HHV-6A expressing green fluorescent protein (GFP). Our findings show

that viral DNA is detectable in blood and lymphoid organs for up to 8 weeks after infection. Viral DNA was detected in the plasma, blood cells, thymus, lymph node, and bone marrow, although no single mouse tested positive for viral DNA in all of these compartments, 11 out of 12 mice were positive in at least one. Specific thymocyte populations were found to be significantly modified in animals infected for longer periods (and via cell-associated transmission); while animals infected with cell-free virus showed a significant increase in $CD4^+CD8^+$ cells in blood. These findings suggest that humanized mice represent a new *in vivo* model to study HHV-6A replication and immunopathogenesis.

Materials and Methods

Cells

Human cord blood samples were obtained with permission from the University of Colorado Cord Blood Bank. The Institutional Review Board does not require a protocol for human cord blood because samples are shipped without patient identifiers. HSCs were purified from human cord blood based upon the CD34 marker using the EasySep Human Cord Blood CD34 positive selection kit (StemCell Technologies). Cells were cultured for two days in IMDM (Invitrogen) supplemented with 10% FCS and 10 ng/ml each of human IL-3, IL-6, and SCF (R&D Systems).

Virus propagation

BAC-derived HHV-6A, strain U1102, was previously engineered to express GFP (176). BAC-derived HHV-6A DNA was isolated from overnight *E. coli* cultures grown at 32°C in LB

containing chloramphenicol (15 μg/ml) and purified using NucleoBond PC 100 columns (Clontech) per the manufacturer's protocols. HHV-6A BAC DNA (5 μg) and 1 μg of the human cytomegalovirus pp71-expressing plasmid pCGN1-pp71 (177) were transfected into 5×10^6 Jjhan cells with transfection reagent "V" utilizing a Nucleofector, (Lonza AG) per the manufacturer's protocols. After transfection the cells were maintained in 3mL RMPI media containing 8% Fetal Bovine Serum (Sigma) and supplemented with 100 U/ml each of penicillin and streptomycin. After 5-7 days the media was changed and supplemented with 20ng/mL TPA (Sigma) and 3mM Na-butyrate (Sigma) for 24 hours. Cells were washed 3x with PBS to remove the TPA and Na-butyrate and co-cultured with an equal number of HSB-2 cells that were pre-stimulated for 24 hours with 2pg/ml IL-2 (Sigma) and 5ng/ml PHA (Sigma). Fresh pre-stimulated HSB2 cells are added every 4-6 days to allow accumulation of the virus by cell-to-cell spread.

To isolate virus, the cultures were pelleted by low-speed centrifugation and the supernatant was reserved. Infected cells were resuspended in 10 ml of media and sonicated to release virus from infected cells. The media was then cleared of cellular debris, and the supernatant was added to the reserved media. Virus was then purified by ultracentrifugation through a 20% sorbitol cushion in a SW28 rotor for 90 minutes at 53,000 x *g*. The resulting pellet was resuspended in media supplemented with 1.5% BSA and aliquots were stored at –80°C following snap-freeze in liquid nitrogen.

Titering of Virus

Titers of HHV-6A were calculated using standard $TCID_{50}$ assays (178). Briefly, Jjhan cells were plated into a 96-well plate at 1×10^5 cells per well and incubated overnight at 37°C. Aliquots of HHV-6A were thawed at 37°C and briefly sonicated. The stock was serially diluted

in 10-fold increments and used to inoculate Jjhan cells. The cultures were incubated in a 37°C incubator with 5% CO_2 for 10-14 days. GFP positive wells were scored to determine the titer of the stock.

Animals

Balb/c-Rag2$^{-/-}$γc$^{-/-}$ mice were humanized by engraftment with CD34^{+} human HSCs purified from human umbilical cord blood as described previously (69). Mice were maintained in the specific pathogen-free room at the Brigham Young University Central Animal Care Facility. These studies have been reviewed and approved by the Institutional Animal Use and Care Committee (Protocol 120101). Briefly, 1-5 day old mice were conditioned by irradiating with 350 rads and then injected intrahepatically with 2-5×10^5 human CD34^{+} cells. Mice were screened for human cell engraftment at 8 weeks post-engraftment. Peripheral blood was collected by tail bleed and stained with antibodies specific to either human or mouse CD45. FACS analysis was performed to determine percent peripheral blood engraftment of human cells (89, 180).

Preparation of carrier cells for viral transmission to humanized mice

1×10^6 fresh CD34 depleted cord blood mononuclear cells were cultured in basal medium (RPMI 1640 + 10% FCS + 1x Pen/Strep) and were stimulated with PHA (20 µg/ml) for 48 hours followed by IL-2 (100 units/ml) for 10 days. We chose to use these cells because 1) they are routinely used for HHV-6A infections and 2) they are readily available in our lab. DNA extraction and quantitative polymerase chain reaction (Q-PCR) were performed on a portion of cells to verify lack of endogenous HHV-6A. 1.7×10^6 cells were infected with 3.3×10^5 infectious units (i.u.) of a recombinant strain of HHV-6A expressing GFP under the CMV IE promoter, and

in the U1102 strain background (176) (hereafter referred to as HHV-6A) + 5 μg/ml polybrene (Sigma) and mock-infected cells were resuspended in basal medium with polybrene. Samples were infected for 2 hours, shaken every 30 min. Final MOI was 0.02. After incubation, cells were resuspended in 3 ml basal medium and plated in a 6-well plate. IL-2 was added and cells were incubated for 48 hours. FACS analysis was performed on infected and mock-infected cells to detect and quantify HHV-6A-infected cells prior to mouse infection. GFP was used to identify infected cells, and samples were stained with anti-human CD3, CD4, and CD8 antibodies (see below) to characterize infected cell types.

HHV-6A transmission to humanized mice

In the cell-associated viral transmission study, 1×10^5 cells (of which ~20% were GFP^+) in 100 μl serum-free RPMI 1640 were injected intraperitoneally (i.p) into mice. Uninfected mice were injected similarly with uninfected cells in the same medium as infected mice. In the cell-free viral transmission study, cell-free HHV-6A-GFP was thawed and immediately diluted in RPMI 1640 (no serum or antibiotics). 100 μl of cell-free virus (4.3×10^5 i.u./mouse) was injected i.p. into mice.

Measurement of blood viral load

Blood was collected by tail bleed for 6 weeks. 70 μl of whole blood was collected per time point and blood was usually centrifuged to separate cellular and plasma fractions. DNA was then extracted with the QIAamp DNA Blood Mini Kit (Qiagen). Q-PCR was performed using an Applied Biosystems StepOne machine to detect and quantify presence of viral genomes using a published assay (181). 10-fold serial dilutions of a plasmid containing the target HHV-6A sequence were used as copy number standards, and the sensitivity of the assay was previously

reported to be 10 DNA copies (181). The limit of detection of the assay was 1,000 normalized copies in plasma/ml or 400 copies in bone marrow, lymph node, thymus, and spleen (see below).

Organ collection and measurement of viral load in organs

In the cell-associated study, mice were sacrificed (time points ranging from 6.5 to 9.5 weeks post-infection, see Table 1) and lymphoid organs collected (thymus, bone marrow, lymph nodes and spleen). Bone marrow was extracted from both femurs. The thymus was divided in half for Q-PCR or FACS analysis in one infected and one mock-infected animal. Subsequently, single cell suspensions were made and divided in half in order to perform both FACS and Q-PCR analysis. For Q-PCR, DNA was extracted using the QIAamp DNA blood mini kit and analyzed by Q-PCR as described above. Similar methods were used for organ collection in the cell-free viral transmission study except mice were sacrificed at 1 week p.i.

FACS analysis

Anti-human CD45 (eBioscience) and anti-mouse CD45 (eBioscience) were used for screening mice pre-infection to determine percent engraftment. Anti-human CD3 (BioLegend), anti-human CD4 (eBioscience), anti-human CD8 (eBioscience) and anti-human CD46 (eBioscience) were used in FACS analysis of regular tail bleeds and on the harvested organs. Samples were run on a BD FACSCanto flow cytometer and analyzed with Summit v4.3 software.

Results

RAG-hu mice produce cells that express the HHV-6A receptor

RAG-hu mice were engrafted with human $CD34^+$ hematopoietic stem cells isolated from cord blood as described previously (69) and as outlined in Methods. Mice were screened for human cell engraftment at 8 weeks post reconstitution by FACS analysis of peripheral blood for the pan-leukocyte markers hCD45 and mCD45.

CD46 is a known receptor involved in HHV-6A entry (185) and serves as an inhibitor of complement-mediated cell lysis. CD46 is thought to be expressed in all nucleated human cells, but is only expressed in murine testis (205) which may explain murine resistance to HHV-6A infection. Thus, we stained cells from RAG-hu mice for the presence of CD46 in order to determine if this animal model might be useful for HHV-6A research. We found that RAG-hu mice produce human $CD46^+$ cells in the blood, thymus, and bone marrow (Fig.1). $CD3^+$ T cells were $CD46^+$, as well as $CD3^-$ cells that were not characterized further.

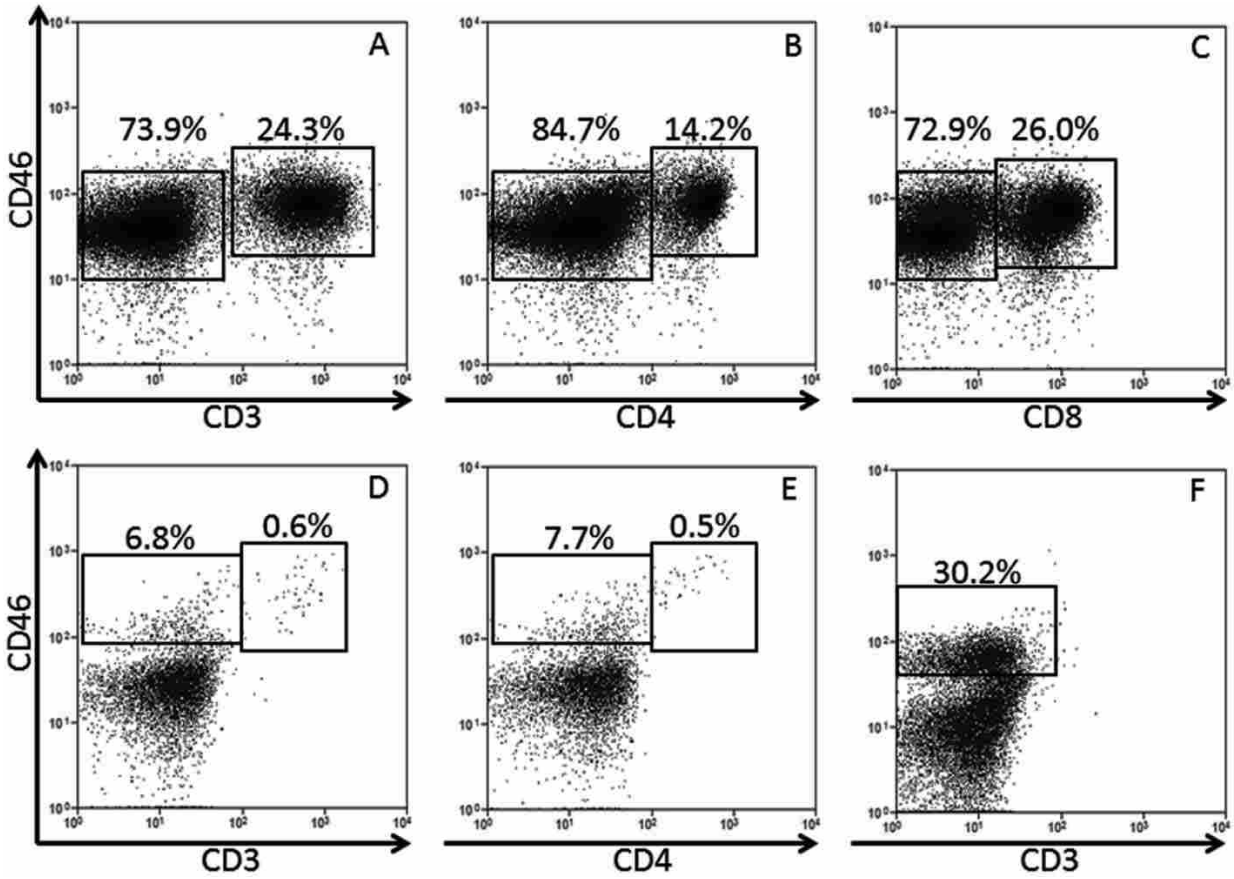

Figure 1. Humanized mice harbor human cells that express the HHV-6A receptor (A-C) RAG-hu thymocytes are $CD46^+$, including (A) $CD3^+$ T cells and the two major subsets of T cells, (B) $CD4^+$ helper T cells (C) and $CD8^+$ cytotoxic T cells. (D-E) RAG-hu blood also contains $CD46^+$ cells, some of which are also (D) $CD3^+$ and (E) $CD4^+$. (F) The bone marrow also harbors $CD46^+$ cells, but only minimal T cells were detected in this organ.

Infection of RAG-hu mice with HHV-6A

Initial attempts at HHV-6A infection used cell-associated virus because HHV-6 is known to be a highly cell-associated virus (206) plus a recent study using the related hCMV in humanized mice was unable to achieve infection with cell-free virus but was successful using infected fibroblasts as carrier cells (204). We also attempted cell-free virus transmission with a high titer stock of HHV-6A to determine if this mechanism would also be viable for inoculation of humanized mice. Detection of cell-free transmission is greater evidence for the permissiveness of *in vivo* infection because in cell-associated transmission the input virus may subsequently be detected whether transmission to the graft takes place or not.

In the cell-associated transmission study mice were divided into 5 groups: 1) non-humanized $Rag2^{-/-}\gamma c^{-/-}$ mice, never irradiated, inoculated with infected cells, 2) 0% engrafted $Rag2^{-/-}\gamma c^{-/-}$ mice, irradiated, inoculated with infected cells, 3) >30% engrafted $Rag2^{-/-}\gamma c^{-/-}$ mice, inoculated with infected cells, 4) >30% engrafted $Rag2^{-/-}\gamma c^{-/-}$ mice, inoculated with uninfected cells, and 5) engrafted $Rag2^{-/-}\gamma c^{-/-}$ mice, not inoculated, uninfected (Table 1). Animals with >30% peripheral blood engraftment (defined as ($hCD45^+$ cells)/($hCD45^+$ cells + $mCD45^+$ cells)) were used in order to ensure that the human immune system is sufficient to support viral infection. Group 1 served as a control for determining if HHV-6A could infect and/or persist in non-humanized immunocompromised mice. Group 2 served as a control for determining if HHV-6A could infect mice that had been sub-lethally irradiated (thus becoming further immunocompromised) and reconstituted but had undetectable engraftment. Group 3 is the experimental group to determine if HHV-6A could infect engrafted RAG-hu mice. Groups 4 and 5 served as uninfected controls. Cells used for viral transmission were not donor matched with cell samples used to engraft, similar to a previous report where successful hCMV transmission

was accomplished with allogeneic human fibroblasts in a related humanized mouse model (204). In the cell-free transmission study mice were divided into 2 groups: 1) non-humanized, never irradiated, inoculated with cell-free virus and 2) >30% engrafted, inoculated with cell-free virus. Mice in the >30% groups in both studies ranged from 30-75% engraftment (see Table 1).

All RAG-hu mice were tested for the presence of HHV-6A DNA by Q-PCR prior to experimental infection. This verification was necessary because a low percentage of human cord blood samples (which are used to initially engraft the humanized mice) are contaminated with HHV-6A (207). All mice tested negative for HHV-6A DNA in whole blood samples analyzed prior to cell-associated HHV-6A inoculation as did PHA+IL-2 stimulated cord blood cells prior to HHV-6A infection (used as carrier cells for transmission).

Table 1. Characteristics of humanized mice used for HHV-6A infections

Mouse #	Injected w/HHV-6A	Age (months)	Engraftment	Irradiated	Sacrificed (weeks)
33	+, CA	2	0%	-	9.5
34	+, CA	2	0%	-	6.5
35	+, CA	2	0%	-	9.5
36	+, CA	2	0%	-	9.5
685	+, CA	3	0%	+	9.5
686	+, CA	3	0%	+	9.5
687	+, CA	3	0%	+	9.5
688	+, CA	3	0%	+	6.5
708	+, CA	5	29%	+	8
3089	+, CA	4	58%	+	8
3090	+, CA	4	56%	+	8
3092	+, CA	4	71%	+	6.5
3099	+, CA	5	36%	+	8
3100	+, CA	5	49%	+	8
698	-, M	3	41%	+	8
3095	-, M	4	42%	+	6.5
3096	-, M	4	32%	+	8
3098	-, M	4	39%	+	8
759	-,U	6	18%	+	NA
767	-,U	6	43%	+	NA
769	-,U	6	68%	+	NA
37	+, CF	2	0%	-	1
38	+, CF	2	0%	-	1
39	+, CF	2	0%	-	1
40	+, CF	2	0%	-	1
711	+, CF	7	38%	+	1
715	+, CF	7	75%	+	1
755	+, CF	4	46%	+	1
756	+, CF	4	36%	+	1
778	+, CF	5	48%	+	1
781	+, CF	5	35%	+	1

Key: CA=cell-associated virus, M=mock-infected cells, U=uninfected, CF=cell-free virus, NA=not applicable

Generation of infected cells for use in cell-associated transmission study

PHA and IL-2 stimulated CD34 depleted cord blood mononuclear cells were infected with HHV-6A or uninfected for 2 hours as described previously in Methods. Cells were cultured for 48 hours p.i. (with green cells present upon visual inspection by fluorescence microscopy at 20 hours p.i. in infected sample; data not shown). We observed an increase in cell size in the infected group as compared to the uninfected group, which is a common cytopathic effect of HHV-6A (data not shown). We also observed a $CD3^{low}CD4^{+}$ subgroup in the infected sample (Fig 2D) that was not present in the uninfected sample (Fig 2C), and downregulation of CD3 is also common upon HHV-6A infection of T cells (208). Approximately 20% of lymphocytes were GFP^{+} in the infected sample (Fig 2B) immediately prior to injection into RAG-hu mice with a low background of GFP expression in the uninfected sample (Fig 2 A).

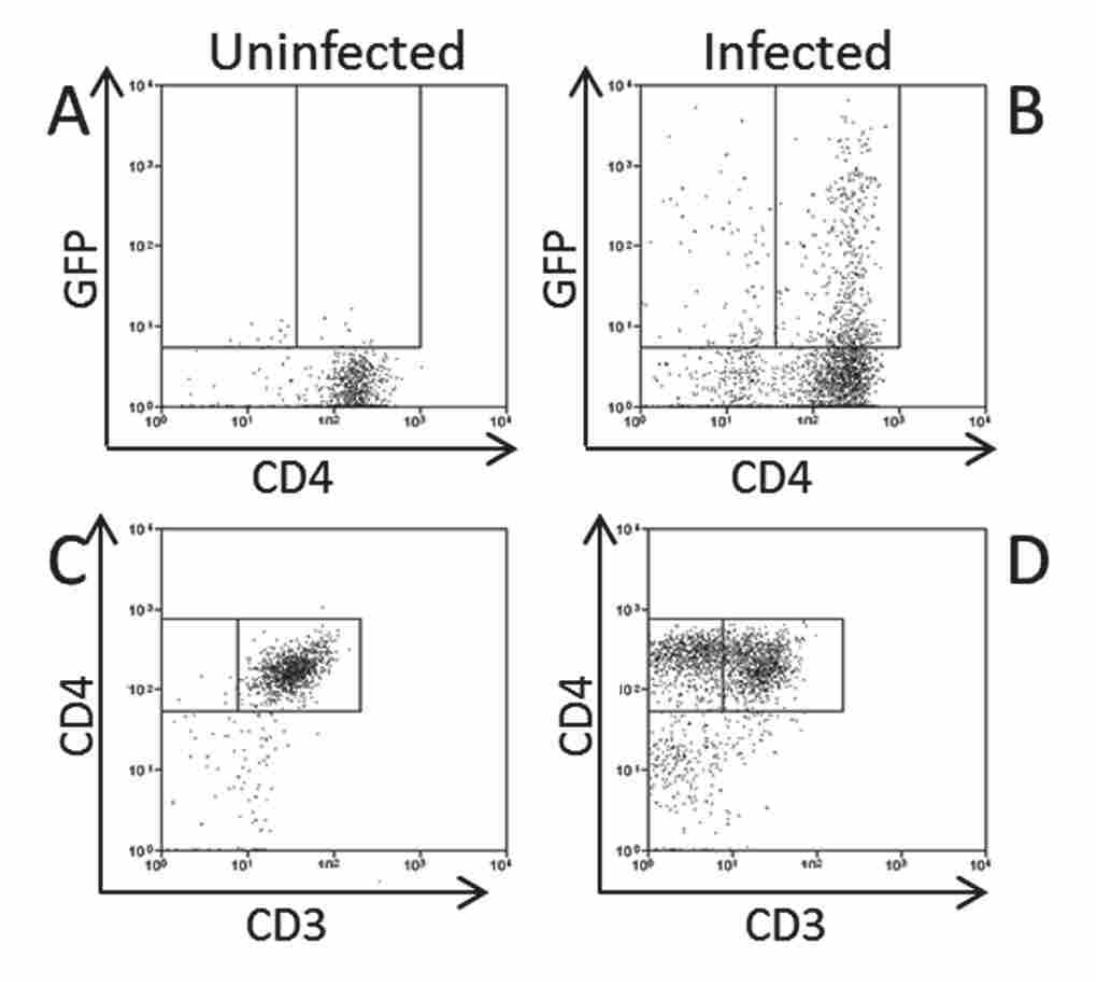

Figure 2. HHV-6A infected carrier cells used in cell-associated transmission to humanized mice (A-D) Flow cytometry of (A,C) uninfected and (B,D) HHV-6A infected cells prior to injection into RAG-hu mice. (A,B) Detection of GFP expression. (C,D) Analysis of CD3 and CD4 expression.

HHV-6A DNA detection in blood and lymphoid organs

All animals were bled regularly and DNA was extracted for Q-PCR analysis of the viral genome from different blood fractions (plasma, blood cell, or whole blood, as indicated in tables 2 and 3). In addition, animals were sacrificed at various time points (see Table 1) in order to examine various organs for viral genome detection and/or to analyze cellular populations for GFP expression and for depletion or enrichment of specific T cell populations. Viral DNA was detected by Q-PCR in nearly all animals at at least one time point in the >30% engrafted, HHV-6A inoculated groups (both cell-free transmission and cell-associated transmission see tables 2, 3 and 4).

In the cell-free transmission study viral DNA was detected in the bone marrow of all 6 >30% engrafted, HHV-6A inoculated mice while no viral DNA was detectable in the non-humanized mice (n=4; see Table 2). 2 of the >30% engrafted, HHV-6A inoculated mice had detectable viral DNA present in the blood whereas no viral DNA was detected in the blood of infected, unengrafted mice. No viral DNA was detected in thymic (n=3) or splenic tissues (n=6) analyzed from cell-free infected RAG-hu mice. All samples analyzed in the cell-free transmission study were done at the time of sacrifice (1 week post infection).

Table 2. Detection of viral DNA in blood and lymphoid organs one week post cell-free infection

Mouse #	Mouse group	Blood(PF,BC)	BM	Thy	Spl
37-40	NH, I	-	-	NT	-
711	H, I	BC=14,000	110,000	-	-
715	H, I	PF=13,000	3,600	NT	-
755	H, I	-	42,000	-	-
756	H, I	-	6,200	-	-
778	H, I	-	1,400	NT	-
781	H, I	-	650	NT	-

Key: NH=non-humanized, H=humanized, I=infected, PF=plasma fraction, BC=blood cell fraction, BM=bone marrow, Thy=thymus, Spl=spleen, (-)=below limit of detection, NT=not tested. Plasma and blood cell fractions reported in DNA copies/ml; BM reported in DNA copies per femur; Thy reported in DNA copies per half thymus; Spl reported in DNA copies per one third spleen. For blood, fractions analyzed are indicated in column headings.

Table 3. Detection of viral DNA in blood after cell-associated infection

Mouse #	Mouse group	1 week(PF)	2 weeks(WB)	3 weeks(PF)	4 weeks(PF;BC)	5 weeks(PF)	6 weeks(PF;BC)
33-36	NH, I	-	-	-	-	-	-
685-688	NH, I	-	-	-	-	-	-
698, 3095, 3096, 3098	H, M	-	-	-	-	-	-
708	H, I	-	-	-	-	-	-
3089	H, I	3,200	5,200	68,000	-	-	1,900; -
3090	H, I	-	-	-	-	-	-; 46,000
3092	H, I	-	-	33,000	130,000; 290,000	2,100	-; 77,000
3099	H, I	-	-	-	15,000; -	1,200	-
3100	H, I	-	-	-	-; 36,000	1,200	-; 9,700

Key: NH=non-humanized, H=humanized, I=infected, M=mock-infected, PF=plasma fraction, BC=blood cell fraction, WB=whole blood, (-)=below limit of detection. Plasma and blood cell fractions reported in DNA copies/ml. Not all samples were analyzed by Q-PCR each week. Blood fractions analyzed are indicated in column headings.

Table 4. Detection of viral DNA in lymphoid organs from mice sacrificed 6 ½ to 9 ½ weeks post cell-associated infection

Mouse #	Mouse group	Bone Marrow	Thymus	Lymph Node	Spleen
33-36	NH, I	-	NT	NT	-
685-688	NH, I	-	NT	NT	-
698	H, M	-	NT	NT	-
3095	H, M	-	-	-	-
3096	H, M	-	NT	NT	-
3098	H, M	-	NT	NT	-
708	H, I	-	NT	NT	-
3089	H, I	9,200	NT	NT	-
3090	H, I	-	NT	NT	-
3092	H, I	-	8,100	2,800	-
3099	H, I	-	NT	NT	-
3100	H, I	2,700	NT	NT	-

Key: NH=non-humanized, H=humanized, I=infected, M=mock-infected, (-)=below limit of detection, NT=not tested. Bone marrow reported in DNA copies per femur; Thymus reported in DNA copies per half thymus; Lymph node reported in DNA copies per node; Spleen reported in DNA copies per one third spleen.

In the cell-associated transmission study, HHV-6A DNA was detected by Q-PCR in plasma and cellular fractions of blood (Table 3), in the bone marrow, lymph node, and thymus but not in spleen (Table 4). Viral DNA was detected in mice in the >30% engrafted, HHV-6A inoculated group in the plasma fraction in 4 of 6 mice, in the blood cell fraction in 3 of 6 mice tested, and in 1 of 6 whole blood samples tested. In addition, 2 of 6 mice in this group had detectable viral DNA in the bone marrow and in the lone mouse thymic and lymph node samples tested from this group (see Table 4). We noted that viral DNA was detected mostly in the plasma from weeks 1-5 and that plasma viral load decreases in copy number after week 4 and in frequency of detection after week 5. 4 of 18 samples collected from engrafted humanized infected mice during the first three weeks of the cell-associated infection experiment were positive for viral DNA, while 15 of 38 samples tested from week 4 onward were positive and had generally higher levels of viral DNA. In total, 5 of 6 mice in the >30% engrafted, HHV-6A inoculated group had viral DNA present in blood or organs. Mouse 708 had undetectable viral DNA in blood or lymphoid organs, but this animal was inadvertently inoculated with about half of the volume of infected carrier cells into the subcutaneous space and the other half into the intended intraperitoneal cavity. No viral DNA was detected in any of the three control groups in the cell-associated transmission study.

Detection of HHV-6A-infected cells *in vivo* via GFP expression

We attempted to detect GFP^+ cells as an additional way to verify successful infection in both the cell-associated and cell-free infection studies. However, no GFP^+ cells were detected in the cell-associated study in blood samples collected weeks 1 and 3 post-infection and analyzed by flow cytometry. Additionally, no GFP^+ cells were detected when lymphoid organs were collected at the time of sacrifice. A single mesenteric lymph node sample (mouse 715) from the

cell-free transmission study was found to harbor GFP^+ cells when animals were sacrificed and analyzed at 1 week post-infection (data not shown). 0.04% of $CD4^+$ cells in the lymph node were GFP^+, while 0.28% of $CD8^+$ cells were GFP^+. Of the $CD4^+GFP^+$ cells, most were $CD3^-$ (95%). Of the GFP^+ cells detected in this sample, 4% were $CD3^+$, 55% were $CD4^+$, and 7% were $CD8^+$.

Thymocyte populations are significantly changed in HHV-6A infected RAG-hu mice

Previous work in humanized mice (SCID-hu *thy/liv* model) infected with HHV-6A or HHV-6B indicated that these viruses are capable of modifying thymic populations after direct viral inoculation into the thymic graft (195). We thus analyzed thymic populations taken from RAG-hu mice infected by either cell-associated or cell-free transmission. Animals infected by cell-free transmission had undetectable levels of viral DNA in the thymus at 1 week post-infection (3 of 3 tested; see Table 2), and their thymocyte populations were similar to uninfected animals (data not shown). Thus, we focused our thymocyte analysis on animals infected by the cell-associated transmission route, noting that these animals were also infected for a longer duration. RAG-hu mice infected by cell-associated transmission did exhibit significant shifts in thymic populations (Fig 3). We noted a significant decrease (P=0.05) in CD3 expression on $CD4^+$ thymocytes with a mean of 3.9% and 17.9% of thymocytes that were $CD3^+CD4^-$ in infected (n=4) and uninfected (n=6) groups, respectively. This is similar to a previous report indicating that HHV-6 can downregulate CD3 expression (209). We also detected a significant loss (P=0.04) of intrathymic T progenitor cells ($CD3^-CD4^+CD8^-$), with a mean of 2.5% in infected mice (n=3) and 11.3% in uninfected mice (n=5) when gating on the $CD4^+$ population. When analyzing this same population on a $CD3^-$ gate, we again found a significant depletion (P=0.03) with a mean of 2.7% in infected mice (n=3) and 32.2% in uninfected mice (n=5). We also detected a significant (P=0.02) increase in the number of $CD3^+CD4^+CD8^+$ thymocytes with

a mean of 36.6% in infected mice (n=3) and 12.8% in uninfected mice (n=5). The $CD3^-CD4^+CD8^+$ population appeared to increase in infected animals but the difference was not significant (P=0.08) and the $CD3^+CD4^+CD8^-$ population appeared to decrease in infected animals but the difference was not significant (P=0.25).

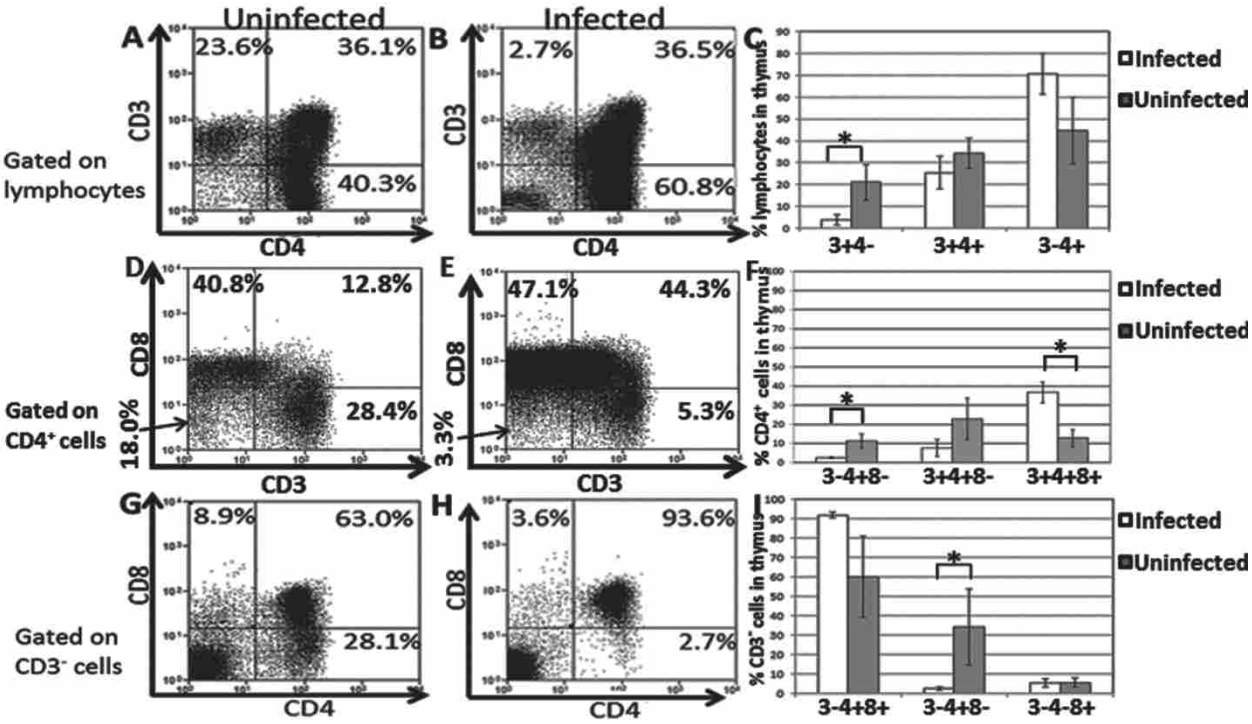

Figure 3. Depletion of specific thymocyte populations in HHV-6A-infected mice RAG-hu mice infected with HHV-6A by cell-associated viral transmission showed modulation of specific thymocyte populations. (A-C) The $CD3^+CD4^-$ population was depleted, while the $CD3^-CD4^+$ was increased in infected animals. Mouse 3095 (uninfected) is shown in A and mouse 3099 (infected) is shown in B. Samples were gated on a lymphocyte gate. N=4 infected N=6 uninfected. (D-F) The $CD3^-CD4^+CD8^-$ and $CD3^+CD4^+CD8^-$ populations were depleted and the $CD3^+CD4^+CD8^+$ population increased when analysis was gated upon $CD4^+$ cells. Mouse 3098 (uninfected) is shown in D and mouse 3099 (infected) is shown in E. N=3 infected N=5 uninfected. (G-I) The $CD3^-CD4^+CD8^+$ population expanded and the $CD3^-CD4^+CD8^-$ population was reduced when analysis was gated on the $CD3^-$ population. Mouse 3098 (uninfected) is shown in G and mouse 3089 (infected) is shown in H. N=3 infected N=5 uninfected. When performing data analysis, the two single positive and the double positive cell populations were normalized to 100%. Mouse 708 was excluded from these analyses because no viral DNA was detected in that mouse at any time point and we concluded that the mouse likely was not successfully infected. Standard error indicated; student's t test used for statistical analysis. *, $p \leq 0.05$.

Detection of $CD4^+CD8^+$ T cells in HHV-6A-infected RAG-hu blood

Previous studies have indicated that HHV-6A infection can induce CD4 expression on primary human CD8 T cells *in vitro* (210). Thus, we analyzed samples by FACS for the presence of $CD4^+CD8^+$ T cells. We detected significantly increased ratios (P=0.04) of $CD3^+CD4^+CD8^+$ cells in the blood of cell-free virus infected RAG-hu mice (Fig. 4). This population represented a mean of 8.8% of $CD3^+$ T cells, while in uninfected humanized mice these cells were 3.1% of all T cells. $CD4^+CD8^+$ cells are normally rare in human blood, with one report showing an average of 2.91% of $CD4^+CD8^+$ cells in normal human blood (n=10) (211) which is similar to our results in uninfected humanized mouse blood. Other blood T cell populations were not significantly altered in infected samples, including an analysis of $CD3^+CD4^-CD8^+$, $CD3^+CD4^+CD8^-$, $CD3^-CD4^+CD8^+$, $CD3^-CD4^+CD8^-$ and $CD3^-CD4^-CD8^+$ populations.

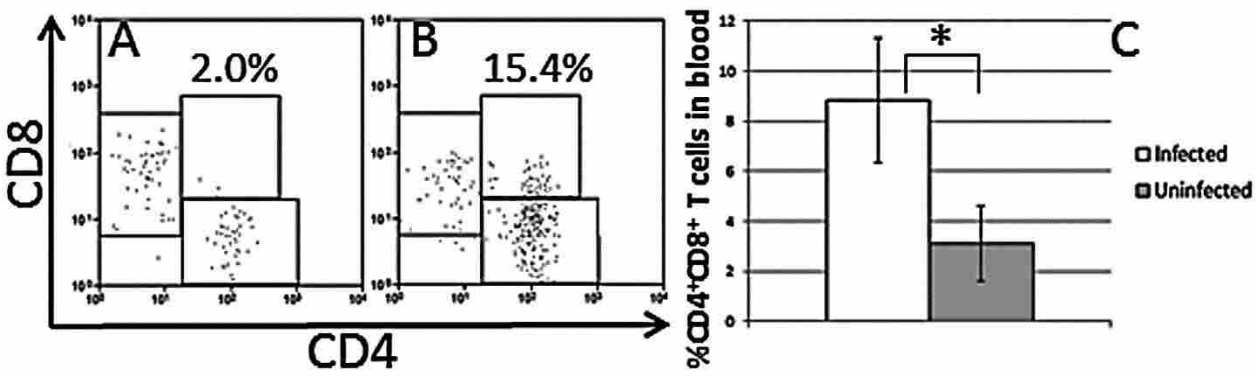

Figure 4. Detection of $CD4^+CD8^+$ T cells in blood of HHV-6A infected mice (A-C) Levels of $CD4^+CD8^+$ T cells in blood were quantified by flow cytometry. (A) Uninfected mouse, (B) HHV-6A infected mouse 715 (cell-free transmission, and highest amount of $CD4^+CD8^+$ cells). All samples were first gated on CD3. (C) Mean levels of $CD4^+CD8^+$ cells were quantified in cell-free infected mice (n=6), uninfected mice (n=4). Standard error indicated; student's t-test used for statistical analysis. * $p \leq 0.05$.

Discussion

Here we have shown that RAG-hu mice are susceptible to infection with HHV-6A by either cell-associated or cell-free transmission. Viral DNA was detected in blood (cellular and plasma fractions), bone marrow, lymph node, and thymic tissues (Tables 2, 3, and 4) although no single mouse tested positive for viral DNA in all of these compartments, as mentioned previously. Following cell-associated transmission, viral DNA was detectable for up to 8 weeks post-infection indicating a persistent infection. No viral DNA was detected in any of the three control groups in the cell-associated study, indicating that viral transmission from the infected carrier cells to the originally engrafted cells and subsequent replication was successful because no viral DNA was detectable in either blood or lymphoid organs in control mice without an HSC graft. Irradiated but non-engrafted animals were included as a control for the higher murine immunodeficiency of irradiated mice and they also had undetectable viral DNA after transmission. Some animals in the cell-associated transmission study had viral DNA detected at early time points and not later, and some animals had no detectable DNA at early time points but it was detected later. We attribute this to a relatively high limit of detection in the assay because only small blood samples can be obtained from mice. We noted that plasma viral DNA levels peaked at 3-4 weeks post-infection, but levels decreased to near the level of detection in plasma by 5 weeks and only a single animal had detectable viral DNA in the plasma at 6 weeks. Viral DNA was still detected in the cellular fraction of blood at 6 weeks in three animals while plasma viral DNA was found in a single mouse at that time point, potentially indicating a shift from lytic infection (extracellular DNA) to latency (intracellular DNA).

Cell-associated transmission was attempted because a similar previous experiment with hCMV was only successful with this method (204). However, cell-free transmission was

successful in all 6 animals in our study. We also noted a greater tendency to detect viral DNA in the bone marrow of animals infected by cell-free transmission, but it is not clear if that finding is due to a different mode of transmission or to different time points (1w for cell-free and 6.5-9.5w for cell-associated). We also detected a significant increase in $CD4^+CD8^+$ cells in the blood of cell-free virus infected mice (Fig. 4). This was possibly due to CD4 upregulation in CD8 T cells, which was previously shown *in vitro* in HHV-6A infected cells (210). When we correlated Q-PCR results of blood cells and plasma to the detection of these $CD4^+CD8^+$ cells there was not a clear trend because one animal (715) had high proportions of these cells and detectable viral DNA in plasma, while other animals also had high proportions of the cells but undetectable viral DNA in either blood fraction. Another animal (711) had low proportions of the cells with only intracellular blood viral DNA. The frequent detection of this effect, combined with relatively rare detection of viral DNA in either blood fraction, indicates that these cells may be uninfected by HHV-6A. These cells largely maintained CD3 expression, which also indicates a lack of infection. It is possible that HHV-6A infection promotes the release of these cells from the thymus because $CD4^+CD8^+$ cells are rare outside of the thymus. However, we failed to detect viral DNA in the thymus in 3 animals tested and so the promotion of releasing cells from the thymus would likely be conducted from a distal site. Evidence exists that the presence of $CD4^+CD8^+$ cells in human blood is upregulated following viral infection, including after infection with persistent viruses such as the herpesvirus EBV (211).

We attempted to use GFP expression from a recombinant virus to further demonstrate successful infection. However, the only animal with detectable GFP^+ cells was mouse 715 from the cell-free transmission group, and those cells were from the mesenteric lymph node. FACS analysis of GFP^+ cells indicated that they were mostly $CD3^-CD4^+$, which is in accordance with

our *in vitro* results in Fig 2D and previously published data showing a tropism for $CD4^+$ T cells and a downregulation of CD3 after infection (209, 212). We later determined that the GFP cassette in this virus is driven by the CMV IE promoter (Y. Mori, personal communication). Since the cell-associated mice were sacrificed at 6.5 to 9.5 weeks p.i. it is possible that the virus was in a latent state at the time of organ collection; this hypothesis is supported by the shift from extracellular to intracellular DNA seen in blood. The activity of the CMV IE promoter in the context of a latent HHV-6A infection is currently unknown, and if that promoter is inactive during latency that may explain a lack of GFP^+ cells in any of the cell-associated infected mice. An interesting observation was made that several thymocyte populations were altered in HHV-6A infected animals versus uninfected animals (Fig. 3). These observations lend further support that successful viral transmission occurred, because similar findings have been reported *in vitro* and in another humanized mouse study. In those studies, CD3 depletion only occurred in infected (not in bystander) cells (195, 210, 212). Thymocyte depletion was only detected in animals infected by the cell-associated pathway, but these animals were also infected for a longer period. It is possible that virus had not trafficked to the thymus in cell-free infected mice, a finding supported by our Q-PCR data where 0 of 3 of these thymic samples harbored viral DNA (Table 2). We noted significant depletion in the $CD3^+CD4^-$ and $CD3^-CD4^+CD8^-$ populations in HHV-6A-infected animals. We also noted a significant increase in the $CD3^+CD4^+CD8^+$ subset, with a marginally significant increase in the $CD3^-CD4^+CD8^+$ population. The significant loss of $CD3^-CD4^+CD8^-$ thymocytes was similarly reported by Gobbi et al. when HHV-6A was directly inoculated into the thymic organoid of SCID-hu *thy/liv* mice (195). In contrast to that report, our results show a significant increase in the $CD3^+CD4^+CD8^+$ subset. These discrepancies may be explained by the use of different virus isolates, with strain GS used in that report and a

recombinant isolate based upon strain U1102 used here. In addition, we have used a newer generation of humanized mice with a wider scope of human cell types and a much broader distribution in the mouse, and we inoculated at a site distant from the thymus. Several of these thymocyte populations that were modified by infection *in vivo* can be explained by a tropism and cytopathogenicity of the virus for $CD4^+$ T cells. Additionally, the tendency of the virus to downregulate CD3 and/or to upregulate CD4 expression can also explain shifting populations (e.g., $CD3^+CD4^-$ and $CD3^+CD4^+CD8^-$ populations expected to decrease, and $CD3^-CD4^+CD8^+$ population expected to increase). The $CD3^+CD4^+CD8^-$ population was previously shown to be more infectable with HHV-6A as compared to other thymocyte populations (195). We have proposed that in the cell-associated study the virus was predominantly latent at the time points that the thymic samples were collected. We are not aware of any studies documenting CD3 downregulation or CD4 upregulation in latently infected primary cells, so it is currently not clear if lytic replication is required for these effects upon host cell gene expression.

We and others have previously shown that RAG-hu mice are also highly susceptible to HIV-1 infection (103, 107, 166, 180). Our current findings indicate higher proportions of $CD4^+$ cells in HHV-6A infected animals, similar to those shown by Lusso et al. *in vitro* where they showed that HHV-6A-infected $CD8^+$ T cells began to express CD4 and were able to replicate HIV-1 (210). If HHV-6A is able to convert $CD8^+$ T cells to become infectable by HIV-1 *in vivo*, then those cells may be depleted by HIV-1 and/or by HHV-6A. Downregulation of CD3, as our results herein have indicated, is expected to cause immunosuppression because CD3 serves as the signaling subunit of the T cell receptor. Hence, T cells could engage the T cell receptor but not be able to respond effectively. Either of these two effects would support the hypothesis that HHV-6A is a co-factor in AIDS progression (197, 198). Our future directions include plans to

perform coinfection studies of HHV-6A and HIV-1 in humanized mice in order to determine if there is a synergistic effect between the two viruses in the progression to AIDS as well as to determine if RAG-hu mice will sustain infection with HHV-6B.

Acknowledgments

We are grateful to Dr. Yasuko Mori (National Institute of Biomedical Innovation, Osaka, Japan) for giving permission to use a recombinant strain of HHV-6A produced in her laboratory. Balb/c-Rag2$^{-/-}$γc$^{-/-}$ mice were generously provided by Dr. Ramesh Akkina at Colorado State University. This work was funded by a Pilot Grant award from the HHV-6 Foundation to BB. This work was partially supported by National Institutes of Health Grant U54 AI057160 to the Midwest Regional Center of Excellence for Biodefense and Emerging Infectious Diseases Research (MRCE) to EM. AT was supported by the Brigham Young University Cancer Research Center and the HHV-6 Foundation.

B. Human B cell development in Rag-hu mice

Development of Human B Cells and Antibodies Following Human Hematopoietic Stem Cell Transplantation to Rag2$^{-/-}$γc$^{-/-}$ mice

Tanner, Anne, Hallam, Steven J., Nielsen, Stanton J., Cuadra, German I., and *Berges, Bradford K.

Abstract

Humanized mice represent a valuable model system to study the development and functionality of the human immune system. In the RAG-hu mouse model highly immunodeficient Rag2$^{-/-}$γc$^{-/-}$ mice are transplanted with human CD34^{+} hematopoietic stem cells, resulting in human hematopoiesis and a predominant production of B and T lymphocytes. Human adaptive immune responses have been detected towards a variety of antigens in humanized mice but both cellular and humoral immune responses tend to be weak and sporadically detected. The underlying mechanisms for inconsistent responses are poorly understood. Here, we analyzed the kinetics of human B cell development and antibody production in RAG-hu mice to better understand the lack of effective antibody responses. We found that T cell levels in blood did not significantly change from 8 to 28 weeks post-engraftment, while B cells reached a peak at 14 weeks. Concentrations of 3 antibody classes (IgM, IgG, IgA) were found to be at levels about 0.1% or less of normal human levels, but human antibodies were still detected up to 32 weeks after engraftment. Human IgM was detected in 92.5% of animals while IgG and IgA were detected in about half of animals. We performed flow cytometric analysis of human B cells in bone marrow, spleen, and blood to

examine the presence of precursor B cells, immature B cells, naïve B cells, and plasma B cells. We detected high levels of surface IgM^+ B cells (immature and naïve B cells) and low levels of plasma B cells in these organs, suggesting that B cells do not mature properly in this model. Low levels of human T cells in the spleen were observed, and we suggest that the lack of T cell help may explain poor B cell development and antibody responses. We conclude that human B cells that develop in humanized mice do not receive the signals necessary to undergo class-switching or to secrete antibody effectively, and we discuss strategies to potentially overcome these barriers.

Key words: Adaptive immunity, B cells, human antibodies, human immunity, humanized mice, RAG-hu mice

1. Introduction

Human immune system mice are a useful tool to study the development and functionality of the human immune system. The most common current human immune system mouse models use human hematopoietic stem cells (HSCs) isolated from either cord blood or fetal liver and are then transferred into highly immunodeficient mice such as the $Rag2^{-/-}\gamma c^{-/-}$ and NOD/SCID$\gamma c^{-/-}$ strains (213). These humanized mice produce a wide variety of human immune cell types, including B cells, T cells, monocytes/macrophage, and dendritic cells (69). Production of other immune components such as granulocytes, erythrocytes, and platelets is typically weak, and the B and T lymphocyte population represents an unusually large proportion of blood, bone marrow, and spleen cells due to poor granulocyte production.

Humanized mouse models have been very useful for studies of viral pathogens of human immune cells such as Human Immunodeficiency Virus type 1 (HIV-1) (166), herpesviruses (2),

Dengue virus (70), and other pathogens. Human antibody responses have been reported against a variety of pathogens in humanized mice, including HIV-1, Dengue virus, Epstein-Barr virus, Kaposi's Sarcoma-associated herpesvirus, Herpes simplex virus type 2, and other pathogens/antigens (70, 103, 122, 172, 203, 214). Neutralizing antibody responses that target similar viral proteins as seen in humans have been reported in the case of Dengue virus (70). Although the current humanized mouse models are capable of producing human humoral and cellular immune responses to these pathogens, in general the results have been inconsistent and when they are detected the immune responses are typically weak (91, 103, 104). The reasons for these findings are currently unclear, but previous studies have indicated that total human antibody concentrations are much lower in humanized mice than in humans and there may be a defect in class-switching, since IgM concentrations tend to be closer to human concentrations than for IgG (69, 89). One study attempted to immortalize human B cells after immunizing humanized mice and was only able to produce IgM monoclonal antibodies and not IgG producing cells, lending further support to the hypothesis that there is a lack of effective class-switching (215). Interestingly, this same paper showed through immunoscope analysis that a broad diversity of human antibody sequences are derived in humanized mice, indicating that derivation of diverse B cell receptors functions very similarly in humanized mice as compared to humans. If there is a defect in effective antibody class-switching in humanized mice the mechanisms are not understood.

Since immune responses are critical to controlling pathogens and for vaccine studies, a better understanding of the reasons for poor B cell responses in humanized mice would be useful to assist in developing better humanized mouse models that reproduce normal human antibody concentrations and more robust antigen-specific responses. Here, we describe the B cell

compartment of HSC-transplanted Rag2$^{-/-}\gamma c^{-/-}$ mice. We have examined blood, bone marrow, and spleen for the presence of human B cells and to analyze the kinetics of B cell engraftment. We have also measured total human antibody levels in serum across a time course in order to determine when B cell development is complete in humanized mice. We found that immature and naive cells are found at a high frequency in spleen and bone marrow and that CD138^{+} plasma B cells are found in low levels in these organs. Few T cells were detected in the spleen, which is an important site for B cell maturation. Our results suggest that early steps in B cell development function properly in humanized mice, but that mechanisms governing class-switching and activation of B cells to become plasma cells are not very effective. Methods used to enhance T cell development and maturation in humanized mice may help to solve these issues.

2. Materials and methods

2.1. Cells

Human cord blood samples were obtained from the University of Colorado Cord Blood Bank. The Brigham Young University Institutional Review Board does not require a protocol for human cord blood samples because they lack patient identifiers. Human hematopoietic stem cells were purified from human cord blood using the CD34 marker with the EasySep human cord blood CD34-positive selection kit (StemCell Technologies). Cells were cultured for 2 days in Iscove's modified Dulbecco's medium (IMDM; Invitrogen) supplemented with 10% fetal calf serum (FCS) and 10 ng/mL each of human interleukin-3 (IL-3), IL-6, and stem cell factor (SCF) (R&D Systems) (216).

2.2. Animals

BALB/c-Rag2$^{-/-}$γc$^{-/-}$ mice were humanized by engraftment with CD34^{+} human HSCs purified from human umbilical cord blood as described previously (216). Mice were maintained in a specific pathogen- free (SPF) room at the Brigham Young University Central Animal Care Facility. Drinking water is supplemented with Trimethoprim-Sulfa antibiotics to prevent bacterial infection. These studies have been reviewed and approved by the Institutional Animal Use and Care Committee (protocols 120101 and 150108). Briefly, 1- to 5-day-old mice were conditioned by gamma irradiation with 350 rads and then injected intrahepatically with 2 x 10^5 to 7 x 10^5 human CD34^{+} cells. Mice were screened for human cell engraftment at 8-10 weeks post-engraftment, at which time plasma was also collected for antibody concentration analysis. Animals were additionally bled at numerous other time points in order to measure human cell types in blood and to collect additional plasma.

2.3. FACS analysis

70 µL of whole blood was obtained through tail bleed and treated with a mouse red blood cell lysis buffer for 15 min. Following this treatment the cells were centrifuged at 3300 rpm for 3 min and the supernatant was discarded. The pellet was then resuspended in 100 µL FACS staining buffer. 3 µL blocking buffer was then added and allowed to incubate in the dark at 4°C for 15 min. This was followed by the addition of 3 µL of the desired fluorescent-linked antibodies and incubated in the dark at 4°C for a period of 30 min. To determine percent human peripheral blood engraftment, peripheral blood was stained with human CD45 PECy-7 and mouse CD45 PE antibodies and FACS analysis was performed (71). Antibodies used for B cell characterization were: hCD45 PECy-7, hCD19 APC eFluor 780 (eBioscience), hCD3 PE, hCD138 PECy5.5 (Invitrogen), hIgM FITC (BioLegend). Immediately following this 30 min step 900 µL of 1% paraformaldehyde in 1x PBS was added to fix samples. Samples were then centrifuged at 3300

rpm for 3 min and the supernatant was discarded. The pellet was then resuspended in 150 µL 1x PBS and submitted for FACS analysis. An Attune Acoustic Focusing Cytometer (Applied Biosystems) was used to run samples, and Attune software v2.1 was used to analyze the results. All antibodies used in these studies do not cross-react with murine antigens, as assessed by staining of unengrafted $Rag2^{-/-}\gamma c^{-/-}$ blood and lymphoid organs.

2.4. Antibody Concentrations

Mouse plasma samples were obtained by centrifuging whole blood at 3300 rpm for 3 min and then collecting the supernatant. ELISA tests were run using the Total Human IgM, Total Human IgG, and Total Human IgA kits (ALerCHEK) according to the manufacturer's instructions. Since human antibody concentrations are typically low in humanized mice, plasma was diluted 1:100 for IgM and IgG assays and 1:20 for IgA assays in order to obtain results in the linear range of the assay.

2.5. Statistics

Human T and B cell development in mouse peripheral blood was analyzed by Welch's ANOVA test (with Games-Howell *post hoc* test when applicable). To compare B cell levels in bone marrow, spleen, and blood, an ANOVA with Tukey-Kramer *post hoc* test was performed. For comparison of the different time points of plasma antibody concentrations an ANOVA with Tukey-Kramer post hoc test (where applicable) were performed. Standard Error (SE) was calculated and indicated in all bar graphs. R^2 values were calculated to determine if a correlation exists between total antibody concentrations and peripheral blood engraftment levels in the humanized mice.

3. Results and Discussion

3.1. Kinetics of human B and T lymphocyte development in peripheral blood of RAG-hu mice

In the RAG-hu model, purified human $CD34^+$ hematopoietic stem cells are transplanted into neonatal $Rag2^{-/-}\gamma c^{-/-}$ mice following sub-lethal irradiation (216). The kinetics of development of the human immune system following transplantation of human HSCs into mice is poorly understood. We hypothesized that one reason for weak adaptive immune responses in this model could be due to immaturity of the human immune system at the time of exposure to antigen. To examine the development of human lymphocytes, we used flow cytometry to monitor the relative frequency of human T cells ($CD3^+$) and B cells ($CD19^+$) in a time course in peripheral blood following human HSC engraftment (Fig. 5). Our findings confirmed previous reports that T and B lymphocytes are the major human cell types in humanized mouse peripheral blood, ranging from a combined sum of 54.6 ± 3.6% (SE) at 8 weeks post-engraftment (wpe) to 90.8 ± 1.2% at 14 wpe. We found that B cells outnumbered T cells at every time point except for 25-28 wpe, where levels were nearly identical. B cell levels ranged from 29.1 ± 5.0% to 76.7 ± 3.0% of human peripheral blood cells, while T cell levels ranged from 14.1 ± 2.6% to 28.3 ± 7.0%. The lowest levels of B cells were detected at 25-28 wpe, while a peak was detected at 14 wpe. The lowest levels of T cells were detected at 8 wpe and 14 wpe, although statistical analysis revealed that no significant differences in T cell populations were detected across the entire time course (Welch's ANOVA test, p=.45). At the 14 week time point there were significantly greater numbers of human B cells as compared to all other time points (Welch's ANOVA test, $p < 10^{-5}$ with *post hoc* Games-Howell test, $p < 0.01$). No significant differences were found between B cell levels at any other time points (*post hoc* Games-Howell test $p > 0.05$).

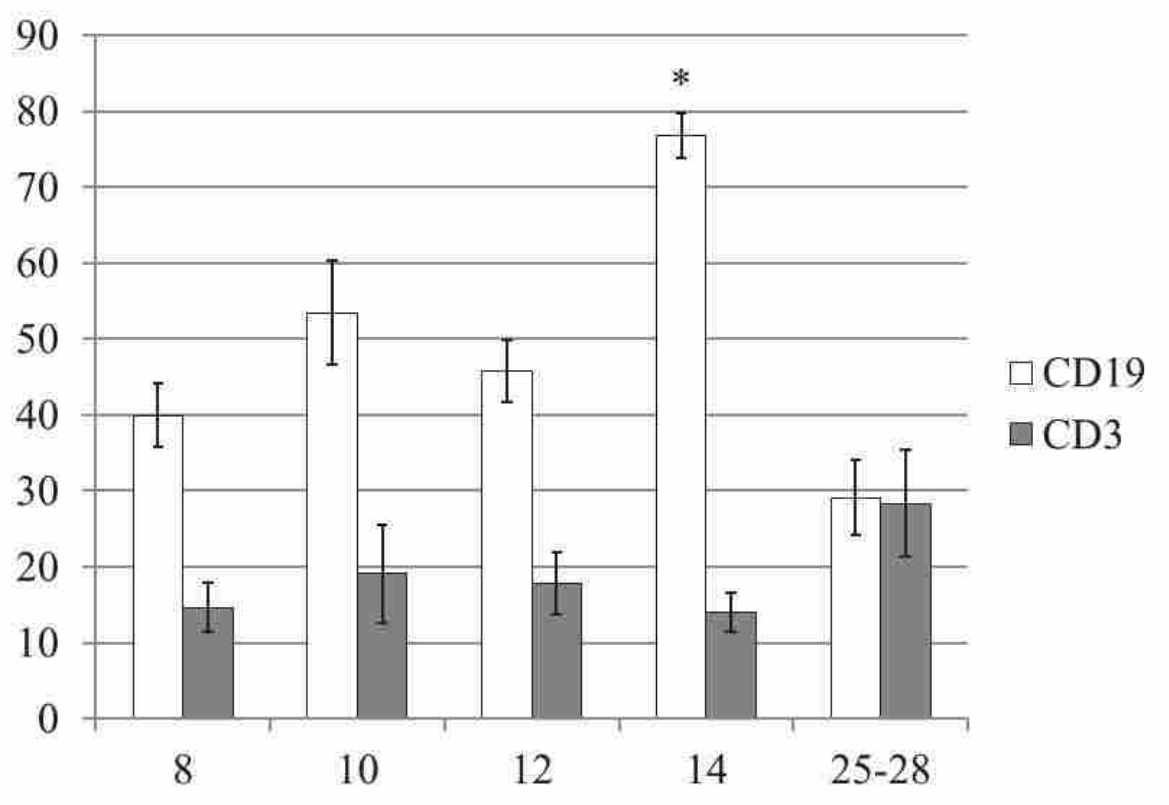

Figure 5. Peripheral blood engraftment of human B and T cells in humanized mice Flow cytometry was used to assess engraftment levels of human T cells ($CD3^+$) and human B cells ($CD19^+$) in peripheral blood. A human leukocyte antibody (anti-hCD45) was initially used for gating purposes to focus on human leukocyte populations. Mean levels in peripheral blood for each cell type were calculated and SE is indicated. (Welch's ANOVA test for B cell levels, $p<0.000001$ with *post hoc* Games-Howell, $p<.01$ for all comparisons with week 14 except week 10 where $p<.05$). No significant differences in T cell populations were detected across the entire time course (Welch's ANOVA test, $p=.45$). Sample sizes per time point are n=11 (8w), n=14 (10w), n=7 (12w), n=6 (14w), and n=9 (25-28w). Unique cord blood samples used for engrafting animals at each time point: n=3 (8w), n=5 (10w), n=1 (12w), n=2 (14w), n=4 (25-28w).

Since only a portion of humanized mice are good human antibody producers, we included data on peripheral blood T and B cell levels over time for individual animals (Table 5). Some animals followed the general trend seen in Fig. 5, while others did not. B cell levels in peripheral blood increased in all tested animals from week 8 to week 14, but then decreased in all tested animals from weeks 14 to 25. Interestingly, T cell levels in Fig. 5 showed insignificant changes over time, while individual mice show several different patterns. One animal steadily decreased from 8-25 weeks (mouse 2070), one animal showed a peak at 14 weeks (2071) and some animals increased across the time course (2072/2073). Mouse 2074 T cell levels increased from weeks 8 to 14, then appeared stable until week 25. These data suggest that T cell levels fluctuate more across a cohort of humanized mice whereas B cell levels follow a more similar pattern across groups of engrafted animals.

Harris et al. studied the duration of human immune system reconstitution in the NOD-Rag1-gammanull model engrafted with $CD34^+$ cells from cord blood (217). They examined human B and T cell fractions in humanized mouse peripheral blood and found that B cells were predominant at early time points but that an inversion took place at about 15-20 wpe and T cells become the predominant lymphocyte in blood. Here, we showed that T cell levels do not significantly change between 8-28 wpe but that B cells had reached a peak at 14 wpe. We suggest that model-specific differences may explain our different results.

Table 5. Peripheral blood levels of human T and B lymphocytes tracked in individual mice over time Human B and T lymphocyte populations were tracked in individual mice over a time course using flow cytometry analysis. Human leukocytes were gated based upon hCD45 expression, followed by analysis of $CD3^+$ cells (T cells) and $CD19^+$ cells (B cells).

	Gender	Cord sample	Cells transplanted
Mouse			
2070	F	A	$7.3x10^5$
2071	F	A	$7.3x10^5$
2072	F	B	$9.0x10^5$
2073	M	B	$9.0x10^5$
2074	M	B	$9.0x10^5$
2077	M	C	$2.8x10^5$
T fraction	Week 8	Week 14	Week 25
Mouse			
2070	19.7	14.1	1.4
2071	5.4	10	1.5
2072	9.5	n/t	36.5
2073	6.6	25.2	53.9
2074	3.3	11.7	10
2077	7.1	6.8	n/t
B fraction	Week 8	Week 14	Week 25
Mouse			
2070	43.4	78.7	46.9
2071	39.4	79.7	46.6
2072	28.6	n/t	2.7
2073	33.7	65.6	20.4
2074	53.7	83.1	28.1
2077	55.5	83.3	n/t

3.2. Proportions of human B cells in lymphoid organs and blood

Human B cell development in humanized mice has not been carefully studied and characterization of B cell development in primary and secondary lymphoid organs is also lacking. We sacrificed humanized mice and then used flow cytometry to detect different categories of B cells in bone marrow, spleen, and blood based upon phenotypic markers. We used CD19 as a marker for most human B cell populations, but also used CD138 as a marker for plasma B cells because CD19 expression is lost upon differentiation to this cell type. Some types of primitive B cells also express CD138, such as pro-B cells, pre-B cells, and immature B cells; however each of these populations also express CD19 which allows for differentiation from plasma B cells which are $CD19^{-}CD138^{+}$. We found that human B cells (sum of $CD19^{+}$ cells and $CD19^{-}IgM^{-}CD138^{+}$ cells) were the predominant human cell type (of the $hCD45^{+}$ population) in bone marrow (88.1 ± 4.3%; see Fig. 6), and to a lesser extent in spleen (60.1 ± 10.1%; see Fig. 7) and in blood (53.9 ± 5.3%; see Fig. 8).

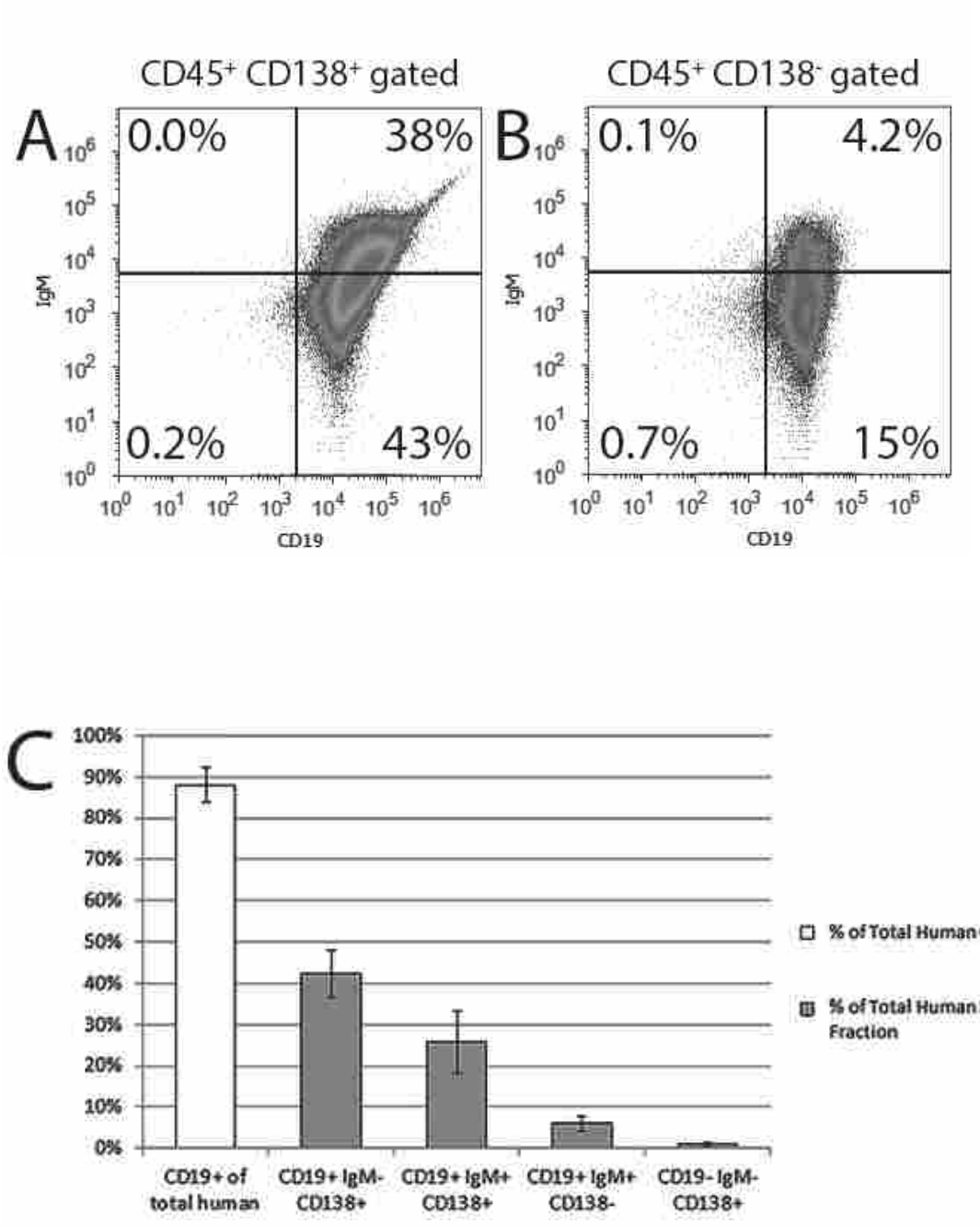

Figure 6. Human B cell populations in humanized mouse bone marrow Human B cells in bone marrow were immunophenotyped by flow cytometry. A human leukocyte antibody (anti-hCD45) was initially used for gating purposes to focus on human leukocyte populations. (A) FACS plot gated on $CD138^+$ cells to observe precursor B cell ($CD19^+IgM^-CD138^+$), immature B

cell ($CD19^+IgM^+CD138^+$), and plasma B cell ($CD19^-IgM^-CD138^+$) populations. Percentages are out of total human B cells. (B) FACS plot gated on $CD138^-$ cells to observe naïve B cell population ($CD19^+IgM^+CD138^-$). Percentages are out of total human B cells. (C) Graph comparing averages of the different bone marrow cell populations in all mice tested. SE is indicated. The precursor B cell population in bone marrow is significantly different from this same population in spleen and blood (compare Fig. 7 and Fig.8) (ANOVA p=.003 with *post hoc* Tukey-Kramer, $p < .05$). Sample sizes per population are n=7 ($CD19^+IgM^-CD138^+$), and n=4 for ($CD19^+IgM^+CD138^+$)($CD19^+IgM^-CD138^-$)($CD19^-IgM^-CD138^+$). Unique cord blood samples used for engrafting animals in each population: n=6 ($CD19^+IgM^-CD138^+$), n=4 for ($CD19^+IgM^+CD138^+$)($CD19^+IgM^-CD138^-$)($CD19^-IgM^-CD138^+$).

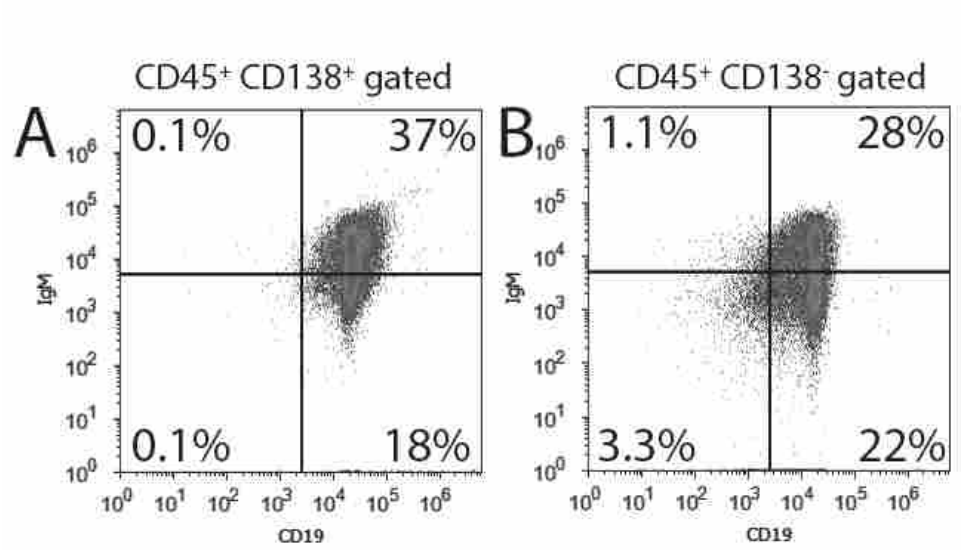

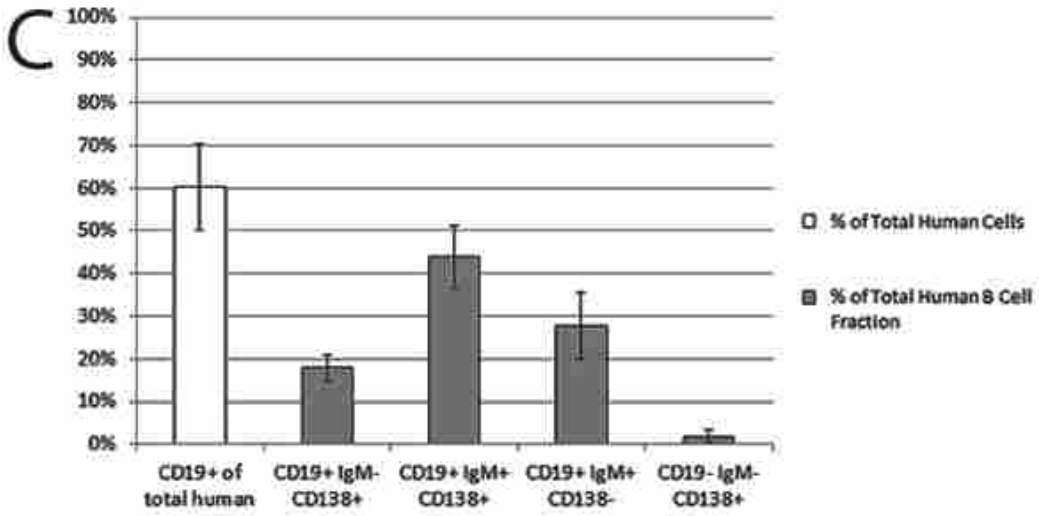

Figure 7. Human B cell populations in humanized mouse spleen Human B cells in spleen were immunophenotyped by flow cytometry. A human leukocyte antibody (anti-hCD45) was initially used for gating purposes to focus on human leukocyte populations. (A) FACS plot gated on $CD138^+$ cells to observe precursor B cell ($CD19^+IgM^-CD138^+$), immature B cell ($CD19^+IgM^+CD138^+$), and plasma B cell ($CD19^-IgM^-CD138^+$) populations. Percentages are out

of total human B cells. (B) FACS plot gated on $CD138^-$ cells to observe naïve B cell population ($CD19^+IgM^+CD138^-$). Percentages are out of total human B cells. (C) Graph comparing averages of the different splenic cell populations in all mice tested. SE is indicated. Sample sizes per population are n=7 ($CD19^+IgM^-CD138^+$), and n=4 for ($CD19^+IgM^+CD138^+$)($CD19^+IgM^-CD138^-$)($CD19^-IgM^-CD138^+$). Unique cord blood samples used for engrafting animals in each population: n=6 ($CD19^+IgM^-CD138^+$), n=4 for ($CD19^+IgM^+CD138^+$)($CD19^+IgM^-CD138^-$)($CD19^-IgM^-CD138^+$).

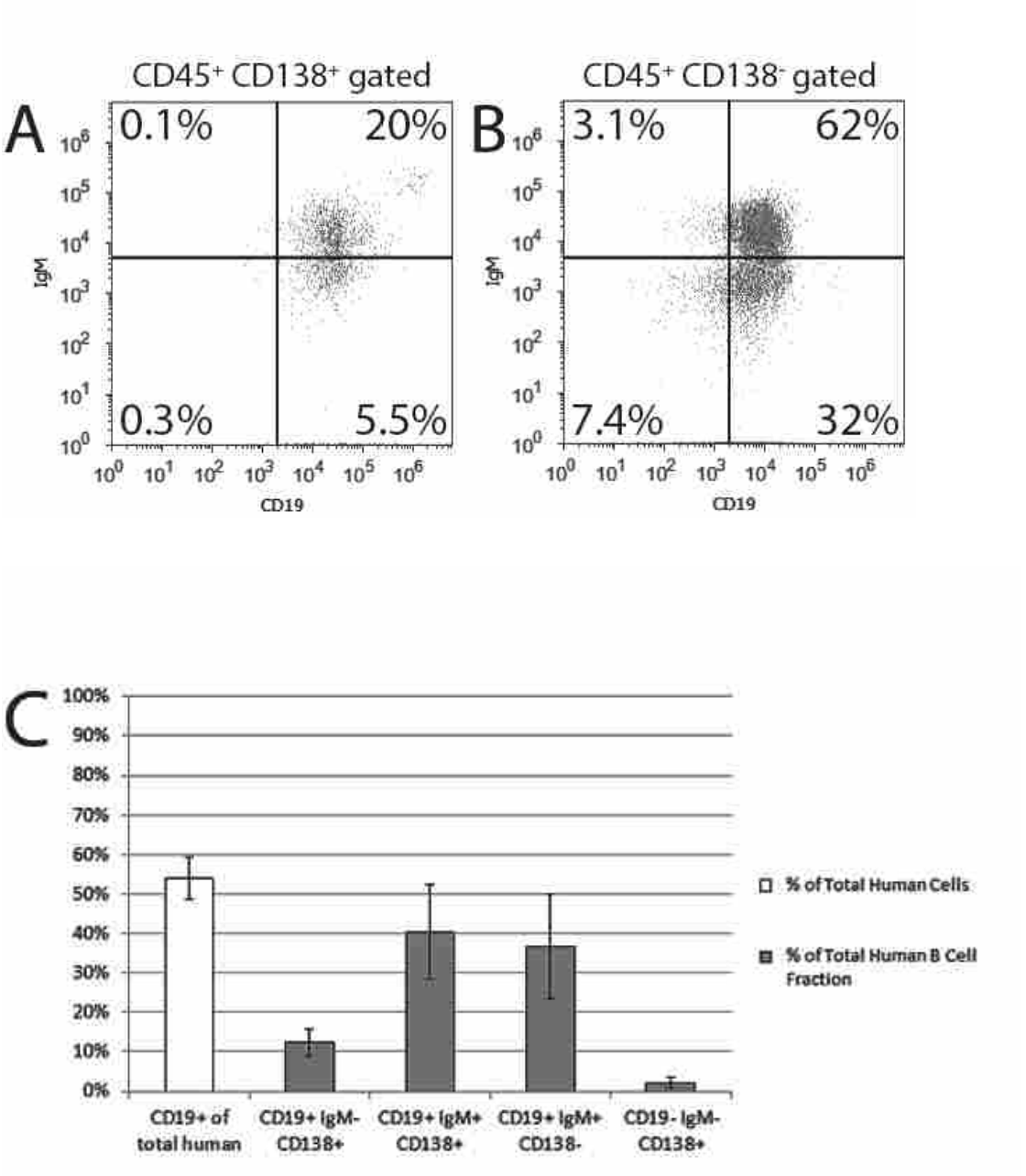

Figure 8. Human B cell populations in humanized mouse peripheral blood Human B cells in blood were immunophenotyped by flow cytometry. A human leukocyte antibody (anti-hCD45) was initially used for gating purposes to focus on human leukocyte populations. (A) FACS plot gated on $CD138^+$ cells to observe precursor B cell ($CD19^+IgM^-CD138^+$), immature B

cell ($CD19^+IgM^+CD138^+$), and plasma B cell ($CD19^-IgM^-CD138^+$) populations. Percentages are out of total human B cells. (B) FACS plot gated on $CD138^-$ cells to observe naïve B cell population ($CD19^+IgM^+CD138^-$). Percentages are out of total human B cells. (C) Graph comparing averages of the different cell populations from blood in all mice tested. SE is indicated. Sample sizes per population are n=6 ($CD19^+IgM^-CD138^+$), and n=3 for ($CD19^+IgM^+CD138^+$)($CD19^+IgM^-CD138^-$)($CD19^-IgM^-CD138^+$). Unique cord blood samples used for engrafting animals in each population: n=5 ($CD19^+IgM^-CD138^+$), n=3 for ($CD19^+IgM^+CD138^+$)($CD19^+IgM^-CD138^-$)($CD19^-IgM^-CD138^+$).

3.3. Characterization of B cell types in bone marrow

In the bone marrow, precursor B cells ($CD19^+IgM^-CD138^+$) and immature B cells ($CD19^+IgM^+CD138^+$) represented the most common human B cells detected, at 42.2 ± 5.7% and 25.8 ± 7.6%, respectively (see Fig. 6C). Naïve B cells ($CD19^+IgM^+CD138^-$) and plasma B cells ($CD19^-IgM^-CD138^+$) were found in lower proportions, at 6.1 ± 1.8% and 1.0 ± 0.5%, respectively. Example FACS plots of stained bone marrow are shown in Fig. 6A, B. Statistical analyses were performed to determine if there were any significant differences between various B cell populations in bone marrow, spleen, and blood. The only significant difference in populations was that the $CD19^+IgM^-CD138^+$ population was larger in bone marrow than in spleen or blood (ANOVA p=.003 with *post hoc* Tukey-Kramer, $p < .05$).

Maturation of B cells to become plasma cells is dependent upon T cell help; specifically, CD40L on T cells interacts with CD40 on B cells to promote antibody secretion (218). We detected only low numbers of human plasma B cells in the bone marrow of RAG-hu mice whereas in normal humans 4-5% of bone marrow cells are plasma cells (219, 220). One problem previously noted with most current humanized mice is that human T cells are largely selected based upon murine major histocompatibility complex (MHC) molecules in the thymus due to the lack of human stromal cells (221). If human helper T cells are positively selected on murine MHC-II in the thymus, then their ability to interact with B cells expressing human MHC-II in the periphery is not expected to be effective and this would prevent effective plasma cell differentiation. Interestingly, many $CD5^+$ B cells have been reported to exist in humanized mice (222, 223). These cells are less prone to undergo class-switching and are more prone to produce IgM antibodies independent of T cell help (224).

The lack of human MHC expression on thymic stromal cells likely has an impact on the ability to derive antigen-specific human T cell responses in humanized mice because humanized mouse T cells undergo selection on mostly murine MHC. Attempts to overcome this barrier to T cell development include the development of the bone marrow/liver/thymus (BLT) model which uses a human fetal thymic transplant to allow for selection on human MHC and various studies indicate that both cellular and humoral immune responses are more frequent and robust in the BLT model as compared to those that lack human thymic stromal cells (214, 221, 225) although careful studies to compare various humanized mouse models are still lacking. The BLT model is technically challenging because it requires human fetal tissues which can be challenging to obtain, and also requires survival surgery to implant the tissues. Another option is the use of human HLA-transgenic animals as another way to generate T cells that are selected on human MHC; this idea has been explored to some degree and appears to result in enhanced T cell responses (226, 227). No examination of human B cell responses in HLA-transgenic mice has been explored to our knowledge. Another hypothesis to explain the lack of human plasma B cells is that they are initially produced, but do not receive the survival signals necessary to persist longer than a few days after differentiation.

3.4. Characterization of B cell types in spleen

In the spleen, the predominant human B cell type was immature B cells (43.8 ± 7.5%), followed by naïve B cells at 27.7 ± 7.8% (see Fig. 3C). Precursor B cells were more rare in spleen (17.9 ± 3.1%) and plasma B cells were the least frequent (1.9 ± 1.6%). Example FACS plots of stained splenocytes are shown in Fig. 7A, B.

We also noted that human T cells are found in low numbers in the spleen of RAG-hu mice, whereas human B cells are found in much greater numbers. T cells represented an average

of 36.6 ± 8.8% of total human leukocytes in the spleen, with a low of 12% and a high of 62%. This finding is similar to that reported in NOD/SCID gammanull mice engrafted with HSCs from cord blood (101). Immature B cells are known to leave the bone marrow and to migrate to the spleen, where maturation to peripheral mature B cells and plasma cells occurs (218). Thus, the paucity of T cells in the spleen of humanized mice may also explain the lack of plasma cells. A study conducted by Lang et al. confirms the necessity of T cells for B cell maturation; in their report they introduced autologous T cells and found increased numbers of mature B cells. Conversely, when T cells were depleted, *in vivo* B cell maturation was delayed (228). In previous work with RAG-hu mice, we characterized levels of helper T cells ($CD3^+CD4^+$) and cytotoxic T cells ($CD3^+CD8^+$) in the blood of 28 humanized mice and found that the ratio of helper T cells to cytotoxic T cells is similar as compared to humans, with a mean ratio of 2.1:1 (±1.2 SD) for helper T cells compared to cytotoxic T cells (76). There was clearly variability present between various engrafted animals, with a high of 6.1:1 and a low of 1.0:1. Poor development of helper T cells may contribute to poor B cell development.

Germinal centers are important locations for antibody class-switching, and structures that histologically resemble germinal centers are found in RAG-hu spleen (69). To our knowledge, no studies have been carried out to analyze the functionality of these germinal centers in humanized mice. Follicular dendritic cells (FDCs) are critical components of germinal centers, but human FDCs are not detectable in humanized mice because these cells originate from a non-HSC source. Interestingly, cells bearing murine FDC markers are present in humanized mice germinal centers (69). The lack of human FDCs in humanized mice may block efficient class-switching, development of memory B cells, and somatic hypermutation (229).

3.5. Characterization of B cell types in blood

In the blood, the most common human B cell types were immature and naïve B cells, at 40.4 ± 11.9% and 36.7 ± 13.2%, respectively (see Fig. 8C). Precursor B cells were found in lower levels (12.3 ± 3.4%) and plasma cells were even lower (2.2 ± 1.3%). Example FACS plots of stained blood cells are shown in Fig. 8A, B. We noted that the particular animal chosen for Fig. 8B had an unusually high level of plasma B cells ($CD19^{-}IgM^{-}CD138^{+}$). There is high variability in the levels of engraftment as well as in antibody production in individual humanized mice.

3.6. Measurement of total human plasma antibody concentrations

To examine the functionality of the human B cells, we measured human antibody concentrations in humanized mouse plasma. Total human IgM, IgG, and IgA concentrations were measured by ELISA. Plasma samples from unengrafted mice did not have detectable human antibody levels for any antibody class (data not shown). Although all 3 antibody classes were detected in plasma, the frequency of detection differed amongst the classes. 49 of 53 samples tested positive for IgM (92.5%), while only 25 of 53 were positive for IgG (47.2%) and 28 of 53 were positive for IgA (52.8%) (Fig. 9A). The total average concentrations across all time points (only counting positive samples) were 2.1 μg/mL for IgM, 10 μg/mL for IgG, and 0.036 μg/mL for IgA (Fig. 9B). By way of comparison, the normal concentrations in human plasma are 1,500 μg/mL for IgM, 14,000 μg/mL for IgG, and 3,500 μg/mL for IgA. Thus, for all antibody classes we consistently measured approximately 0.1% or less of normal antibody concentrations in humanized mouse plasma as compared to normal humans. IgA concentrations were farthest from the normal human values (0.001% of normal), IgM levels were the closest (0.14%), and IgG levels were similar to IgM (0.07%).

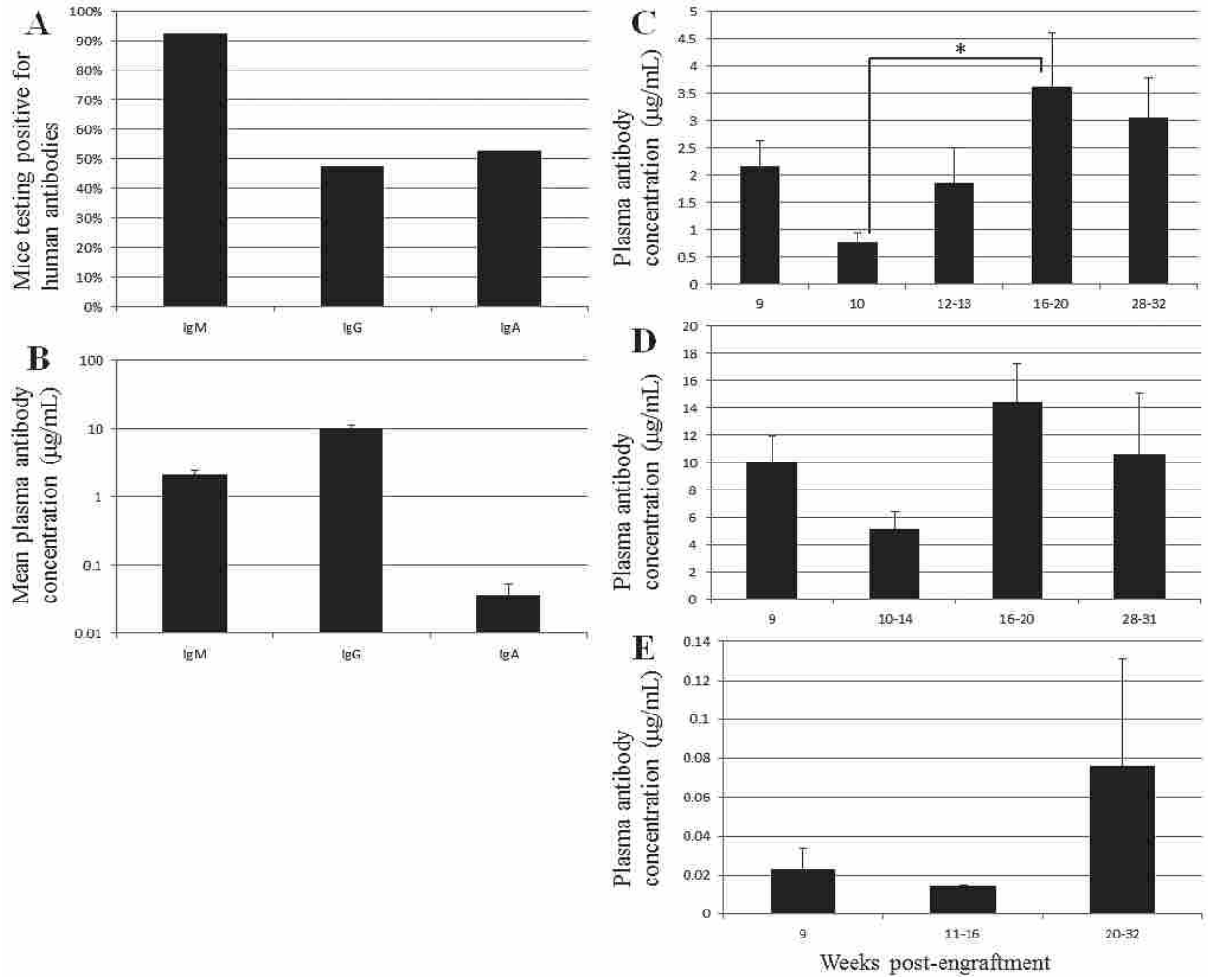

Figure 9. Total human antibody concentrations in humanized mouse plasma . ELISA was used to measure total human antibody concentrations in plasma. (A) Fraction of animals testing positive for IgM, IgG, or IgA (n=53 animals for each group). (B) Mean antibody concentrations for IgM, IgG, IgA; only including positive animals (n=49, 25, and 28, respectively). A time course of (C) IgM, (D) IgG, and (E) IgA in plasma after human cell engraftment. (* ANOVA p=.04 with *post hoc* Tukey-Kramer, $p < .05$). Sample sizes per time point are: C) n=10 (9w), n=6 (10w), n=3 (12-13w), n=4 (16-20w), and n=3 (28-32w); D) n=4 for all time points; and E) n=4 (9w), n=3 (11-16w), and n=3 (20-32w).

Traggiai et al. monitored human B and T cell development over time in RAG-hu mice (69). They showed that human antibody levels are immature at 8 wpe, with a rise in total IgM from 8 to 16 wpe and undetectable levels of IgG at 8 wpe with higher levels at 16 wpe. Our results somewhat agree in terms of the kinetics of the response, although we did detect IgG at 9 wpe in many animals. They showed total human antibody concentrations higher than what we have detected, but the defect in class-switching is similar. They reported a mean IgM concentration of about 15 μg/mL and a mean IgG of about 200 μg/mL (69) while Chen et al. reported mean IgM levels of 119 μg/mL and 1.1 μg/mL IgG in humanized NOD/SCID gammanull mice (230), while Wang et al. showed ~7 mg/mL IgM in humanized NOD/SCID mice with undetectable IgG (223). Our results show a mean IgM titer of 2 μg/mL and a mean IgG titer of 10 μg/mL. The use of different mouse strains and sources of HSCs may explain the differing results.

Wang et al. examined IgG responses and T cell development in NOD/SCID mice transplanted with $CD34^+$ cells from cord blood (223). They showed very little IgG responses, and also very few human T cells engrafted (appears to be much less than in RAG-hu mice). Since NOD/SCID mice are considered to have higher residual murine immunity than $Rag2^{-/-}\gamma c^{-/-}$ mice, the mouse strain might explain the differences in our results. B cells require T cell help for effective antibody responses, so we surmise that the increased numbers of human T cells might explain why the RAG-hu model has higher IgG production.

3.7. Kinetics of production of human antibody classes

In order to study the kinetics of human antibody development in humanized mice, we measured human antibody concentrations in plasma across a time course that lasted up to 32 wpe. All 3 antibody classes (IgM, IgG, IgA) were detectable in plasma by 9 wpe, and only minor

differences in antibody concentrations were noted at later time points. No significant differences in total antibody concentrations were detected across the time course for IgG (Welch's ANOVA test, p=0.11) (Fig. 9D) or IgA (Welch's ANOVA test, p=0.53) (Fig. 9E). A single significant difference was detected in IgM from 10 wpe to 16-20 wpe where an increase was detected (ANOVA p=.04 with *post hoc* Tukey-Kramer, $p < 0.05$) (Fig. 9C). However, this significant increase was not maintained to the 28-32 wpe time point. Our results show that human antibody production persists through at least 32 wpe, with no significant decreases at late time points.

3.8. No correlation exists between peripheral blood engraftment and plasma antibody concentration

Since only a fraction of humanized mice produce detectable antigen-specific responses to infection or immunization, it would be useful if a marker could be developed which would allow one to predict the likelihood of an animal producing a detectable response. However, such a marker has not yet been reported. We analyzed our data to see if a correlation exists between the percent peripheral blood engraftment (defined as $hCD45^+$ cells divided by the sum of ($hCD45^+$ plus $mCD45^+$ cells)) and the plasma concentrations of various human antibody classes. We failed to detect a correlation between animals with higher peripheral blood engraftment and those with higher levels of IgM, IgG, or IgA (Supplementary Fig. 1). These findings suggest that the level of chimerism in humanized mice is not the most critical aspect involved in antibody responses.

Improvements in human erythrocyte and platelet development have been made by eliminating murine macrophages which may engulf human immune system components (73, 231, 232). In contrast, little research has been conducted to specifically improve B cell development and functionality. One interesting study analyzed the defect in class-switching

from IgM to IgG responses in humanized mice. Chen et al. used NOD/SCID gammanull mice engrafted with either fetal liver or cord blood $CD34^+$ cells and found that better human antibody responses and enhanced class-switching were detected following administration of human Interleukin 4 (IL-4) and Granulocyte-Macrophage Colony-Stimulating Factor (GM-CSF) to humanized mice (230). IgM responses were 42% higher in cytokine-treated animals and IgG responses were over 10.5-fold higher using this protocol. In addition, tetanus toxin-specific IgG went from undetectable to detectable levels in many animals administered IL-4 and GM-CSF. Thus, the production of humanized mice in a background strain that produces human cytokines may also be beneficial to achieve normal human antibody responses.

Conclusions

We have shown that RAG-hu mice produce human B cells which are dispersed in blood, bone marrow, and spleen. B cell engraftment in peripheral blood reached a peak in relative numbers of cells at 14 wpe, while T cell levels were stable from 8-28 wpe. The vast majority of mice had detectable levels of human IgM in plasma, while only about half had detectable IgG or IgA. The mean antibody concentrations were considerably lower than those seen humans, and in general antibody concentrations did not significantly change over time from 9 to ~30 wpe. We detected relatively few $CD138^+$ plasma cells in the bone marrow, despite the fact that most plasma cells reside in this site in humans. Taken together, our results indicate that in the RAG-hu model there are defects in class-switching from IgM to IgG or IgA production, and that naïve B cells are not effectively matured to become plasma B cells. Further work can now be done to test the hypothesis that improvements in T cell levels may enhance the reproducibility of human antibody responses in humanized mice.

The following are supplementary data related to this article.

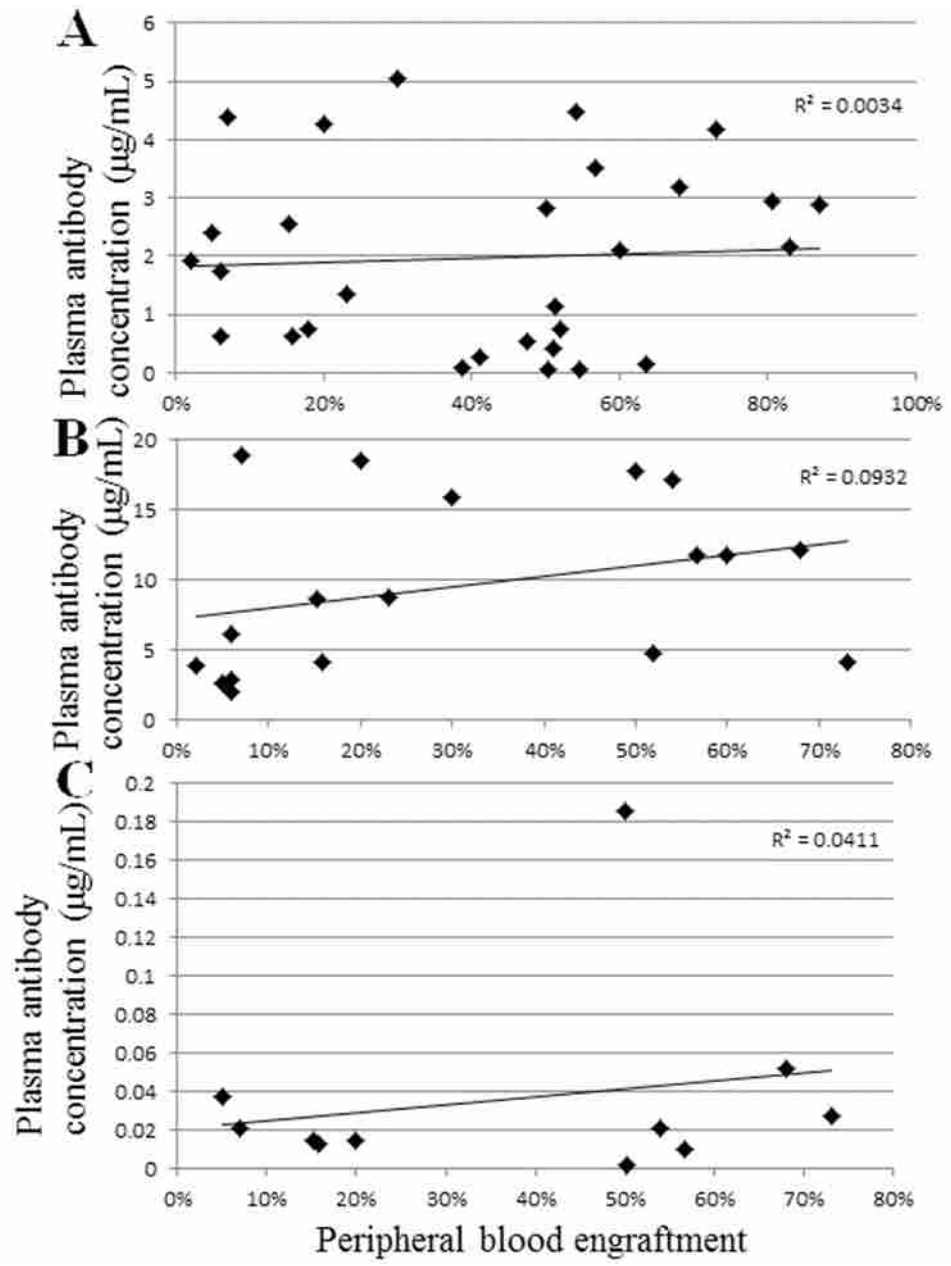

Supplementary Figure 1. Total human antibody concentration as a function of peripheral blood engraftment Total antibody concentrations were plotted relative to the peripheral blood engraftment levels to determine if there was a correlation between engraftment levels and concentrations of human antibodies. Various antibody classes were tested, including (A) IgM (n=29), (B) IgG (n=18), and (C) IgA (n=11). R^2 values were calculated and are indicated on each graph.

Acknowledgements

The authors declare no conflict of interests. We thank Stephen Taylor, Eakachai Prompetchara, Sterling Adams, Jacob Hatch, Greg Low, and Mary Ann Taylor for assistance in extracting cord blood samples, and for engrafting and screening humanized mice. This work was supported by a Brigham Young University Mentoring Environment Grant to BB. SH, GC, and SN were recipients of Office of Research and Creative Activities grant awards from Brigham Young University.

Abbreviations

FACS	Fluorescence activated cell sorting
Rag2	Recombinase activating gene 2
γc	Common gamma chain receptor
Wpe	Weeks post-engraftment
Ig	Immunoglobulin
NOD	Non-obese diabetic
SCID	Severe combined immunodeficiency
ELISA	Enzyme-linked immunosorbent assay
HSC	Hematopoietic stem cell
MHC	Major histocompability complex
BLT	Bone marrow/liver/thymus humanized mice
GM-CSF	Granulocyte macrophage colony stimulating factor

C. Coinfection with human herpesvirus 6A and HIV and immunopathogenesis in humanized Rag2$^{-/-}\gamma c^{-/-}$ mice and relevance to HIV/AIDS

1. Rationale for the study

The interactions between human immunodeficiency virus 1 (HIV-1) and human herpesvirus 6A (HHV-6A) have been examined previously and there is evidence suggesting that these viruses can have a synergistic effect on one another (57, 161) and may be working synergistically in the progression to Acquired immunodeficiency syndrome (AIDS). Our humanized mouse model for HHV-6A (233) has been used extensively to study HIV-1 infection and pathogenesis. This model, the Rag2$^{-/-}\gamma c^{-/-}$ or Rag-hu model, is an improvement to the SCID-hu thy/liv model used by Gobbi et al. in their HIV/HHV-6 coinfection study (55), as the Rag-hu model produces a variety of human blood cell types that are found in the organs and blood of the Rag-hu mice, rather than only having human thymocytes in the thymus/liver graft of the SCID-hu thy/liv mice. Also, human thymocytes do not express CCR5 and therefore any CCR5-tropic HIV cannot be studied in the SCID-hu thy/liv model. Both CCR5 and CXCR4 coreceptors are expressed in cells in the Rag-hu model, providing the target cells for HIV-1. These mice also express CD46, the receptor for HHV-6A, creating a new model to study the effects these viruses have on each other *in vivo*.

There are a number of evidences that suggest that HHV-6A and HIV-1 may be working synergistically. HHV-6A shares primary tropism for CD4$^+$ T cells along with HIV-1 and these cells can simultaneously be infected with both viruses (161). HHV-6A transactivates the genome of HIV which increases replication of HIV (161, 163, 164, 234, 235). HIV has also been shown to activate HHV-6A in a tat-dependent manner, increasing the titer of HHV-6A as well as the kinetics of the infection (236, 237). The reactivation of HHV-6A by HIV has been hypothesized

to cause a more rapid progression to AIDS than the patient would have with HIV infection alone because HHV-6A causes a downregulation of CD3 (238) (the depletion of which is the basis for AIDS), potentially compromising T cell function by inhibiting expression of the CD3/TCR complex. Infection with HHV-6A also causes an upregulation of CD4 (17) on $CD4^+$ T cells as well as cells that do not normally express CD4, including $CD8^+$ T cells, causing these previously unsusceptible cells to become susceptible to HIV-1(17).

Limited *in vivo* studies have been performed looking at the interactions between HIV-1 and HHV-6A due to the large expense and need for specialized facilities associated with non-human primate research. Lusso et al. performed an *in vivo* coinfection study using HHV-6A and simian immunodeficiency virus (SIV) in macaques, where the coinfected animals progressed to an AIDS-like state more rapidly than those infected with SIV only (57). As the majority of people (~90%) are infected with HHV-6, it is difficult to study this question in humans as an HIV+ HHV-6(-) individual is rare. This is one reason why we developed the Rag-hu mouse model for HHV-6A infection, so proper control groups could be in place to study the effects of coinfection with these viruses. Here we report on a coinfection study of HIV-1 and HHV-6A in Rag-hu mice.

2. Experimental design

In order to determine the effects of coinfection with HHV-6A and HIV-1 in Rag-hu mice, mice were challenged with recombinant HHV-6A expressing green fluorescent protein strain U1102, HIV-1 strain JRCSF (CCR5 tropic), or both viruses. Mice in the coinfected group were infected with HHV-6A and then 2 weeks later they were infected with HIV-1. HHV-6A only, HIV-1 only, and mock infected mouse groups were used as controls. The four groups in the coinfection study consisted of 25 mice total. Both male and female mice were used, with ages

ranging from 4 ½ to 7 ½ months old. Initially, $CD34^-$ cells extracted from human umbilical cord blood were infected with HHV-6A and injected into the HHV-6A only group as well as the coinfected group. The HIV-1 only and mock infected groups were mock infected with uninfected $CD34^-$ cells. Two weeks after infection with HHV-6A, the HIV-1 only and coinfected mouse groups were infected intraperitoneally with cell-free HIV-1 (strain JRCSF, which is CCR5 tropic). Mice were bled weekly and blood was analyzed by flow cytometry and Q-PCR. Mice were sacrificed at ~12 weeks p.i. with HHV-6A (~10 weeks p.i. with HIV-1). Blood, spleen, bone marrow, thymus, and lymph nodes were harvested at time of sacrifice.

Due to mechanical errors with the Q-PCR machine, proof of infection could not be verified and these results were therefore unable to be published. However, the observed pathogenesis in the animals indicates successful infection which is why these results are being reported here. The cells we used for the cell-associated infection with GFP tagged HHV-6A were green prior to infection just as they had been in our previous HHV-6A mouse study (233) so there is no reason to believe the infection would not have worked this time and we used cell-free HIV stock which has been used a number of times to infect Rag-hu mice with HIV previously (129, 130) so there is no reason to believe these infections did not work in this study. The different pathogenesis observed between the groups also indicates that these groups were in fact different.

Table 6. Characteristics of mice used in HIV-1/HHV-6A coinfection study

Cage #	Sex- Mouse #	D.O.B	Engrafted	# of Cells	Date Screened	% Engraftment
Coinfected						
220	F-898	9/30/2013	10/4/2013	2.5-3 x 10^5	12/5/2013	73%
222	F-2001	10/17/2013	10/18/2013	3.6 x 10^5	12/12/2013	69%
216	F-887	9/19/2013	9/20/2013	2.3-2.5 x 10^5	11/21/2013	44%
230	F-2024	11/20/2013	11/22/2013	2.25-2.6 x 10^5	1/14/2013	74%
215	M-885/2054	9/19/2013	9/20/2013	2.3-2.5 x 10^5	11/21/2013	30%
222	F-2002	10/17/2013	10/18/2013	3.6 x 10^5	12/12/2013	53%
218	M-892/2052	9/26/2013	9/27/2013	2.3 x 10^5 *	12/5/2013	22%
HIV						
220	F-900	9/30/2013	10/4/2013	2.5-3 x 10^5	12/5/2013	84%
213	F-874	9/18/2013	9/20/2013	2.3-2.5 x 10^5	11/21/2013	58%
229	M-2020	11/15/2013	11/15/2013	4.5-4.6 x 10^5	1/14/2013	54%
231	M-2026/2055	11/20/2013	11/22/2013	2.25-2.6 x 10^5	1/14/2013	35%
216	F-886	9/19/2013	9/20/2013	2.3-2.5 x 10^5	11/21/2013	40%
220	F-1115/2027	10/1/2013	10/4/2013	2.5 x 10^5	12/5/2013	57%
HHV-6A						
230	F-2025	11/20/2013	11/22/2013	2.25-2.6 x 10^5	1/14/2013	49%
225	M-2011	10/30/2013	11/1/2013	2.5-2.9 x 10^5	1/3/2013	60%
213	F-875	9/18/2013	9/20/2013	2.3-2.5 x 10^5	11/21/2013	65%
203	F-852	8/12/2013	8/16/2013	4.0 x 10^5	10/25/2013	51%
207	M-862	9/5/2013	9/6/2013	1.3-2.25 x 10^5	11/7/2013	28%
219	F-894/895	9/26/2013	9/27/2013	2.3 x 10^5 *	12/5/2013	55%
Mock						
228	F-2016	11/15/2013	11/15/2013	4.5-4.6 x 10^5	1/14/2013	58%
209	F-865	9/11/2013	9/13/2013		11/7/2013	49%
218	M-893/2053	9/26/2013	9/27/2013	2.3 x 10^5 *	12/5/2013	51%
219	F-896/897	9/26/2013	9/27/2013	2.3 x 10^5 *	12/5/2013	40%
205	M-856	8/15/2013	8/16/2013	3.5-4.0 x 10^5	10/25/2013	23%
210	M-869/2051	9/10/2013	9/13/2013		11/7/2013	33%

* Expired cord blood was used for extraction (meaning it was older than 24 hours old) and subsequent engraftment.

3. Analysis of thymocyte populations in Rag-hu mice

Our findings show a decrease in overall number of thymocytes in the thymi of coinfected animals compared to the other experimental groups as seen by FACS analysis. Coinfected mice had considerably fewer thymocytes as compared to HIV only, HHV-6A only, and mock infected groups. ANOVA was performed on all of the data from the coinfection study with no significance. As scientific studies often use t-tests when ANOVA tests are more appropriate, t-test values are reported to provide an estimate of the significance of some of the findings but all findings should be considered not statistically significant by ANOVA. When comparing coinfected vs. HIV infected groups, a t-test gave $p = .05$. A t-test of coinfected vs. mock infected groups was $p = .07$ and coinfected vs. HHV-6A infected is not significant with $p = .19$ (Fig. 10). We observed a depletion of $CD3^+CD4^-$ cellular population in coinfected mouse thymocytes compared to HIV infected mice. A t-test of coinfected vs. HIV was $p = .04$ and for HHV-6A vs. HIV it was $p = .08$ (Fig. 11). An increase in $CD3^+CD4^+$ cellular population (gated on lymphocytes) in coinfected mice compared to both HIV only and HHV-6A only groups was observed. A t-test of coinfected vs. HIV was $p = .03$ and coinfected vs. HHV-6A was $p = .05$ (Fig. 12). An increase in $CD3^-CD4^+$ cellular population (gated on lymphocytes) in HHV-6A compared to HIV infected mice was observed. When comparing HIV vs. HHV-6A, the groups with the greatest variation in this chart, the t-test was $p = .08$. An increase in $CD3^+CD4^+CD8^+$ cellular population (gated on CD4) in HIV infected mice compared to mock infected group was observed. T-test of HIV vs. mock was $p = .02$ and coinfected vs. mock was $p = .12$ and HHV-6A vs. mock was $p = .10$.

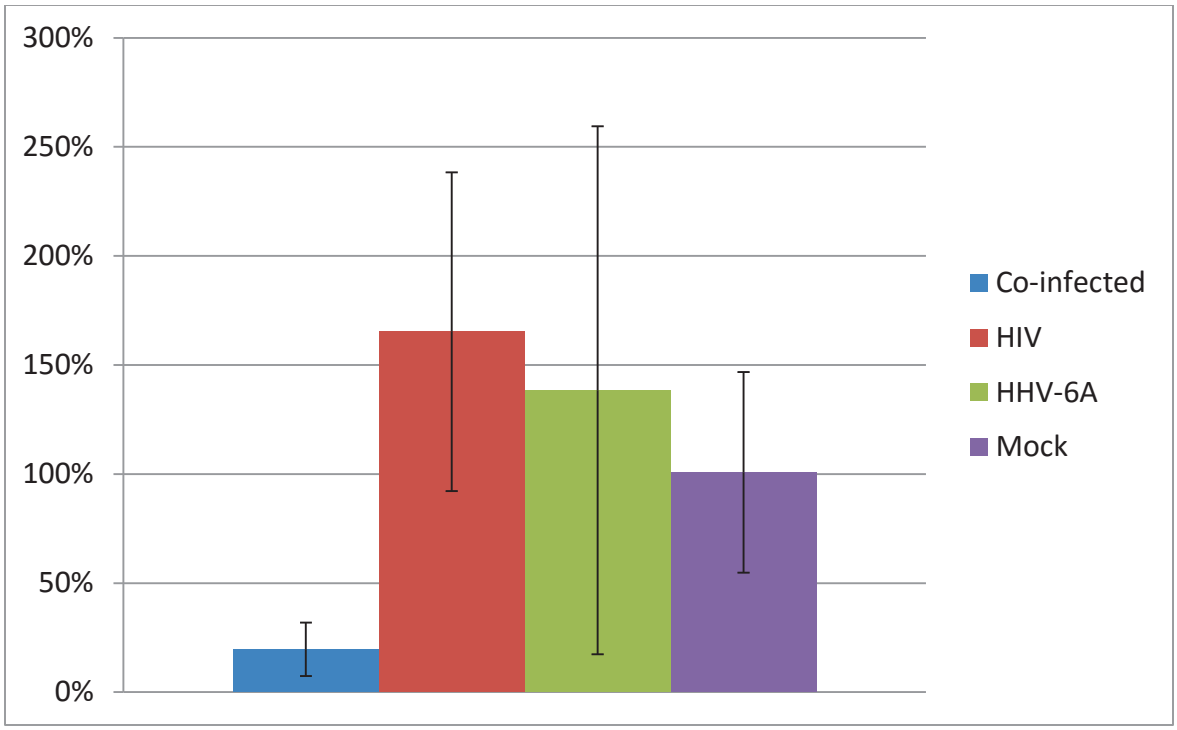

Figure 10. Depletion of total thymocyte population in coinfected Rag-hu mice

Flow cytometry analysis of total thymocytes gated on human $CD45^{+}$ cells. Averages of coinfected, HIV only, HHV-6A only, and mock infected groups are represented. When comparing coinfected vs. HIV infected groups, a t-test gave $p = .05$. A t-test of coinfected vs. mock infected groups was $p = .07$ and coinfected vs. HHV-6A infected was $p = .19$ (n=6 and error bars = SE).

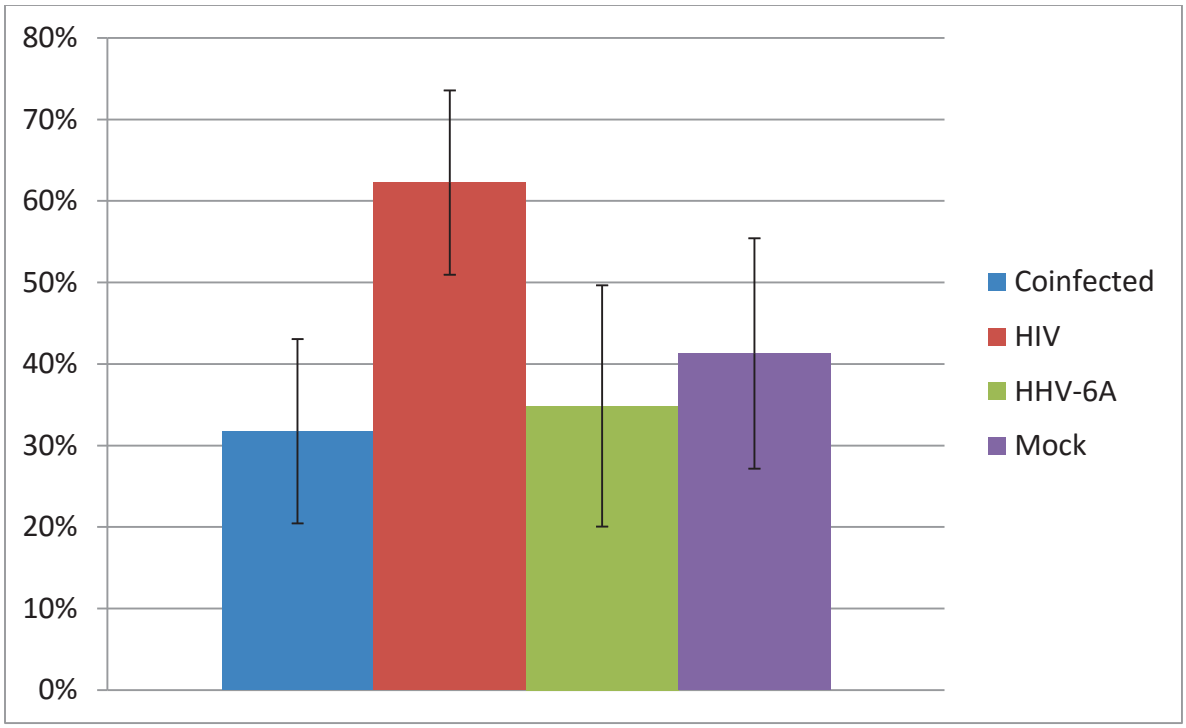

Figure 11. Depletion of $CD3^{+}CD4^{-}$ thymocytes in coinfected Rag-hu mice

Flow cytometry analysis showed a depletion of $CD3^{+}CD4^{-}$ cellular population (gated on lymphocytes) in coinfected mouse thymocytes compared to HIV infected mice. Averages of the four different groups are represented. A t-test of coinfected vs. HIV was p = .04 and for HHV-6A vs. HIV was p = .08. (n=6 and error bars = SE).

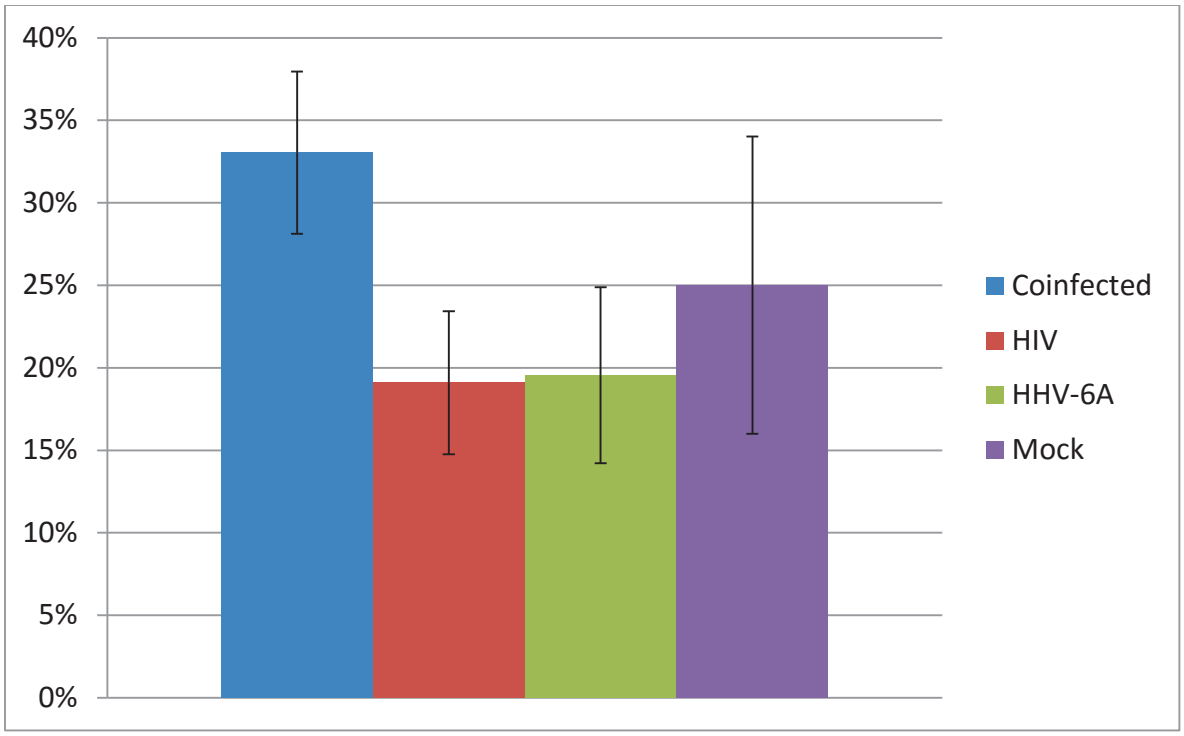

Figure 12. Increase in $CD3^+CD4^+$ cellular population in coinfected Rag-hu mice

Flow cytometry analysis showed an increase in $CD3^+CD4^+$ cellular population (gated on lymphocytes) in coinfected mice compared to both HIV only and HHV-6A only groups. Averages of the four different groups are represented. A t-test of coinfected vs. HIV was $p = .03$ and coinfected vs. HHV-6A was $p = .05$. (n=6 and error bars=SE).

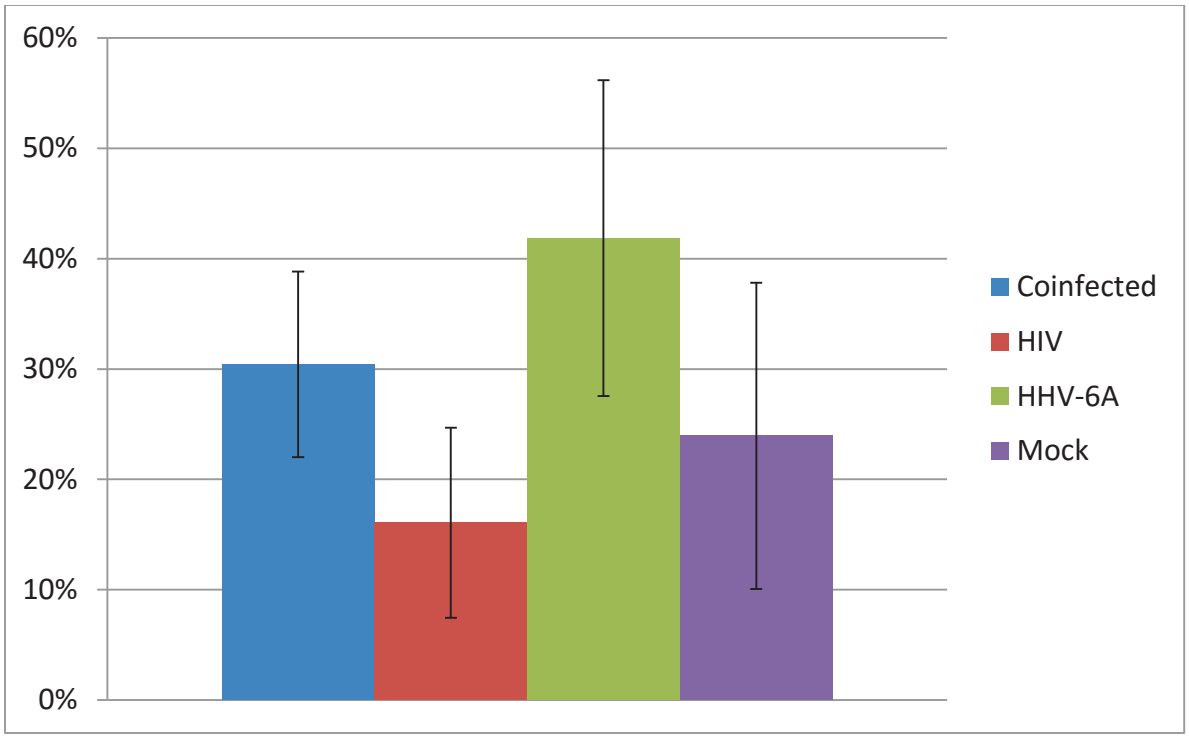

Figure 13. Increase in $CD3^{-}CD4^{+}$ cellular population in HHV-6A-infected Rag-hu mice

Flow cytometry analysis showed a trend where the $CD3^{-}CD4^{+}$ cellular population (gated on lymphocytes) increased in HHV-6A as compared to HIV infected mice. When comparing HIV vs. HHV-6A the t-test was $p = .08$. Averages of the four different groups are represented. (n=6 and error bars = SE).

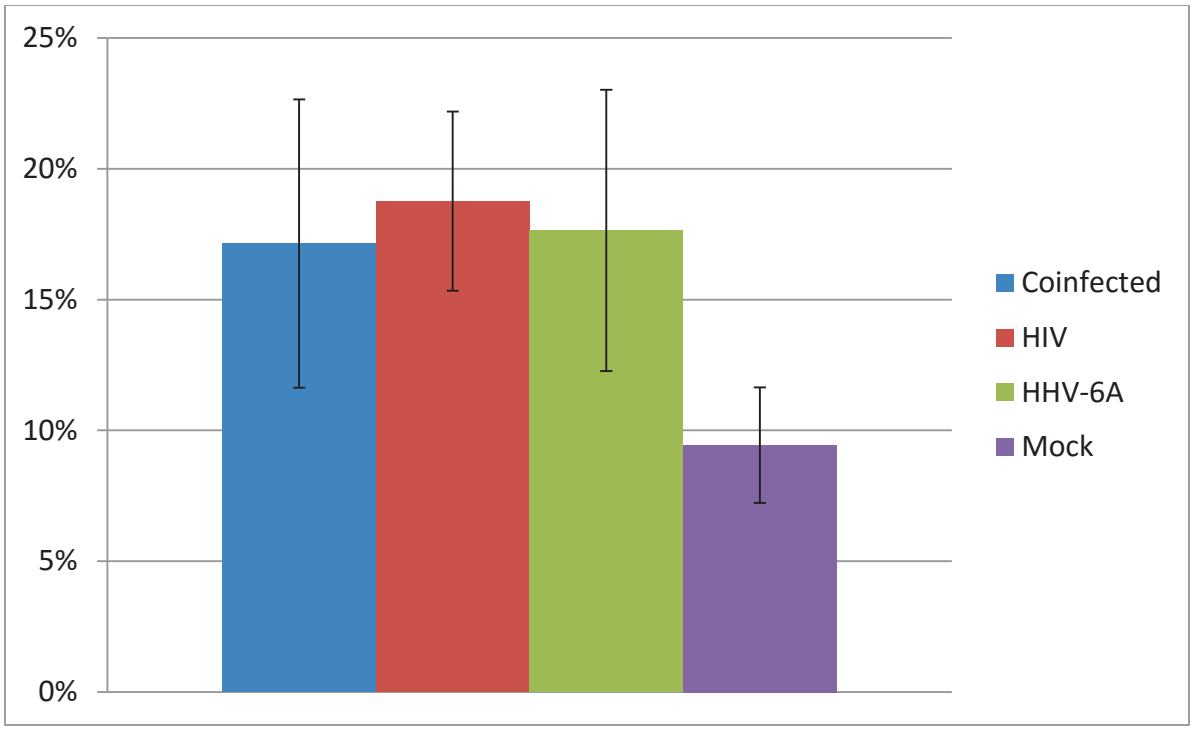

Figure 14. Increase in $CD3^+CD4^+CD8^+$ cellular population in HIV-infected Rag-hu mice

Flow cytometry analysis showed an increase in $CD3^+CD4^+CD8^+$ cellular population (gated on CD4) in HIV infected mice compared to mock infected group. The t-test of HIV vs. mock was $p = .02$ with coinfected vs. mock at $p = .12$ and HHV-6A vs. mock at $p = .10$. Averages of the four different groups are represented. (n=6 and error bars = SE).

Other Results

Bone marrow and spleen of all mice were analyzed by flow cytometry with no significant differences between the four groups of mice tested. Mouse #898 (in the coinfected group) died 5 days post infection with HIV-1. The death occurred hours prior to the daily mouse checks so organs were not harvested.

Acknowledgements

We are grateful to Yasuko Mori (National Institute of Biomedical Innovation, Osaka, Japan) for giving permission to use a recombinant strain of HHV-6A produced in her laboratory. The following reagent was obtained through the NIH AIDS Reagent Program, Division of AIDS, NIAID, NIH: GHOST Cell Transfectants - GHOST (3) Hi-5 from Dr. Vineet N. KewalRamani and Dr. Dan R. Littman.

D. Preferential targeting of HHV-6A towards HIV or vice versa

1. Rationale for the study

In coinfection studies with HIV and HHV-6A, a majority of HIV+ cells were also HHV-6A+ (161). It was not known whether the coinfected cells were due to both viruses having primary tropism for $CD4^+$ T cells or whether there was preferential targeting of an already infected cell. Migration assays were performed to determine if one of the viruses was preferentially migrating towards infected cells of the other virus. Preferential targeting of either of these viruses by the other could prove to be a useful finding as that virus could be designed to inhibit or stop replication of its natural target.

2. Experimental Design

Infected JJhan cells were placed in transwells (Corning) with either RPMI only, HHV-6A GS supernatant, or HIV-1 NL4-3 supernatant in the well below. Cells were stained for viruses as well as CD3, CD4, CD8, CCR7, CXCR4, and S1P1. CCL21, the ligand which attracts CCR7, was used as a positive control. A total of 10 wells were used in this experiment and were as follows:

Figure 15. Experimental design of cell-associated HIV/HHV-6A migration assay

White boxes on top represent tissue culture well above the transwell membrane while shaded boxes on bottom represent tissue culture well below the transwell. Cells were placed in top and cell culture supernatant was placed in bottom.

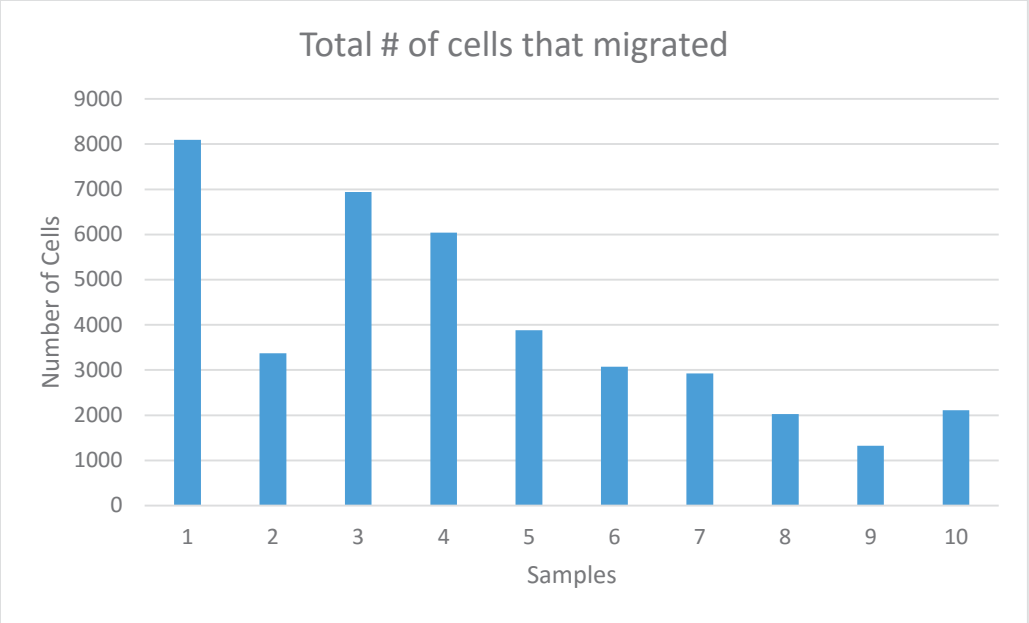

Figure 16. No preferential targeting observed in HHV-6A or HIV infected cells

No significant difference was observed in the migration assays. Samples 1,3, and 4 had more migration as was expected with the addition of CCL21. Samples are as follows:

1) Uninfected towards CCL21

2) Uninfected towards uninfected

3) HIV towards CCL21

4) HHV-6A towards CCL21

5) HIV towards uninfected

6) Uninfected towards HIV

7) HHV-6A towards uninfected

8) Uninfected towards HHV-6A

9) HHV-6A towards HIV

10) HIV towards HHV-6A

3. HHV-6A and HIV-1 infected cells showed no preferential targeting to each other

No significant difference was observed between any of the wells. The migration assay was performed 4 days post infection.

4. Increased migration of HHV-6A+ cells towards chemokine CCL21

An increase in migration of HHV-6A+ $CD34^-$ cord blood cells towards CCL21 was observed in our migration studies. HHV-6A infected cells were placed in transwells with varying concentrations of CCL21 in the well below. 50, 100, and 150 ng/ml concentrations were used with 150 ng/ml determined to induce the most cellular migration. On day 1 post infection there was 71% migration of the HHV-6A infected cells towards CCL21 verses only 31% migration of infected cells towards RPMI, 25% migration of mock infected cells towards CCL21, and 14% migration of mock infected cells towards RPMI. Day 2 post infection results were similar with 88% migration of the HHV-6A infected cells towards CCL21 verses only 33% migration of infected cells towards RPMI, 42% migration of mock infected cells towards CCL21, and 15% migration of mock infected cells towards RPMI. On day 3 and 4 post infection the cells migrated much more similarly between the groups.

5. Time course of HHV-6A towards CCL21

A time course study was done to determine if HHV-6A-infected $CD34^-$ cord blood cells exhibited increased migration towards CCL21 depending on time post infection. Increased migration of HHV-6A infected cells on day 2 post infection was observed. PHA and IL-2 stimulated $CD34^-$ cord blood cells were used in this study and infected with HHV-6A wild type strain GS as described previously in "Viral propagation" section at an MOI of 11.0.

6. Cell-free viral migration assays

A migration assay was performed with cell-free virus with HHV-6A GS wild type and HIV NL4-3. Four different assays using transwells were run consisting of HIV over RPMI, HHV-6A over RPMI, HIV over HHV-6A, and HHV-6A over HIV. As additional controls, HIV and HHV-6A were incubated in separate microcentrifuge tubes and incubated the same as the migration assays. Also as controls, freshly thawed HIV and HHV-6A were immediately loaded onto electron microscopy grid and stained with phosphotungstic acid (PTA) for imaging with an electron microscope. Viral clusters were observed on the grid from the HIV over HHV-6A migration well, with different sized particles being observed (Fig. 16-18). Pairs of viruses were also observed on the grid from the HHV-6A over HIV migration well (Fig. 19), although much fewer particles were observed than the HIV over HHV-6A grid. No other viral particles were observed on any of the other grids.

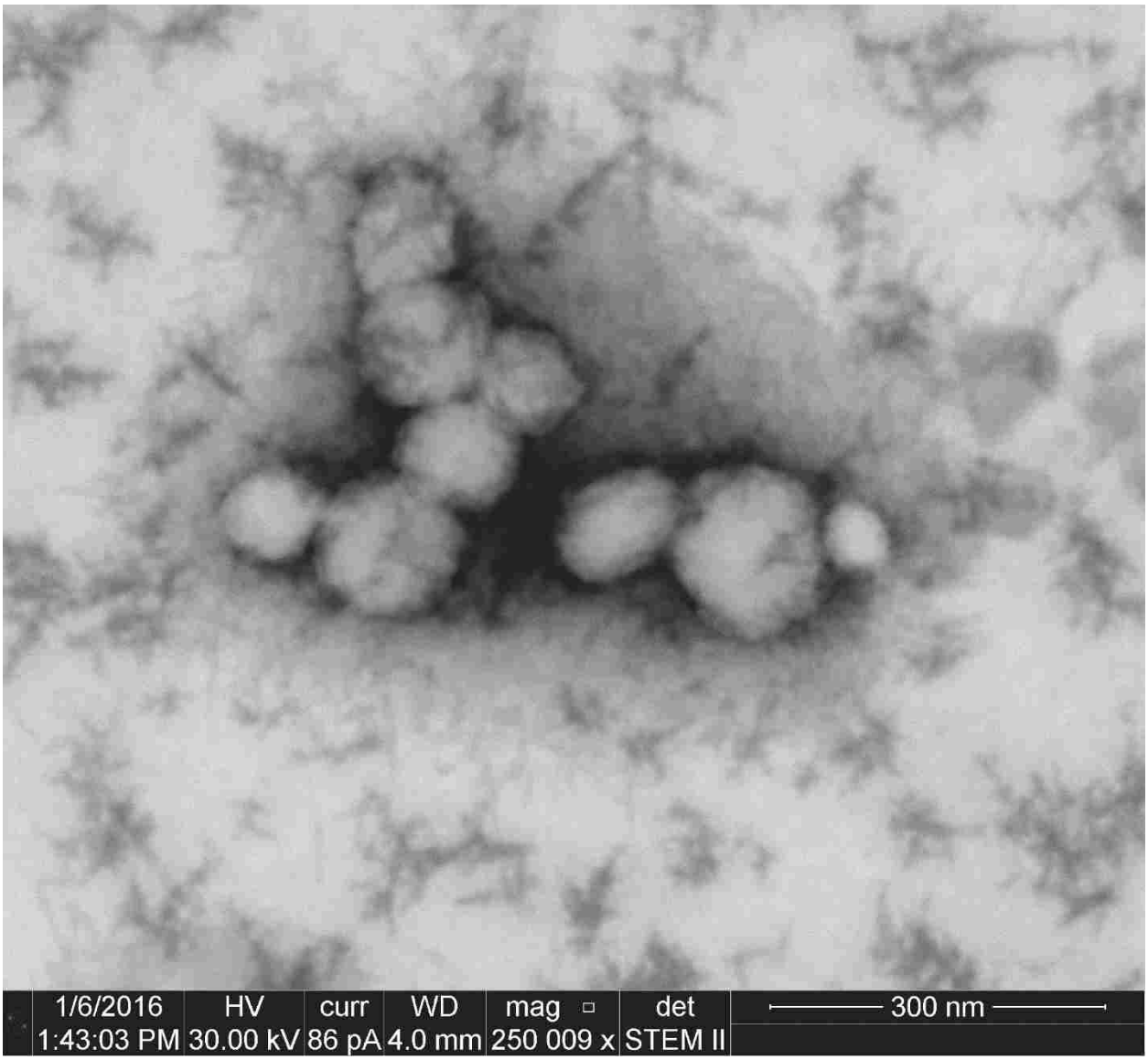

Figure 17. Electron microscopy of cell-free migration assay sample HIV-1 NL4-3 over HHV-6A GS wild type

FEI Helios NanoLab 600 DualBeam FIB/SEM was used for imaging.

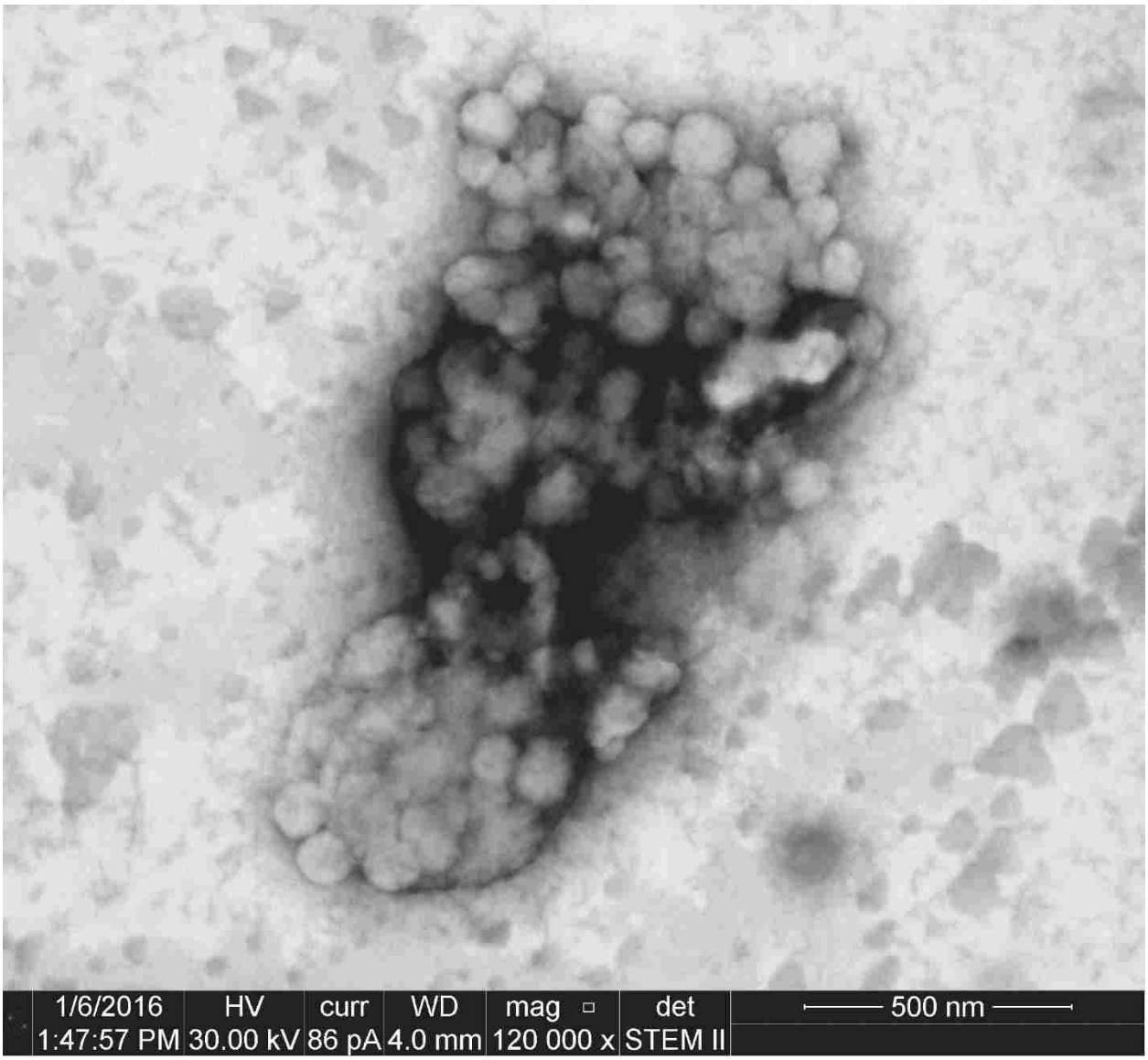

Figure 18. Electron microscopy of cell-free migration assay sample HIV-1 NL4-3 over HHV-6A GS wild type

FEI Helios NanoLab 600 DualBeam FIB/SEM was used for imaging.

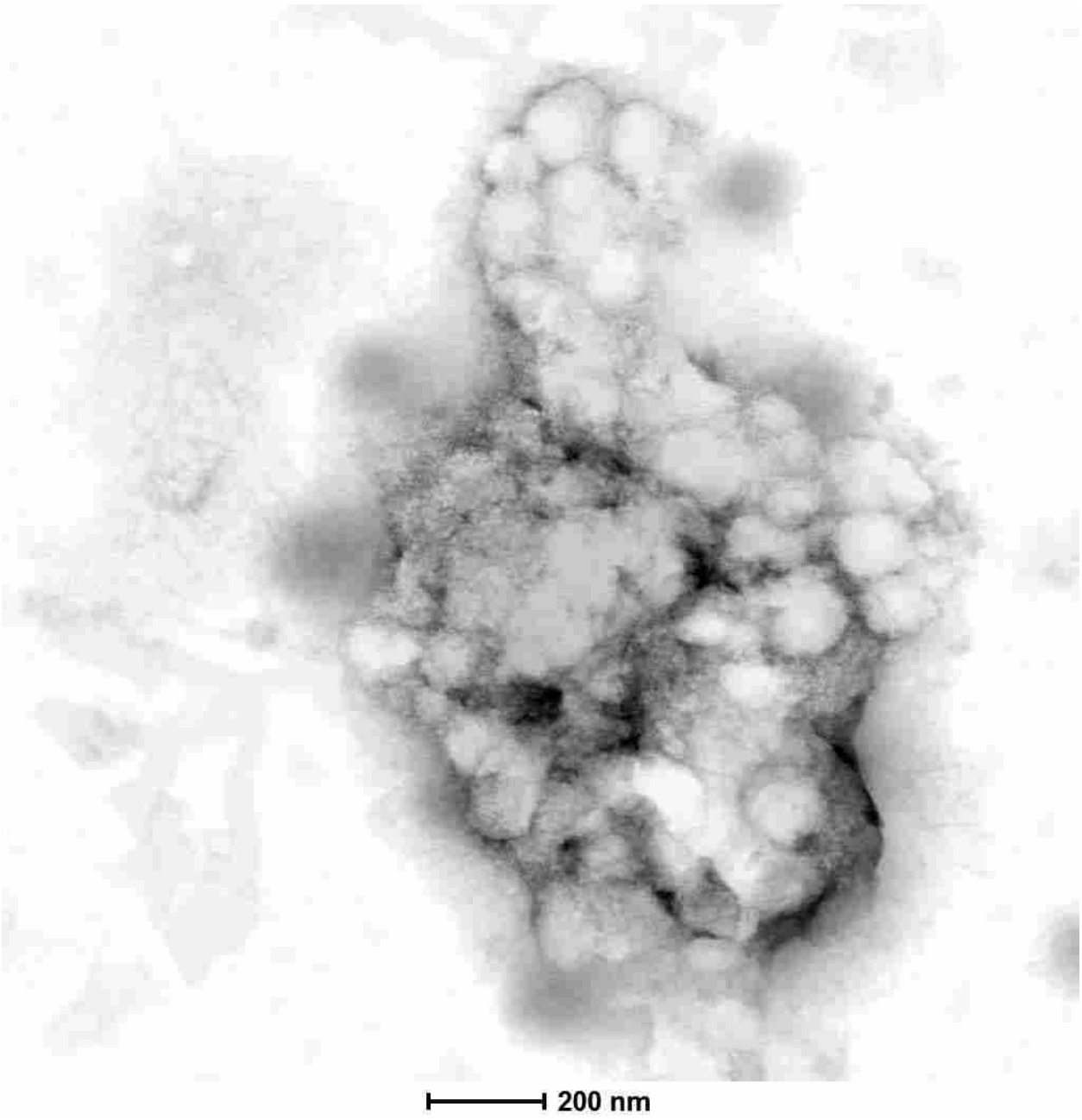

Figure 19. Electron microscopy of cell-free migration assay sample HIV-1 NL4-3 over HHV-6A GS wild type

FEI Tecnai F20 TEM/STEM/AEM was used for imaging.

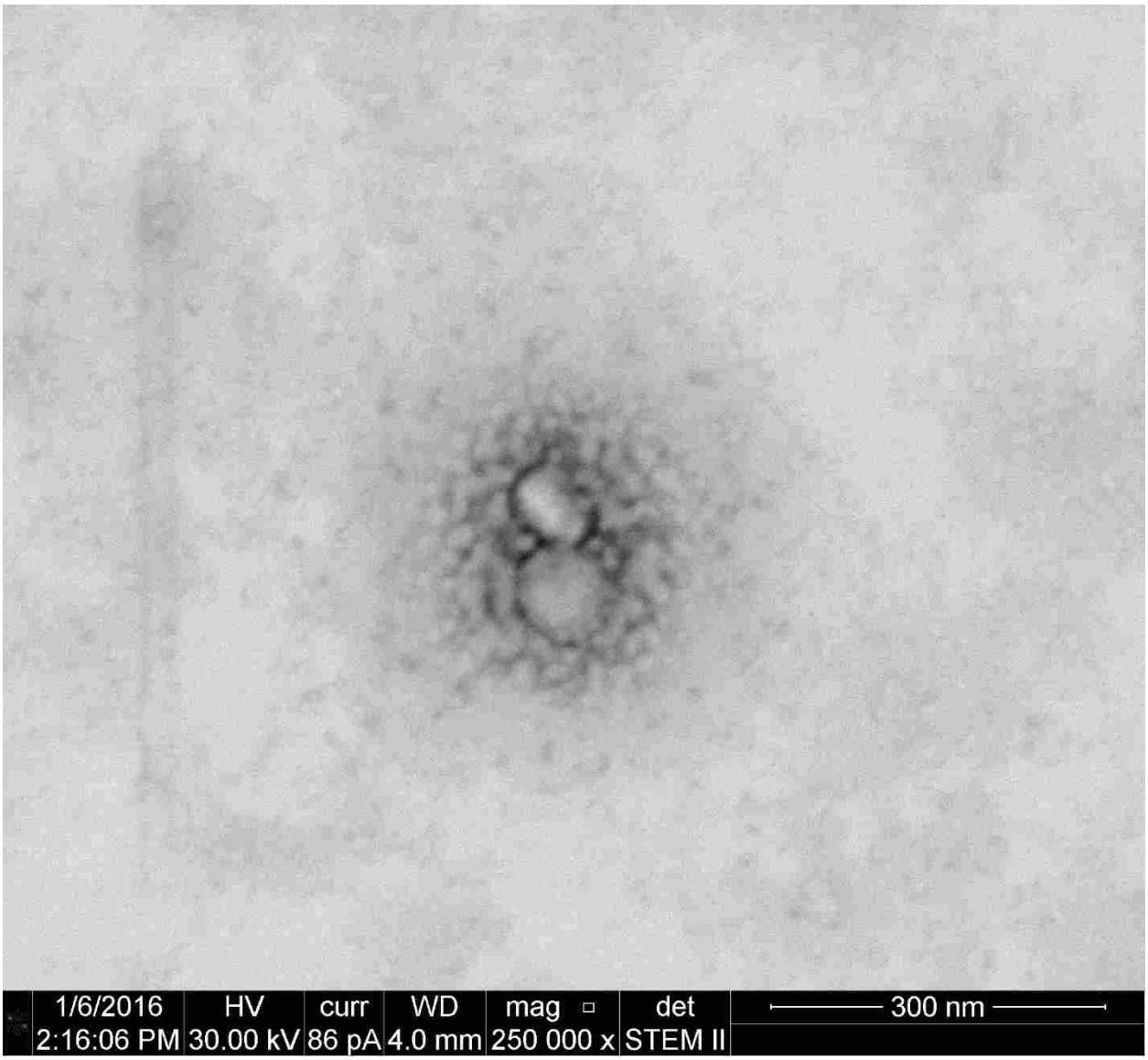

Figure 20. Electron microscopy of cell-free migration assay sample HHV-6A GS wild type over HIV-1 NL4-3

FEI Helios NanoLab 600 DualBeam FIB/SEM was used for imaging.

E. Impact of HHV-6A infection on S1P1 expression

1. Rationale for the study

Sphingosine-1 phosphate receptor (S1P1) is necessary to induce T cell egress from the thymus. As our previous mouse studies had shown $CD4^+CD8^+$ double positive cells in the blood, the possibility of viral manipulation of S1P1 expression to induce T cell egress was explored. We determined to identify the impact, if any, HHV-6A infection has on S1P1 expression as it has not to our knowledge been previously investigated.

2. Experimental Design

Four groups were used in this study consisting of JJhan cells that were infected with HIV-1 only, HHV-6A only, both HIV-1 and HHV-6A, or mock infected. S1P1 expression was measured by flow cytometry over a time course at days 2, 3, 4, 5, 9, 17, and 31 to determine if HHV-6A or HIV-1 altered expression of S1P1 compared with uninfected controls. At each time point, each group had an unstained control for increased accuracy of altered expression.

3. S1P1 expression altered at late time points

Preliminary data indicate that S1P1 expression in HIV-1 and HHV-6A coinfected cells at late time points (31 days post infection) is increased in the $S1P1^{hi}$ population from 2.9 % at day 17 to 21.9 % at day 31 as compared with the HIV-1 only and HHV-6A only groups, with only 6.3% and 8.4% on day 31 respectively. Interestingly, the mock infected group also showed an increase in $S1P1^{hi}$ expression at later time points, with 22.3 % at day 31.

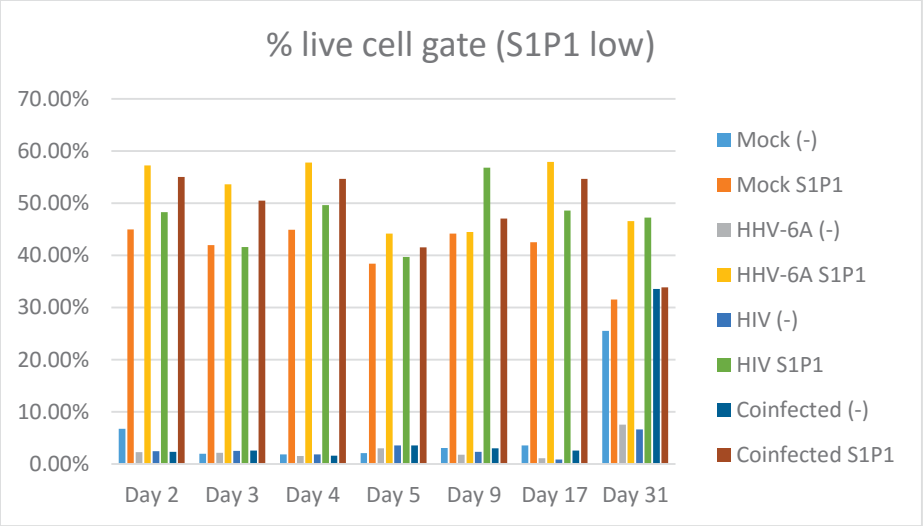
% live cell gate (S1P1 low)
70.00%
60.00%
50.00%
40.00%
30.00%
20.00%
10.00%
0.00%
Day 2
Day 3
Day 4
Day 5
Day 9
Day 17
Day 31
Mock (-)
Mock S1P1
HHV-6A (-)
HHV-6A S1P1
HIV (-)
HIV S1P1
Coinfected (-)
Coinfected S1P1

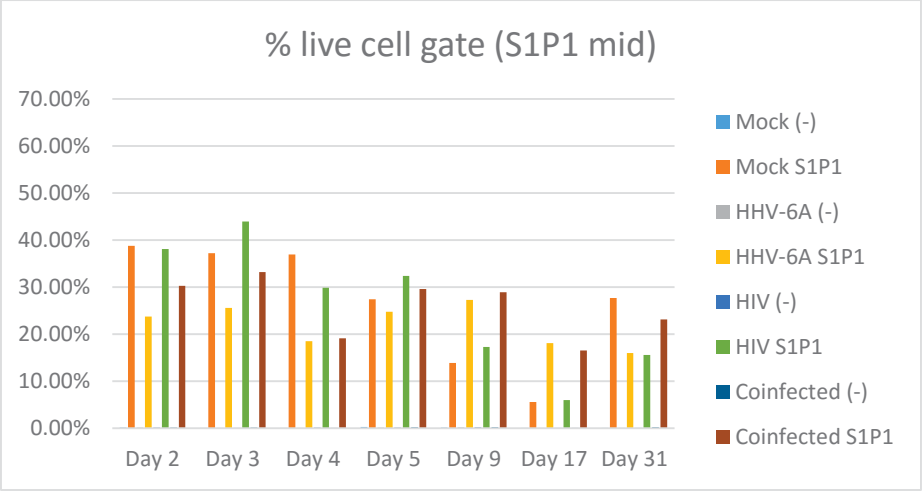
% live cell gate (S1P1 mid)
70.00%
60.00%
50.00%
40.00%
30.00%
20.00%
10.00%
0.00%
Day 2
Day 3
Day 4
Day 5
Day 9
Day 17
Day 31
Mock (-)
Mock S1P1
HHV-6A (-)
HHV-6A S1P1
HIV (-)
HIV S1P1
Coinfected (-)
Coinfected S1P1

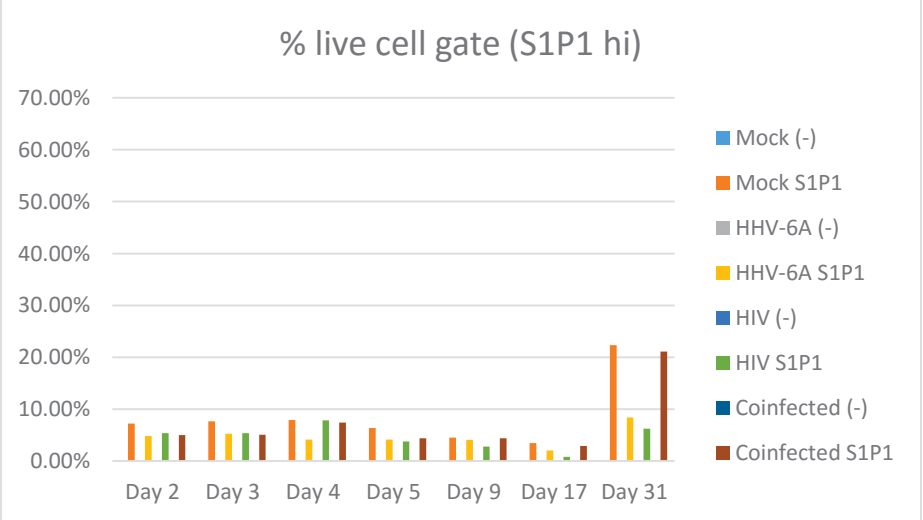
% live cell gate (S1P1 hi)
70.00%
60.00%
50.00%
40.00%
30.00%
20.00%
10.00%
0.00%
Day 2
Day 3
Day 4
Day 5
Day 9
Day 17
Day 31
Mock (-)
Mock S1P1
HHV-6A (-)
HHV-6A S1P1
HIV (-)
HIV S1P1
Coinfected (-)
Coinfected S1P1

Figure 21. Changes in S1P1 expression over time

JJhan cells that were infected with HIV-1 only, HHV-6A only, both HIV-1 and HHV-6A, or mock infected. S1P1 expression was measured by flow cytometry over a time course at days 2, 3, 4, 5, 9, 17, and 31 to determine if HHV-6A or HIV-1 altered expression of S1P1 compared with uninfected controls. At each time point, each group had an unstained control for increased accuracy of altered expression.

IV. Discussion

Here we have shown that RAG-hu mice are susceptible to infection with HHV-6A by either cell-associated or cell-free transmission. Viral DNA was detected in blood (cellular and plasma fractions), bone marrow, lymph node, and thymic tissues (Tables 2, 3, and 4) although no single mouse tested positive for viral DNA in all of these compartments, as mentioned previously. Following cell-associated transmission, viral DNA was detectable for up to 8 weeks post-infection indicating a persistent infection. No viral DNA was detected in any of the three control groups in the cell-associated study, indicating that viral transmission from the infected carrier cells to the originally engrafted cells and subsequent replication was successful because no viral DNA was detectable in either blood or lymphoid organs in control mice without an HSC graft. Irradiated but non-engrafted animals were included as a control for the higher murine immunodeficiency of irradiated mice and they also had undetectable viral DNA after transmission. Some animals in the cell-associated transmission study had viral DNA detected at early time points and not later, and some animals had no detectable DNA at early time points but it was detected later. We attribute this to a relatively high limit of detection in the assay because only small blood samples can be obtained from mice. We noted that plasma viral DNA levels peaked at 3-4 weeks post-infection, but levels decreased to near the level of detection in plasma by 5 weeks and only a single animal had detectable viral DNA in the plasma at 6 weeks. Viral DNA was still detected in the cellular fraction of blood at 6 weeks in three animals while plasma viral DNA was found in a single mouse at that time point, potentially indicating a shift from lytic infection (extracellular DNA) to latency (intracellular DNA).

Cell-associated transmission was attempted because a similar previous experiment with hCMV was only successful with this method (204). However, cell-free transmission was

successful in all 6 animals in our study. We also noted a greater tendency to detect viral DNA in the bone marrow of animals infected by cell-free transmission, but it is not clear if that finding is due to a different mode of transmission or to different time points (1w for cell-free and 6.5-9.5w for cell-associated). We also detected a significant increase in $CD4^+CD8^+$ cells in the blood of cell-free virus infected mice (Fig. 4). This was possibly due to CD4 upregulation in CD8+ T cells, which was previously shown *in vitro* in HHV-6A infected cells (210). When we correlated Q-PCR results of blood cells and plasma to the detection of these $CD4^+CD8^+$ cells there was not a clear trend because one animal (#715) had high proportions of these cells and detectable viral DNA in plasma, while other animals also had high proportions of the cells but undetectable viral DNA in either blood fraction. Another animal (#711) had low proportions of the cells with only intracellular blood viral DNA. The frequent detection of this effect, combined with relatively rare detection of viral DNA in either blood fraction, indicates that these cells may be uninfected by HHV-6A. These cells largely maintained CD3 expression, which also indicates a lack of infection. It is possible that HHV-6A infection promotes the release of these cells from the thymus because $CD4^+CD8^+$ cells are rare outside of the thymus. However, we failed to detect viral DNA in the thymus in 3 animals tested and so the promotion of releasing cells from the thymus would likely be conducted from a distal site. Evidence exists that the presence of $CD4^+CD8^+$ cells in human blood is upregulated following viral infection, including after infection with persistent viruses such as the herpesvirus EBV (211).

The increased levels of CD4+CD8+ cells in the blood of some of the HHV-6A-infected mice could also indicate a mechanism whereby HHV-6A contributes to autoimmunity. As mentioned, these double positive cells are rare outside of the thymus so the increased levels of CD4+CD8+ cells could be due to a premature departure of these cells from the thymus while still

in the double positive state, prior to undergoing positive or negative selection or both where they would become single positive CD4 or CD8 cells. Typically, as cells enter the thymus from the bone marrow CCR7 is expressed until the DN3 (double negative 3) stage where it is downregulated to allow the cell sufficient time to undergo proper development, part of which includes undergoing positive selection in the cortex where CCR7 is then upregulated, causing migration of the cell to the CCL19/CCL21-rich thymic medulla where negative selection occurs prior to the cell exiting the thymus (134). However, HHV-6A infection can cause an upregulation of CCR7 which could cause a premature migration of these cells directly to the medulla, thus bypassing important processes including positive selection and transitioning to a single positive cell. If these untrained cells gained access to the periphery, they would be highly autoreactive. The overexpression of CCR7 could also promote migration of these cells into the CNS and brain as has been demonstrated in mouse models (239), which is our hypothesis for the involvement of HHV-6A in multiple sclerosis.

EBV has also been implicated in autoimmune diseases such as systemic lupus erythematosus (SLE) and MS. It has been shown to alter a number of cellular receptors as well as use viral proteins to mimic cellular signals such as the Latent membrane protein 2A (LMP2A) of EBV that promotes survival and proliferation of B cells in the absence of cellular signals (240). HHV-6B protein U20 has been shown to interfere with tumor necrosis factor receptor 1 (TNFR1) signaling and could be a way the virus prevents programmed cell death (241). It is possible that HHV-6A could also be employing a similar strategy of using of a viral protein to mimic a survival signal in the absence of these cellular signals and to evade a death signal. This could lead to improperly trained, potentially autoreactive, T cells exiting the thymus and contributing to different autoimmune diseases, depending on where these cells migrate. Furthermore, HHV-

6A protein U51A binds CCL19 and the presence of U51A-binding chemokines in the brain (135) may induce migration of the potentially autoreactive HHV-6A infected cells into this area, where MS disease occurs.

Sphingosine-1 phosphate receptor (S1P1) causes cellular trafficking towards its ligand, Sphingosine 1-phosphate (S1P) (a membrane-derived lysophospholipid), and is necessary to induce T cell egress from the thymus whereas CCR7 has been shown to promote T cell sequestration in the thymus. S1P1 counteracts and eventually overrides the CCR7 retention signal, allowing cells to enter the periphery. As an additional component in our theory of MS we considered the possible involvement of HHV-6A in manipulating S1P1 expression and subsequent T cell migration or sequestration. The upregulation of S1P1 by HHV-6A would provide an explanation for the larger quantities of double positive cells observed in the blood of our infected mice, as these cells would be prematurely located in the thymic medulla due to overexpression of CCR7 and the upregulation of S1P1 would allow them to exit prior to appropriate selection. We recognize that HHV-6A could likewise cause a downregulation of S1P1, as previous mouse studies have shown an absence of T cells in the periphery of mice whose hematopoietic cells lack S1P1 (134) and we have also observed lower levels of T cells in the periphery of our infected mice.

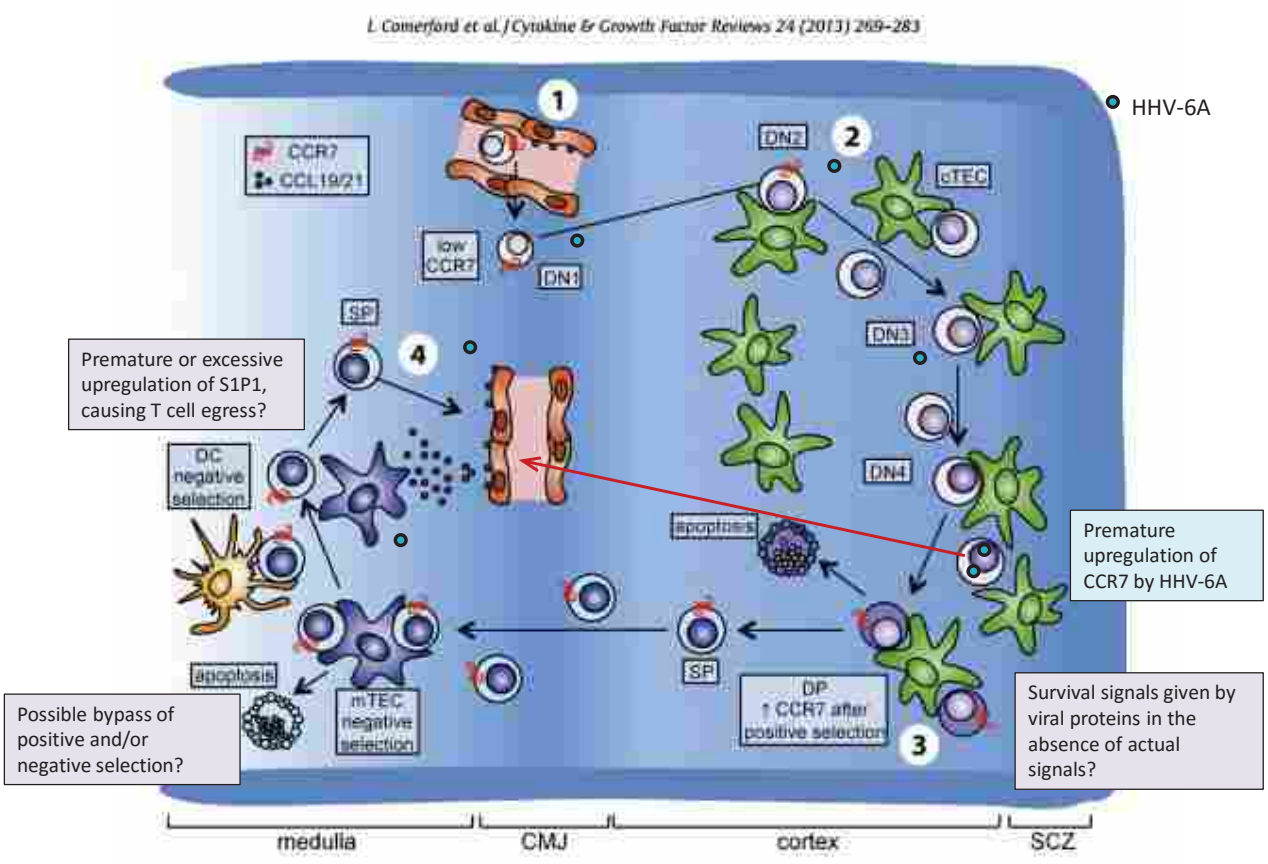

Figure 22. Diagram of HHV-6A alterations in CCR7 and S1P1 expression in human thymocytes and implications in disease

Diagram represents the human thymus. The alteration of CCR7 expression could cause T cells to bypass positive and/or negative selection in the thymus (represented by red arrow) and the upregulation of S1P1 could promote premature egress of these inadequately selected T cells into the periphery, possibly resulting in autoimmunity. This figure is adapted from "A myriad of functions and complex regulation of the CCR7/CCL19/CCL21 chemokine axis in the adaptive immune system." by Comerford et al. (134).

We attempted to use GFP expression from a recombinant virus to further demonstrate successful infection in our HHV-6A Rag-hu mouse study. However, the only animal with detectable GFP^+ cells was mouse 715 from the cell-free transmission group, and those cells were from the mesenteric lymph node. FACS analysis of GFP^+ cells indicated that they were mostly $CD3^-$ $CD4^+$, which is in accordance with our *in vitro* results in Fig 2D and previously published data showing a tropism for $CD4^+$ T cells and a downregulation of CD3 after infection (209, 212). We later determined that the GFP cassette in this virus is driven by the CMV IE promoter (Y. Mori, personal communication). Since the cell-associated mice were sacrificed at 6.5 to 9.5 weeks p.i. it is possible that the virus was in a latent state at the time of organ collection; this hypothesis is supported by the shift from extracellular to intracellular DNA seen in blood. The activity of the CMV IE promoter in the context of a latent HHV-6A infection is currently unknown, and if that promoter is inactive during latency that may explain a lack of GFP^+ cells in any of the cell-associated infected mice. An interesting observation was made that several thymocyte populations were altered in HHV-6A infected animals versus uninfected animals (Fig. 3). These observations lend further support that successful viral transmission occurred, because similar findings have been reported *in vitro* and in another humanized mouse study. In those studies, CD3 depletion only occurred in infected (not in bystander) cells (195, 210, 212). Thymocyte depletion was only detected in animals infected by the cell-associated pathway, but these animals were also infected for a longer period. It is possible that virus had not trafficked to the thymus in cell-free infected mice, a finding supported by our Q-PCR data where 0 of 3 of these thymic samples harbored viral DNA (Table 2). We noted significant depletion in the $CD3^+CD4^-$ and $CD3^-CD4^+CD8^-$ populations in HHV-6A-infected animals. We also noted a significant increase in the $CD3^+CD4^+CD8^+$ subset, with a marginally significant increase in the $CD3^-CD4^+CD8^+$

population. The significant loss of $CD3^-CD4^+CD8^-$ thymocytes was similarly reported by Gobbi et al. when HHV-6A was directly inoculated into the thymic organoid of SCID-hu *thy/liv* mice (195). In contrast to that report, our results show a significant increase in the $CD3^+CD4^+CD8^+$ subset. These discrepancies may be explained by the use of different virus isolates, with strain GS used in that report and a recombinant isolate based upon strain U1102 used here. In addition, we have used a newer generation of humanized mice with a wider scope of human cell types and a much broader distribution in the mouse, and we inoculated at a site distant from the thymus. Several of these thymocyte populations that were modified by infection *in vivo* can be explained by a tropism and cytopathogenicity of the virus for $CD4^+$ T cells. Additionally, the tendency of the virus to downregulate CD3 and/or to upregulate CD4 expression can also explain shifting populations (e.g., $CD3^+CD4^-$ and $CD3^+CD4^+CD8^-$ populations expected to decrease, and $CD3^-CD4^+CD8^+$ population expected to increase). The $CD3^+CD4^+CD8^-$ population was previously shown to be more infectable with HHV-6A as compared to other thymocyte populations (195). We have proposed that in the cell-associated study the virus was predominantly latent at the time points that the thymic samples were collected. We are not aware of any studies documenting CD3 downregulation or CD4 upregulation in latently infected primary cells, so it is currently not clear if lytic replication is required for these effects upon host cell gene expression.

We and others have previously shown that RAG-hu mice are also highly susceptible to HIV-1 infection (103, 107, 166, 180). Our current findings indicate higher proportions of $CD4^+$ cells in HHV-6A infected animals, similar to those shown by Lusso et al. *in vitro* where they showed that HHV-6A-infected $CD8^+$ T cells began to express CD4 and were able to replicate HIV-1 (210). If HHV-6A is able to convert $CD8^+$ T cells to become infectable by HIV-1 *in vivo*, then those cells may be depleted by HIV-1 and/or by HHV-6A. Downregulation of CD3, as our

results herein have indicated, is expected to cause immunosuppression because CD3 serves as the signaling subunit of the T cell receptor. Hence, T cells could engage the T cell receptor but not be able to respond effectively. Either of these two effects would support the hypothesis that HHV-6A is a co-factor in AIDS progression (197, 198).

All mice in the HIV and HHV-6A coinfection study (excluding mouse # 875, due to erratic behavior, thus creating a potential hazard for handling) were bled weekly by tail bleed according to IACUC standards. Because of previous experiments done on HIV we expected to be able to track T cell levels in the blood of the mice and compare the T cell levels between the different groups. The blood cell fraction of the mice was analyzed by FACS for about the first 4 weeks of the study with very few $CD3^+$ T cells being present. One explanation for the low levels of peripheral blood T cells is the mode of engraftment. We are unable to use fetal liver for engraftment as this source of stem cells has ethical constraints and few suppliers exist so we engraft our mice instead using $CD34^+$ stem cells obtained from human cord blood (167). Although this method is effective in obtaining positively engrafted humanized mice, the different source of engrafted cells may result in a less robust engraftment. For the age of the mice used in this study, we would expect between ~14-28% of human lymphocytes to be $CD3^+$ (242). Because so few T cells were present in the tail bleeds, FACS analysis was halted and preference was given instead to performing DNA/RNA extractions from the weekly blood samples to determine viral load of both HIV and HHV-6A. Very few mice were positive by Q-PCR for HHV-6A in the blood during the 12 week span of the study. This is not surprising, as HHV-6A primarily infects $CD4^+$ T cells, few of which were present in the peripheral blood.

Although human T and B cell responses are commonly detected in humanized mice following exposure to human herpesviruses (HHVs) and other antigens, many experiments have

shown sporadic detection of these responses and the amplitude of responses also varies. Although the reasons for these findings are not well understood, it has been hypothesized that since T cell maturation occurs in a thymus that expresses both murine and human MHC-I molecules that this unusual selection mechanism may play a role in relatively weak adaptive immune responses (94). The very high frequency of EBV-induced cancers in humanized mice is possibly promoted by weak adaptive immunity and hence a lack of immunological control of EBV. Efforts to improve human adaptive immunity in these models revolve around the introduction of human MHC-I expression into the thymus by two main mechanisms: by transplantation of human thymic stromal cells, referred to as a BLT (bone marrow, liver, thymus) humanized mouse (221) or by a genetic knock-in of human MHC-I into the mouse genome (227). These improvements will be critical for future vaccine studies because weak adaptive immunity will not allow for effective challenge studies to determine vaccine efficacy.

Coinfected mice had considerably fewer thymocytes as compared to the other 3 groups in the study. When comparing coinfected vs. HIV infected, $p = .05$. A t test of coinfected vs. mock infected groups is $p = .07$ and coinfected vs. HHV-6A infected is not significant with $p = .19$. The depletion of human $CD45^+$ cells seen in the coinfected mouse group suggest that coinfection with HIV-1 and HHV-6A has a more severe effect on thymocyte cellular populations than either HIV-1 or HHV-6A alone. The results seen in the HHV-6A and mock groups in this study are similar to those seen previously (233). This evidence could support the hypothesis that HIV and HHV-6A are having a synergistic effect on each other, leading to more severe cell death in the thymus. An alternate hypothesis could be that cells in the coinfected mice are getting sequestered in another area of the body, possibly the bone marrow, as CXCR4 is downregulated in HHV-6A infected cells and is necessary for cellular trafficking from the bone marrow to the thymus (134).

There is a depletion of the $CD3^+CD4^-$ cellular population (gated on lymphocytes) in coinfected mouse thymocytes compared to HIV infected mice. This population would be expected to be depleted as HHV-6A downregulates CD3 and upregulates CD4. For these same reasons it is also not surprising that a similar trend was seen when comparing HHV-6A vs. HIV and would also explain the increase in the $CD3^-CD4^+$ cellular population in HHV-6A compared to HIV infected mice. An increase in the $CD3^+CD4^+$ cellular population (gated on lymphocytes) was seen in coinfected mice compared to both HIV only and HHV-6A only groups. As previously stated, CD4 is upregulated by HHV-6A but it is unclear as to why the CD3 marker would be more highly expressed in the coinfected mice. An increase in the $CD3^+CD4^+CD8^+$ cellular population (gated on CD4) in HIV infected mice compared to mock infected group was observed and to a lesser extent this trend was also seen in the HHV-6A and coinfected groups, perhaps highlighting another important aspect of infection with these viruses contributing to higher numbers of double positive cells in the thymus which could then migrate into the periphery. Similar results were seen in our previous study with HHV-6A infected mice showing an increase in $CD3^+CD4^+CD8^+$ cells in the thymus and $CD4^+CD8^+$ cells in the blood (233).

While the results of the cell-free migration assay are strictly qualitative and do not provide conclusive evidence, they could provide insight into modes of coinfection and are sufficient to warrant further investigation. If viruses are commonly clustered as is seen in these images, it is possible that coinfection is occurring as one virus attaches to a cellular receptor and the other virus is also able to enter the cell as it is attached to that virus, regardless of attachment or tropism. This viral piggybacking could result in cells that are normally refractory to infection with a certain virus becoming infected. Clustering of viruses could prove advantageous to the virus as their mass is increased dramatically when clustered as compared to a single virion,

which may allow them greater probability of coming in contact with cells or having more than one virus infect a single cell to increase chances of replication and survival. As HIV and HHV-6A appear to have a synergistic effect on one another, increasing chances of coinfection in cells could also prove to be mutually beneficial for these viruses.

The mechanisms behind how cell-free virus would locate and come in contact with other cell-free virus are not known. Even though the mechanisms are currently unknown, the likelihood of this phenomenon occurring by chance seems unlikely, as it is observed even in low viral titer conditions. If the process of viruses encountering cells they can infect is as random as seeds blowing in the wind as some suggest, we would expect to almost always observe individual virions by electron microscopy (except under high titer conditions when the likelihood of them colliding by chance is greatly increased) and very rarely see two together, with the chances of more than two together being even less likely. This, however, is not the case, and electron micrographs of all types of viruses commonly show large viral clusters. It is possible that the properties of the cellular membrane would not allow more than one virus particle entry with any given attachment and the viral clustering could just provide a way for more individual viruses to come in contact with the cell but that each individual virion would still have to attach and enter separately.

V. Future Directions

Although there was an overexpression of $S1P1^{hi}$ at late time points in the coinfected sample of the S1P1 time course study, this data is preliminary and needs further examination. Additional studies should look at *in vivo* expression of S1P1 in blood, bone marrow, spleen, thymus, lymph nodes, and brain of HHV-6A infected animals as well as HIV-1 and HHV-6A coinfected animals, as this is the group that showed overexpression *in vitro*. Additional coinfection studies would be beneficial to determine mechanism behind coinfection with HIV and HHV-6A of a single cell. Performing an experiment with $CD4^+$ T cells that are only susceptible to infection with HHV-6A but not HIV (use a CCR5 tropic strain of HIV and a $CCR5^-CD4^+$ T cell line) and then coinfecting the cells to determine if HIV infection can still occur would be a method to further investigate the "viral piggybacking" hypothesis. The origin of the CD4+CD8+ double positive T cells in the blood of HHV-6A infected Rag-hu mice requires additional investigation. These could be double positive cells that have prematurely left the thymus as has been suggested, however different explanations are possible such as these were single positive CD4 or CD8 cells in the periphery that became double positive cells due to the infection. Identification of thymic stage markers or T cell maturation markers would help determine the origin of these double positive cells found in the blood of HHV-6A infected mice.

VI. References

1. **Cornaby C, Tanner A, Stutz EW, Poole BD, Berges BK.** 2016. Piracy on the molecular level: human herpesviruses manipulate cellular chemotaxis. J Gen Virol **97:**543-560.
2. **Berges BK, Tanner A.** 2014. Modeling of human herpesvirus infections in humanized mice. J Gen Virol **95:**2106-2117.
3. **Tanner A, Taylor SE, Decottignies W, Berges BK.** 2014. Humanized mice as a model to study human hematopoietic stem cell transplantation. Stem Cells Dev **23:**76-82.
4. **Salahuddin SZ, Ablashi DV, Markham PD, Josephs SF, Sturzenegger S, Kaplan M, Halligan G, Biberfeld P, Wong-Staal F, Kramarsky B, et al.** 1986. Isolation of a new virus, HBLV, in patients with lymphoproliferative disorders. Science **234:**596-601.
5. **Ablashi DV, Balachandran N, Josephs SF, Hung CL, Krueger GR, Kramarsky B, Salahuddin SZ, Gallo RC.** 1991. Genomic polymorphism, growth properties, and immunologic variations in human herpesvirus-6 isolates. Virology **184:**545-552.
6. **Aubin JT, Collandre H, Candotti D, Ingrand D, Rouzioux C, Burgard M, Richard S, Huraux JM, Agut H.** 1992. Several groups among human herpesvirus 6 strains can be distinguished by Southern blotting and polymerase chain reaction. J Clin Microbiol **30:**2524.
7. **Schirmer EC, Wyatt LS, Yamanishi K, Rodriguez WJ, Frenkel N.** 1991. Differentiation between two distinct classes of viruses now classified as human herpesvirus 6. Proc Natl Acad Sci U S A **88:**5922-5926.
8. **Adams MJ, Carstens EB.** 2012. Ratification vote on taxonomic proposals to the International Committee on Taxonomy of Viruses (2012). Arch Virol **157:**1411-1422.
9. **Dominguez G, Dambaugh TR, Stamey FR, Dewhurst S, Inoue N, Pellett PE.** 1999. Human herpesvirus 6B genome sequence: coding content and comparison with human herpesvirus 6A. J Virol **73:**8040-8052.
10. **Ablashi D, Agut H, Alvarez-Lafuente R, Clark DA, Dewhurst S, DiLuca D, Flamand L, Frenkel N, Gallo R, Gompels UA, Höllsberg P, Jacobson S, Luppi M, Lusso P, Malnati M, Medveczky P, Mori Y, Pellett PE, Pritchett JC, Yamanishi K, Yoshikawa T.** 2014. Classification of HHV-6A and HHV-6B as distinct viruses. Arch Virol **159:**863-870.
11. **Mori YaY, Koichi.** 2007. HHV-6A, 6B, and 7: pathogenesis, host response, and clinical disease - Human Herpesviruses - NCBI Bookshelf, Human Herpesviruses. Cambridge University Press.
12. **Kondo K, Hayakawa Y, Mori H, Sato S, Kondo T, Takahashi K, Minamishima Y, Takahashi M, Yamanishi K.** 1990. Detection by polymerase chain reaction amplification of human herpesvirus 6 DNA in peripheral blood of patients with exanthem subitum. J Clin Microbiol **28:**970-974.
13. **Gompels UA, Nicholas J, Lawrence G, Jones M, Thomson BJ, Martin ME, Efstathiou S, Craxton M, Macaulay HA.** 1995. The DNA sequence of human herpesvirus-6: structure, coding content, and genome evolution. Virology **209:**29-51.
14. **De Bolle L, Naesens L, De Clercq E.** 2005. Update on human herpesvirus 6 biology, clinical features, and therapy. Clin Microbiol Rev **18:**217-245.
15. **Biberfeld P, Kramarsky B, Salahuddin SZ, Gallo RC.** 1987. Ultrastructural characterization of a new human B lymphotropic DNA virus (human herpesvirus 6) isolated from patients with lymphoproliferative disease. J Natl Cancer Inst **79:**933-941.
16. **Yoshida M, Uno F, Bai ZL, Yamada M, Nii S, Sata T, Kurata T, Yamanishi K, Takahashi M.** 1989. Electron microscopic study of a herpes-type virus isolated from an infant with exanthem subitum. Microbiol Immunol **33:**147-154.

17. **Lusso P, De Maria A, Malnati M, Lori F, DeRocco SE, Baseler M, Gallo RC.** 1991. Induction of CD4 and susceptibility to HIV-1 infection in human CD8+ T lymphocytes by human herpesvirus 6. Nature **349:**533-535.
18. **Lusso P, Malnati MS, Garzino-Demo A, Crowley RW, Long EO, Gallo RC.** 1993. Infection of natural killer cells by human herpesvirus 6. Nature **362:**458-462.
19. **Lusso P, Garzino-Demo A, Crowley RW, Malnati MS.** 1995. Infection of gamma/delta T lymphocytes by human herpesvirus 6: transcriptional induction of CD4 and susceptibility to HIV infection. J Exp Med **181:**1303-1310.
20. **Ablashi DV, Lusso P, Hung CL, Salahuddin SZ, Josephs SF, Llana T, Kramarsky B, Biberfeld P, Markham PD, Gallo RC.** 1989. Utilization of human hematopoietic cell lines for the propagation and characterization of HBLV (human herpesvirus 6). Dev Biol Stand **70:**139-146.
21. **Gravel A, Dubuc I, Morissette G, Sedlak RH, Jerome KR, Flamand L.** 2015. Inherited chromosomally integrated human herpesvirus 6 as a predisposing risk factor for the development of angina pectoris. Proc Natl Acad Sci U S A **112:**8058-8063.
22. **Sada E, Yasukawa M, Ito C, Takeda A, Shiosaka T, Tanioka H, Fujita S.** 1996. Detection of human herpesvirus 6 and human herpesvirus 7 in the submandibular gland, parotid gland, and lip salivary gland by PCR. J Clin Microbiol **34:**2320-2321.
23. **Okuno T, Takahashi K, Balachandra K, Shiraki K, Yamanishi K, Takahashi M, Baba K.** 1989. Seroepidemiology of human herpesvirus 6 infection in normal children and adults. J Clin Microbiol **27:**651-653.
24. **Cone RW, Huang ML, Hackman RC, Corey L.** 1996. Coinfection with human herpesvirus 6 variants A and B in lung tissue. J Clin Microbiol **34:**877-881.
25. **Fillet AM, Raphael M, Visse B, Audouin J, Poirel L, Agut H.** 1995. Controlled study of human herpesvirus 6 detection in acquired immunodeficiency syndrome-associated non-Hodgkin's lymphoma. The French Study Group for HIV-Associated Tumors. J Med Virol **45:**106-112.
26. **Saxinger C, Polesky H, Eby N, Grufferman S, Murphy R, Tegtmeir G, Parekh V, Memon S, Hung C.** 1988. Antibody reactivity with HBLV (HHV-6) in U.S. populations. J Virol Methods **21:**199-208.
27. **Gerdemann U, Keukens L, Keirnan JM, Katari UL, Nguyen CT, de Pagter AP, Ramos CA, Kennedy-Nasser A, Gottschalk SM, Heslop HE, Brenner MK, Rooney CM, Leen AM.** 2013. Immunotherapeutic strategies to prevent and treat human herpesvirus 6 reactivation after allogeneic stem cell transplantation. Blood **121:**207-218.
28. **Virtanen JO, Farkkila M, Multanen J, Uotila L, Jaaskelainen AJ, Vaheri A, Koskiniemi M.** 2007. Evidence for human herpesvirus 6 variant A antibodies in multiple sclerosis: diagnostic and therapeutic implications. J Neurovirol **13:**347-352.
29. **Appleton AL, Sviland L, Peiris JS, Taylor CE, Wilkes J, Green MA, Pearson AD, Kelly PJ, Malcolm AJ, Proctor SJ, et al.** 1995. Human herpes virus-6 infection in marrow graft recipients: role in pathogenesis of graft-versus-host disease. Newcastle upon Tyne Bone Marrow Transport Group. Bone Marrow Transplant **16:**777-782.
30. **Ablashi DV, Eastman HB, Owen CB, Roman MM, Friedman J, Zabriskie JB, Peterson DL, Pearson GR, Whitman JE.** 2000. Frequent HHV-6 reactivation in multiple sclerosis (MS) and chronic fatigue syndrome (CFS) patients. J Clin Virol **16:**179-191.
31. **Ablashi DV, Devin CL, Yoshikawa T, Lautenschlager I, Luppi M, Kuhl U, Komaroff AL.** 2010. Review Part 3: Human herpesvirus-6 in multiple non-neurological diseases. J Med Virol **82:**1903-1910.
32. **Yao K, Crawford JR, Komaroff AL, Ablashi DV, Jacobson S.** 2010. Review part 2: Human herpesvirus-6 in central nervous system diseases. J Med Virol **82:**1669-1678.

33. **Caselli E, Zatelli MC, Rizzo R, Benedetti S, Martorelli D, Trasforini G, Cassai E, degli Uberti EC, Di Luca D, Dolcetti R.** 2012. Virologic and immunologic evidence supporting an association between HHV-6 and Hashimoto's thyroiditis. PLoS Pathog **8:**e1002951.
34. **Gobbi A, Stoddart CA, Malnati MS, Locatelli G, Santoro F, Abbey NW, Bare C, Linquist-Stepps V, Moreno MB, Herndier BG, Lusso P, McCune JM.** 1999. Human herpesvirus 6 (HHV-6) causes severe thymocyte depletion in SCID-hu Thy/Liv mice. J Exp Med **189:**1953-1960.
35. **Emery VC, Atkins MC, Bowen EF, Clark DA, Johnson MA, Kidd IM, McLaughlin JE, Phillips AN, Strappe PM, Griffiths PD.** 1999. Interactions between beta-herpesviruses and human immunodeficiency virus in vivo: evidence for increased human immunodeficiency viral load in the presence of human herpesvirus 6. J Med Virol **57:**278-282.
36. **Lusso P, Gallo RC.** 1995. Human herpesvirus 6 in AIDS. Immunol Today **16:**67-71.
37. **Broccolo F, Cassina G, Chiari S, Garcia-Parra R, Villa A, Leone BE, Brenna A, Locatelli G, Mangioni C, Cocuzza CE.** 2008. Frequency and clinical significance of human beta-herpesviruses in cervical samples from Italian women. J Med Virol **80:**147-153.
38. **Nakayama-Ichiyama S, Yokote T, Iwaki K, Miyoshi T, Takubo T, Tsuji M, Hanafusa T.** 2011. Co-infection of human herpesvirus-6 and human herpesvirus-8 in primary cutaneous diffuse large B cell lymphoma, leg type. Br J Haematol **155:**514-516.
39. **Lacroix A, Collot-Teixeira S, Mardivirin L, Jaccard A, Petit B, Piguet C, Sturtz F, Preux PM, Bordessoule D, Ranger-Rogez S.** 2010. Involvement of human herpesvirus-6 variant B in classic Hodgkin's lymphoma via DR7 oncoprotein. Clin Cancer Res **16:**4711-4721.
40. **Luppi M, Marasca R, Barozzi P, Artusi T, Torelli G.** 1993. Frequent detection of human herpesvirus-6 sequences by polymerase chain reaction in paraffin-embedded lymph nodes from patients with angioimmunoblastic lymphadenopathy and angioimmunoblastic lymphadenopathy-like lymphoma. Leuk Res **17:**1003-1011.
41. **Nakayama-Ichiyama S, Yokote T, Kobayashi K, Hirata Y, Hiraoka N, Iwaki K, Takayama A, Akioka T, Oka S, Miyoshi T, Fukui H, Tsuda Y, Takubo T, Tsuji M, Higuchi K, Hanafusa T.** 2011. Primary effusion lymphoma of T-cell origin with t(7;8)(q32;q13) in an HIV-negative patient with HCV-related liver cirrhosis and hepatocellular carcinoma positive for HHV6 and HHV8. Ann Hematol **90:**1229-1231.
42. **Razzaque A.** 1990. Oncogenic potential of human herpesvirus-6 DNA. Oncogene **5:**1365-1370.
43. **Thomson BJ, Efstathiou S, Honess RW.** 1991. Acquisition of the human adeno-associated virus type-2 rep gene by human herpesvirus type-6. Nature **351:**78-80.
44. **Leibovitch EC, Jacobson S.** 2014. Evidence linking HHV-6 with multiple sclerosis: an update. Curr Opin Virol **9:**127-133.
45. **Gordon L, McQuaid S, Cosby SL.** 1996. Detection of herpes simplex virus (types 1 and 2) and human herpesvirus 6 DNA in human brain tissue by polymerase chain reaction. Clin Diagn Virol **6:**33-40.
46. **Liedtke W, Malessa R, Faustmann PM, Eis-Hübinger AM.** 1995. Human herpesvirus 6 polymerase chain reaction findings in human immunodeficiency virus associated neurological disease and multiple sclerosis. J Neurovirol **1:**253-258.
47. **Sanders VJ, Felisan S, Waddell A, Tourtellotte WW.** 1996. Detection of herpesviridae in postmortem multiple sclerosis brain tissue and controls by polymerase chain reaction. J Neurovirol **2:**249-258.
48. **Cermelli C, Berti R, Soldan SS, Mayne M, D'ambrosia JM, Ludwin SK, Jacobson S.** 2003. High frequency of human herpesvirus 6 DNA in multiple sclerosis plaques isolated by laser microdissection. J Infect Dis **187:**1377-1387.

49. **Reynaud JM, Jégou JF, Welsch JC, Horvat B.** 2014. Human Herpesvirus 6A Infection in CD46 Transgenic Mice: Viral Persistence in the Brain and Increased Production of Proinflammatory Chemokines via Toll-Like Receptor 9. J Virol **88:**5421-5436.
50. **Leibovitch E, Wohler JE, Cummings Macri SM, Motanic K, Harberts E, Gaitán MI, Maggi P, Ellis M, Westmoreland S, Silva A, Reich DS, Jacobson S.** 2013. Novel marmoset (Callithrix jacchus) model of human Herpesvirus 6A and 6B infections: immunologic, virologic and radiologic characterization. PLoS Pathog **9:**e1003138.
51. **Reynaud JM, Horvat B.** 2013. Animal models for human herpesvirus 6 infection. Front Microbiol **4:**174.
52. **Mock DJ, Strathmann F, Blumberg BM, Mayer-Proschel M.** 2006. Infection of murine oligodendroglial precursor cells with Human Herpesvirus 6 (HHV-6)--establishment of a murine in vitro model. J Clin Virol **37 Suppl 1:**S17-23.
53. **Greiner DL, Hesselton RA, Shultz LD.** 1998. SCID mouse models of human stem cell engraftment. Stem Cells **16:**166-177.
54. **Kraft DL, Weissman IL, Waller EK.** 1993. Differentiation of CD3-4-8- human fetal thymocytes in vivo: characterization of a CD3-4+8- intermediate. J Exp Med **178:**265-277.
55. **Gobbi A, Stoddart CA, Locatelli G, Santoro F, Bare C, Linquist-Stepps V, Moreno ME, Abbey NW, Herndier BG, Malnati MS, McCune JM, Lusso P.** 2000. Coinfection of SCID-hu Thy/Liv mice with human herpesvirus 6 and human immunodeficiency virus type 1. J Virol **74:**8726-8731.
56. **Reynaud JM, Jégou JF, Welsch JC, Horvat B.** 2014. Human Herpesvirus 6A Infection in CD46 Transgenic Mice: Viral Persistence in the Brain and Increased Production of Proinflammatory Chemokines via Toll-Like Receptor 9. J Virol **88:**5421-5436.
57. **Lusso P, Crowley RW, Malnati MS, Di Serio C, Ponzoni M, Biancotto A, Markham PD, Gallo RC.** 2007. Human herpesvirus 6A accelerates AIDS progression in macaques. Proc Natl Acad Sci U S A **104:**5067-5072.
58. **Yalcin S, Mukai T, Kondo K, Ami Y, Okawa T, Kojima A, Kurata T, Yamanishi K.** 1992. Experimental infection of cynomolgus and African green monkeys with human herpesvirus 6. J Gen Virol **73 (Pt 7):**1673-1677.
59. **Gardner MB, Luciw PA.** 2008. Macaque models of human infectious disease. ILAR J **49:**220-255.
60. **Lusso P, Secchiero P, Crowley RW.** 1994. In vitro susceptibility of Macaca nemestrina to human herpesvirus 6: a potential animal model of coinfection with primate immunodeficiency viruses. AIDS Res Hum Retroviruses **10:**181-187.
61. **Lusso P, Markham PD, DeRocco SE, Gallo RC.** 1990. In vitro susceptibility of T lymphocytes from chimpanzees (Pan troglodytes) to human herpesvirus 6 (HHV-6): a potential animal model to study the interaction between HHV-6 and human immunodeficiency virus type 1 in vivo. J Virol **64:**2751-2758.
62. **Lacoste V, Verschoor EJ, Nerrienet E, Gessain A.** 2005. A novel homologue of Human herpesvirus 6 in chimpanzees. J Gen Virol **86:**2135-2140.
63. **McCune JM, Namikawa R, Kaneshima H, Shultz LD, Lieberman M, Weissman IL.** 1988. The SCID-hu mouse: murine model for the analysis of human hematolymphoid differentiation and function. Science **241:**1632-1639.
64. **Mosier DE, Gulizia RJ, Baird SM, Wilson DB.** 1988. Transfer of a functional human immune system to mice with severe combined immunodeficiency. Nature **335:**256-259.
65. **Berges BK, Rowan MR.** 2011. The utility of the new generation of humanized mice to study HIV-1 infection: transmission, prevention, pathogenesis, and treatment, p 65, Retrovirology, vol 8, England.
66. **Smith MS, Goldman DC, Bailey AS, Pfaffle DL, Kreklywich CN, Spencer DB, Othieno FA, Streblow DN, Garcia JV, Fleming WH, Nelson JA.** 2010. Granulocyte-colony stimulating factor

reactivates human cytomegalovirus in a latently infected humanized mouse model. Cell Host Microbe **8:**284-291.

67. **Ma SD, Hegde S, Young KH, Sullivan R, Rajesh D, Zhou Y, Jankowska-Gan E, Burlingham WJ, Sun X, Gulley ML, Tang W, Gumperz JE, Kenney SC.** 2011. A new model of Epstein-Barr virus infection reveals an important role for early lytic viral protein expression in the development of lymphomas. J Virol **85:**165-177.
68. **Banerjee P, Tripp A, Lairmore MD, Crawford L, Sieburg M, Ramos JC, Harrington W, Jr., Beilke MA, Feuer G.** 2010. Adult T-cell leukemia/lymphoma development in HTLV-1-infected humanized SCID mice. Blood **115:**2640-2648.
69. **Traggiai E, Chicha L, Mazzucchelli L, Bronz L, Piffaretti JC, Lanzavecchia A, Manz MG.** 2004. Development of a human adaptive immune system in cord blood cell-transplanted mice. Science **304:**104-107.
70. **Kuruvilla JG, Troyer RM, Devi S, Akkina R.** 2007. Dengue virus infection and immune response in humanized Rag2$^{-/-}\gamma c^{-/-}$ (RAG-hu) mice. Virol **369:**143-152.
71. **Berges BK, Wheat WH, Palmer BE, Connick E, Akkina R.** 2006. HIV-1 infection and CD4 T cell depletion in the humanized Rag2-/-gc-/- (RAG-hu) mouse model. Retrovirology **3:**76.
72. **Ishikawa F, Yasukawa M, Lyons B, Yoshida S, Miyamoto T, Yoshimoto G, Watanabe T, Akashi K, Shultz LD, Harada M.** 2005. Development of functional human blood and immune systems in NOD/SCID/IL2 receptor {gamma} chain(null) mice. Blood **106:**1565-1573.
73. **Chen Q, Khoury M, Chen J.** 2010. Expression of human cytokines dramatically improves reconstitution of specific human-blood lineage cells in humanized mice. Proc Natl Acad Sci U S A **106:**21783-21788.
74. **Hu Z, Van Rooijen N, Yang YG.** 2011. Macrophages prevent human red blood cell reconstitution in immunodeficient mice. Blood **118:**5938-5946.
75. **Hu Z, Yang YG.** 2012. Full reconstitution of human platelets in humanized mice after macrophage depletion. Blood **120:**1713-1716.
76. **Berges BK, Akkina SR, Folkvord JM, Connick E, Akkina R.** 2008. Mucosal transmission of R5 and X4 tropic HIV-1 via vaginal and rectal routes in humanized Rag2-/-gc-/- (RAG-hu) mice. Virology **373:**342-351.
77. **Sun Z, Denton PW, Estes JD, Othieno FA, Wei BL, Wege AK, Melkus MW, Padgett-Thomas A, Zupancic M, Haase AT, Garcia JV.** 2007. Intrarectal transmission, systemic infection, and CD4+ T cell depletion in humanized mice infected with HIV-1. J Exp Med **204:**705-714.
78. **Dash PK, Gorantla S, Gendelman HE, Knibbe J, Casale GP, Makarov E, Epstein AA, Gelbard HA, Boska MD, Poluektova LY.** 2011. Loss of Neuronal Integrity during Progressive HIV-1 Infection of Humanized Mice. J Neurosci **31:**3148-3157.
79. **Gorantla S, Makarov E, Finke-Dwyer J, Castanedo A, Holguin A, Gebhart CL, Gendelman HE, Poluektova L.** 2010. Links between Progressive HIV-1 Infection of Humanized Mice and Viral Neuropathogenesis. Am J Pathol **177:**2938-2949.
80. **Bonnet D.** 2001. Normal and leukemic CD34-negative human hematopoietic stem cells. Rev Clin Exp Hematol **5:**42-61.
81. **Notta F, Doulatov S, Laurenti E, Poeppl A, Jurisica I, Dick JE.** 2011. Isolation of single human hematopoietic stem cells capable of long-term multilineage engraftment. Science **333:**218-221.
82. **Kalscheuer H, Danzl N, Onoe T, Faust T, Winchester R, Goland R, Greenberg E, Spitzer TR, Savage DG, Tahara H, Choi G, Yang YG, Sykes M.** 2012. A model for personalized in vivo analysis of human immune responsiveness. Sci Transl Med **4:**125ra130.
83. **Shultz LD, Lyons BL, Burzenski LM, Gott B, Chen X, Chaleff S, Kotb M, Gillies SD, King M, Mangada J, Greiner DL, Handgretinger R.** 2005. Human lymphoid and myeloid cell development

in NOD/LtSz-scid IL2R gamma null mice engrafted with mobilized human hemopoietic stem cells. J Immun **174:**6477-6489.

84. **van der Loo JC, Hanenberg H, Cooper RJ, Luo FY, Lazaridis EN, Williams DA.** 1998. Nonobese diabetic/severe combined immunodeficiency (NOD/SCID) mouse as a model system to study the engraftment and mobilization of human peripheral blood stem cells. Blood **92:**2556-2570.
85. **Anderson JS, Bandi S, Kaufman DS, Akkina R.** 2006. Derivation of normal macrophages from human embryonic stem (hES) cells for applications in HIV gene therapy. Retrovirology **3:**24.
86. **Choi KD, Yu J, Smuga-Otto K, Salvagiotto G, Rehrauer W, Vodyanik M, Thomson J, Slukvin I.** 2009. Hematopoietic and endothelial differentiation of human induced pluripotent stem cells. Stem Cells **27:**559-567.
87. **Kaufman DS, Hanson ET, Lewis RL, Auerbach R, Thomson JA.** 2001. Hematopoietic colony-forming cells derived from human embryonic stem cells. Proc Natl Acad Sci U S A **98:**10716-10721.
88. **Tian X, Woll PS, Morris JK, Linehan JL, Kaufman DS.** 2006. Hematopoietic engraftment of human embryonic stem cell-derived cells is regulated by recipient innate immunity. Stem Cells **24:**1370-1380.
89. **Akkina R, Berges BK, Palmer BE, Remling L, Neff CP, Kuruvilla J, Connick E, Folkvord J, Gagliardi K, Kassu A, Akkina SR.** 2011. Humanized Rag1-/-gamma-chain-/- mice support multilineage hematopoiesis and are susceptible to HIV-1 infection via systemic and vaginal routes. PLos ONE **6:**e20169.
90. **Bente DA, Melkus MW, Garcia JV, Rico-Hesse R.** 2005. Dengue fever in humanized NOD/SCID mice. J Virol **79:**13797-13799.
91. **Watanabe S, Terashima K, Ohta S, Horibata S, Yajima M, Shiozawa Y, Dewan MZ, Yu Z, Ito M, Morio T, Shimizu N, Honda M, Yamamoto N.** 2007. Hematopoietic stem cell-engrafted NOD/SCID/IL2R{gamma}null mice develop human lymphoid system and induce long-lasting HIV-1 infection with specific humoral immune responses. Blood **109:**212-218.
92. **Brehm MA, Cuthbert A, Yang C, Miller DM, DiIorio P, Laning J, Burzenski L, Gott B, Foreman O, Kavirayani A, Herlihy M, Rossini AA, Shultz LD, Greiner DL.** 2010. Parameters for establishing humanized mouse models to study human immunity: analysis of human hematopoietic stem cell engraftment in three immunodeficient strains of mice bearing the IL2rgamma(null) mutation. Clin Immunol **135:**84-98.
93. **Waskow C, Madan V, Bartels S, Costa C, Blasig R, Rodewald HR.** 2009. Hematopoietic stem cell transplantation without irradiation. Nat Methods **6:**267-269.
94. **Shultz LD, Brehm MA, Garcia-Martinez JV, Greiner DL.** 2012. Humanized mice for immune system investigation: progress, promise and challenges. Nat Rev Immunol **12:**786-798.
95. **Shultz LD, Ishikawa F, Greiner DL.** 2007. Humanized mice in translational biomedical research. Nat Rev Immunol **7:**118-130.
96. **Zhang B, Duan Z, Zhao Y.** 2009. Mouse models with human immunity and their application in biomedical research. J Cell Mol Med **13:**1043-1058.
97. **Joo SY, Choi BK, Kang MJ, Jung DY, Park KS, Park JB, Choi GS, Joh J, Kwon CH, Jung GO, Lee SK, Kim SJ.** 2009. Development of Functional Human Immune System With the Transplantations of Human Fetal Liver/Thymus Tissues and Expanded Hematopoietic Stem Cells in RAG2(-/-
)gamma(c)(-/-) Mice. Transplant Proc **41:**1885-1890.
98. **Denton PW, García JV.** 2011. Humanized Mouse Models of HIV Infection. AIDS Rev **13:**135-148.
99. **Stoddart CA, Maidji E, Galkina SA, Kosikova G, Rivera JM, Moreno ME, Sloan B, Joshi P, Long BR.** 2011. Superior human leukocyte reconstitution and susceptibility to vaginal HIV transmission in humanized NOD-scid IL-2Rγ(-/-) (NSG) BLT mice. Virol **417:**154-160.

100. **Hall KM, Horvath TL, Abonour R, Cornetta K, Srour EF.** 2006. Decreased homing of retrovirally transduced human bone marrow CD34+ cells in the NOD/SCID mouse model. Exp Hematol **34:**433-442.
101. **Takahashi M, Tsujimura N, Otsuka K, Yoshino T, Mori T, Matsunaga T, Nakasono S.** 2012. Comprehensive evaluation of leukocyte lineage derived from human hematopoietic cells in humanized mice. J Biosci Bioeng **113:**529-535.
102. **Berges BK, Akkina SR, Remling L, Akkina R.** 2010. Humanized Rag2(-/-)gammac(-/-) (RAG-hu) mice can sustain long-term chronic HIV-1 infection lasting more than a year. Virol **397:**100-103.
103. **Baenziger S, Tussiwand R, Schlaepfer E, Mazzucchelli L, Heikenwalder M, Kurrer MO, Behnke S, Frey J, Oxenius A, Joller H, Aguzzi A, Manz MG, Speck RF.** 2006. Disseminated and sustained HIV infection in CD34+ cord blood cell-transplanted Rag2-/-{gamma}c-/- mice. Proc Natl Acad Sci USA **103:**15951-15956.
104. **Sato K, Nie C, Misawa N, Tanaka Y, Ito M, Koyanagi Y.** 2010. Dynamics of memory and naïve CD8(+) T lymphocytes in humanized NOD/SCID/IL-2Rgamma(null) mice infected with CCR5-tropic HIV-1. Vaccine **28S2:**B32-B37.
105. **Gorantla S, Sneller H, Walters L, Sharp JG, Pirruccello SJ, West JT, Wood C, Dewhurst S, Gendelman HE, Poluektova L.** 2007. Human Immunodeficiency Virus Type 1 pathobiology studied in humanized Balb/c-Rag2-/-{gamma}c-/- mice. J Virol **81:**2700-2712.
106. **Lang J, Weiss N, Freed BM, Torres RM, Pelanda R.** 2011. Generation of hematopoietic humanized mice in the newborn BALB/c-Rag2(null)Il2rγ(null) mouse model: A multivariable optimization approach. Clin Immunol **140:**102-116.
107. **Zhang L, Kovalev GI, Su L.** 2006. HIV-1 infection and pathogenesis in a novel humanized mouse model. Blood **109:**2978-2981.
108. **Ishikawa F, Livingston AG, Wingard JR, Nishikawa S, Ogawa M.** 2002. An assay for long-term engrafting human hematopoietic cells based on newborn NOD/SCID/beta2-microglobulin(null) mice. Exp Hematol **30:**488-494.
109. **Campadelli-Fiume G, Mirandola P, Menotti L.** 1999. Human herpesvirus 6: An emerging pathogen. Emerg Infect Dis **5:**353-366.
110. **Traggiai E, Chicha L, Mazzucchelli L, Bronz L, Piffaretti JC, Lanzavecchia A, Manz MG.** 2004. Development of a human adaptive immune system in cord blood cell-transplanted mice. Science **304:**104-107.
111. **Schleiss MR.** 2006. Nonprimate models of congenital cytomegalovirus (CMV) infection: gaining insight into pathogenesis and prevention of disease in newborns. ILAR J **47:**65-72.
112. **Wakiguchi H.** 2002. Overview of Epstein-Barr virus-associated diseases in Japan. Crit Rev Oncol Hematol **44:**193-202.
113. **Rickinson AB, Kieff E.** 2007. Epstein-Barr Virus, p 2655-2700. *In* Knipe DM (ed), Field's Virology, vol 2. Lippincott Williams & Wilkins, Philadelphia.
114. **Longnecker RM, Kieff E, Cohen JI.** 2013. Epstein-Barr virus, p 1898-1959. *In* Knipe DM, Howley PM (ed), Fields Virology, 6th ed. Lippincott Williams and Wilkins, Philadelphia, PA.
115. **Fuzzati-Armentero MT, Duchosal MA.** 1998. hu-PBL-SCID mice: an in vivo model of Epstein-Barr virus-dependent lymphoproliferative disease. Histol Histopathol **13:**155-168.
116. **Mosier DE, Gulizia RJ, Baird SM, Spector S, Spector D, Kipps TJ, Fox RI, Carson DA, Cooper N, Richman DD.** 1989. Studies of HIV infection and the development of Epstein-Barr virus-related B cell lymphomas following transfer of human lymphocytes to mice with severe combined immunodeficiency. Curr Top Micro Immun **152:**195-199.
117. **Islas-Ohlmayer M, Padgett-Thomas A, Domiati-Saad R, Melkus MW, Cravens PD, Martin Mdel P, Netto G, Garcia JV.** 2004. Experimental infection of NOD/SCID mice reconstituted with human CD34+ cells with Epstein-Barr virus. J Virol **78:**13891-13900.

118. **Wahl A, Linnstaedt SD, Esoda C, Krisko JF, Martinez-Torres F, Delecluse HJ, Cullen BR, Garcia JV.** 2013. A Cluster of Virus-encoded microRNAs Accelerates Acute Systemic Epstein-Barr Virus Infection but does not Significantly Enhance Virus-induced Oncogenesis In Vivo. J Virol **87:**5437-5446.
119. **Cocco M, Bellan C, Tussiwand R, Corti D, Traggiai E, Lazzi S, Mannucci S, Bronz L, Palummo N, Ginanneschi C, Tosi P, Lanzavecchia A, Manz MG, Leoncini L.** 2008. CD34+ Cord Blood Cell-Transplanted Rag2-/- {gamma}c-/- Mice as a Model for Epstein-Barr Virus Infection. Am J Pathol **173:**1369-1378.
120. **Heuts F, Rottenberg ME, Salamon D, Rasul E, Adori M, Klein G, Klein E, Nagy N.** 2014. T Cells Modulate Epstein-Barr Virus Latency Phenotypes During Infection of Humanized Mice. J Virol **88:**3235-3245.
121. **Strowig T, Gurer C, Ploss A, Liu YF, Arrey F, Sashihara J, Koo G, Rice CM, Young JW, Chadburn A, Cohen JI, Münz C.** 2009. Priming of protective T cell responses against virus-induced tumors in mice with human immune system components. J Exp Med **206:**1423-1434.
122. **Yajima M, Imadome K, Nakagawa A, Watanabe S, Terashima K, Nakamura H, Ito M, Shimizu N, Honda M, Yamamoto N, Fujiwara S.** 2008. A new humanized mouse model of Epstein-Barr virus infection that reproduces persistent infection, lymphoproliferative disorder, and cell-mediated and humoral immune responses. J Inf Dis **198:**673-682.
123. **Sato K, Misawa N, Nie C, Satou Y, Iwakiri D, Matsuoka M, Takahashi R, Kuzushima K, Ito M, Takada K, Koyanagi Y.** 2011. A novel animal model of Epstein-Barr virus-associated hemophagocytic lymphohistiocytosis in humanized mice. Blood **117:**5663-5673.
124. **Kuwana Y, Takei M, Yajima M, Imadome K, Inomata H, Shiozaki M, Ikumi N, Nozaki T, Shiraiwa H, Kitamura N, Takeuchi J, Sawada S, Yamamoto N, Shimizu N, Ito M, Fujiwara S.** 2011. Epstein-barr virus induces erosive arthritis in humanized mice. PLoS ONE **6:**e26630.
125. **Yajima M, Imadome KI, Nakagawa A, Watanabe S, Terashima K, Nakamura H, Ito M, Shimizu N, Yamamoto N, Fujiwara S.** 2009. T Cell-Mediated Control of Epstein-Barr Virus Infection in Humanized Mice. J Inf Dis **200:**1611-1615.
126. **Ma SD, Hegde S, Young KH, Sullivan R, Rajesh D, Zhou Y, Jankowska-Gan E, Burlingham WJ, Sun X, Gulley ML, Tang W, Gumperz JE, Kenney SC.** 2011. A new model of EBV infection reveals an important role for early lytic viral protein expression in the development of lymphomas. J Virol **85:**165-177.
127. **Van Duyne R, Pedati C, Guedel I, Carpio L, Kehn-Hall K, Saifuddin M, Kashanchi F.** 2009. Th**e utilization of humanized mouse models for the study of human retroviral infections**. Retrovirology **76**.
128. **Baenziger S, Tussiwand R, Schlaepfer E, Mazzucchelli L, Heikenwalder M, Kurrer MO, Behnke S, Frey J, Oxenius A, Joller H, Aguzzi A, Manz MG, Speck RF.** 2006. Disseminated and sustained HIV infection in CD34+ cord blood cell-transplanted Rag2-/-gamma c-/- mice. Proc Natl Acad Sci U S A **103:**15951-15956.
129. **Berges BK, Akkina SR, Remling L, Akkina R.** 2010. Humanized Rag2(-/-)gammac(-/-) (RAG-hu) mice can sustain long-term chronic HIV-1 infection lasting more than a year. Virology **397:**100-103.
130. **Berges BK, Wheat WH, Palmer BE, Connick E, Akkina R.** 2006. HIV-1 infection and CD4 T cell depletion in the humanized Rag2-/-γc-/- (RAG-hu) mouse model. Retrovirology.
131. **Zhang L, Kovalev GI, Su L.** 2007. HIV-1 infection and pathogenesis in a novel humanized mouse model. Blood **109:**2978-2981.
132. **Marsden MD, Kovochich M, Suree N, Shimizu S, Mehta R, Cortado R, Bristol G, An DS, Zack JA.** 2011. HIV latency in the humanized BLT mouse. J Virol.

133. **Flamand L, Komaroff AL, Arbuckle JH, Medveczky PG, Ablashi DV.** 2010. Review, part 1: Human herpesvirus-6-basic biology, diagnostic testing, and antiviral efficacy. J Med Virol **82:**1560-1568.
134. **Comerford I, Harata-Lee Y, Bunting MD, Gregor C, Kara EE, McColl SR.** 2013. A myriad of functions and complex regulation of the CCR7/CCL19/CCL21 chemokine axis in the adaptive immune system. Cytokine Growth Factor Rev **24:**269-283.
135. **Catusse J, Spinks J, Mattick C, Dyer A, Laing K, Fitzsimons C, Smit MJ, Gompels UA.** 2008. Immunomodulation by herpesvirus U51A chemokine receptor via CCL5 and FOG-2 down-regulation plus XCR1 and CCR7 mimicry in human leukocytes. Eur J Immunol **38:**763-777.
136. **Dewin DR, Catusse J, Gompels UA.** 2006. Identification and characterization of U83A viral chemokine, a broad and potent beta-chemokine agonist for human CCRs with unique selectivity and inhibition by spliced isoform. J Immunol **176:**544-556.
137. **Clark DJ, Catusse J, Stacey A, Borrow P, Gompels UA.** 2013. Activation of CCR2+ human proinflammatory monocytes by human herpesvirus-6B chemokine N-terminal peptide. J Gen Virol **94:**1624-1635.
138. **French C, Menegazzi P, Nicholson L, Macaulay H, DiLuca D, Gompels UA.** 1999. Novel, nonconsensus cellular splicing regulates expression of a gene encoding a chemokine-like protein that shows high variation and is specific for human herpesvirus 6. Virology **262:**139-151.
139. **Catusse J, Parry CM, Dewin DR, Gompels UA.** 2007. Inhibition of HIV-1 infection by viral chemokine U83A via high-affinity CCR5 interactions that block human chemokine-induced leukocyte chemotaxis and receptor internalization. Blood **109:**3633-3639.
140. **Fitzsimons CP, Gompels UA, Verzijl D, Vischer HF, Mattick C, Leurs R, Smit MJ.** 2006. Chemokine-directed trafficking of receptor stimulus to different g proteins: selective inducible and constitutive signaling by human herpesvirus 6-encoded chemokine receptor U51. Mol Pharmacol **69:**888-898.
141. **Cerdan C, Devilard E, Xerri L, Olive D.** 2001. The C-class chemokine lymphotactin costimulates the apoptosis of human CD4(+) T cells. Blood **97:**2205-2212.
142. **Hasegawa H, Utsunomiya Y, Yasukawa M, Yanagisawa K, Fujita S.** 1994. Induction of G protein-coupled peptide receptor EBI 1 by human herpesvirus 6 and 7 infection in CD4+ T cells. J Virol **68:**5326-5329.
143. **Tadagaki K, Nakano K, Yamanishi K.** 2005. Human herpesvirus 7 open reading frames U12 and U51 encode functional beta-chemokine receptors. J Virol **79:**7068-7076.
144. **Grivel JC, Santoro F, Chen S, Faga G, Malnati MS, Ito Y, Margolis L, Lusso P.** 2003. Pathogenic effects of human herpesvirus 6 in human lymphoid tissue ex vivo. J Virol **77:**8280-8289.
145. **Yasukawa M, Hasegawa A, Sakai I, Ohminami H, Arai J, Kaneko S, Yakushijin Y, Maeyama K, Nakashima H, Arakaki R, Fujita S.** 1999. Down-regulation of CXCR4 by human herpesvirus 6 (HHV-6) and HHV-7. J Immunol **162:**5417-5422.
146. **Karpova D, Bonig H.** 2015. Concise Review: CXCR4/CXCL12 Signaling in Immature Hematopoiesis--Lessons From Pharmacological and Genetic Models. Stem Cells **33:**2391-2399.
147. **Poznansky MC, Olszak IT, Evans RH, Wang Z, Foxall RB, Olson DP, Weibrecht K, Luster AD, Scadden DT.** 2002. Thymocyte emigration is mediated by active movement away from stroma-derived factors. J Clin Invest **109:**1101-1110.
148. **Weinreich MA, Hogquist KA.** 2008. Thymic emigration: when and how T cells leave home. J Immunol **181:**2265-2270.
149. **Calderón L, Boehm T.** 2011. Three chemokine receptors cooperatively regulate homing of hematopoietic progenitors to the embryonic mouse thymus. Proc Natl Acad Sci U S A **108:**7517-7522.

150. **Grivel JC, Ito Y, Fagà G, Santoro F, Shaheen F, Malnati MS, Fitzgerald W, Lusso P, Margolis L.** 2001. Suppression of CCR5- but not CXCR4-tropic HIV-1 in lymphoid tissue by human herpesvirus 6. Nat Med **7:**1232-1235.
151. **Milne RS, Mattick C, Nicholson L, Devaraj P, Alcami A, Gompels UA.** 2000. RANTES binding and down-regulation by a novel human herpesvirus-6 beta chemokine receptor. J Immunol **164:**2396-2404.
152. **Yamanishi K, Okuno T, Shiraki K, Takahashi M, Kondo T, Asano Y, Kurata T.** 1988. Identification of human herpesvirus-6 as a causal agent for exanthem subitum. Lancet **1:**1065-1067.
153. **Martin LK, Schub A, Dillinger S, Moosmann A.** 2012. Specific CD8$^+$ T cells recognize human herpesvirus 6B. Eur J Immunol **42:**2901-2912.
154. **Tang H, Serada S, Kawabata A, Ota M, Hayashi E, Naka T, Yamanishi K, Mori Y.** 2013. CD134 is a cellular receptor specific for human herpesvirus-6B entry. Proc Natl Acad Sci U S A **110:**9096-9099.
155. **Lüttichau HR, Clark-Lewis I, Jensen P, Moser C, Gerstoft J, Schwartz TW.** 2003. A highly selective CCR2 chemokine agonist encoded by human herpesvirus 6. J Biol Chem **278:**10928-10933.
156. **Zou P, Isegawa Y, Nakano K, Haque M, Horiguchi Y, Yamanishi K.** 1999. Human herpesvirus 6 open reading frame U83 encodes a functional chemokine. J Virol **73:**5926-5933.
157. **Balkwill F.** 2004. Cancer and the chemokine network. Nat Rev Cancer **4:**540-550.
158. **Isegawa Y, Ping Z, Nakano K, Sugimoto N, Yamanishi K.** 1998. Human herpesvirus 6 open reading frame U12 encodes a functional beta-chemokine receptor. J Virol **72:**6104-6112.
159. **Vahlne A.** 2009. A historical reflection on the discovery of human retroviruses. Retrovirology **6:**40.
160. **Sierra S, Kupfer B, Kaiser R.** 2005. Basics of the virology of HIV-1 and its replication. J Clin Virol **34:**233-244.
161. **Lusso P, Ensoli B, Markham PD, Ablashi DV, Salahuddin SZ, Tschachler E, Wong-Staal F, Gallo RC.** 1989. Productive dual infection of human CD4+ T lymphocytes by HIV-1 and HHV-6. Nature **337:**370-373.
162. **Flamand L, Romerio F, Reitz MS, Gallo RC.** 1998. CD4 promoter transactivation by human herpesvirus 6. J Virol **72:**8797-8805.
163. **Ensoli B, Lusso P, Schachter F, Josephs SF, Rappaport J, Negro F, Gallo RC, Wong-Staal F.** 1989. Human herpes virus-6 increases HIV-1 expression in co-infected T cells via nuclear factors binding to the HIV-1 enhancer. EMBO J **8:**3019-3027.
164. **Kashanchi F, Thompson J, Sadaie MR, Doniger J, Duvall J, Brady JN, Rosenthal LJ.** 1994. Transcriptional activation of minimal HIV-1 promoter by ORF-1 protein expressed from the SalI-L fragment of human herpesvirus 6. Virology **201:**95-106.
165. **Denton PW, García JV.** 2011. Humanized mouse models of HIV infection. AIDS Rev **13:**135-148.
166. **Berges BK, Rowan MR.** 2011. The utility of the new generation of humanized mice to study HIV-1 infection: transmission, prevention, pathogenesis, and treatment. Retrovirology **8:**65.
167. **Sanchez FM, Cuadra GI, Nielsen SJ, Tanner A, Berges BK.** 2013. Production and characterization of humanized Rag2-/-γc -/- mice. Methods Mol Biol **1031:**19-26.
168. **Shultz LD, Ishikawa F, Greiner DL.** 2007. Humanized mice in translational biomedical research. Nat Rev Immunol **7:**118-130.
169. **Manz MG.** 2007. Human-hemato-lymphoid-system mice: opportunities and challenges. Immunity **26:**537-541.
170. **Lang J, Weiss N, Freed BM, Torres RM, Pelanda R.** 2011. Generation of hematopoietic humanized mice in the newborn BALB/c-Rag2null Il2rγnull mouse model: a multivariable optimization approach. Clin Immunol **140:**102-116.

171. **Shultz LD, Lyons BL, Burzenski LM, Gott B, Chen X, Chaleff S, Kotb M, Gillies SD, King M, Mangada J, Greiner DL, Handgretinger R.** 2005. Human lymphoid and myeloid cell development in NOD/LtSz-scid IL2R gamma null mice engrafted with mobilized human hemopoietic stem cells. J Immunol **174:**6477-6489.
172. **Kwant-Mitchell A, Ashkar AA, Rosenthal KL.** 2009. Mucosal innate and adaptive immune responses against HSV-2 in a humanized mouse model. J Virol **83:**10664-10676.
173. **Brehm MA, Cuthbert A, Yang C, Miller DM, DiIorio P, Laning J, Burzenski L, Gott B, Foreman O, Kavirayani A, Herlihy M, Rossini AA, Shultz LD, Greiner DL.** 2010. Parameters for establishing humanized mouse models to study human immunity: analysis of human hematopoietic stem cell engraftment in three immunodeficient strains of mice bearing the IL2rgamma(null) mutation. Clin Immunol **135:**84-98.
174. **Pearson T, Shultz LD, Miller D, King M, Laning J, Fodor W, Cuthbert A, Burzenski L, Gott B, Lyons B, Foreman O, Rossini AA, Greiner DL.** 2008. Non-obese diabetic-recombination activating gene-1 (NOD-Rag1 null) interleukin (IL)-2 receptor common gamma chain (IL2r gamma null) null mice: a radioresistant model for human lymphohaematopoietic engraftment. Clin Exp Immunol **154:**270-284.
175. **Rozemuller H, Knaän-Shanzer S, Hagenbeek A, van Bloois L, Storm G, Martens AC.** 2004. Enhanced engraftment of human cells in RAG2/gammac double-knockout mice after treatment with CL2MDP liposomes. Exp Hematol **32:**1118-1125.
176. **Tang H, Kawabata A, Yoshida M, Oyaizu H, Maeki T, Yamanishi K, Mori Y.** 2010. Human herpesvirus 6 encoded glycoprotein Q1 gene is essential for virus growth. Virology **407:**360-367.
177. **Kalejta RF, Bechtel JT, Shenk T.** 2003. Human cytomegalovirus pp71 stimulates cell cycle progression by inducing the proteasome-dependent degradation of the retinoblastoma family of tumor suppressors. Mol Cell Biol **23:**1885-1895.
178. **Reed LJ, Muench H.** 1938. A simple method of estimating fifty per cent endpoints. Am J Hyg **27:**493-497.
179. **Mörner A, Björndal A, Albert J, Kewalramani VN, Littman DR, Inoue R, Thorstensson R, Fenyö EM, Björling E.** 1999. Primary human immunodeficiency virus type 2 (HIV-2) isolates, like HIV-1 isolates, frequently use CCR5 but show promiscuity in coreceptor usage. J Virol **73:**2343-2349.
180. **Berges BK, Wheat WH, Palmer BE, Connick E, Akkina R.** 2006. HIV-1 infection and CD4 T cell depletion in the humanized Rag2-/-gamma c-/- (RAG-hu) mouse model. Retrovirology **3:**76.
181. **Gautheret-Dejean A, Manichanh C, Thien-Ah-Koon F, Fillet AM, Mangeney N, Vidaud M, Dhedin N, Vernant JP, Agut H.** 2002. Development of a real-time polymerase chain reaction assay for the diagnosis of human herpesvirus-6 infection and application to bone marrow transplant patients. J Virol Methods **100:**27-35.
182. **Salahuddin SZ, Ablashi DV, Markham PD, Josephs SF, Sturzenegger S, Kaplan M, Halligan G, Biberfeld P, Wong-Staal F, Kramarsky B, Gallo RC.** 1986. Isolation of a new virus, HBLV, in patients with lymphoproliferative disorders. Science **234:**596-601.
183. **Emery VC.** 2007. HHV-6A, 6B, and 7: persistence in the population, epidemiology and transmission - Human Herpesviruses - NCBI Bookshelf.
184. **Burbelo PD, Bayat A, Wagner J, Nutman TB, Baraniuk JN, Iadarola MJ.** 2012. No serological evidence for a role of HHV-6 infection in chronic fatigue syndrome. Am J Transl Res **4:**443-451.
185. **Santoro F, Kennedy PE, Locatelli G, Malnati MS, Berger EA, Lusso P.** 1999. CD46 is a cellular receptor for human herpesvirus 6. Cell **99:**817-827.
186. **Yamanishi K, Okuno T, Shiraki K, Takahashi M, Kondo T, Asano Y, Kurata T.** 1988. Identification of human herpesvirus-6 as a causal agent for exanthem subitum. Lancet **1:**1065-1067.
187. **Sola P, Merelli E, Marasca R, Poggi M, Luppi M, Montorsi M, Torelli G.** 1993. Human herpesvirus 6 and multiple sclerosis: survey of anti-HHV-6 antibodies by immunofluorescence

analysis and of viral sequences by polymerase chain reaction. J Neurol Neurosurg Psychiatry **56:**917-919.

188. **Behzad-Behbahani A, Mikaeili MH, Entezam M, Mojiri A, Pour GY, Arasteh MM, Rahsaz M, Banihashemi M, Khadang B, Moaddeb A, Nematollahi Z, Azarpira N.** 2011. Human herpesvirus-6 viral load and antibody titer in serum samples of patients with multiple sclerosis. J Microbiol Immunol Infect **44:**247-251.
189. **Agut H.** 2011. Deciphering the clinical impact of acute human herpesvirus 6 (HHV-6) infections. J Clin Virol **52:**164-171.
190. **Le J, Gantt S, Practice AIDCo.** 2013. Human herpesvirus 6, 7 and 8 in solid organ transplantation. Am J Transplant **13 Suppl 4:**128-137.
191. **Razonable RR, Zerr DM, Practice AIDCo.** 2009. HHV-6, HHV-7 and HHV-8 in solid organ transplant recipients. Am J Transplant **9 Suppl 4:**S97-100.
192. **Saraya T, Mikoshiba M, Kamiyama H, Yoshizumi M, Tsuchida S, Tsukagoshi H, Ishioka T, Terada M, Tanabe E, Tomioka C, Ishii H, Kimura H, Kozawa K, Shiohara T, Takizawa H, Goto H.** 2013. Evidence for reactivation of human herpesvirus 6 in generalized lymphadenopathy in a patient with drug-induced hypersensitivity syndrome. J Clin Microbiol **51:**1979-1982.
193. **Tohyama M, Hashimoto K, Yasukawa M, Kimura H, Horikawa T, Nakajima K, Urano Y, Matsumoto K, Iijima M, Shear NH.** 2007. Association of human herpesvirus 6 reactivation with the flaring and severity of drug-induced hypersensitivity syndrome. Br J Dermatol **157:**934-940.
194. **Ablashi DV, Devin CL, Yoshikawa T, Lautenschlager I, Luppi M, Kühl U, Komaroff AL.** 2010. Review Part 3: Human herpesvirus-6 in multiple non-neurological diseases. J Med Virol **82:**1903-1910.
195. **Gobbi A, Stoddart CA, Malnati MS, Locatelli G, Santoro F, Abbey NW, Bare C, Linquist-Stepps V, Moreno MB, Herndier BG, Lusso P, McCune JM.** 1999. Human herpesvirus 6 (HHV-6) causes severe thymocyte depletion in SCID-hu Thy/Liv mice. J Exp Med **189:**1953-1960.
196. **Emery VC, Atkins MC, Bowen EF, Clark DA, Johnson MA, Kidd IM, McLaughlin JE, Phillips AN, Strappe PM, Griffiths PD.** 1999. Interactions between beta-herpesviruses and human immunodeficiency virus in vivo: evidence for increased human immunodeficiency viral load in the presence of human herpesvirus 6. J Med Virol **57:**278-282.
197. **Lusso P, Gallo RC.** 1995. Human herpesvirus 6 in AIDS. Immunol Today **16:**67-71.
198. **Lusso P, Crowley RW, Malnati MS, Di Serio C, Ponzoni M, Biancotto A, Markham PD, Gallo RC.** 2007. Human herpesvirus 6A accelerates AIDS progression in macaques. Proc Natl Acad Sci U S A **104:**5067-5072.
199. **Lusso P, Markham PD, DeRocco SE, Gallo RC.** 1990. In vitro susceptibility of T lymphocytes from chimpanzees (Pan troglodytes) to human herpesvirus 6 (HHV-6): a potential animal model to study the interaction between HHV-6 and human immunodeficiency virus type 1 in vivo. J Virol **64:**2751-2758.
200. **Lusso P, Secchiero P, Crowley RW.** 1994. In vitro susceptibility of Macaca nemestrina to human herpesvirus 6: a potential animal model of coinfection with primate immunodeficiency viruses. AIDS Res Hum Retroviruses **10:**181-187.
201. **Leibovitch E, Wohler JE, Cummings Macri SM, Motanic K, Harberts E, Gaitán MI, Maggi P, Ellis M, Westmoreland S, Silva A, Reich DS, Jacobson S.** 2013. Novel marmoset (Callithrix jacchus) model of human Herpesvirus 6A and 6B infections: immunologic, virologic and radiologic characterization. PLoS Pathog **9:**e1003138.
202. **Wu W, Vieira J, Fiore N, Banerjee P, Sieburg M, Rochford R, Harrington WJ, Feuer G.** 2006. KSHV/HHV-8 infection of human hematopoietic progenitor (CD34+) cells: persistence of infection during hematopoiesis in vitro and in vivo. Blood **108:**141-151.

203. **Parsons CH, Adang LA, Overdevest J, O'Connor CM, Taylor JRJ, Camerini D, Kedes DH.** 2006. KSHV targets multiple leukocyte lineages during long-term productive infection in NOD/SCID mice. J Clin Invest **116:**1963-1973.
204. **Smith MS, Goldman DC, Bailey AS, Pfaffle DL, Kreklywich CN, Spencer DB, Othieno FA, Streblow DN, Garcia JV, Fleming WH, Nelson JA.** 2011. Granulocyte-colony stimulating factor reactivates human cytomegalovirus in a latently infected humanized mouse model. Cell Host Microbe **8:**284-291.
205. **Tsujimura A, Shida K, Kitamura M, Nomura M, Takeda J, Tanaka H, Matsumoto M, Matsumiya K, Okuyama A, Nishimune Y, Okabe M, Seya T.** 1998. Molecular cloning of a murine homologue of membrane cofactor protein (CD46): preferential expression in testicular germ cells. Biochem J **330:**163-168.
206. **Zhen Z, Bradel-Tretheway B, Sumagin S, Bidlack JM, Dewhurst S.** 2005. The human herpesvirus 6 G protein-coupled receptor homolog U51 positively regulates virus replication and enhances cell-cell fusion in vitro. J Virol **79:**11914-11924.
207. **Adams O, Krempe C, Kögler G, Wernet P, Scheid A.** 1998. Congenital infections with human herpesvirus 6. J Inf Dis **178:**544-546.
208. **Braun DK, Dominguez G, Pellett PE.** 1997. Human herpesvirus 6. Clin Microbiol Rev **10:**521-567.
209. **Lusso P, Malnati M, De Maria A, Balotta C, DeRocco SE, Markham PD, Gallo RC.** 1991. Productive infection of CD4+ and CD8+ mature human T cell populations and clones by human herpesvirus 6. Transcriptional down-regulation of CD3. J Immun **147:**685-691.
210. **Lusso P, De Maria A, Malnati M, Lori F, DeRocco SE, Baseler M, Gallo RC.** 1991. Induction of CD4 and susceptibility to HIV-1 infection in human CD8+ T lymphocytes by human herpesvirus 6. Nature **349:**533-535.
211. **Nascimbeni M, Shin EC, Chiriboga L, Kleiner DE, Rehermann B.** 2004. Peripheral CD4(+)CD8(+) T cells are differentiated effector memory cells with antiviral functions. Blood **104:**478-486.
212. **Grivel JC, Santoro F, Chen S, Fagá G, Malnati MS, Ito Y, Margolis L, Lusso P.** 2003. Pathogenic effects of human herpesvirus 6 in human lymphoid tissue ex vivo. J Virol **77:**8280-8289.
213. **Tanner A, Taylor SE, Decottignies W, Berges BK.** 2014. Humanized mice as a model to study human hematopoietic stem cell transplantation. Stem Cells Dev **23:**76-82.
214. **Brainard DM, Seung E, Frahm N, Cariappa A, Bailey CC, Hart WK, Shin HS, Brooks SF, Knight HL, Eichbaum Q, Yang YG, Sykes M, Walker BD, Freeman GJ, Pillai S, Westmoreland SV, Brander C, Luster AD, Tager AM.** 2009. Induction of robust cellular and humoral virus-specific adaptive immune responses in HIV-infected humanized BLT mice. J Virol **83:**7305-7321.
215. **Becker PD, Legrand N, van Geelen CM, Noerder M, Huntington ND, Lim A, Yasuda E, Diehl SA, Scheeren FA, Ott M, Weijer K, Wedemeyer H, Di Santo JP, Beaumont T, Guzman CA, Spits H.** 2010. Generation of human antigen-specific monoclonal IgM antibodies using vaccinated "human immune system" mice. PLoS One **5:**e13137.
216. **Sanchez FM, Cuadra GI, Nielsen SJ, Tanner A, Berges BK.** 2013. Production and Characterization of Humanized Rag2(-/-)γc (-/-) Mice. Methods Mol Biol **1031:**19-26.
217. **Harris DT, Badowski M.** 2014. Long term human reconstitution and immune aging in NOD-Rag (-)-γ chain (-) mice. Immunobiology **219:**131-137.
218. **Nagasawa T.** 2006. Microenvironmental niches in the bone marrow required for B-cell development. Nat Rev Immunol **6:**107-116.
219. **Bladé J, Samson D, Reece D, Apperley J, Björkstrand B, Gahrton G, Gertz M, Giralt S, Jagannath S, Vesole D.** 1998. Criteria for evaluating disease response and progression in patients with multiple myeloma treated by high-dose therapy and haemopoietic stem cell transplantation. Myeloma Subcommittee of the EBMT. European Group for Blood and Marrow Transplant. Br J Haematol **102:**1115-1123.

220. **Durie BG, Harousseau JL, Miguel JS, Bladé J, Barlogie B, Anderson K, Gertz M, Dimopoulos M, Westin J, Sonneveld P, Ludwig H, Gahrton G, Beksac M, Crowley J, Belch A, Boccadaro M, Cavo M, Turesson I, Joshua D, Vesole D, Kyle R, Alexanian R, Tricot G, Attal M, Merlini G, Powles R, Richardson P, Shimizu K, Tosi P, Morgan G, Rajkumar SV.** 2006. International uniform response criteria for multiple myeloma. Leukemia **20:**1467-1473.
221. **Melkus MW, Estes JD, Padgett-Thomas A, Gatlin J, Denton PW, Othieno FA, Wege AK, Haase AT, Garcia JV.** 2006. Humanized mice mount specific adaptive and innate immune responses to EBV and TSST-1. Nat Med **12:**1316-1322.
222. **Biswas S, Chang H, Sarkis PT, Fikrig E, Zhu Q, Marasco WA.** 2011. Humoral immune responses in humanized BLT mice immunized with West Nile virus and HIV-1 envelope proteins are largely mediated via human CD5(+) B cells. Immunology **134:**419-433.
223. **Wang X, Qi Z, Wei H, Tian Z, Sun R.** 2012. Characterization of human B cells in umbilical cord blood-transplanted NOD/SCID mice. Transpl Immunol **26:**156-162.
224. **Baumgarth N, Tung J, Herzenberg L.** 2005. Inherent specificities in natural 689 antibodies: a key to immune defense against pathogen invasion. Springer Semin Immunopathol **26:**347.
225. **Akkina R.** 2013. New generation humanized mice for virus research: Comparative aspects and future prospects. Virology **435:**14-28.
226. **Serra-Hassoun M, Bourgine M, Boniotto M, Berges J, Langa F, Michel ML, Freitas AA, Garcia S.** 2014. Human Hematopoietic Reconstitution and HLA-Restricted Responses in Nonpermissive Alymphoid Mice. J Immun **193:**1504-1511.
227. **Shultz LD, Saito Y, Najima Y, Tanaka S, Ochi T, Tomizawa M, Doi T, Sone A, Suzuki N, Fujiwara H, Yasukawa M, Ishikawa F.** 2010. Generation of functional human T-cell subsets with HLA-restricted immune responses in HLA class I expressing NOD/SCID/IL2r{gamma}null humanized mice. Proc Natl Acad Sci U S A **107:**13022-13027.
228. **Lang J, Kelly M, Freed BM, McCarter MD, Kedl RM, Torres RM, Pelanda R.** 2013. Studies of Lymphocyte Reconstitution in a Humanized Mouse Model Reveal a Requirement of T Cells for Human B Cell Maturation. J Immun **190:**2090-2101.
229. **Tew JG, Phipps RP, Mandel TE.** 1980. The maintenance and regulation of the humoral immune response: persisting antigen and the role of follicular antigen-binding dendritic cells as accessory cells. Immunol Rev **53:**175-201.
230. **Chen Q, He F, Kwang J, Chan JK, Chen J.** 2012. GM-CSF and IL-4 Stimulate Antibody Responses in Humanized Mice by Promoting T, B, and Dendritic Cell Maturation. J Immunol **189:**5223-5229.
231. **Pek EA, Chan T, Reid S, Ashkar AA.** 2011. Characterization and IL-15 dependence of NK cells in humanized mice. Immunobiology **216:**218-224.
232. **Huntington ND, Legrand N, Alves NL, Jaron B, Weijer K, Plet A, Corcuff E, Mortier E, Jacques Y, Spits H, Di Santo JP.** 2009. IL-15 trans-presentation promotes human NK cell development and differentiation in vivo. J Exp Med **206:**25-34.
233. **Tanner A, Carlson SA, Nukui M, Murphy EA, Berges BK.** 2013. Human herpesvirus 6A infection and immunopathogenesis in humanized Rag2$^{-/-}$ $\gamma c^{-/-}$ mice. J Virol **87:**12020-12028.
234. **Wang J, Jones C, Norcross M, Bohnlein E, Razzaque A.** 1994. Identification and characterization of a human herpesvirus 6 gene segment capable of transactivating the human immunodeficiency virus type 1 long terminal repeat in an Sp1 binding site-dependent manner. J Virol **68:**1706-1713.
235. **Gravel A, Tomoiu A, Cloutier N, Gosselin J, Flamand L.** 2003. Characterization of the immediate-early 2 protein of human herpesvirus 6, a promiscuous transcriptional activator. Virology **308:**340-353.
236. **Sieczkowski L, Chandran B, Wood C.** 1995. The human immunodeficiency virus tat gene enhances replication of human herpesvirus-6. Virology **211:**544-553.

237. **Knox KK, Carrigan DR.** 1996. Active HHV-6 infection in the lymph nodes of HIV-infected patients: in vitro evidence that HHV-6 can break HIV latency. J Acquir Immune Defic Syndr Hum Retrovirol **11:**370-378.
238. **Lusso P, Malnati M, De Maria A, Balotta C, DeRocco SE, Markham PD, Gallo RC.** 1991. Productive infection of CD4+ and CD8+ mature human T cell populations and clones by human herpesvirus 6. Transcriptional down-regulation of CD3. J Immunol **147:**685-691.
239. **Buonamici S, Trimarchi T, Ruocco MG, Reavie L, Cathelin S, Mar BG, Klinakis A, Lukyanov Y, Tseng JC, Sen F, Gehrie E, Li M, Newcomb E, Zavadil J, Meruelo D, Lipp M, Ibrahim S, Efstratiadis A, Zagzag D, Bromberg JS, Dustin ML, Aifantis I.** 2009. CCR7 signalling as an essential regulator of CNS infiltration in T-cell leukaemia. Nature **459:**1000-1004.
240. **Anderson LJ, Longnecker R.** 2008. EBV LMP2A provides a surrogate pre-B cell receptor signal through constitutive activation of the ERK/MAPK pathway. J Gen Virol **89:**1563-1568.
241. **Kofod-Olsen E, Ross-Hansen K, Schleimann MH, Jensen DK, Møller JM, Bundgaard B, Mikkelsen JG, Höllsberg P.** 2012. U20 is responsible for human herpesvirus 6B inhibition of tumor necrosis factor receptor-dependent signaling and apoptosis. J Virol **86:**11483-11492.
242. **Tanner A, Hallam SJ, Nielsen SJ, Cuadra GI, Berges BK.** 2015. Development of human B cells and antibodies following human hematopoietic stem cell transplantation to Rag2(-/-)γc(-/-) mice. Transpl Immunol **32:**144-150.

VII. Appendix
(See next page)

Journal of General Virology (2016), **97**, 543–560 **DOI** 10.1099/jgv.0.000370

Review

Piracy on the molecular level: human herpesviruses manipulate cellular chemotaxis

Caleb Cornaby, Anne Tanner, Eric W. Stutz, Brian D. Poole and Bradford K. Berges

Department of Microbiology and Molecular Biology, Brigham Young University, Provo, UT 84602, USA

Correspondence
Bradford K. Berges
brad.berges@gmail.com

Cellular chemotaxis is important to tissue homeostasis and proper development. Human herpesvirus species influence cellular chemotaxis by regulating cellular chemokines and chemokine receptors. Herpesviruses also express various viral chemokines and chemokine receptors during infection. These changes to chemokine concentrations and receptor availability assist in the pathogenesis of herpesviruses and contribute to a variety of diseases and malignancies. By interfering with the positioning of host cells during herpesvirus infection, viral spread is assisted, latency can be established and the immune system is prevented from eradicating viral infection.

INTRODUCTION

Cells respond to a variety of cytokines and chemokines that allow them to migrate in different areas in the body depending on where they are needed. This process is essential for appropriate tissue maintenance, homeostasis, formation, repair and pathogen clearance (Turner *et al.*, 2014; Zhou *et al.*, 2014). Dysregulation of the delicate balance of cellular signals and/or improper positioning could impede these processes. Aside from being related to a range of diseases, viral-induced chemotaxis contributes to the epidemiology and persistence of human herpesviruses. These viruses regulate a multitude of cellular genes that direct cellular chemotaxis, thereby manipulating these genes for the benefit of the invading virus. Herpesviruses also produce various chemokines and chemokine receptors from genes in the viral genome, further affecting cellular chemotaxis. In essence, viral infection results in the piracy of cellular function as it directs cell movement in both infected and uninfected cell types.

The family *Herpesviridae* is divided into various subfamilies including *Alphaherpesvirinae*, *Betaherpesvirinae*, and *Gammaherpesvirinae* (Flint & American Society for Microbiology, 2009; Yoshida & Yamada, 2006). The nine human herpesviruses (HHVs) include herpes simplex virus type 1 (HHV-1 or HSV-1) and 2 (HHV-2 or HSV-2), varicella–zoster virus (HHV-3 or VZV), Epstein–Barr virus (HHV-4 or EBV), human cytomegalovirus (HHV-5 or hCMV), human herpesvirus 6A (HHV-6A) and 6B (HHV-6B or roseola virus), human herpesvirus 7 (HHV-7) and Kaposi's sarcoma-associated herpesvirus (HHV-8 or KSHV) (Siakallis *et al.*, 2009). All of these viral species share similar structural characteristics with a genome composed of double-stranded DNA, an icosahedral capsid, an envelope studded with a variety of viral and host proteins, and viral tegument proteins in an amorphous layer between the capsid and envelope (Flint & American Society for Microbiology, 2009). Herpesviruses are able to remain latent in host cells for the life of the individual, during which time viral particles are undetectable but viral nucleic acids can be found, and viral gene expression is very limited. Various stimuli can cause viral reactivation, wherein viral gene expression recommences and infectious particles can be detected and shed to new hosts. Herpesviruses encode a complex assortment of proteins that manipulate cellular functions during infection in order to promote viral persistence. Human herpesviruses are an integral part of human existence, with over 90% of adults being persistently infected with one or more of these nine herpesviruses in their lifetimes. Although the incidence of serious herpesvirus-induced diseases is rare in most cases, the prevalence of infection is so high that the overall disease burden takes a toll on society.

It has been hypothesized that several herpesvirus species affect development or progression of diseases, including lymphomas, atherosclerosis, autoimmune disorders, and disruption of angiogenesis, through interference with cellular chemotaxis (Ehlin-Henriksson *et al.*, 2009; Franciotta *et al.*, 2008; Rosenkilde & Schwartz, 2004; Stern & Slobedman, 2008; Streblow *et al.*, 2001). In this review we will elaborate on the known human HHV mechanisms and pathways that influence cellular chemotaxis during viral infection. Potential benefits to herpesviruses in evolving these mechanisms will be presented as well as the resulting potential for their roles in disease development.

ALPHAHERPESVIRINAE

HSV-1, HSV-2 and VZV encompass the human pathogens of the subfamily *Alphaherpesvirinae*, typically showing lytic replication in epithelial cells and harboured as a latent infection in neuronal cells. HSV-1 is quite common in industrialized countries, with a seroprevalence of around 90% (Viejo-Borbolla *et al.*, 2012) in the adult population. Symptoms of viral infection include cold sores and redness of the skin; however, many infections are asymptomatic. HSV-1 transmittance only occurs when viral replication takes place, either during primary infection or in a reactivation event. The most common methods of transferring HSV-1 include direct skin contact and via saliva. Similar to HSV-1, HSV-2 can mask its presence from the host's immune system, demonstrating a preference to lie dormant in the sacral ganglia (HSV-1 in trigeminal ganglia) and manifest occasional lytic outbreaks, typically in the genital area. HSV-2 is one of the most common sexually transmitted diseases, with a seroprevalence of 12–20% in the USA. HSV-2 infection is of greater concern in developing countries, where seroprevalence is much higher (Weiss, 2004; Xu *et al.*, 2006). VZV primary infection results in the common childhood disease varicella (chickenpox) after which the virus establishes latency in the ganglia of a variety of neurons (Gilden *et al.*, 2014). Reactivation of the virus results in zoster (shingles) and other chronic pain diseases, which can be manifest in various places on the epithelium (Gilden *et al.*, 2014).

Until recently, not much was known about HSV and how it affects chemotaxis; however, current work has demonstrated that HSV infection has a strong influence on chemotaxis (see Table 1). Viejo-Borbolla *et al.* (2012) showed that a secreted form of viral glycoprotein G (SgG) from both HSV-1 and HSV-2 binds chemokines with high affinity. Membrane-bound glycoprotein G (gG) was shown to be necessary for chemokine-binding activity. They found that HSV SgG in both HSV-1 and HSV-2 increased chemotaxis of monocytes in infected individuals towards CXCL12 and that gG attaches to glycosaminoglycans (GAGs) at the surface of cells without negative effects on G-protein-coupled receptors (GPCRs). Another, more recent, study further investigated the mechanism by which viral SgG enhances chemotaxis. It was found that gG binds to GAGs, which induces lipid raft clustering, leading to increased CXCR4 incorporation. The conformational change causes an increase in functional chemokine–receptor complexes at the cell surface (Martinez-Martin *et al.*, 2015). CXCL12 is the natural ligand for CXCR4 and is secreted constitutively in a variety of tissues, including the lymph nodes, bone marrow, lungs and adrenal glands (Alkhatib, 2009; Luker & Luker, 2006). It is also known that CXCR4 signalling is important in modulating the survival of neuronal cells and modulating synaptic function (Nash & Meucci, 2014). The increased functionality of CXCR4 could potentially allow infected cells to migrate to these areas *in vivo*. By migrating to areas secreting CXCL12, infected cells could come into contact with more target cells. Similar results had been observed by Bellner *et al.* (2005) when they tested the chemotactic ability of HSV-2 gG (gG-2p20). These authors found that isolated human neutrophils and monocytes followed a gradient of gG-2p20 via binding of the formyl peptide receptor (FPR) on the surface of these cells. While the chemoattractant properties have never been displayed using the full-length gG2 protein, several speculations can be made based on the findings that suggest that neutrophils and monocytes could be attracted to areas with infected cells expressing gG-2p20. This could possibly be beneficial for HSV-2 infection. Attracting a large number of phagocytic cells would increase tissue damage and activated cells, potentially enabling viral spread and propagation (Bellner *et al.*, 2005). It was shown that gG-2p20 is an FPR-activating agonist. Activation of FPR *in vivo* led to the downregulation of other chemotactic receptors. These observations suggest the possibility that the change in expression could lead to impaired clearance of HSV-2 during infection (Bellner *et al.*, 2005). In summary, a variety of studies have demonstrated the effectiveness of HSV-1 and HSV-2 in manipulating CXCR4 in infected cells.

HSV-2 has demonstrated the ability to manipulate chemotaxis via a host chemokine as well. A study performed by Huang *et al.* (2012) demonstrated an elevated expression of CXCL9 in the cervical mucosa of HSV-2-positive women. Further research confirmed that HSV-2 regulated the expression of CXCL9 in human cervical epithelial cells by inducing the phosphorylation and translocation of C/EBP-β to the nucleus, where it transactivates CXCL9. The known receptor for CXCL9 is CXCR3, which is expressed predominantly in non-resting T cells (Van Raemdonck *et al.*, 2015). Expression has also been observed in epithelial, endothelial, fibroblast and smooth muscle cells (SMCs) (Billottet *et al.*, 2013; Van Raemdonck

Table 1. Alphaherpesviruses change cellular receptors/chemokines

Cell type	Receptor or chemokine	Virus	Amount or functionality	References
Monocyte	CXCR4	HSV-1, HSV-2	Increase	Bellner *et al.* (2005); Viejo-Borbolla *et al.* (2012)
Neutrophil	CXCR4	HSV-1, HSV-2	Increase	Bellner *et al.* (2005)
Epithelial	CXCL9	HSV-2	Increase	Huang *et al.* (2012)

et al., 2015). This upregulation of CXCL9 was shown to result in increased migration of activated peripheral blood leukocytes (PBLs) and CD4+T lymphocytes (Huang *et al.*, 2012). Huang and associates postulate that HSV-2 is responsible for upregulating CXCL9; however, it was not shown what viral protein induced the expression or if the increase in CXCL9 expression was a cellular response to viral infection. The viral benefits for inducing migration of CD4+T cells and PBLs to sites of infection are unclear. The ability of HSV-2 to regulate CXCL9 could be investigated more in depth as this is the only study demonstrating this type of subversion in epithelial cells.

Past research has also suggested that VZV could utilize glycoproteins as chemoattractants, inducing migration of polymorphonuclear leukocytes (Ihara *et al.*, 1991). No other recent research has been conducted to determine if VZV affects chemotaxis of other infected cell types, although several studies do provide evidence for how VZV might influence cellular chemotaxis (Desloges *et al.*, 2008; Shavit *et al.*, 1999; Steain *et al.*, 2011). We now understand that HSV-1 and HSV-2 can manipulate monocytes through increasing the functionality of CXCR4 by making lipid rafts with the viral SgG protein. HSV-2 can further change the migration of cells by increasing the expression of CXCL9 in infected epithelial cells, potentially attracting CD4+T cells and PBLs to sites of infection.

BETAHERPESVIRINAE

Human cytomegalovirus (hCMV)

Also known as human herpesvirus 5, hCMV is a prominent member of the *Betaherpesvirinae* subfamily. With a seroprevalence worldwide ranging from 45 to 100%, hCMV is a common human pathogen that is often asymptomatic in infected adults and children (Cannon *et al.*, 2010; Chen *et al.*, 1999; McGavran & Smith, 1965). hCMV has gained public scrutiny and awareness owing to further understanding of its prevalence in causing congenital infections leading to birth defects (Bialas *et al.*, 2015). In the USA it is a more common cause of birth defects than many other causes, including fetal alcohol syndrome, Down syndrome, spina bifida, HIV/AIDS, Haemophilus influenzae type B and congenital rubella syndrome (Cannon & Davis, 2005). Like other herpesviruses, hCMV is associated with various post-transplant complications and is a main viral cause of solid organ transplant and haematopoietic stem cell transplant morbidity and mortality (Ariza-Heredia *et al.*, 2014; Gandhi & Khanna, 2004). It is also known to cause severe disease in other immunocompromised individuals, such as AIDS patients. Viral shedding can occur via saliva, urine, breast milk, semen and tears. hCMV is known to infect various cell types, including epithelial cells, endothelial cells, smooth muscle cells, fibroblasts, dendritic cells and lymphocytes, the latter cell type typically remaining latently infected for the life of the host.

Using a variety of viral proteins to manipulate migration of host cells and potential target cells, hCMV uses both surface receptors and secreted chemokines (see Tables 2 and 3). Among the viral chemokines secreted by hCMV-infected cells are the products of the *UL128* and *UL146* genes. Numerous studies have been performed demonstrating how these viral gene products affect the migration of hCMV-infected cells. It has been noted that hCMV-infected monocytes demonstrate a reduced chemotactic ability owing to a downregulation of CCR1, CCR2 and CCR5 (Frascaroli *et al.*, 2006). A similar downregulation of various chemokines was observed along with an increase in migratory inhibitory factor in hCMV-infected macrophages, resulting in a lack of motility (Frascaroli *et al.*, 2009).

Table 2. Human herpesvirus-encoded chemokine receptors

Virus	Viral receptor	Result	References
hCMV	US27	Potentiates CXCR4, increases migration to various tissues	Arnolds *et al.* (2013)
	US28	Migration of infected cells to areas of inflammation	Streblow *et al.* (1999); Vomaske *et al.* (2009)
	UL33 and UL78	Prevents migration to sites of inflammation and certain tissues	Tadagaki *et al.* (2012); Tschische *et al.* (2011)
HHV-6A	U51	Prevents NK cell interaction and prevents apoptotic signals	Catusse *et al.* (2008); Fitzsimons *et al.* (2006)
HHV-6B	U12	Migrates to inflammatory and T cell-rich zones	Isegawa *et al.* (1998)
HHV-7	U51 U12	Migration of infected cells to T cell-rich and inflammatory areas	Nicholas (1996); Tadagaki *et al.* (2005)
KSHV	KSHV-GPCR	Increases cell survival	Couty *et al.* (2009); Pati *et al.* (2001); Shepard *et al.* (2001)

Table 3. Human herpesvirus-encoded chemokines

Virus	Viral chemokine	Result	References
VZV	GP I and GP II	Chemoattractant for polymorphonuclear leukocytes	Ihara *et al.* (1991)
HSV	gG2	Chemoattractant for monocytes	Bellner *et al.* (2005)
hCMV	UL146	Chemoattractant for neutrophils	Lüttichau, (2010); Penfold *et al.* (1999)
hCMV	UL128 and UL146	Attracts PBMCs and prevents monocyte migration	Frascaroli *et al.* (2006); Gao *et al.* (2013); Straschewski *et al.* (2011)
HHV-6A	U83A	Chemoattractant for T cells, monocytes and immature dendritic cells	Catusse *et al.* (2007); Dewin *et al.* (2006)
HHV-6B	U83B	Chemoattractant for monocytes	Clark *et al.* (2013); Lüttichau *et al.* (2003)
KSHV	vCCL1	Chemoattractant for monocytes	Nakano *et al.* (2003); Weber *et al.* (2001)
KSHV	vCCL2	Prevents Th1 T cell chemotaxis and attracts monocytes	Nakano *et al.* (2003); Weber *et al.* (2001)
KSHV	vCCL3	Inhibits chemotaxis of Th1 T cells and NK cells	Lüttichau *et al.* (2007)
KSHV	vIL-6	Attracts endothelial cells	Wu *et al.* (2014)

Later it was demonstrated by Frascaroli and associates that in the presence of UL128 there was a resulting downregulation of CCR1, CCR2 and CCR5 in monocytes (Straschewski *et al.*, 2011). Because of this impairment, monocytes could no longer migrate following the chemokines CCL5 and CCL2, which are ligands of the aforementioned receptors. CCL2 and CCL5 are known to be involved in the recruitment of monocytes and T cells and are secreted as pro-inflammatory cytokines in response to tissue damage or viral detection (Ansari *et al.*, 2013; Soria & Ben-Baruch, 2008). Recently, using a *UL128*-transfected cell line (CHO-UL128) to produce UL128, Gao *et al.* (2013) studied the effects of this β chemokine on cell migration. They found that UL128 acted as a chemoattractant for peripheral blood mononuclear cells (PBMCs) *in vitro* and functioned similarly to CCL3 as a chemoattractant. These results suggest that UL128 could act to prevent chemotaxis of monocytes following other gradients, such as CCL5 and CCL2, and could use a separate receptor to attract the monocytes to areas of infected cells (Gao *et al.*, 2013). This increases the cells available to be infected by hCMV, potentially furthering viral spread. The other known chemokine produced, UL146, codes for an α chemokine and viral homologue to CXCL1 (vCXCL1) (Penfold *et al.*, 1999). Two studies demonstrated that vCXCL1 could induce the chemotaxis of neutrophils *in vitro* (Lüttichau, 2010; Penfold *et al.*, 1999). Using calcium mobilization, chemotaxis and phosphatidylinositol turnover assays, it was found that vCXCL1 was a ligand for CXCR1 and CXCR2. CXCR1 and CXCR2 are both expressed on neutrophils, and it is expected that hCMV-infected endothelial cells express vCXCL1 as a chemoattractant to increase the numbers of neutrophils and assist in viral spread to other endothelial cells (Lüttichau, 2010). In a study conducted by Smith *et al.* (2004), it was observed that hCMV-infected monocytes induced transendothelial migration *in vitro*, although the viral mechanism is unknown (Smith *et al.*, 2004).

Regulating host cell chemokines can also result in chemotactic changes (see Table 4). hCMV UL144 is a viral protein that activates NF-κB (Poole *et al.*, 2006). This leads to a cascade of multiple pathways, including induced expression of host CCL22, which acts as a chemoattractant for Th2 and regulatory T cells (Tregs). By recruiting these cells to sites of viral infection it is possible to suppress T helper and CD8 + T cells, tapering the immune response (Fielding, 2015). It has also been found that granulocyte macrophage progenitors (GMPs) latently infected with hCMV demonstrate increased expression of CCL2 (Stern & Slobedman, 2008). CCL2 is a pro-inflammatory cytokine that acts as a chemoattractant to monocytes, macrophages, dendritic cells and T cells expressing CCR2. This increase in CCL2 acts to attract CD14 + monocytes to latently infected GMPs (Stern & Slobedman, 2008). This behaviour of latently infected GMPs is likely a viral strategy employed to recruit new leukocytes to be infected; however, too little is known about *in vivo* hCMV reactivation to know if this spread and reactivation occurs before or after GMPs develop into macrophages. Further research could be done into the manipulation of hCMV-infected GMPs as there is currently just one study demonstrating this change in chemotaxis.

There are a variety of hCMV chemokine receptors shown to affect cell migration, including US27, US28, UL33 and UL78 (Fielding, 2015), all of which are homologous to human GPCRs. US27 is expressed late during lytic infection and has no known ligand (Fraile-Ramos *et al.*, 2002; Stapleton *et al.*, 2012). However, it was found to potentiate CXCR4-mediated chemotaxis, increasing the expression and amount of surface CXCR4 (Arnolds *et al.*, 2013). As previously explained, CXCR4 is a seven-membrane-

Table 4. Betaherpesviruses change cellular receptors/chemokines

Cell type	Receptor or chemokine	Virus	Amount or functionality	References
Dendritic cell	CCR7	hCMV	Decrease	Moutaftsi *et al.* (2004)
	CCR1	hCMV	Decrease	Varani *et al.* (2005)
	CCR5	hCMV	Decrease	Varani *et al.* (2005)
GMP	CCL2	hCMV	Increase	Stern & Slobedman (2008)
Monocyte	CCR1	hCMV	Decrease	Frascaroli *et al.* (2006, 2009);
	CCR2	hCMV	Decrease	Straschewski *et al.* (2011)
	CCR5	hCMV	Decrease	
	CCL22	hCMV	Increase	Poole *et al.* (2006)
T cell	CCL5	HHV-6A	Decrease/increase	Cerdan *et al.* (2001)
	CCR7	HHV-6	Increase	Hasegawa *et al.* (1994)
	CXCR4	HHV-6	Decrease	Yasukawa *et al.* (1999)
	CXCR4	HHV-7	Decrease	Yasukawa *et al.* (1999)
	CCR7	HHV-7	Increase	Hasegawa *et al.* (1994)

spanning GPCR that allows the cell to follow the chemokine gradient of its natural ligand, CXCL12, which is secreted constitutively in a variety of tissues, including the lymph nodes, thymus, bone marrow, lungs and adrenal glands (Alkhatib, 2009; Luker & Luker, 2006). The potentiation of CXCR4 resulted in increased migration to CXCL12 during *in vitro* migration assays (Arnolds *et al.*, 2013). It has been speculated that increased CXCR4 levels at appropriate times could allow hCMV-infected cells to migrate to bone marrow or lymph nodes, where there would be an increased opportunity to spread to susceptible cells (Arnolds *et al.*, 2013).

US28 was first shown to affect migration in vascular SMCs (Streblow *et al.*, 1999). It was found that US28 directed cell migration following the chemokines CCL2 and possibly CCL5. In the absence of CCL2, there was no migration of hCMV-infected SMCs (Streblow *et al.*, 1999). This would allow infected SMCs to migrate to areas of inflammation, potentially providing opportunity for viral spread to leukocytes. Later it was demonstrated that US28 acted to control migration of both infected SMCs and infected macrophages. Kledal *et al.* (1998) found that US28 also bound CX3CL1, which is a chemokine that is found on the cell surface and extracellularly in a secreted form; this work was later followed up by others (Murphy *et al.*, 2008; Vomaske *et al.*, 2009). CX3CL1 is only known to be produced by endothelial cells and results in the recruitment of inflammatory cells (Bazan *et al.*, 1997; Vomaske *et al.*, 2009). These authors found that the presence of CX3CL1 inhibited the migration of hCMV-infected SMCs, but induced the migration of hCMV-infected macrophages. It was also demonstrated that the inverse was true, in the presence of CCL5, hCMV-infected macrophages US28-mediated migration was inhibited, but hCMV-infected SMCs demonstrated normal chemotaxis, as expected (Vomaske *et al.*, 2009). This makes the viral GPCR US28 unique in that it is chemokine- and cell-type-specific. It seems important for the virus to control cellular migration during hCMV infection. Evidence for how US28 functions was provided by Tschische *et al.* (2011), when they found that hCMV chemokine receptors heteromerize with each other. It was observed that UL33 and UL78 heteromerization resulted in silencing of US28-mediated activation of the NF-κB pathway. Tadagaki *et al.* (2012) investigated UL33 and UL78, and found that these two GPCR homologues formed heteromers with CCR5 and CXCR4 on the surface of infected THP-1 cells. This was found to prevent cell chemotaxis facilitated by CCR5 and CXCR4 *in vitro*. CCR5 allows the cell to follow a variety of chemokines, including CCL3, CCL4 and CCL5, these being the best agonists, while CXCR4 is known to be chemoattracted to CXCL12 (Alkhatib, 2009). The majority of chemokines that act as CCR5 ligands are pro-inflammatory.

During hCMV infection the virus is able to regulate host receptors in various ways to prevent chemotaxis. It has been demonstrated that hCMV prevents CCR7 expression in monocyte-derived dendritic cells, preventing chemotaxis following CCL19 and CCL21 chemokine gradients *in vitro* (Moutaftsi *et al.*, 2004). hCMV-infected Langerhans cells also demonstrate reduced chemotaxis in response to lymphoid chemokines (Lee *et al.*, 2006). After these observations it was found by Wagner *et al.* (2008) that hCMV UL18 inhibited chemotaxis of dendritic cells *in vitro*. The extracellular UL18 is expressed late in hCMV infection and binds the leukocyte immunoglobulin-like receptor 1 molecule on the surface of dendritic cells. This results in various changes, including reduced chemotaxis, increased pro-inflammatory cytokine production, upregulation of CD83 and inhibition of CD40 (Park *et al.*, 2002; Wagner *et al.*, 2008). It was also observed that hCMV-infected dendritic cells showed downregulated chemokine expression and inhibited maturation due to vIL-10, a product of the hCMV *UL111A* gene. Dendritic cells that were able to

mature during hCMV infection showed an increase in chemotactic ability to follow the lymph node homing chemokine (Chang *et al.*, 2004). It has further been observed that chemotaxis is disrupted in infected endothelial cells. Reinhardt *et al.* (2014) demonstrated how hCMV-infected human coronary artery endothelial cell (HCAEC) chemotaxis to vascular endothelial growth factor is inhibited. HCAEC migration is important for repair post-vascular injury (Deanfield *et al.*, 2007; Waltenberger, 2007). While the observation explains how hCMV can play a role in contributing to pro-atherosclerotic phenotypes, the viral strategy for inhibiting HCAEC migration remains unknown. A further way to inhibit chemotaxis of cells is by secreting chemokine-binding proteins. hCMV-produced UL21.5 acts in this capacity by binding CCL5, acting as a chemokine sink or decoy receptor (Wang *et al.*, 2004a). This would prevent the cellular receptor from being able to bind CCL5 and follow the chemoattractant. hCMV also utilizes miR-UL148D to silence CCL5 protein synthesis in infected cells (Kim *et al.*, 2012). These studies emphasize the importance of CCL5 regulation during hCMV infection. Preventing immune cell production and detection of CCL5 would assist in preventing the attraction of monocytes and T cells to areas of hCMV infection. While a certain number of monocytes would be beneficial for viral spread, an overabundance of monocytes and the presence of T cells could result in the impairment of viral spread.

To better enhance viral spread, hCMV uses virally encoded chemokines UL128, UL146 and vCXCL1 to attract target immune cells. The piracy of host chemokine CCL22 further assists in this process. By upregulation of CCL22 in infected monocytes, Tregs are attracted, and could assist in downregulation of an immune response to viral infection. By increasing the functionality of CXCR4, chemotaxis of virally infected cells to other tissues could be encouraged. By manipulating host chemokine receptor CCR7, hCMV can avoid migration to primary and secondary lymph tissue, evading possible detection. The dysregulation of virus-infected cell movement appears to allow hCMV the edge in evading immune detection and increase the opportunity for viral spread (see Fig. 1). Future studies investigating the function of viral chemokines and chemokine receptors could examine their effects *in vivo* utilizing

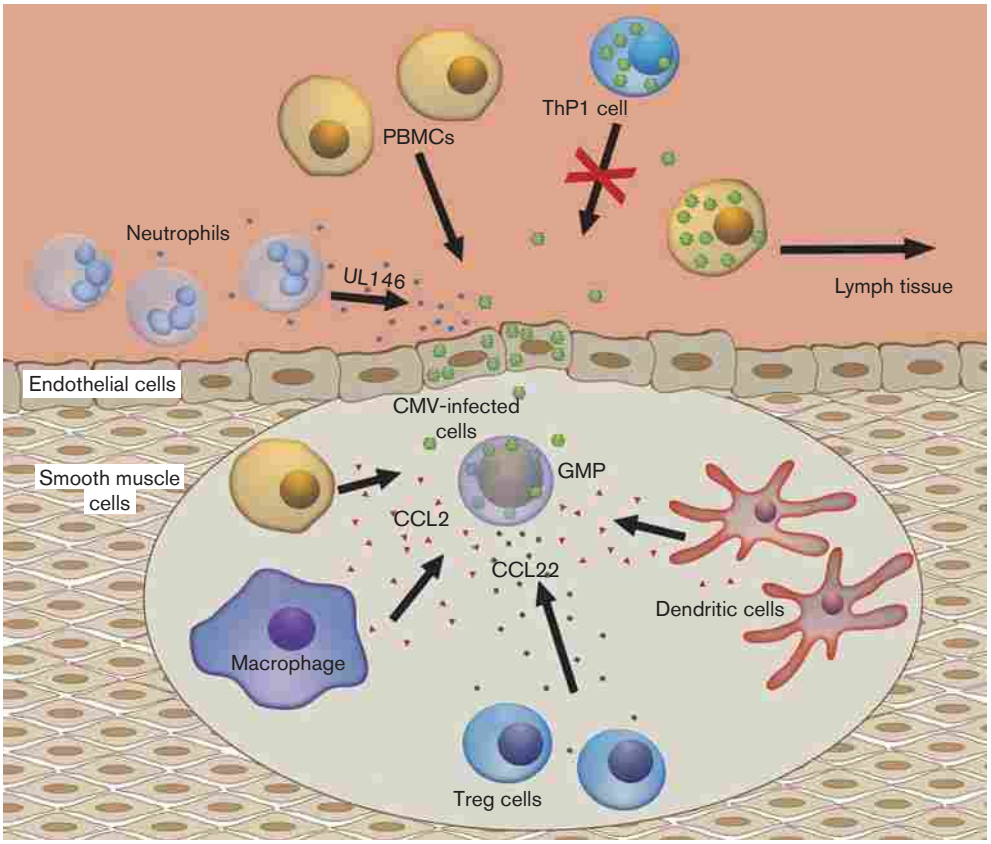

Fig. 1. Changes in cellular chemotaxis resulting from hCMV infection. hCMV uses virally encoded chemokines UL128, UL146 and vCXCL1 to attract target immune cells such as neutrophils and PBMCs. Increases in CCL2 expression further assist in attracting monocytes, macrophages and dendritic cells. Upregulation of CCL22 in infected monocytes attracts Treg cells, which can assist in downregulation of an effective immune response to viral infection. Increasing the functionality of CXCR4 allows virally infected cells to migrate to other tissues, including secondary lymphoid tissues.

animal models, as has been done with hCMV US28 (Bongers *et al.*, 2010).

Human herpesvirus 6 (HHV-6)

HHV-6, initially named human B lymphotropic virus, was first discovered in 1986 in patients with lymphoproliferative disorders (Salahuddin *et al.*, 1986). HHV-6A and HHV-6B were recognized as different variants of the same species in 1992, and in 2012 the International Committee on Taxonomy of Viruses classified them as two distinct viruses (Ablashi *et al.*, 1993; Adams & Carstens, 2012). Because classification as two distinct viruses has come relatively recently, it makes it difficult to distinguish between HHV-6A and HHV-6B in some of the early literature. The seroprevalence of HHV-6 in adults worldwide is approximately 83–100% (Hall *et al.*, 2006).

HHV-6A

HHV-6A is a betaherpesvirus that has primary tropism for CD4+T cells and can also infect CD8+T cells, natural killer (NK) cells, gamma/delta T cells, human neural stem cells, human progenitor-derived astrocytes, and oligodendrocyte progenitor cells (Ablashi *et al.*, 2014; Lusso *et al.*, 1991, 1993, 1995). It has also been shown to lytically infect B cells that have been immortalized with EBV (Ablashi *et al.*, 1989). HHV-6A can alter the expression of different cellular markers involved in cellular homing and trafficking, which causes significant disruption to immune cell function and viability. The virus has been implicated in a number of diseases including multiple sclerosis, Hashimoto's thyroiditis, and AIDS. *In vitro* studies show that HHV-6A causes upregulation of CD4 on cells that do not typically express this marker, making these cells susceptible to HIV infection and possibly contributing in the progression to AIDS (Lusso *et al.*, 1991, 2007).

HHV-6 has one functional chemokine-like protein, U83 (see Table 3). The viral chemokine U83A from HHV-6A is involved in chemoattraction and has selective specificity for receptors CCR1, CCR4, CCR5, CCR6 and CCR8. These are found on T cells, monocytes/macrophages and activated T lymphocytes (CCR1, CCR5, CCR8), skin-homing T lymphocytes (CCR4, CCR8), immature dendritic cells (CCR1, CCR6) and NK cells (CCR8) (Ablashi *et al.*, 2014; Catusse *et al.*, 2008; Dewin *et al.*, 2006). The difference in specificity of U83A (from HHV-6A) and U83B (from HHV-6B) to attract diverse cell types (see Table 3) could account for the variable tropism of the two viruses (Clark *et al.*, 2013). U83A is found in a full-length form as well as a truncated splice variant (French *et al.*, 1999). It is thought that, because of the different forms of the peptide, U83A could block both innate and adaptive immune responses, as well as attract the cells involved in these responses for further infection (Dewin *et al.*, 2006). U83A induces chemotaxis and morphological changes in cells expressing CCR5 in a manner similar to CCL4, but with a significantly delayed internalization of CCR5 compared with CCL4. Interestingly, binding of U83A to CCR5 has been shown to inhibit CCR5 tropic HIV-1 infection (Catusse *et al.*, 2007).

HHV-6 has two GPCRs, U12 and U51, which encode chemokine receptors (see Table 2). U51, known to affect migration in HHV-6A infected cells, is expressed at early time points post-infection, whereas U12 is expressed late and influences chemotaxis of HHV-6B-infected cells. HHV-6A U51A has novel specificity for CCL5 and can also bind CCL2, CCL11, CCL7 and CCL13. This makes U51A unique among viral and cellular receptors in that it overlaps activity with CCR1, CCR2, CCR3 and CCR5 in the binding of CCL5 (Catusse *et al.*, 2008). There is also overlap with CCR2, CCR4, US28, UL12, D6 and Duffy in the binding of CCL2; CCR3 and E1 in the binding of CCL11; CCR1, CCR3, US28 and D6 in the binding of CCL7; and CCR2 and CCR3 in the binding of CCL13. Unlike many viral GPCRs that have constitutive signalling, U51A has been shown to perform both inducible and constitutive signalling (Catusse *et al.*, 2008; Fitzsimons *et al.*, 2006).

U51A expression has been shown to cause a reduction of CCL5 expression using the Hut78 human CD4+T lymphocyte cell line. U51A has high relative affinity for XCL1, which normally binds human receptor XCR1 found on NK cells and T lymphocytes. This binding could have a number of effects, including: preventing infected cells from interacting with NK cells; inducing chemotaxis to T lymphocytes, which could spread infection; and preventing apoptotic signals within infected cells (Cerdan *et al.*, 2001). CCL19, normally bound by human receptor CCR7, can also be bound by U51A. This could cause infected cells to migrate to the T cell-rich lymph node, promoting viral spread. HHV-6A U83A chemokine does not bind U51A. Expression of U51A ligands in the brain could also allow migration of infected cells into the central nervous system. Damaged epithelial lung cells and airway parasympathetic nerves express CCL2 and CCL11, which both bind U51A, and could promote migration of the infected cells to these areas to be transmitted to new hosts.

CCR7, which is expressed in various lymphoid tissues, is another receptor that is modulated by herpesviruses (see Table 4). HHV-6A and HHV-6B upregulate CCR7 expression in CD4+T cells (Hasegawa *et al.*, 1994). CCR7 is specific for CCL19 and CCL21 and plays roles in cell migration and proliferation (Tadagaki *et al.*, 2005). This upregulation of CCR7 could be an important aspect of HHV-6 pathogenesis as upregulation of CCR7 promotes migration of T cells and dendritic cells to the paracortex in lymph nodes (where T cell priming occurs) and the periarteriolar lymphoid sheath in the spleen, both of which are T cell-rich (Comerford *et al.*, 2013).

As mentioned previously, HHV-6A can also downregulate cellular receptors. Along with downregulation of CD46 (its entry receptor) and CD3 (Grivel *et al.*, 2003), CXCR4 is downregulated by HHV-6A in primary CD4+ T lymphocytes and the Jjhan T cell line, which affect the chemotactic response of the cells to CXCL12, the natural ligand of CXCR4 (Yasukawa *et al.*, 1999). The disruption of CXCR4/CXCL12 signalling by downregulation of CXCR4 by HHV-6A could prevent the retention of haematopoietic stem/progenitor cells (HSPCs) and more mature leukocytes in the bone marrow, allowing these cells to be mobilized and enter into circulation (Karpova & Bonig, 2015). The migration of CXCR4-expressing thymocytes out of the thymus was shown to occur in a CXCL12-dependent manner (Poznansky *et al.*, 2002; Weinreich & Hogquist, 2008); so the downregulation of CXCR4 by HHV-6A could be another way the virus prevents migration away from areas where target cells are present. Additionally, the downregulation of CXCR4 by HHV-6A could prevent homing of bone marrow-derived precursor cells to the thymus (Calderón & Boehm, 2011), possibly preventing positive and negative selection from occurring in these cells.

HHV-6 has been shown to cause modulations to CCL5 expression. This chemokine has selective chemoattractive activity on resting CD4+ memory T cells (Hasegawa *et al.*, 1994) and has been shown to be upregulated by HHV-6 in an *ex vivo* study where human tonsil blocks were infected with both HHV-6 and HIV-1. This upregulation of CCL5 was shown to suppress HIV-1 CCR5-tropic variants and possibly to stimulate replication of CXCR4-utilizing variants, which gives evidence that HHV-6 may play a role in HIV pathogenesis by promoting the switch between CCR5-tropic to CXCR4-tropic HIV-1 (Grivel *et al.*, 2001). In contrast, CCL5 expression in epithelial cells is downregulated by U51A from HHV-6A (Milne *et al.*, 2000). Epithelial cells expressing U51A also had morphological changes and exhibited increased spreading and flattening, which could increase the ability of HHV-6 to spread to uninfected cells as it is primarily spread by cell-to-cell contact (Milne *et al.*, 2000). As has been observed with other viral chemokines and chemokine receptors, their functions could be multipurpose in attracting cells to the area of infection, and also in evading the immune cells of the host so replication and latency can take place.

As described above, HHV-6A alters the expression of different cellular markers. Many of these markers are involved in cellular homing and tracking to specific areas of the body, and when altered can cause significant disruption to immune cell function and viability. Further research into HHV-6A effects on cellular trafficking could serve as a critical guide for developing new treatments to prevent these disease-causing disruptions.

HHV-6B

HHV-6B causes exanthem subitum (roseola) (Yamanishi *et al.*, 1988) and is found in approximately 95–100% of adults worldwide. Unlike HHV-6A, HHV-6B has very little to no ability to infect CD8+T cells, NK cells and gamma/delta T cells (Grivel *et al.*, 2003; Martin *et al.*, 2012). The cellular receptor for HHV-6B is CD134 which, like the cellular receptor for HHV-6A, CD46, is expressed on almost all human cells (Tang *et al.*, 2013), indicating that other factors are required for effective viral replication.

The HHV-6B viral chemokine U83B is specific for CCR2 and can cause chemoattraction of CCR2-expressing cells (classical and intermediate monocytes) for infection (Ablashi *et al.*, 2014; Clark *et al.*, 2013; Lüttichau *et al.*, 2003) (see Table 3). U83 from HHV-6B induced transient calcium mobilization and efficient migration in THP-1 cells (a monocyte cell line derived from monocytic leukaemia) (Zou *et al.*, 1999). U83B has been shown to have a different specificity from U83A as U83B chemoattracts CCR2-expressing monocytes, whereas U83A has a broader but still selective specificity as mentioned previously (Catusse *et al.*, 2008; Dewin *et al.*, 2006). The specificity of U83B for CCR2 appears to be due to its N-terminal region. Human chemokines can induce rapid internalization of CCR2 upon binding, whereas *in vitro* experiments show U83B does not cause CCR2 internalization. This finding is similar to the delayed internalization of CCR5 observed with U83A. CCR2 expression is induced in pro-inflammatory conditions and, interestingly, HHV-6B is associated with inflammatory diseases such as encephalitis and myocarditis (Clark *et al.*, 2013).

The HHV-6B GPCR U12 efficiently binds CCL2, CCL5 and CCL4, so it has overlapping activity with the receptors for CCL2 and CCL5 as in HHV-6A, but also has overlapping activity with the receptors for CCL4 (Balkwill, 2004; Isegawa *et al.*, 1998) (see Table 2). The exact role of chemokine receptors with these viruses is still unknown, but they could be multipurpose, in that they could have been developed for immune evasion to intercept chemokines that would otherwise be attracting immune cells to the area of infection, to attract uninfected cells that could then be infected, to induce latency, or to transition from latency to active replication.

Similar to HHV-6A, HHV-6B was shown to downregulate CXCR4 in CD4+T lymphocytes as well as MT-4 cells. This downregulation impaired the chemotactic response of the cells to the natural ligand, CXCL12 (Yasukawa *et al.*, 1999). Similar to HHV-6A, this could induce mobilization of HSPCs into the circulation as well as prevent migration of cells out of the thymus, both of which aid in the propagation and survival of the virus.

Human herpesvirus 7 (HHV-7)

As part of the same subfamily as HHV-6A and -6B, HHV-7 shares similar characteristics, including also being a T-lymphotropic virus, although it can infect other cell types (Ablashi *et al.*, 1995; Ward, 2005). Like other human

herpesviruses, once HHV-7 is acquired, the host is infected for life. The virus is shed in saliva and spread through this route of transmission. Compared with the other human herpesviruses, much less research has been conducted on HHV-7 infection and pathogenesis. Clinically it has been associated with the development of pityriasis rosea, post-infectious myeloradiculoneuropathy, encephalopathy and other syndromes. There is some speculation on the involvement of HHV-7 in the development and progression of these diseases (Chuh *et al.*, 2004; Mihara *et al.*, 2005; van den Berg *et al.*, 1999). HHV-7 infections can have a variety of symptoms, including fever, rash, febrile respiratory problems, vomiting and diarrhoea (Clark *et al.*, 1997; van den Berg *et al.*, 1999). Infections typically occur in children and are most often asymptomatic (Ward, 2005).

HHV-7 has been shown to influence migration in human cells in a variety of ways (see Tables 1 and 4). Yasukawa *et al.* (1999) showed that it downregulated transcription and surface expression of CXCR4 in CD4+T cells. As described before, CXCR4 is the receptor for CXCL12, which is secreted by various cells in the lymph nodes, bone marrow, etc. With CXCR4 assistance, T cells can follow a CXCL12 gradient to sites of inflammation (Domanska *et al.*, 2013). After infection with HHV-7, Yasukawa *et al.* (1999) tested the migration and intracellular levels of Ca^{2+} of CD4+T cells. It was found that infected cells demonstrated less migration following the CXCL12 gradient and decreased levels of intracellular Ca^{2+} compared with the mock-infected cells used as controls. It is currently unknown what viral factor(s) contribute to the downregulation of CXCR4. It has been demonstrated that lower levels of CXCR4 in HHV-7-positive T lymphocytes prevent infection by CXCR5-tropic HIV-1 (Yasukawa *et al.*, 1999). Future research could explore how HHV-7 manipulates CXCR4 in infected cells and further confirm the findings of Yasukawa *et al.* (1999), as theirs is the only study investigating this change in chemotaxis.

While CXCR4 is a cellular GPCR that is influenced post-viral infection, HHV-7 has two known viral chemokine receptors, products of the U12 and U51 genes. These genes were identified as GPCR homologues and later Tadagaki *et al.* investigated the functionality of the protein products of these genes (Nicholas, 1996; Tadagaki *et al.*, 2005). They verified that these proteins do accumulate on the surface of the cell. Further, they verified that they could act as functional chemokine signal receptors. Cells expressing U12 and U51 expressed heightened levels of intracellular Ca^{2+} after appropriate signalling through the U12 and U51 GPCRs. Testing the chemotactic effect of the expression of these proteins in the Jurkat T cell line using microchannel migration techniques, it was found that cells expressing U12 migrated effectively following a gradient of CCL19 and CCL21. This would make U12 a viral homologue of the cellular GPCR CCR7, as it also responds to both CCL19 and CCL21. Both of these chemokines are strongly expressed in the T cell zone of secondary lymphoid tissues and are important in lymphocyte homing and migration (Nomura *et al.*, 2001). It has also been observed that CCR7 expression is upregulated during HHV-7 infection (Hasegawa *et al.*, 1994). While the strategy behind the manipulation of cellular chemotaxis following these ligand chemokines is still unclear, it could be speculated that migration to such areas could be beneficial for HHV-7 transmission as T cells are preferential targets of infection. Tadagaki *et al.* (2005) also speculated that expression of these viral proteins could aid in immune evasion and viral replication. Further research in murine L1.2 cells showed that U12 and U51 products could respond to CCL22 and CCL19, respectively (Tadagaki *et al.*, 2007). Gene products U12 and U51 could act with CCR4 and CCR7, respectively, to direct migration in this cell line in response to CCL22 and CCL19 (Luther *et al.*, 2002). If this were to hold true in human cells infected with HHV-7, then infected cells would be expected to migrate more to areas of inflammation, as CCL22 is a pro-inflammatory chemokine secreted by a wide variety of cells, and areas of high T cell density as CCL19 is constitutively expressed by stromal cells in the T cell zone (Luther *et al.*, 2002). These areas would be attractive locations for the viral spread of HHV-7.

GAMMAHERPESVIRINAE

Epstein–Barr virus (EBV)

The main cause of viral mononucleosis, EBV infects nasopharyngeal epithelial cells and B lymphocytes (Balfour *et al.*, 2005; Cohen, 2000). Viral spread is mainly accomplished through shedding in saliva (Balfour *et al.*, 2005). EBV gains access to appropriate host cells by using viral gp350 to bind CD21 (a type 2 complement receptor) on the cell surface; the viral envelope then fuses with the cell membrane, releasing the viral capsid and associated tegument proteins into the cytoplasm (Toussirot & Roudier, 2008). The virus uses major histocompatibility complex class II molecules as cofactors when infecting B lymphocytes (Li *et al.*, 1997). During its latent infection of host B cells, EBV expresses one of four possible latency programmes, depending on cellular development and conditions (Young & Rickinson, 2004). It is likely that reactivation *in vivo* of latent virus is due to the differentiation of infected memory B lymphocytes (Amon & Farrell, 2005; Hochberg *et al.*, 2004b). EBV is associated with a variety of malignancies owing to its ability to regulate cell proliferation, including Burkitt's lymphoma, Hodgkin's lymphoma, nasopharyngeal carcinoma, gastric carcinoma, and post-transplant lymphoproliferative disorder (Hochberg *et al.*, 2004a; Kutok & Wang, 2006; Shibata & Weiss, 1992; Young & Rickinson, 2004).

During infection of B cells, EBV controls the expression of various endogenous chemokines and chemokine receptors (see Table 5). One such manipulated receptor that is shown to affect migration is CXCR4. As previously described it is

Table 5. Gammaherpesvirus changes cellular receptors/chemokines

Cell type	Receptor or chemokine	Virus	Amount or functionality	References
B cell	CXCR4	EBV	Decrease	Ehlin-Henriksson *et al.* (2006, 2009);
	CCR7	EBV	Decrease/increase	Nakayama *et al.* (2002)
	CCR6	EBV	Increase	Nakayama *et al.* (2002)
	CCR10	EBV	Increase	
	CXCR5	EBV	Decrease	Ehlin-Henriksson *et al.* (2009); Nakayama *et al.* (2002)
	EBI2	EBV	Increase	Birkenbach *et al.* (1993); Kelly *et al.* (2011)
Endothelial	CXCL8	KSHV	Increase	Wang *et al.* (2004b)
	CCL2	KSHV	Increase	Pati *et al.* (2001); Xu & Ganem (2007)
	CCL5	KSHV	Increase	
	CXCL7	KSHV	Increase	
	CXCL16	KSHV	Increase	

the receptor for CXCL12, which is secreted by various cells in a number of organs, including the lymph nodes, lungs, liver, kidneys, heart and bone marrow (Teicher & Fricker, 2010). Ehlin-Henriksson *et al.* (2006) demonstrated that tonsillar B cells infected with EBV showed reduced expression of CXCR4 (Ehlin-Henriksson *et al.*, 2006). Assays of chemotactic migration further showed that infected tonsillar B cells had decreased ability to migrate towards CXCL12. This decreased expression and the subsequent lack of chemotaxis was demonstrated in EBV-immortalized B cells as well (Nakayama *et al.*, 2002). The inability to follow the CXCL12 gradient would prevent infected B cells from migrating to tissues expressing only this chemokine. CCR7 is another host receptor that is virally regulated during EBV infection. In a later study by Ehlin-Henriksson *et al.* (2009), it was found that CCR7 is downregulated in tonsillar B cells post-infection. This change in expression led to decreased migration following the natural chemokine ligand CCL21. CCL21 is produced by stromal cells in primary and secondary lymphoid tissues and lymphatic endothelial cells in the peripheral tissue (Comerford *et al.*, 2013). It is critical for directing the formation of secondary lymphoid tissues such as spleen, Peyer's patches, and lymph nodes (Ohl *et al.*, 2003). It has also been surmised that CCR7 ligands are influential in tertiary lymphoid organs (Comerford *et al.*, 2013). Immortalized B lymphoblast cell lines (LCLs) have been shown to have an increased expression of CCR7 compared with uninfected cells. This upregulation resulted in increased migration following a CCL21 gradient in assays of chemotaxis (Nakayama *et al.*, 2002). While these results may seem to be paradoxical, it is possible that the difference in expression could be a result of a different latency programme or stage of viral infection. Ehlin-Henriksson *et al.* (2009) used harvested tonsillar B cells and measured CCR7 expression and cellular migration 7 days post-infection. In contrast, LCLs are a result of EBV immortalization of B lymphocytes, the process taking several weeks to establish the cell line and expressing a type III latency programme (Young & Rickinson, 2004). The difference in expression could be a result of either the length of infection or the latency programme employed by the virus post-infection.

In that same study of LCLs, it was found that they expressed increased amounts of CCR6 and CCR10, the natural ligands of which are CCL20 and CCL28, respectively. Migration assays confirmed that this change resulted in increased chemotaxis towards CCL20 and CCL28 chemokine gradients (Nakayama *et al.*, 2002). CCL20 is an inflammatory chemokine involved in the recruitment of dendritic cells, CD4 + T lymphocytes and B lymphocytes (Zhao *et al.*, 2014). CCL28 is secreted by epithelial cells that line the mucosa and is used to recruit IgA^+ plasma cells (Vazquez *et al.*, 2015; Wilson & Butcher, 2004). CCL28 expression is highest in the salivary glands (Liu *et al.*, 2012). It would be in the best interest of EBV to regulate these receptors, allowing the virus to migrate to mucosal tissues, such as the salivary gland, for effective viral spread. Chemotaxis to sites of inflammation could result in viral reactivation and increased targets for further infection. A final cellular receptor that is downregulated during infection, effecting a change in chemotaxis, is CXCR5. The inability to migrate owing to lowered levels of CXCR5 was observed in LCLs and infected tonsillar B cells (Ehlin-Henriksson *et al.*, 2009; Nakayama *et al.*, 2002). CXCR5 allows B cells to migrate in response to CXCL13 (Carlsen *et al.*, 2004). CXCL13 is an important chemokine for secondary lymphoid tissue development, and the main cells responsible for secretion of CXCL13 are follicular dendritic cells (Cyster *et al.*, 2000; Legler *et al.*, 1998). It is expressed in vascular tissue, Peyer's patches, and inflamed lymphoid tissue (Ebisuno *et al.*, 2003; Mazzucchelli *et al.*, 1999; Okada *et al.*, 2002; Shi *et al.*, 2001). A recent study of murine B lymphocyte positioning in CXCR5-negative mice demonstrated that CXCR5 is important for the retention of B cells in Peyer's patches (Schmidt & Zillikens, 2013). While avoiding tissue types expressing CXCL13 could be beneficial for the virus, possibly assisting in immune avoidance, the exact reason for regulating CXCR5 is still unclear. Another receptor thought to be

influenced by EBV is EBV-induced gene 2 (*EBI2*). Infected B cells display a heightened expression of EBI2 (Birkenbach *et al.*, 1993; Kelly *et al.*, 2011). While it remains unknown how EBV manipulates EBI2 expression in B lymphocytes, it has been observed that $EBI2^+$ cells migrate following a 7α-OHC gradient (Liu *et al.*, 2011). 7α-OHC is the natural ligand of EBI2 and is expressed by stromal cells of secondary lymph tissue, assisting in directed migration during cell chemotaxis in these areas (Gatto & Brink, 2013; Hannedouche *et al.*, 2011). Exaggerated expression of EBI2 by EBV could result in migration to the outer follicular zone in secondary lymph tissue, preventing migration toward T cell zones and germinal centres (Cyster, 2010).

The viral regulation of host lymphocytes extends to controlling various chemokines produced during infection, resulting in a change in the chemotaxis of uninfected cells. EBNA-3C, a viral product essential in establishing latency and immortalization of B cells, acts to regulate two host-produced chemokines, CXCL10 and CXCL11 (McClellan *et al.*, 2012). EBNA-3C has been found to interact with both transcriptional co-repressors and co-activators (Cotter & Robertson, 2000; Radkov *et al.*, 1999; Touitou *et al.*, 2001). Using the EBV-negative BJAB cell line, McClellan *et al.* (2012) showed that expression of EBNA-3C reduces expression of these two chemokines. The result is decreased migration of $CXCR3^+$ cells (McClellan *et al.*, 2012). Cells that express and migrate in response to CXCL10 and CXCL11 via CXCR3 include various T lymphocytes, including CD8 + T cells. CXCL10 and CXCL11 are typically expressed to attract Th1 cells in response to infection. EBV has also demonstrated the ability to influence the expression of chemokines via microRNAs (miRNAs). miR-BHRF1-3, an EBV-produced miRNA, has the ability to silence CXCL11 protein synthesis (Xia *et al.*, 2008). Downregulation of these chemokines suggests that immune avoidance could be a reason behind viral manipulation. Repression of CXCL11 would prevent attraction of cytotoxic T cells that might recognize virally infected B lymphocytes.

The chemokine receptor CXCR4 is a popular target for manipulation, and EBV, like other herpesviruses, uses it to prevent cell migration to certain tissue areas, probably to avoid immune detection. To achieve this same purpose, EBV also downregulates CCR7. During infection, the virus increases the host chemokine CCR6, allowing infected cells to more readily migrate to areas of inflammation. CCR10 function is also pirated, allowing infected cells to migrate toward epithelial cells, such as mucosal epithelial cells. This is likely vital for the spread of EBV. Reduction in expression of CXCL10 and CXCL11 could help in immune avoidance by suppressing the ability to attract T lymphocytes via these chemokines (see Fig. 2).

Kaposi's sarcoma herpesvirus (KSHV)

KSHV, also known as human herpesvirus 8 (HHV-8), is named after Moritz Kaposi, who originally described a unique skin lesion in the 1870s. The discovery of the association of herpesviral DNA sequences in Kaposi's sarcoma (KS) did not occur until 1994 (Chang *et al.*, 1994; Ganem, 2010). KS presents as tumours most often found in the dermis but can also be found in lungs, liver and intestines (Moore & Chang, 2003). KSHV is also linked to primary effusion lymphoma and multicentric Castleman's disease (Avey *et al.*, 2015; Cesarman *et al.*, 1995; Soulier *et al.*, 1995).

KSHV encodes three secreted chemokines; vCCL1 (ORF K6 or vMIP-I/MIP-1a), vCCL2 (ORF K4 or vMIP-II/MIP-1b) and vCCL3 (ORF K4.1 or vMIP-III/BCK), which activate CCR8, CCR3 and CCR4, respectively (see Table 3). This set of chemokines antagonizes the recruitment of Th1 and NK cells. This redirects the immune response from a Th1-like response towards a Th2 profile. vCCL2 has also been shown to prevent CCL5-mediated chemotaxis of Th1-like lymphocytes (Moore & Chang, 2003; Stebbing *et al.*, 2003; Weber *et al.*, 2001). The receptor XCR1, which normally binds the ligand XCL1 and is involved in T-cell recruitment, is selectively activated by vCCL3 but is also blocked by vCCL2. The opposing function and differing time of expression of the two viral chemokines could indicate the importance of the regulation of the XCR1 receptor in KSHV infection and pathogenesis. Neutrophils have high levels of XCR1, and vCCL3 chemoattracts these cells, which may indicate that neutrophils play a role in viral spread (Lüttichau *et al.*, 2007). vCCL1 and vCCL2 expression were also shown to induce migration of monocytes. This could play a role in the process of tumour development in KS as circulating monocytes could be recruited to KSHV-infected cells, thus propagating the infection (Nakano *et al.*, 2003).

KSHV encodes a GPCR (vGPCR or ORF74) that is homologous to CXCR2 and has a high level of constitutive activity (Arvanitakis *et al.*, 1997; Cesarman *et al.*, 1996; Hensbergen *et al.*, 2004; Pati *et al.*, 2001) (see Table 2). Constitutive expression of ORF74 in microvascular lung endothelial cells inhibits migration and increases cell survival. This inhibitory effect on migration can be reversed by endogenous chemokines CXCL10 and CXCL12. These act as inverse agonists of ORF74, as seen in an *in vitro* wound closure assay, where CXCL10 increased migration of ORF74-expressing cells. Limiting migration of infected cells may aid in immune evasion and KSHV survival. Constitutive expression of ORF74 has also been shown to attract uninfected endothelial cells, which could then be infected and propagate the infection (Couty *et al.*, 2009).

ORF74 has been shown to activate the transcriptional activators NF-κB and activator protein 1 (AP-1), leading to the downstream production of signals including IL-6, IL-8, granulocyte-macrophage colony-stimulating factor (GM-CSF) and CCL5 (Pati *et al.*, 2001; Schwarz & Murphy, 2001; Shepard *et al.*, 2001). Elevated levels of CXCL8 are observed in KS patients and can activate KSHV-infected cell growth and induce chemotaxis (Wang

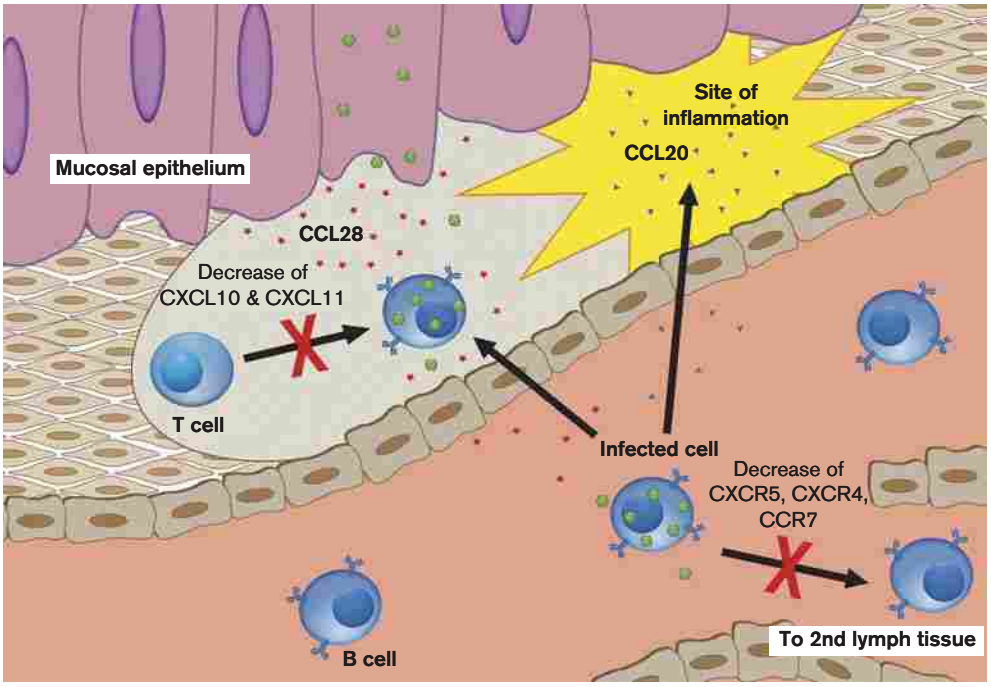

Fig. 2. Changes in cellular chemotaxis resulting from EBV infection. EBV decreases expression of cellular CXCR4 and CCR7 to prevent migration to certain tissue areas, probably to avoid immune detection. Increases in host chemokine CCR6 allow infected cells to migrate to areas of inflammation. CCR10 function is also pirated, allowing infected cells to migrate toward epithelial cells, such as mucosal epithelial cells. Downregulation of CXCL10 and CXCL11 could help in immune avoidance by suppressing the ability of infected cells to attract T lymphocytes.

et al., 2004b). CXCR1 and CXCR2, receptors that bind CXCL8, have been found to be expressed in KS lesions. CXCR4 has also been found to be expressed on cells in these lesions, which is important as this receptor acts as a co-receptor for CXCR4-tropic strains of HIV (Masood *et al.*, 2001; Pati *et al.*, 2001; Wang *et al.*, 2004b). These combined effects of ORF74 could stimulate the proliferation, migration and chemotaxis of endothelial cells in KS.

KSHV encodes a homologue of IL-6, vIL-6, that has been shown to promote migration of endothelial cells in both autocrine and paracrine fashions. Inhibition of this migration can be specifically inhibited by a DNA methyltransferase 1 (DNMT1) inhibitor, suggesting that the mechanism of vIL-6 is dependent on enhancing expression of DNMT1. As the control of DNA methylation is crucial for gene expression and other cellular processes, disruption of methylation could be a mechanism for KS tumorigenesis (Wu *et al.*, 2014).

There are a number of different cellular chemotactic proteins shown to be upregulated by KSHV, including: CCL2, CXCL7, CCL5, GM-CSF, CXCL16 and angiogenin (Xu & Ganem, 2007) (see Table 5). Some of these, such as CCL5 and GM-CSF, likely increase migration of endothelial cells toward KSHV-GPCR-expressing KS cells (Bussolino *et al.*, 1989; Pati *et al.*, 2001). In contrast, CXCL16 appears to play an indirect role in tumour growth and expansion through migration of activated T cells (Xu & Ganem, 2007). KSHV also causes downregulation of certain genes. The KSHV miRNA miR-K12-10a downregulates the cytokine receptor TNF-like weak inducer of apoptosis (TWEAK) receptor. This inhibits the pro-inflammatory response and also provides protection from TWEAK-induced apoptosis (Abend *et al.*, 2010).

Latency-associated nuclear antigen 1 (LANA-1; encoded by ORF73), a latently expressed gene, has been shown to hinder neutrophil chemotaxis, which interferes with recruitment of neutrophils to infected areas and could be a way in which latent KSHV survives host-induced acute inflammation. Neutrophil recruitment is restored in LANA-1 knockdowns, although not to the level of uninfected cells, indicating that KSHV has other mechanisms to repress neutrophil recruitment (Li *et al.*, 2011).

As seen with other herpesviruses, KSHV can induce or inhibit cellular migration, according to what is most beneficial for viral infection at the given stage. It not only interferes with cellular marker expression, it also induces increased production of specific chemokines and cytokines, which leads to other issues in cellular function and trafficking.

CONCLUDING REMARKS

With exposure to human herpesviruses being very common, it is important to understand how these infectious human pathogens influence infected and uninfected cell types. The viruses of the subfamily *Alphaherpesvirinae* use gG to increase the functionality of CXCR4, leading to increased chemotaxis to a variety of tissues while being able to manipulate cellular chemokines, such as CXCL9, to attract PBLs. Viruses of the subfamily *Betaherpesvirinae*, also capable of producing and manipulating chemokine and chemokine receptors, influence a variety of cells during infection. hCMV inhibits migration in infected monocytes and potentially attracts monocytes, PBMCs, macrophages, dendritic cells and regulatory T cells to sites of infection. Similarly, through its ability to attract target cells, HHV-6 is able to induce chemotaxis of T lymphocytes, monocytes, immature dendritic cells, and NK cells to areas of infected cells using viral U83. T cells infected with HHV-6 are further manipulated, as viral and cellular GPCRs allow cells to migrate to sites of inflammation and areas rich in T cells. Also manipulating T cells, HHV-7 prevents infected T lymphocytes from migrating to various organs and tissues by downregulating CXCR4. However, it too potentially encourages migration to inflammatory sites and locations high in T cells by inducing cells to follow chemokine gradients of CCR7, CCL21, CCL22 and CCL19.

Further masters of cellular piracy, viruses of the subfamily *Gammaherpesvirinae* also influence cellular chemotaxis to avoid immune detection and spread viral infection throughout the host until latency can be established. To prevent newly infected cells from potentially migrating to lymph tissue and other organs, EBV reduces expression of CXCR4, CCR7 and CXCR5. By downregulating the chemokines CXCL10 and CXCL11, EBV could prevent infected cells from attracting cytotoxic T cells. To regulate chemotaxis of cells during infection, KSHV regulates the attraction or avoidance of neutrophils and monocytes by viral chemokines vCCL1, 2 and 3. KSHV would be able to induce the chemotaxis of uninfected endothelial cells by upregulating various cellular chemokines and activating the NF-κB pathway, enabling viral spread.

Though our current understanding of how human herpesviruses affect host cell migration during infection is rather expansive, there still remain various areas for future research opportunities. In this review we have elaborated on the cells potentially affected by virally encoded and virally induced chemokines and chemokine receptors. However, the full range of cells affected by these chemokines remains to be tested and investigated further. Several virally regulated cell chemokine receptors suspected of influencing viral spread and immune avoidance are in need of confirmatory scientific inquiry. Several human herpesviruses have not been studied extensively for effects on cellular chemotaxis, such as the viruses of the subfamily *Alphaherpesvirinae* and HHV-7. These areas leave a variety of opportunities for future research that could contribute to our understanding of how these viruses lead to disease pathogenesis and progression.

REFERENCES

Abend, J. R., Uldrick, T. & Ziegelbauer, J. M. (2010). Regulation of tumor necrosis factor-like weak inducer of apoptosis receptor protein (TWEAKR) expression by Kaposi's sarcoma-associated herpesvirus microRNA prevents TWEAK-induced apoptosis and inflammatory cytokine expression. *J Virol* **84**, 12139–12151.

Ablashi, D. V., Lusso, P., Hung, C. L., Salahuddin, S. Z., Josephs, S. F., Llana, T., Kramarsky, B., Biberfeld, P., P, D. & Gallo, R. C. (1989). Utilization of human hematopoietic cell lines for the propagation and characterization of HBLV (human herpesvirus 6). *Dev Biol Stand* **70**, 139–146.

Ablashi, D., Agut, H., Berneman, Z., Campadelli-Fiume, G., Carrigan, D., Ceccerini-Nelli, L., Chandran, B., Chou, S., Collandre, H. & other authors (1993). Human herpesvirus-6 strain groups: a nomenclature. *Arch Virol* **129**, 363–366.

Ablashi, D. V., Berneman, Z. N., Kramarsky, B., Whitman, J., Jr., Asano, Y. & Pearson, G. R. (1995). Human herpesvirus-7 (HHV-7): current status. *Clin Diagn Virol* **4**, 1–13.

Ablashi, D., Agut, H., Alvarez-Lafuente, R., Clark, D. A., Dewhurst, S., DiLuca, D., Flamand, L., Frenkel, N., Gallo, R. & other authors (2014). Classification of HHV-6A and HHV-6B as distinct viruses. *Arch Virol* **159**, 863–870.

Adams, M. J. & Carstens, E. B. (2012). Ratification vote on taxonomic proposals to the International Committee on Taxonomy of Viruses (2012). *Arch Virol* **157**, 1411–1422.

Alkhatib, G. (2009). The biology of CCR5 and CXCR4. *Curr Opin HIV AIDS* **4**, 96–103.

Amon, W. & Farrell, P. J. (2005). Reactivation of Epstein-Barr virus from latency. *Rev Med Virol* **15**, 149–156.

Ansari, A. W., Kamarulzaman, A. & Schmidt, R. E. (2013). Multifaceted impact of host C-C chemokine CCL2 in the immuno-pathogenesis of HIV-1/M. tuberculosis co-infection. *Front Immunol* **4**, 312.

Ariza-Heredia, E. J., Nesher, L. & Chemaly, R. F. (2014). Cytomegalovirus diseases after hematopoietic stem cell transplantation: a mini-review. *Cancer Lett* **342**, 1–8.

Arnolds, K. L., Lares, A. P. & Spencer, J. V. (2013). The US27 gene product of human cytomegalovirus enhances signaling of host chemokine receptor CXCR4. *Virology* **439**, 122–131.

Arvanitakis, L., Geras-Raaka, E., Varma, A., Gershengorn, M. C. & Cesarman, E. (1997). Human herpesvirus KSHV encodes a constitutively active G-protein-coupled receptor linked to cell proliferation. *Nature* **385**, 347–350.

Avey, D., Brewers, B. & Zhu, F. (2015). Recent advances in the study of Kaposi's sarcoma-associated herpesvirus replication and pathogenesis. *Virol Sin* **30**, 130–145.

Balfour, H. H., Jr., Holman, C. J., Hokanson, K. M., Lelonek, M. M., Giesbrecht, J. E., White, D. R., Schmeling, D. O., Webb, C. H., Cavert, W. & other authors (2005). A prospective clinical study of Epstein-Barr virus and host interactions during acute infectious mononucleosis. *J Infect Dis* **192**, 1505–1512.

Balkwill, F. (2004). Cancer and the chemokine network. *Nat Rev Cancer* **4**, 540–550.

Bazan, J. F., Bacon, K. B., Hardiman, G., Wang, W., Soo, K., Rossi, D., Greaves, D. R., Zlotnik, A. & Schall, T. J. (1997). A new class of membrane-bound chemokine with a CX3C motif. *Nature* **385**, 640–644.

Bellner, L., Thorén, F., Nygren, E., Liljeqvist, J. A., Karlsson, A. & Eriksson, K. (2005). A proinflammatory peptide from herpes simplex virus type 2 glycoprotein G affects neutrophil, monocyte, and NK cell functions. *J Immunol* **174**, 2235–2241.

Bialas, K. M., Swamy, G. K. & Permar, S. R. (2015). Perinatal cytomegalovirus and varicella zoster virus infections: epidemiology, prevention, and treatment. *Clin Perinatol* **42**, 61–75.

Billottet, C., Quemener, C. & Bikfalvi, A. (2013). CXCR3, a double-edged sword in tumor progression and angiogenesis. *Biochim Biophys Acta* **1836**, 287–295.

Birkenbach, M., Josefsen, K., Yalamanchili, R., Lenoir, G. & Kieff, E. (1993). Epstein-Barr virus-induced genes: first lymphocyte-specific G protein-coupled peptide receptors. *J Virol* **67**, 2209–2220.

Bongers, G., Maussang, D., Muniz, L. R., Noriega, V. M., Fraile-Ramos, A., Barker, N., Marchesi, F., Thirunarayanan, N., Vischer, H. F. & other authors (2010). The cytomegalovirus-encoded chemokine receptor US28 promotes intestinal neoplasia in transgenic mice. *J Clin Invest* **120**, 3969–3978.

Bussolino, F., Wang, J. M., Defilippi, P., Turrini, F., Sanavio, F., Edgell, C. J., Aglietta, M., Arese, P. & Mantovani, A. (1989). Granulocyte- and granulocyte-macrophage-colony stimulating factors induce human endothelial cells to migrate and proliferate. *Nature* **337**, 471–473.

Calderón, L. & Boehm, T. (2011). Three chemokine receptors cooperatively regulate homing of hematopoietic progenitors to the embryonic mouse thymus. *Proc Natl Acad Sci U S A* **108**, 7517–7522.

Cannon, M. J. & Davis, K. F. (2005). Washing our hands of the congenital cytomegalovirus disease epidemic. *BMC Public Health* **5**, 70.

Cannon, M. J., Schmid, D. S. & Hyde, T. B. (2010). Review of cytomegalovirus seroprevalence and demographic characteristics associated with infection. *Rev Med Virol* **20**, 202–213.

Carlsen, H. S., Baekkevold, E. S., Morton, H. C., Haraldsen, G. & Brandtzaeg, P. (2004). Monocyte-like and mature macrophages produce CXCL13 (B cell-attracting chemokine 1) in inflammatory lesions with lymphoid neogenesis. *Blood* **104**, 3021–3027.

Catusse, J., Parry, C. M., Dewin, D. R. & Gompels, U. A. (2007). Inhibition of HIV-1 infection by viral chemokine U83A via high-affinity CCR5 interactions that block human chemokine-induced leukocyte chemotaxis and receptor internalization. *Blood* **109**, 3633–3639.

Catusse, J., Spinks, J., Mattick, C., Dyer, A., Laing, K., Fitzsimons, C., Smit, M. J. & Gompels, U. A. (2008). Immunomodulation by herpesvirus U51A chemokine receptor via CCL5 and FOG-2 down-regulation plus XCR1 and CCR7 mimicry in human leukocytes. *Eur J Immunol* **38**, 763–777.

Cerdan, C., Devilard, E., Xerri, L. & Olive, D. (2001). The C-class chemokine lymphotactin costimulates the apoptosis of human $CD4^+$T cells. *Blood* **97**, 2205–2212.

Cesarman, E., Chang, Y., Moore, P. S., Said, J. W. & Knowles, D. M. (1995). Kaposi's sarcoma-associated herpesvirus-like DNA sequences in AIDS-related body-cavity-based lymphomas. *N Engl J Med* **332**, 1186–1191.

Cesarman, E., Nador, R. G., Bai, F., Bohenzky, R. A., Russo, J. J., Moore, P. S., Chang, Y. & Knowles, D. M. (1996). Kaposi's sarcoma-associated herpesvirus contains G protein-coupled receptor and cyclin D homologs which are expressed in Kaposi's sarcoma and malignant lymphoma. *J Virol* **70**, 8218–8223.

Chang, Y., Cesarman, E., Pessin, M. S., Lee, F., Culpepper, J., Knowles, D. M. & Moore, P. S. (1994). Identification of herpesvirus-like DNA sequences in AIDS-associated Kaposi's sarcoma. *Science* **266**, 1865–1869.

Chang, W. L., Baumgarth, N., Yu, D. & Barry, P. A. (2004). Human cytomegalovirus-encoded interleukin-10 homolog inhibits maturation of dendritic cells and alters their functionality. *J Virol* **78**, 8720–8731.

Chen, D. H., Jiang, H., Lee, M., Liu, F. & Zhou, Z. H. (1999). Three-dimensional visualization of tegument/capsid interactions in the intact human cytomegalovirus. *Virology* **260**, 10–16.

Chuh, A., Chan, H. & Zawar, V. (2004). Pityriasis rosea—evidence for and against an infectious aetiology. *Epidemiol Infect* **132**, 381–390.

Clark, D. A., Kidd, I. M., Collingham, K. E., Tarlow, M., Ayeni, T., Riordan, A., Griffiths, P. D., Emery, V. C. & Pillay, D. (1997). Diagnosis of primary human herpesvirus 6 and 7 infections in febrile infants by polymerase chain reaction. *Arch Dis Child* **77**, 42–45.

Clark, D. J., Catusse, J., Stacey, A., Borrow, P. & Gompels, U. A. (2013). Activation of CCR2+ human proinflammatory monocytes by human herpesvirus-6B chemokine N-terminal peptide. *J Gen Virol* **94**, 1624–1635.

Cohen, J. I. (2000). Epstein-Barr virus infection. *N Engl J Med* **343**, 481–492.

Comerford, I., Harata-Lee, Y., Bunting, M. D., Gregor, C., Kara, E. E. & McColl, S. R. (2013). A myriad of functions and complex regulation of the CCR7/CCL19/CCL21 chemokine axis in the adaptive immune system. *Cytokine Growth Factor Rev* **24**, 269–283.

Cotter, M. A., II & Robertson, E. S. (2000). Modulation of histone acetyltransferase activity through interaction of Epstein-Barr nuclear antigen 3C with prothymosin alpha. *Mol Cell Biol* **20**, 5722–5735.

Couty, J. P., Lupu-Meiri, M., Oron, Y. & Gershengorn, M. C. (2009). Kaposi's sarcoma-associated herpesvirus-G protein-coupled receptor-expressing endothelial cells exhibit reduced migration and stimulated chemotaxis by chemokine inverse agonists. *J Pharmacol Exp Ther* **329**, 1142–1147.

Cyster, J. G. (2010). B cell follicles and antigen encounters of the third kind. *Nat Immunol* **11**, 989–996.

Cyster, J. G., Ansel, K. M., Reif, K., Ekland, E. H., Hyman, P. L., Tang, H. L., Luther, S. A. & Ngo, V. N. (2000). Follicular stromal cells and lymphocyte homing to follicles. *Immunol Rev* **176**, 181–193.

Deanfield, J. E., Halcox, J. P. & Rabelink, T. J. (2007). Endothelial function and dysfunction: testing and clinical relevance. *Circulation* **115**, 1285–1295.

Desloges, N., Schubert, C., Wolff, M. H. & Rahaus, M. (2008). Varicella-zoster virus infection induces the secretion of interleukin-8. *Med Microbiol Immunol (Berl)* **197**, 277–284.

Dewin, D. R., Catusse, J. & Gompels, U. A. (2006). Identification and characterization of U83A viral chemokine, a broad and potent β-chemokine agonist for human CCRs with unique selectivity and inhibition by spliced isoform. *J Immunol* **176**, 544–556.

Domanska, U. M., Kruizinga, R. C., Nagengast, W. B., Timmer-Bosscha, H., Huls, G., de Vries, E. G. & Walenkamp, A. M. (2013). A review on CXCR4/CXCL12 axis in oncology: no place to hide. *Eur J Cancer* **49**, 219–230.

Ebisuno, Y., Tanaka, T., Kanemitsu, N., Kanda, H., Yamaguchi, K., Kaisho, T., Akira, S. & Miyasaka, M. (2003). Cutting edge: the B cell chemokine CXC chemokine ligand 13/B lymphocyte chemoattractant is expressed in the high endothelial venules of lymph nodes and Peyer's patches and affects B cell trafficking across high endothelial venules. *J Immunol* **171**, 1642–1646.

Ehlin-Henriksson, B., Mowafi, F., Klein, G. & Nilsson, A. (2006). Epstein-Barr virus infection negatively impacts the CXCR4-dependent migration of tonsillar B cells. *Immunology* **117**, 379–385.

Ehlin-Henriksson, B., Liang, W., Cagigi, A., Mowafi, F., Klein, G. & Nilsson, A. (2009). Changes in chemokines and chemokine receptor

expression on tonsillar B cells upon Epstein-Barr virus infection. *Immunology* **127**, 549–557.

Fielding, C. A. (2015). Mimicry of cytokine pathways by human herpesviruses. *Future Virol* **10**, 41–51.

Fitzsimons, C. P., Gompels, U. A., Verzijl, D., Vischer, H. F., Mattick, C., Leurs, R. & Smit, M. J. (2006). Chemokine-directed trafficking of receptor stimulus to different G proteins: selective inducible and constitutive signaling by human herpesvirus 6-encoded chemokine receptor U51. *Mol Pharmacol* **69**, 888–898.

Flint, S. J. & American Society for Microbiology (2009). *Principles of Virology*. Washington, DC: American Society for Microbiology.

Fraile-Ramos, A., Pelchen-Matthews, A., Kledal, T. N., Browne, H., Schwartz, T. W. & Marsh, M. (2002). Localization of HCMV UL33 and US27 in endocytic compartments and viral membranes. *Traffic* **3**, 218–232.

Franciotta, D., Salvetti, M., Lolli, F., Serafini, B. & Aloisi, F. (2008). B cells and multiple sclerosis. *Lancet Neurol* **7**, 852–858.

Frascaroli, G., Varani, S., Moepps, B., Sinzger, C., Landini, M. P. & Mertens, T. (2006). Human cytomegalovirus subverts the functions of monocytes, impairing chemokine-mediated migration and leukocyte recruitment. *J Virol* **80**, 7578–7589.

Frascaroli, G., Varani, S., Blankenhorn, N., Pretsch, R., Bacher, M., Leng, L., Bucala, R., Landini, M. P. & Mertens, T. (2009). Human cytomegalovirus paralyzes macrophage motility through down-regulation of chemokine receptors, reorganization of the cyto-skeleton, and release of macrophage migration inhibitory factor. *J Immunol* **182**, 477–488.

French, C., Menegazzi, P., Nicholson, L., Macaulay, H., DiLuca, D. & Gompels, U. A. (1999). Novel, nonconsensus cellular splicing regulates expression of a gene encoding a chemokine-like protein that shows high variation and is specific for human herpesvirus 6. *Virology* **262**, 139–151.

Gandhi, M. K. & Khanna, R. (2004). Human cytomegalovirus: clinical aspects, immune regulation, and emerging treatments. *Lancet Infect Dis* **4**, 725–738.

Ganem, D. (2010). KSHV and the pathogenesis of Kaposi sarcoma: listening to human biology and medicine. *J Clin Invest* **120**, 939–949.

Gao, H., Tao, R., Zheng, Q., Xu, J. & Shang, S. (2013). Recombinant HCMV UL128 expression and functional identification of PBMC-attracting activity in vitro. *Arch Virol* **158**, 173–177, 179.

Gatto, D. & Brink, R. (2013). B cell localization: regulation by EBI2 and its oxysterol ligand. *Trends Immunol* **34**, 336–341.

Gilden, D., Nagel, M. A. & Cohrs, R. J. (2014). Varicella-zoster. *Handb Clin Neurol* **123**, 265–283.

Grivel, J. C., Ito, Y., Fagà, G., Santoro, F., Shaheen, F., Malnati, M. S., Fitzgerald, W., Lusso, P. & Margolis, L. (2001). Suppression of CCR5- but not CXCR4-tropic HIV-1 in lymphoid tissue by human herpesvirus 6. *Nat Med* **7**, 1232–1235.

Grivel, J. C., Santoro, F., Chen, S., Fagá, G., Malnati, M. S., Ito, Y., Margolis, L. & Lusso, P. (2003). Pathogenic effects of human herpesvirus 6 in human lymphoid tissue ex vivo. *J Virol* **77**, 8280–8289.

Hall, C. B., Caserta, M. T., Schnabel, K. C., McDermott, M. P., Lofthus, G. K., Carnahan, J. A., Gilbert, L. M. & Dewhurst, S. (2006). Characteristics and acquisition of human herpesvirus (HHV) 7 infections in relation to infection with HHV-6. *J Infect Dis* **193**, 1063–1069.

Hannedouche, S., Zhang, J., Yi, T., Shen, W., Nguyen, D., Pereira, J. P., Guerini, D., Baumgarten, B. U., Roggo, S. & other authors (2011). Oxysterols direct immune cell migration via EBI2. *Nature* **475**, 524–527.

Hasegawa, H., Utsunomiya, Y., Yasukawa, M., Yanagisawa, K. & Fujita, S. (1994). Induction of G protein-coupled peptide receptor EBI 1 by human herpesvirus 6 and 7 infection in CD4+T cells. *J Virol* **68**, 5326–5329.

Hensbergen, P. J., Verzijl, D., Balog, C. I., Dijkman, R., van der Schors, R. C., van der Raaij-Helmer, E. M., van der Plas, M. J., Leurs, R., Deelder, A. M. & other authors (2004). Furin is a chemokine-modifying enzyme: in vitro and in vivo processing of CXCL10 generates a C-terminally truncated chemokine retaining full activity. *J Biol Chem* **279**, 13402–13411.

Hochberg, D., Middeldorp, J. M., Catalina, M., Sullivan, J. L., Luzuriaga, K. & Thorley-Lawson, D. A. (2004a). Demonstration of the Burkitt's lymphoma Epstein-Barr virus phenotype in dividing latently infected memory cells in vivo. *Proc Natl Acad Sci U S A* **101**, 239–244.

Hochberg, D., Souza, T., Catalina, M., Sullivan, J. L., Luzuriaga, K. & Thorley-Lawson, D. A. (2004b). Acute infection with Epstein-Barr virus targets and overwhelms the peripheral memory B-cell compartment with resting, latently infected cells. *J Virol* **78**, 5194–5204.

Huang, W., Hu, K., Luo, S., Zhang, M., Li, C., Jin, W., Liu, Y., Griffin, G. E., Shattock, R. J. & Hu, Q. (2012). Herpes simplex virus type 2 infection of human epithelial cells induces CXCL9 expression and CD4+T cell migration via activation of p38-CCAAT/enhancer-binding protein-β pathway. *J Immunol* **188**, 6247–6257.

Ihara, T., Yasuda, N., Kamiya, H., Torigoe, S. & Sakurai, M. (1991). Chemotaxis of polymorphonuclear leukocytes to varicella-zoster virus antigens. *Microb Pathog* **10**, 451–458.

Isegawa, Y., Ping, Z., Nakano, K., Sugimoto, N. & Yamanishi, K. (1998). Human herpesvirus 6 open reading frame U12 encodes a functional beta-chemokine receptor. *J Virol* **72**, 6104–6112.

Karpova, D. & Bonig, H. (2015). Concise review: CXCR4/CXCL12 signaling in immature hematopoiesis—lessons from pharmacological and genetic models. *Stem Cells* **33**, 2391–2399.

Kelly, L. M., Pereira, J. P., Yi, T., Xu, Y. & Cyster, J. G. (2011). EBI2 guides serial movements of activated B cells and ligand activity is detectable in lymphoid and nonlymphoid tissues. *J Immunol* **187**, 3026–3032.

Kim, Y., Lee, S., Kim, S., Kim, D., Ahn, J. H. & Ahn, K. (2012). Human cytomegalovirus clinical strain-specific microRNA miR-UL148D targets the human chemokine RANTES during infection. *PLoS Pathog* **8**, e1002577.

Kledal, T. N., Rosenkilde, M. M. & Schwartz, T. W. (1998). Selective recognition of the membrane-bound CX3C chemokine, fractalkine, by the human cytomegalovirus-encoded broad-spectrum receptor US28. *FEBS Lett* **441**, 209–214.

Kutok, J. L. & Wang, F. (2006). Spectrum of Epstein-Barr virus-associated diseases. *Annu Rev Pathol* **1**, 375–404.

Lee, A. W., Hertel, L., Louie, R. K., Burster, T., Lacaille, V., Pashine, A., Abate, D. A., Mocarski, E. S. & Mellins, E. D. (2006). Human cytomegalovirus alters localization of MHC class II and dendrite morphology in mature Langerhans cells. *J Immunol* **177**, 3960–3971.

Legler, D. F., Loetscher, M., Roos, R. S., Clark-Lewis, I., Baggiolini, M. & Moser, B. (1998). B cell-attracting chemokine 1, a human CXC chemokine expressed in lymphoid tissues, selectively attracts B lymphocytes via BLR1/CXCR5. *J Exp Med* **187**, 655–660.

Li, Q., Spriggs, M. K., Kovats, S., Turk, S. M., Comeau, M. R., Nepom, B. & Hutt-Fletcher, L. M. (1997). Epstein-Barr virus uses HLA class II as a cofactor for infection of B lymphocytes. *J Virol* **71**, 4657–4662.

Li, X., Liang, D., Lin, X., Robertson, E. S. & Lan, K. (2011). Kaposi's sarcoma-associated herpesvirus-encoded latency-associated nuclear antigen reduces interleukin-8 expression in endothelial cells and

impairs neutrophil chemotaxis by degrading nuclear p65. *J Virol* **85**, 8606–8615.

Liu, C., Yang, X. V., Wu, J., Kuei, C., Mani, N. S., Zhang, L., Yu, J., Sutton, S. W., Qin, N. & other authors (2011). Oxysterols direct B-cell migration through EBI2. *Nature* **475**, 519–523.

Liu, G. X., Lan, J., Sun, Y., Hu, Y. J. & Jiang, G. S. (2012). Expression of the chemokine CCL28 in pleomorphic adenoma and adenolymphoma of the human salivary glands. *Exp Ther Med* **4**, 65–69.

Luker, K. E. & Luker, G. D. (2006). Functions of CXCL12 and CXCR4 in breast cancer. *Cancer Lett* **238**, 30–41.

Lusso, P., De Maria, A., Malnati, M., Lori, F., DeRocco, S. E., Baseler, M. & Gallo, R. C. (1991). Induction of CD4 and susceptibility to HIV-1 infection in human $CD8^+$T lymphocytes by human herpesvirus 6. *Nature* **349**, 533–535.

Lusso, P., Malnati, M. S., Garzino-Demo, A., Crowley, R. W., Long, E. O. & Gallo, R. C. (1993). Infection of natural killer cells by human herpesvirus 6. *Nature* **362**, 458–462.

Lusso, P., Garzino-Demo, A., Crowley, R. W. & Malnati, M. S. (1995). Infection of gamma/delta T lymphocytes by human herpesvirus 6: transcriptional induction of CD4 and susceptibility to HIV infection. *J Exp Med* **181**, 1303–1310.

Lusso, P., Crowley, R. W., Malnati, M. S., Di Serio, C., Ponzoni, M., Biancotto, A., Markham, P. D. & Gallo, R. C. (2007). Human herpesvirus 6A accelerates AIDS progression in macaques. *Proc Natl Acad Sci U S A* **104**, 5067–5072.

Luther, S. A., Bidgol, A., Hargreaves, D. C., Schmidt, A., Xu, Y., Paniyadi, J., Matloubian, M. & Cyster, J. G. (2002). Differing activities of homeostatic chemokines CCL19, CCL21, and CXCL12 in lymphocyte and dendritic cell recruitment and lymphoid neogenesis. *J Immunol* **169**, 424–433.

Lüttichau, H. R. (2010). The cytomegalovirus UL146 gene product vCXCL1 targets both CXCR1 and CXCR2 as an agonist. *J Biol Chem* **285**, 9137–9146.

Lüttichau, H. R., Clark-Lewis, I., Jensen, P. Ø., Moser, C., Gerstoft, J. & Schwartz, T. W. (2003). A highly selective CCR2 chemokine agonist encoded by human herpesvirus 6. *J Biol Chem* **278**, 10928–10933.

Lüttichau, H. R., Johnsen, A. H., Jurlander, J., Rosenkilde, M. M. & Schwartz, T. W. (2007). Kaposi sarcoma-associated herpes virus targets the lymphotactin receptor with both a broad spectrum antagonist vCCL2 and a highly selective and potent agonist vCCL3. *J Biol Chem* **282**, 17794–17805.

Martin, L. K., Schub, A., Dillinger, S. & Moosmann, A. (2012). Specific CD8 T cells recognize human herpesvirus 6B. *Eur J Immunol* **42**, 2901–2912.

Martinez-Martin, N., Viejo-Borbolla, A., Martín, R., Blanco, S., Benovic, J. L., Thelen, M. & Alcamí, A. (2015). Herpes simplex virus enhances chemokine function through modulation of receptor trafficking and oligomerization. *Nat Commun* **6**, 6163.

Masood, R., Cai, J., Tulpule, A., Zheng, T., Hamilton, A., Sharma, S., Espina, B. M., Smith, D. L. & Gill, P. S. (2001). Interleukin 8 is an autocrine growth factor and a surrogate marker for Kaposi's sarcoma. *Clin Cancer Res* **7**, 2693–2702.

Mazzucchelli, L., Blaser, A., Kappeler, A., Schärli, P., Laissue, J. A., Baggiolini, M. & Uguccioni, M. (1999). BCA-1 is highly expressed in Helicobacter pylori-induced mucosa-associated lymphoid tissue and gastric lymphoma. *J Clin Invest* **104**, R49–R54.

McClellan, M. J., Khasnis, S., Wood, C. D., Palermo, R. D., Schlick, S. N., Kanhere, A. S., Jenner, R. G. & West, M. J. (2012). Downregulation of integrin receptor-signaling genes by Epstein-Barr virus EBNA 3C via promoter-proximal and -distal binding elements. *J Virol* **86**, 5165–5178.

McGavran, M. H. & Smith, M. G. (1965). Ultrastructural, cytochemical, and microchemical observations on cytomegalovirus (salivary gland virus) infection of human cells in tissue culture. *Exp Mol Pathol* **4**, 1–10.

Mihara, T., Mutoh, T., Yoshikawa, T., Yano, S., Asano, Y. & Yamamoto, H. (2005). Postinfectious myeloradiculoneuropathy with cranial nerve involvements associated with human herpesvirus 7 infection. *Arch Neurol* **62**, 1755–1757.

Milne, R. S., Mattick, C., Nicholson, L., Devaraj, P., Alcami, A. & Gompels, U. A. (2000). RANTES binding and down-regulation by a novel human herpesvirus-6 β chemokine receptor. *J Immunol* **164**, 2396–2404.

Moore, P. S. & Chang, Y. (2003). Kaposi's sarcoma-associated herpesvirus immunoevasion and tumorigenesis: two sides of the same coin? *Annu Rev Microbiol* **57**, 609–639.

Moutaftsi, M., Brennan, P., Spector, S. A. & Tabi, Z. (2004). Impaired lymphoid chemokine-mediated migration due to a block on the chemokine receptor switch in human cytomegalovirus-infected dendritic cells. *J Virol* **78**, 3046–3054.

Murphy, G., Caplice, N. & Molloy, M. (2008). Fractalkine in rheumatoid arthritis: a review to date. *Rheumatology (Oxford)* **47**, 1446–1451.

Nakano, K., Isegawa, Y., Zou, P., Tadagaki, K., Inagi, R. & Yamanishi, K. (2003). Kaposi's sarcoma-associated herpesvirus (KSHV)-encoded vMIP-I and vMIP-II induce signal transduction and chemotaxis in monocytic cells. *Arch Virol* **148**, 871–890.

Nakayama, T., Fujisawa, R., Izawa, D., Hieshima, K., Takada, K. & Yoshie, O. (2002). Human B cells immortalized with Epstein-Barr virus upregulate CCR6 and CCR10 and downregulate CXCR4 and CXCR5. *J Virol* **76**, 3072–3077.

Nash, B. & Meucci, O. (2014). Functions of the chemokine receptor CXCR4 in the central nervous system and its regulation by μ-opioid receptors. *Int Rev Neurobiol* **118**, 105–128.

Nicholas, J. (1996). Determination and analysis of the complete nucleotide sequence of human herpesvirus. *J Virol* **70**, 5975–5989.

Nomura, T., Hasegawa, H., Kohno, M., Sasaki, M. & Fujita, S. (2001). Enhancement of anti-tumor immunity by tumor cells transfected with the secondary lymphoid tissue chemokine EBI-1-ligand chemokine and stromal cell-derived factor-1α chemokine genes. *Int J Cancer* **91**, 597–606.

Ohl, L., Henning, G., Krautwald, S., Lipp, M., Hardtke, S., Bernhardt, G., Pabst, O. & Förster, R. (2003). Cooperating mechanisms of CXCR5 and CCR7 in development and organization of secondary lymphoid organs. *J Exp Med* **197**, 1199–1204.

Okada, T., Ngo, V. N., Ekland, E. H., Förster, R., Lipp, M., Littman, D. R. & Cyster, J. G. (2002). Chemokine requirements for B cell entry to lymph nodes and Peyer's patches. *J Exp Med* **196**, 65–75.

Park, B., Oh, H., Lee, S., Song, Y., Shin, J., Sung, Y. C., Hwang, S. Y. & Ahn, K. (2002). The MHC class I homolog of human cytomegalovirus is resistant to down-regulation mediated by the unique short region protein (US)2, US3, US6, and US11 gene products. *J Immunol* **168**, 3464–3469.

Pati, S., Cavrois, M., Guo, H. G., Foulke, J. S., Jr., Kim, J., Feldman, R. A. & Reitz, M. (2001). Activation of NF-κB by the human herpesvirus 8 chemokine receptor ORF74: evidence for a paracrine model of Kaposi's sarcoma pathogenesis. *J Virol* **75**, 8660–8673.

Penfold, M. E., Dairaghi, D. J., Duke, G. M., Saederup, N., Mocarski, E. S., Kemble, G. W. & Schall, T. J. (1999). Cytomegalovirus encodes a potent α chemokine. *Proc Natl Acad Sci U S A* **96**, 9839–9844.

Poole, E., King, C. A., Sinclair, J. H. & Alcami, A. (2006). The UL144 gene product of human cytomegalovirus activates NFκB via a TRAF6-dependent mechanism. *EMBO J* **25**, 4390–4399.

Poznansky, M. C., Olszak, I. T., Evans, R. H., Wang, Z., Foxall, R. B., Olson, D. P., Weibrecht, K., Luster, A. D. & Scadden, D. T. (2002). Thymocyte emigration is mediated by active movement away from stroma-derived factors. *J Clin Invest* **109**, 1101–1110.

Radkov, S. A., Touitou, R., Brehm, A., Rowe, M., M, ., Kouzarides, T. & Allday, M. J. (1999). Epstein-Barr virus nuclear antigen 3C interacts with histone deacetylase to repress transcription. *J Virol* **73**, 5688–5697.

Reinhardt, B., Godfrey, R., Fellbrich, G., Frank, H., Lüske, A., Olieslagers, S., Mertens, T. & Waltenberger, J. (2014). Human cytomegalovirus infection impairs endothelial cell chemotaxis by disturbing VEGF signalling and actin polymerization. *Cardiovasc Res* **104**, 315–325.

Rosenkilde, M. M. & Schwartz, T. W. (2004). The chemokine system - a major regulator of angiogenesis in health and disease. *Acta Path Microbiol Immunol Scand* **112**, 481–495.

Salahuddin, S. Z., Ablashi, D. V., Markham, P. D., Josephs, S. F., Sturzenegger, S., Kaplan, M., Halligan, G., Biberfeld, P., Wong-Staal, F. & other authors (1986). Isolation of a new virus, HBLV, in patients with lymphoproliferative disorders. *Science* **234**, 596–601.

Schmidt, E. & Zillikens, D. (2013). Pemphigoid diseases. *Lancet* **381**, 320–332.

Schwarz, M. & Murphy, P. M. (2001). Kaposi's sarcoma-associated herpesvirus G protein-coupled receptor constitutively activates NF-κB and induces proinflammatory cytokine and chemokine production via a C-terminal signaling determinant. *J Immunol* **167**, 505–513.

Shavit, I., Shehadeh, N., Zmora, O., Avidor, I. & Etzioni, A. (1999). Severe necrotizing otitis and varicella associated with transient neutrophil chemotactic defect. *Isr Med Assoc J* **1**, 60–61.

Shepard, L. W., Yang, M., Xie, P., Browning, D. D., Voyno-Yasenetskaya, T., Kozasa, T. & Ye, R. D. (2001). Constitutive activation of NF-κB and secretion of interleukin-8 induced by the G protein-coupled receptor of Kaposi's sarcoma-associated herpesvirus involve Gα13 and RhoA. *J Biol Chem* **276**, 45979–45987.

Shi, K., Hayashida, K., Kaneko, M., Hashimoto, J., Tomita, T., Lipsky, P. E., Yoshikawa, H. & Ochi, T. (2001). Lymphoid chemokine B cell-attracting chemokine-1 (CXCL13) is expressed in germinal center of ectopic lymphoid follicles within the synovium of chronic arthritis patients. *J Immunol* **166**, 650–655.

Shibata, D. & Weiss, L. M. (1992). Epstein-Barr virus-associated gastric adenocarcinoma. *Am J Pathol* **140**, 769–774.

Siakallis, G., Spandidos, D. A. & Sourvinos, G. (2009). Herpesviridae and novel inhibitors. *Antivir Ther* **14**, 1051–1064.

Smith, M. S., Bentz, G. L., Alexander, J. S. & Yurochko, A. D. (2004). Human cytomegalovirus induces monocyte differentiation and migration as a strategy for dissemination and persistence. *J Virol* **78**, 4444–4453.

Soria, G. & Ben-Baruch, A. (2008). The inflammatory chemokines CCL2 and CCL5 in breast cancer. *Cancer Lett* **267**, 271–285.

Soulier, J., Grollet, L., Oksenhendler, E., Cacoub, P., Cazals-Hatem, D., Babinet, P., d'Agay, M. F., Clauvel, J. P. & Raphael, M. (1995). Kaposi's sarcoma-associated herpesvirus-like DNA sequences in multicentric Castleman's disease. *Blood* **86**, 1276–1280.

Stapleton, L. K., Arnolds, K. L., Lares, A. P., Devito, T. M. & Spencer, J. V. (2012). Receptor chimeras demonstrate that the C-terminal domain of the human cytomegalovirus US27 gene product is necessary and sufficient for intracellular receptor localization. *Virol J* **9**, 42.

Steain, M., Gowrishankar, K., Rodriguez, M., Slobedman, B. & Abendroth, A. (2011). Upregulation of CXCL10 in human dorsal root ganglia during experimental and natural varicella-zoster virus infection. *J Virol* **85**, 626–631.

Stebbing, J., Portsmouth, S. & Bower, M. (2003). Insights into the molecular biology and sero-epidemiology of Kaposi's sarcoma. *Curr Opin Infect Dis* **16**, 25–31.

Stern, J. L. & Slobedman, B. (2008). Human cytomegalovirus latent infection of myeloid cells directs monocyte migration by up-regulating monocyte chemotactic protein-1. *J Immunol* **180**, 6577–6585.

Straschewski, S., Patrone, M., Walther, P., Gallina, A., Mertens, T. & Frascaroli, G. (2011). Protein pUL128 of human cytomegalovirus is necessary for monocyte infection and blocking of migration. *J Virol* **85**, 5150–5158.

Streblow, D. N., Soderberg-Naucler, C., Vieira, J., Smith, P., Wakabayashi, E., Ruchti, F., Mattison, K., Altschuler, Y. & Nelson, J. A. (1999). The human cytomegalovirus chemokine receptor US28 mediates vascular smooth muscle cell migration. *Cell* **99**, 511–520.

Streblow, D. N., Orloff, S. L. & J, A. (2001). Do pathogens accelerate atherosclerosis? *J Nutr* **131**, 2798S–2804S.

Tadagaki, K., Nakano, K. & Yamanishi, K. (2005). Human herpesvirus 7 open reading frames U12 and U51 encode functional β-chemokine receptors. *J Virol* **79**, 7068–7076.

Tadagaki, K., Yamanishi, K. & Mori, Y. (2007). Reciprocal roles of cellular chemokine receptors and human herpesvirus 7-encoded chemokine receptors, U12 and U51. *J Gen Virol* **88**, 1423–1428.

Tadagaki, K., Tudor, D., Gbahou, F., Tschische, P., Waldhoer, M., Bomsel, M., Jockers, R. & Kamal, M. (2012). Human cytomegalovirus-encoded UL33 and UL78 heteromerize with host CCR5 and CXCR4 impairing their HIV coreceptor activity. *Blood* **119**, 4908–4918.

Tang, H., Serada, S., Kawabata, A., Ota, M., Hayashi, E., Naka, T., Yamanishi, K. & Mori, Y. (2013). CD134 is a cellular receptor specific for human herpesvirus-6B entry. *Proc Natl Acad Sci U S A* **110**, 9096–9099.

Teicher, B. A. & Fricker, S. P. (2010). CXCL12 (SDF-1)/CXCR4 pathway in cancer. *Clin Cancer Res* **16**, 2927–2931.

Touitou, R., Hickabottom, M., Parker, G., Crook, T. & Allday, M. J. (2001). Physical and functional interactions between the corepressor CtBP and the Epstein-Barr virus nuclear antigen EBNA3C. *J Virol* **75**, 7749–7755.

Toussirot, E. & Roudier, J. (2008). Epstein-Barr virus in autoimmune diseases. *Best Pract Res Clin Rheumatol* **22**, 883–896.

Tschische, P., Tadagaki, K., Kamal, M., Jockers, R. & Waldhoer, M. (2011). Heteromerization of human cytomegalovirus encoded chemokine receptors. *Biochem Pharmacol* **82**, 610–619.

Turner, M. D., Nedjai, B., Hurst, T. & Pennington, D. J. (2014). Cytokines and chemokines: at the crossroads of cell signalling and inflammatory disease. *Biochim Biophys Acta* **1843**, 2563–2582.

van den Berg, J. S., van Zeijl, J. H., Rotteveel, J. J., Melchers, W. J., Gabreëls, F. J. & Galama, J. M. (1999). Neuroinvasion by human herpesvirus type 7 in a case of exanthem subitum with severe neurologic manifestations. *Neurology* **52**, 1077–1079.

Van Raemdonck, K., Van den Steen, P. E., Liekens, S., Van Damme, J. & Struyf, S. (2015). CXCR3 ligands in disease and therapy. *Cytokine Growth Factor Rev* **26**, 311–327.

Varani, S., Frascaroli, G., Homman-Loudiyi, M., Feld, S., Landini, M. P. & Söderberg-Nauclér, C. (2005). Human cytomegalovirus inhibits the migration of immature dendritic cells by down-regulating cell-surface CCR1 and CCR5. *J Leukoc Biol* **77**, 219–228.

Vazquez, M. I., Catalan-Dibene, J. & Zlotnik, A. (2015). B cells responses and cytokine production are regulated by their immune microenvironment. *Cytokine* **74**, 318–326.

Viejo-Borbolla, A., Martinez-Martin, N., Nel, H. J., Rueda, P., Martín, R., Blanco, S., Arenzana-Seisdedos, F., Thelen, M., Fallon, P. G. &

Alcami, A. (2012). Enhancement of chemokine function as an immunomodulatory strategy employed by human herpesviruses. *PLoS Pathog* **8**, e1002497.

Vomaske, J., Melnychuk, R. M., Smith, P. P., Powell, J., Hall, L., DeFilippis, V., Früh, K., Smit, M., Schlaepfer, D. D. & other authors (2009). Differential ligand binding to a human cytomegalovirus chemokine receptor determines cell type-specific motility. *PLoS Pathog* **5**, e1000304.

Wagner, C. S., Walther-Jallow, L., Buentke, E., Ljunggren, H. G., Achour, A. & Chambers, B. J. (2008). Human cytomegalovirus-derived protein UL18 alters the phenotype and function of monocyte-derived dendritic cells. *J Leukoc Biol* **83**, 56–63.

Waltenberger, J. (2007). Stress testing at the cellular and molecular level to unravel cellular dysfunction and growth factor signal transduction defects: what molecular cell biology can learn from cardiology. *Thromb Haemost* **98**, 975–979.

Wang, D., Bresnahan, W. & Shenk, T. (2004a). Human cytomegalovirus encodes a highly specific RANTES decoy receptor. *Proc Natl Acad Sci U S A* **101**, 16642–16647.

Wang, J. F., Liu, Z. Y., Anand, A. R., Zhang, X., Brown, L. F., Dezube, B. J., Gill, P. & Ganju, R. K. (2004b). Alpha-chemokine-mediated signal transduction in human Kaposi's sarcoma spindle cells. *Biochim Biophys Acta* **1691**, 129–139.

Ward, K. N. (2005). Human herpesviruses-6 and -7 infections. *Curr Opin Infect Dis* **18**, 247–252.

Weber, K. S., Gröne, H. J., Röcken, M., Klier, C., Gu, S., Wank, R., Proudfoot, A. E., Nelson, P. J. & Weber, C. (2001). Selective recruitment of Th2-type cells and evasion from a cytotoxic immune response mediated by viral macrophage inhibitory protein-II. *Eur J Immunol* **31**, 2458–2466.

Weinreich, M. A. & Hogquist, K. A. (2008). Thymic emigration: when and how T cells leave home. *J Immunol* **181**, 2265–2270.

Weiss, H. (2004). Epidemiology of herpes simplex virus type 2 infection in the developing world. *Herpes* **11** (Suppl. 1), 24A–35A.

Wilson, E. & Butcher, E. C. (2004). CCL28 controls immunoglobulin (Ig)A plasma cell accumulation in the lactating mammary gland and IgA antibody transfer to the neonate. *J Exp Med* **200**, 805–809.

Wu, J., Xu, Y., Mo, D., Huang, P., Sun, R., Huang, L., Pan, S. & Xu, J. (2014). Kaposi's sarcoma-associated herpesvirus (KSHV) vIL-6 promotes cell proliferation and migration by upregulating DNMT1 via STAT3 activation. *PLoS One* **9**, e93478.

Xia, T., O'Hara, A., Araujo, I., Barreto, J., Carvalho, E., Sapucaia, J. B., Ramos, J. C., Luz, E., Pedroso, C. & other authors (2008). EBV microRNAs in primary lymphomas and targeting of CXCL-11 by ebv-mir-BHRF1-3. *Cancer Res* **68**, 1436–1442.

Xu, Y. & Ganem, D. (2007). Induction of chemokine production by latent Kaposi's sarcoma-associated herpesvirus infection of endothelial cells. *J Gen Virol* **88**, 46–50.

Xu, F., Sternberg, M. R., Kottiri, B. J., McQuillan, G. M., Lee, F. K., Nahmias, A. J., Berman, S. M. & Markowitz, L. E. (2006). Trends in herpes simplex virus type 1 and type 2 seroprevalence in the United States. *J Am Med Assoc* **296**, 964–973.

Yamanishi, K., Shiraki, K., Kondo, T., Okuno, T., Takahashi, M., Asano, Y. & Kurata, T. (1988). Identification of human herpesvirus-6 as a causal agent for exanthem subitum. *Lancet* **331**, 1065–1067.

Yasukawa, M., Hasegawa, A., Sakai, I., Ohminami, H., Arai, J., Kaneko, S., Yakushijin, Y., Maeyama, K. & Nakashima, H. (1999). Down-regulation of CXCR4 by human herpesvirus 6 (HHV-6) and HHV-7.J. *J Immunol* **162**, 5417–5422.

Yoshida, M. & Yamada, M. (2006). [Morphology of human alpha-herpesviruses]. *Nihon Rinsho* **64** (Suppl. 3), 121–126, (in Japanese). 16615452.

Young, L. S. & Rickinson, A. B. (2004). Epstein-Barr virus: 40 years on. *Nat Rev Cancer* **4**, 757–768.

Zhao, L., Xia, J., Wang, X. & Xu, F. (2014). Transcriptional regulation of CCL20 expression. *Microbes Infect* **16**, 864–870.

Zhou, J., Xiang, Y., Yoshimura, T., Chen, K., Gong, W., Huang, J., Zhou, Y., Yao, X., Bian, X. & Wang, J. M. (2014). The role of chemoattractant receptors in shaping the tumor microenvironment. *BioMed Res Int* **2014**, 751392.

Zou, P., Isegawa, Y., Nakano, K., Haque, M., Horiguchi, Y. & Yamanishi, K. (1999). Human herpesvirus 6 open reading frame U83 encodes a functional chemokine. *J Virol* **73**, 5926–5933.

Transplant Immunology 32 (2015) 144–150

Contents lists available at ScienceDirect

Transplant Immunology

journal homepage: www.elsevier.com/locate/trim

Development of human B cells and antibodies following human hematopoietic stem cell transplantation to Rag2$^{-/-}$γc$^{-/-}$ mice

Anne Tanner, Steven J. Hallam, Stanton J. Nielsen, German I. Cuadra, Bradford K. Berges *

Department of Microbiology and Molecular Biology, Brigham Young University, Provo, UT 84602, USA

ARTICLE INFO

Article history:
Received 11 March 2015
Received in revised form 25 March 2015
Accepted 26 March 2015
Available online 2 April 2015

Keywords:
Adaptive immunity
B cells
Human antibodies
Human immunity
Humanized mice
RAG-hu mice

ABSTRACT

Humanized mice represent a valuable model system to study the development and functionality of the human immune system. In the RAG-hu mouse model highly immunodeficient Rag2$^{-/-}$γc$^{-/-}$ mice are transplanted with human CD34^{+} hematopoietic stem cells, resulting in human hematopoiesis and a predominant production of B and T lymphocytes. Human adaptive immune responses have been detected towards a variety of antigens in humanized mice but both cellular and humoral immune responses tend to be weak and sporadically detected. The underlying mechanisms for inconsistent responses are poorly understood. Here, we analyzed the kinetics of human B cell development and antibody production in RAG-hu mice to better understand the lack of effective antibody responses. We found that T cell levels in blood did not significantly change from 8 to 28 weeks post-engraftment, while B cells reached a peak at 14 weeks. Concentrations of 3 antibody classes (IgM, IgG, IgA) were found to be at levels about 0.1% or less of normal human levels, but human antibodies were still detected up to 32 weeks after engraftment. Human IgM was detected in 92.5% of animals while IgG and IgA were detected in about half of animals. We performed flow cytometric analysis of human B cells in bone marrow, spleen, and blood to examine the presence of precursor B cells, immature B cells, naïve B cells, and plasma B cells. We detected high levels of surface IgM^{+} B cells (immature and naïve B cells) and low levels of plasma B cells in these organs, suggesting that B cells do not mature properly in this model. Low levels of human T cells in the spleen were observed, and we suggest that the lack of T cell help may explain poor B cell development and antibody responses. We conclude that human B cells that develop in humanized mice do not receive the signals necessary to undergo class-switching or to secrete antibody effectively, and we discuss strategies to potentially overcome these barriers.

1. Introduction

Human immune system mice are a useful tool to study the development and functionality of the human immune system. The most common current human immune system mouse models use human hematopoietic stem cells (HSCs) isolated from either cord blood or fetal liver and are then transferred into highly immunodeficient mice such as the Rag2$^{-/-}$γc$^{-/-}$ and NOD/SCIDγc$^{-/-}$ strains [1]. These humanized mice produce a wide variety of human immune cell types, including B cells, T cells, monocytes/macrophage, and dendritic cells [2]. Production of other immune components such as granulocytes, erythrocytes, and platelets is typically weak, and the B and T lymphocyte population represents an unusually large proportion of blood, bone marrow, and spleen cells due to poor granulocyte production.

Humanized mouse models have been very useful for studies of viral pathogens of human immune cells such as Human Immunodeficiency Virus type 1 (HIV-1) [3], herpesviruses [4], Dengue virus [5], and other pathogens. Human antibody responses have been reported against a variety of pathogens in humanized mice, including HIV-1, Dengue virus, Epstein–Barr virus, Kaposi's Sarcoma-associated herpesvirus, Herpes simplex virus type 2, and other pathogens/antigens [5–10]. Neutralizing antibody responses that target similar viral proteins as seen in humans have been reported in the case of Dengue virus [5]. Although the current humanized mouse models are capable of producing human humoral and cellular immune responses to these pathogens, in general the results have been inconsistent and when they are detected the immune responses are typically weak [6,11,12]. The reasons for these findings are currently unclear, but previous studies have indicated that total human antibody concentrations are much lower in humanized mice than in humans and there may be a defect in class-switching, since IgM concentrations tend to be closer to human concentrations than for IgG [2,13]. One study attempted to immortalize human B cells after immunizing humanized mice and was only able to produce IgM monoclonal antibodies and not IgG producing cells, lending further support to the hypothesis that there is a lack of effective class-switching [14]. Interestingly, this same paper showed through immunoscope analysis that a broad diversity of human antibody sequences are derived in humanized mice, indicating that derivation of diverse B cell receptors functions very similarly in humanized mice as compared to humans. If

* Corresponding author. Tel.: +1 801 422 8112.
E-mail address: brad.berges@gmail.com (B.K. Berges).

http://dx.doi.org/10.1016/j.trim.2015.03.002
0966-3274/

there is a defect in effective antibody class-switching in humanized mice the mechanisms are not understood.

Since immune responses are critical to controlling pathogens and for vaccine studies, a better understanding of the reasons for poor B cell responses in humanized mice would be useful to assist in developing better humanized mouse models that reproduce normal human antibody concentrations and more robust antigen-specific responses. Here, we describe the B cell compartment of HSC-transplanted Rag2$^{-/-}\gamma c^{-/-}$ mice. We have examined blood, bone marrow, and spleen for the presence of human B cells and to analyze the kinetics of B cell engraftment. We have also measured total human antibody levels in serum across a time course in order to determine when B cell development is complete in humanized mice. We found that immature and naive cells are found at a high frequency in spleen and bone marrow and that CD138^{+} plasma B cells are found in low levels in these organs. Few T cells were detected in the spleen, which is an important site for B cell maturation. Our results suggest that early steps in B cell development function properly in humanized mice, but that mechanisms governing class-switching and activation of B cells to become plasma cells are not very effective. Methods used to enhance T cell development and maturation in humanized mice may help to solve these issues.

2. Materials and methods

2.1. Cells

Human cord blood samples were obtained from the University of Colorado Cord Blood Bank. The Brigham Young University Institutional Review Board does not require a protocol for human cord blood samples because they lack patient identifiers. Human hematopoietic stem cells were purified from human cord blood using the CD34 marker with the EasySep human cord blood CD34-positive selection kit (StemCell Technologies). Cells were cultured for 2 days in Iscove's modified Dulbecco's medium (IMDM; Invitrogen) supplemented with 10% fetal calf serum (FCS) and 10 ng/mL each of human interleukin-3 (IL-3), IL-6, and stem cell factor (SCF) (R&D Systems) [15].

2.2. Animals

BALB/c-Rag2$^{-/-}\gamma c^{-/-}$ mice were humanized by engraftment with CD34^{+} human HSCs purified from human umbilical cord blood as described previously [15]. Mice were maintained in a specific pathogen-free (SPF) room at the Brigham Young University Central Animal Care Facility. Drinking water is supplemented with Trimethoprim-Sulfa antibiotics to prevent bacterial infection. These studies have been reviewed and approved by the Institutional Animal Use and Care Committee (protocols 120101 and 150108). Briefly, 1- to 5-day-old mice were conditioned by gamma irradiation with 350 rads and then injected intrahepatically with 2×10^5 to 7×10^5 human CD34^{+} cells. Mice were screened for human cell engraftment at 8–10 weeks post-engraftment, at which time plasma was also collected for antibody concentration analysis. Animals were additionally bled at numerous other time points in order to measure human cell types in blood and to collect additional plasma.

2.3. FACS analysis

70 μL of whole blood was obtained through tail bleed and treated with a mouse red blood cell lysis buffer for 15 min. Following this treatment the cells were centrifuged at 3300 rpm for 3 min and the supernatant was discarded. The pellet was then resuspended in 100 μL FACS staining buffer. 3 μL blocking buffer was then added and allowed to incubate in the dark at 4 °C for 15 min. This was followed by the addition of 3 μL of the desired fluorescent-linked antibodies and incubated in the dark at 4 °C for a period of 30 min. To determine percent human peripheral blood engraftment, peripheral blood was stained with human CD45 PECy-7 and mouse CD45 PE antibodies and FACS analysis was performed [16]. Antibodies used for B cell characterization were: hCD45 PECy-7, hCD19 APC eFluor 780 (eBioscience), hCD3 PE, hCD138 PECy5.5 (Invitrogen), and hIgM FITC (BioLegend). Immediately following this 30 min step 900 μL of 1% paraformaldehyde in 1× PBS was added to fix samples. Samples were then centrifuged at 3300 rpm for 3 min and the supernatant was discarded. The pellet was then resuspended in 150 μL 1× PBS and submitted for FACS analysis. An Attune Acoustic Focusing Cytometer (Applied Biosystems) was used to run samples, and Attune software v2.1 was used to analyze the results. All antibodies used in these studies do not cross-react with murine antigens, as assessed by staining of unengrafted Rag2$^{-/-}\gamma c^{-/-}$ blood and lymphoid organs.

2.4. Antibody concentrations

Mouse plasma samples were obtained by centrifuging whole blood at 3300 rpm for 3 min and then collecting the supernatant. ELISA tests were run using the Total Human IgM, Total Human IgG, and Total Human IgA kits (ALerCHEK) according to the manufacturer's instructions. Since human antibody concentrations are typically low in humanized mice, plasma was diluted 1:100 for IgM and IgG assays and 1:20 for IgA assays in order to obtain results in the linear range of the assay.

2.5. Statistics

Human T and B cell development in mouse peripheral blood was analyzed by Welch's ANOVA test (with Games–Howell post hoc test when applicable). To compare B cell levels in bone marrow, spleen, and blood, an ANOVA with Tukey–Kramer *post hoc* test was performed. For comparison of the different time points of plasma antibody concentrations an ANOVA with Tukey–Kramer post hoc test (where applicable) were performed. Standard error (SE) was calculated and indicated in all bar graphs. R^2 values were calculated to determine if a correlation exists between total antibody concentrations and peripheral blood engraftment levels in the humanized mice.

3. Results and discussion

3.1. Kinetics of human B and T lymphocyte development in peripheral blood of RAG-hu mice

In the RAG-hu model, purified human CD34^{+} hematopoietic stem cells are transplanted into neonatal Rag2$^{-/-}\gamma c^{-/-}$ mice following sub-lethal irradiation [15]. The kinetics of development of the human immune system following transplantation of human HSCs into mice is poorly understood. We hypothesized that one reason for weak adaptive immune responses in this model could be due to immaturity of the human immune system at the time of exposure to antigen. To examine the development of human lymphocytes, we used flow cytometry to monitor the relative frequency of human T cells (CD3^{+}) and B cells (CD19^{+}) in a time course in peripheral blood following human HSC engraftment (Fig. 1). Our findings confirmed previous reports that T and B lymphocytes are the major human cell types in humanized mouse peripheral blood, ranging from a combined sum of 54.6 ± 3.6% (SE) at 8 weeks post-engraftment (wpe) to 90.8 ± 1.2% at 14 wpe. We found that B cells outnumbered T cells at every time point except for 25–28 wpe, where levels were nearly identical. B cell levels ranged from 29.1 ± 5.0% to 76.7 ± 3.0% of human peripheral blood cells, while T cell levels ranged from 14.1 ± 2.6% to 28.3 ± 7.0%. The lowest levels of B cells were detected at 25–28 wpe, while a peak was detected at 14 wpe. The lowest levels of T cells were detected at 8 wpe and 14 wpe, although statistical analysis revealed that no significant differences in T cell populations were detected across the entire time course (Welch's ANOVA test, $p = .45$). At the 14 week time point there were significantly greater numbers of human B cells as compared to all other time points (Welch's ANOVA test, $p < 10^{-5}$ with *post hoc* Games–Howell test, $p < 0.01$). No significant differences were found between B cell levels at any other time points (*post hoc* Games–Howell test $p > 0.05$).

Since only a portion of humanized mice are good human antibody producers, we included data on peripheral blood T and B cell levels over time for individual animals

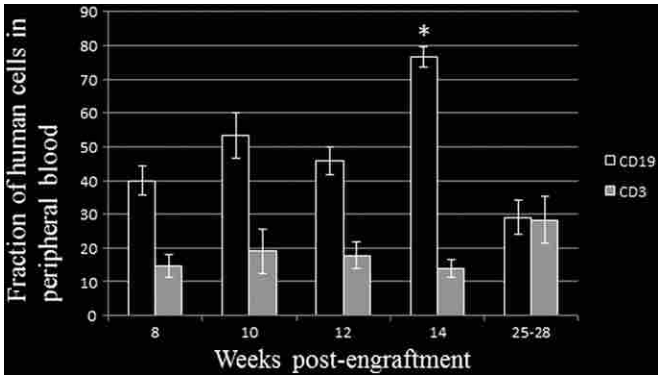

Fig. 1. Peripheral blood engraftment of human B and T cells in humanized mice. Flow cytometry was used to assess engraftment levels of human T cells ($CD3^+$) and human B cells ($CD19^+$) in peripheral blood. A human leukocyte antibody (anti-hCD45) was initially used for gating purposes to focus on human leukocyte populations. Mean levels in peripheral blood for each cell type were calculated and SE is indicated. (Welch's ANOVA test for B cell levels, $p < 0.000001$ with *post hoc* Games–Howell, $p < .01$ for all comparisons with week 14 except week 10 where $p < .05$). No significant differences in T cell populations were detected across the entire time course (Welch's ANOVA test, $p = .45$). Sample sizes per time point are $n = 11$ (8 w), $n = 14$ (10 w), $n = 7$ (12 w), $n = 6$ (14 w), and $n = 9$ (25–28 w). Unique cord blood samples used for engrafting animals at each time point: $n = 3$ (8 w), $n = 5$ (10 w), $n = 1$ (12 w), $n = 2$ (14 w), $n = 4$ (25–28 w).

(Table 1). Some animals followed the general trend seen in Fig. 1, while others did not. B cell levels in peripheral blood increased in all tested animals from week 8 to week 14, but then decreased in all tested animals from weeks 14 to 25. Interestingly, T cell levels in Fig. 1 showed insignificant changes over time, while individual mice show several different patterns. One animal steadily decreased from 8 to 25 weeks (mouse 2070), one animal showed a peak at 14 weeks (2071) and some animals increased across the time course (2072/2073). Mouse 2074 T cell levels increased from weeks 8 to 14, then appeared stable until week 25. These data suggest that T cell levels fluctuate more across a cohort of humanized mice whereas B cell levels follow a more similar pattern across groups of engrafted animals.

Table 1
Peripheral blood levels of human T and B lymphocytes tracked in individual mice over time. Human B and T lymphocyte populations were tracked in individual mice over a time course using flow cytometry analysis. Human leukocytes were gated based upon hCD45 expression, followed by analysis of $CD3^+$ cells (T cells) and $CD19^+$ cells (B cells).

	Gender	Cord sample	Cells transplanted
Mouse			
2070	F	A	7.3×10^5
2071	F	A	7.3×10^5
2072	F	B	9.0×10^5
2073	M	B	9.0×10^5
2074	M	B	9.0×10^5
2077	M	C	2.8×10^5

T fraction	Week 8	Week 14	Week 25
Mouse			
2070	19.7	14.1	1.4
2071	5.4	10	1.5
2072	9.5	n/t	36.5
2073	6.6	25.2	53.9
2074	3.3	11.7	10
2077	7.1	6.8	n/t

B fraction	Week 8	Week 14	Week 25
Mouse			
2070	43.4	78.7	46.9
2071	39.4	79.7	46.6
2072	28.6	n/t	2.7
2073	33.7	65.6	20.4
2074	53.7	83.1	28.1
2077	55.5	83.3	n/t

Harris et al. studied the duration of human immune system reconstitution in the NOD-Rag1-gammanull model engrafted with $CD34^+$ cells from cord blood [17]. They examined human B and T cell fractions in humanized mouse peripheral blood and found that B cells were predominant at early time points but that an inversion took place at about 15–20 wpe and T cells become the predominant lymphocyte in blood. Here, we showed that T cell levels do not significantly change between 8 and 28 wpe but that B cells had reached a peak at 14 wpe. We suggest that model-specific differences may explain our different results.

3.2. Proportions of human B cells in lymphoid organs and blood

Human B cell development in humanized mice has not been carefully studied and characterization of B cell development in primary and secondary lymphoid organs is also lacking. We sacrificed humanized mice and then used flow cytometry to detect different categories of B cells in bone marrow, spleen, and blood based upon phenotypic markers. We used CD19 as a marker for most human B cell populations, but also used CD138 as a marker for plasma B cells because CD19 expression is lost upon differentiation to this cell type. Some types of primitive B cells also express CD138, such as pro-B cells, pre-B cells, and immature B cells; however each of these populations also expresses CD19 which allows for differentiation from plasma B cells which are $CD19^-CD138^+$. We found that human B cells (sum of $CD19^+$ cells and $CD19^-IgM^-CD138^+$ cells) were the predominant human cell type (of the $hCD45^+$ population) in bone marrow (88.1 ± 4.3%; see Fig. 2), and to a lesser extent in spleen (60.1 ± 10.1%; see Fig. 3) and in blood (53.9 ± 5.3%; see Fig. 4).

3.3. Characterization of B cell types in bone marrow

In the bone marrow, precursor B cells ($CD19^+IgM^-CD138^+$) and immature B cells ($CD19^+IgM^+CD138^+$) represented the most common human B cells detected, at 42.2 ± 5.7% and 25.8 ± 7.6%, respectively (see Fig. 2C). Naïve B cells ($CD19^+IgM^+CD138^-$) and plasma B cells ($CD19^-IgM^-CD138^+$) were found in lower proportions, at 6.1 ± 1.8% and 1.0 ± 0.5%, respectively. Example FACS plots of stained bone marrow are shown in Fig. 2A, B. Statistical analyses were performed to determine if there were any significant differences between various B cell populations in bone marrow, spleen, and blood. The only significant difference in populations was that the $CD19^+IgM^-CD138^+$ population was larger in bone marrow than in spleen or blood (ANOVA $p = .003$ with *post hoc* Tukey–Kramer, $p < .05$).

Maturation of B cells to become plasma cells is dependent upon T cell help; specifically, CD40L on T cells interacts with CD40 on B cells to promote antibody secretion [18]. We detected only low numbers of human plasma B cells in the bone marrow of RAG-hu mice whereas in normal humans 4–5% of bone marrow cells are plasma cells [19,20]. One problem previously noted with most current humanized mice is that human T cells are largely selected based upon murine major histocompatibility complex (MHC) molecules in the thymus due to the lack of human stromal cells [21]. If human helper T cells are positively selected on murine MHC-II in the thymus, then their ability to interact with B cells expressing human MHC-II in the periphery is not expected to be effective and this would prevent effective plasma cell differentiation. Interestingly, many $CD5^+$ B cells have been reported to exist in humanized mice [22,23]. These cells are less prone to undergo class-switching and are more prone to produce IgM antibodies independent of T cell help [24].

The lack of human MHC expression on thymic stromal cells likely has an impact on the ability to derive antigen-specific human T cell responses in humanized mice because humanized mouse T cells undergo selection on mostly murine MHC. Attempts to overcome this barrier to T cell development include the development of the bone marrow/liver/thymus (BLT) model which uses a human fetal thymic transplant to allow for selection on human MHC and various studies indicate that both cellular and humoral immune responses are more frequent and robust in the BLT model as compared to those that lack human thymic stromal cells [8,21,25] although careful studies to compare various humanized mouse models are still lacking. The BLT model is technically challenging because it requires human fetal tissues which can be challenging to obtain, and also requires survival surgery to implant the tissues. Another option is the use of human HLA-transgenic animals as another way to generate T cells that are selected on human MHC; this idea has been explored to some degree and appears to result in enhanced T cell responses [26,27]. No examination of human B cell responses in HLA-transgenic mice has been explored to our knowledge. Another hypothesis to explain the lack of human plasma B cells is that they are initially produced, but do not receive the survival signals necessary to persist longer than a few days after differentiation.

3.4. Characterization of B cell types in spleen

In the spleen, the predominant human B cell type was immature B cells (43.8 ± 7.5%), followed by naïve B cells at 27.7 ± 7.8% (see Fig. 3C). Precursor B cells were more rare in spleen (17.9 ± 3.1%) and plasma B cells were the least frequent (1.9 ± 1.6%). Example FACS plots of stained splenocytes are shown in Fig. 3A, B.

We also noted that human T cells are found in low numbers in the spleen of RAG-hu mice, whereas human B cells are found in much greater numbers. T cells represented an average of 36.6 ± 8.8% of total human leukocytes in the spleen,

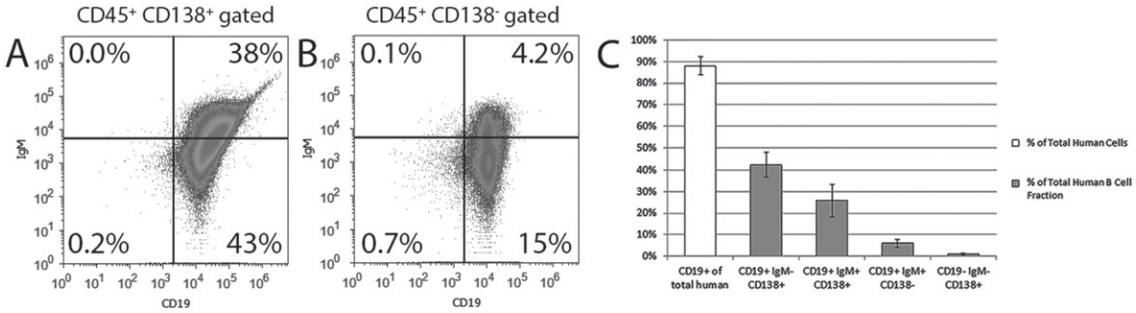

Fig. 2. Human B cell populations in humanized mouse bone marrow. Human B cells in bone marrow were immunophenotyped by flow cytometry. A human leukocyte antibody (anti-hCD45) was initially used for gating purposes to focus on human leukocyte populations. (A) FACS plot gated on $CD138^+$ cells to observe precursor B cell ($CD19^+IgM^-CD138^+$), immature B cell ($CD19^+IgM^+CD138^+$), and plasma B cell ($CD19^-IgM^-CD138^+$) populations. Percentages are out of total human B cells. (B) FACS plot gated on $CD138^-$ cells to observe naïve B cell population ($CD19^+IgM^+CD138^-$). Percentages are out of total human B cells. (C) Graph comparing averages of the different bone marrow cell populations in all mice tested. SE is indicated. The precursor B cell population in bone marrow is significantly different from this same population in spleen and blood (compare Fig. 3 and Fig. 4) (ANOVA $p = .003$ with *post hoc* Tukey–Kramer, $p < .05$). Sample sizes per population are $n = 7$ ($CD19^+IgM^-CD138^+$), and $n = 4$ for ($CD19^+IgM^+CD138^+$)($CD19^+IgM^-CD138^-$)($CD19^-IgM^-CD138^+$). Unique cord blood samples used for engrafting animals in each population: $n = 6$ ($CD19^+IgM^-CD138^+$), $n = 4$ for ($CD19^+IgM^+CD138^+$)($CD19^+IgM^-CD138^-$)($CD19^-IgM^-CD138^+$).

with a low of 12% and a high of 62%. This finding is similar to that reported in NOD/SCID gammanull mice engrafted with HSCs from cord blood [28]. Immature B cells are known to leave the bone marrow and to migrate to the spleen, where maturation to peripheral mature B cells and plasma cells occurs [18]. Thus, the paucity of T cells in the spleen of humanized mice may also explain the lack of plasma cells. A study conducted by Lang et al. confirms the necessity of T cells for B cell maturation; in their report they introduced autologous T cells and found increased numbers of mature B cells. Conversely, when T cells were depleted, in vivo B cell maturation was delayed [29]. In previous work with RAG-hu mice, we characterized levels of helper T cells ($CD3^+CD4^+$) and cytotoxic T cells ($CD3^+CD8^+$) in the blood of 28 humanized mice and found that the ratio of helper T cells to cytotoxic T cells is similar as compared to humans, with a mean ratio of 2.1:1 ($\pm$1.2 SD) for helper T cells compared to cytotoxic T cells [30]. There was clearly variability present between various engrafted animals, with a high of 6.1:1 and a low of 1.0:1. Poor development of helper T cells may contribute to poor B cell development.

Germinal centers are important locations for antibody class-switching, and structures that histologically resemble germinal centers are found in RAG-hu spleen [2]. To our knowledge, no studies have been carried out to analyze the functionality of these germinal centers in humanized mice. Follicular dendritic cells (FDCs) are critical components of germinal centers, but human FDCs are not detectable in humanized mice because these cells originate from a non-HSC source. Interestingly, cells bearing murine FDC markers are present in humanized mice germinal centers [2]. The lack of human FDCs in humanized mice may block efficient class-switching, development of memory B cells, and somatic hypermutation [31].

3.5. Characterization of B cell types in blood

In the blood, the most common human B cell types were immature and naïve B cells, at 40.4 $\pm$ 11.9% and 36.7 $\pm$ 13.2%, respectively (see Fig. 4C). Precursor B cells were found in lower levels (12.3 $\pm$ 3.4%) and plasma cells were even lower (2.2 $\pm$ 1.3%). Example FACS plots of stained blood cells are shown in Fig. 4A, B. We noted that the particular animal chosen for Fig. 4B had an unusually high level of plasma B cells ($CD19^-IgM^-CD138^+$). There is high variability in the levels of engraftment as well as in antibody production in individual humanized mice.

3.6. Measurement of total human plasma antibody concentrations

To examine the functionality of the human B cells, we measured human antibody concentrations in humanized mouse plasma. Total human IgM, IgG, and IgA concentrations were measured by ELISA. Plasma samples from unengrafted mice did not have detectable human antibody levels for any antibody class (data not shown). Although all 3 antibody classes were detected in plasma, the frequency of detection differed amongst the classes. 49 of 53 samples tested positive for IgM (92.5%), while only 25 of 53 were positive for IgG (47.2%) and 28 of 53 were positive for IgA (52.8%) (Fig. 5A). The total average concentrations across all time points (only counting positive samples) were 2.1 μg/mL for IgM, 10 μg/mL for IgG, and 0.036 μg/mL for IgA (Fig. 5B). By way of comparison, the normal concentrations in human plasma are 1500 μg/mL for IgM, 14,000 μg/mL for IgG, and 3500 μg/mL for IgA. Thus, for all antibody classes we consistently measured approximately 0.1% or less of normal antibody concentrations in humanized mouse plasma as compared to normal humans. IgA concentrations were farthest from the normal human values (0.001% of normal), IgM levels were the closest (0.14%), and IgG levels were similar to IgM (0.07%).

Traggiai et al. monitored human B and T cell development over time in RAG-hu mice [2]. They showed that human antibody levels are immature at 8 wpe, with a rise in total IgM from 8 to 16 wpe and undetectable levels of IgG at 8 wpe with higher levels at 16 wpe. Our results somewhat agree in terms of the kinetics of the response, although we did detect IgG at 9 wpe in many animals. They showed total human antibody concentrations higher than what we have detected, but the

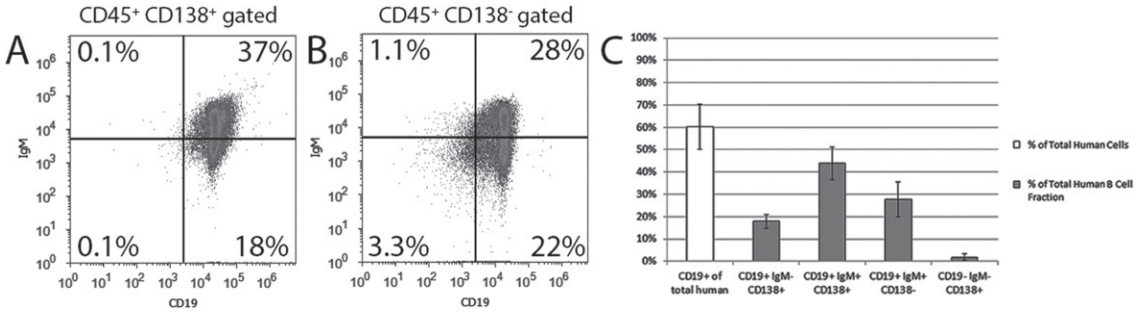

Fig. 3. Human B cell populations in humanized mouse spleen. Human B cells in spleen were immunophenotyped by flow cytometry. A human leukocyte antibody (anti-hCD45) was initially used for gating purposes to focus on human leukocyte populations. (A) FACS plot gated on $CD138^+$ cells to observe precursor B cell ($CD19^+IgM^-CD138^+$), immature B cell ($CD19^+IgM^+CD138^+$), and plasma B cell ($CD19^-IgM^-CD138^+$) populations. Percentages are out of total human B cells. (B) FACS plot gated on $CD138^-$ cells to observe naïve B cell population ($CD19^+IgM^+CD138^-$). Percentages are out of total human B cells. (C) Graph comparing averages of the different splenic cell populations in all mice tested. SE is indicated. Sample sizes per population are $n = 7$ ($CD19^+IgM^-CD138^+$), and $n = 4$ for ($CD19^+IgM^+CD138^+$)($CD19^+IgM^-CD138^-$)($CD19^-IgM^-CD138^+$). Unique cord blood samples used for engrafting animals in each population: $n = 6$ ($CD19^+IgM^-CD138^+$), $n = 4$ for ($CD19^+IgM^+CD138^+$)($CD19^+IgM^-CD138^-$)($CD19^-IgM^-CD138^+$).

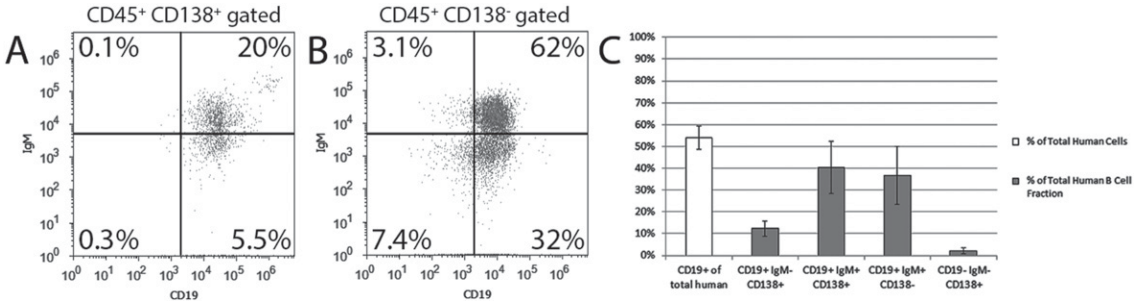

Fig. 4. Human B cell populations in humanized mouse peripheral blood. Human B cells in blood were immunophenotyped by flow cytometry. A human leukocyte antibody (anti-hCD45) was initially used for gating purposes to focus on human leukocyte populations. (A) FACS plot gated on $CD138^+$ cells to observe precursor B cell ($CD19^+IgM^-CD138^+$), immature B cell ($CD19^+IgM^+CD138^+$), and plasma B cell ($CD19^-IgM^-CD138^+$) populations. Percentages are out of total human B cells. (B) FACS plot gated on $CD138^-$ cells to observe naïve B cell population ($CD19^+IgM^+CD138^-$). Percentages are out of total human B cells. (C) Graph comparing averages of the different cell populations from blood in all mice tested. SE is indicated. Sample sizes per population are $n = 6$ ($CD19^+IgM^-CD138^+$), and $n = 3$ for ($CD19^+IgM^+CD138^+$)($CD19^+IgM^-CD138^-$)($CD19^-IgM^-CD138^+$). Unique cord blood samples used for engrafting animals in each population: $n = 5$ ($CD19^+IgM^-CD138^+$), $n = 3$ for ($CD19^+IgM^+CD138^+$)($CD19^+IgM^-CD138^-$)($CD19^-IgM^-CD138^+$).

defect in class-switching is similar. They reported a mean IgM concentration of about 15 μg/mL and a mean IgG of about 200 μg/mL [2] while Chen et al. reported mean IgM levels of 119 μg/mL and 1.1 μg/mL IgG in humanized NOD/SCID gammanull mice [32], while Wang et al. showed ~7 mg/mL IgM in humanized NOD/SCID mice with undetectable IgG [23]. Our results show a mean IgM titer of 2 μg/mL and a mean IgG titer of 10 μg/mL. The use of different mouse strains and sources of HSCs may explain the differing results.

Wang et al. examined IgG responses and T cell development in NOD/SCID mice transplanted with $CD34^+$ cells from cord blood [23]. They showed very little IgG responses, and also very few human T cells engrafted (appears to be much less than in RAG-hu mice). Since NOD/SCID mice are considered to have higher residual murine immunity than $Rag2^{-/-}\gamma c^{-/-}$ mice, the mouse strain might explain the differences in our results. B cells require T cell help for effective antibody responses, so we surmise that the increased numbers of human T cells might explain why the RAG-hu model has higher IgG production.

3.7. Kinetics of production of human antibody classes

In order to study the kinetics of human antibody development in humanized mice, we measured human antibody concentrations in plasma across a time course

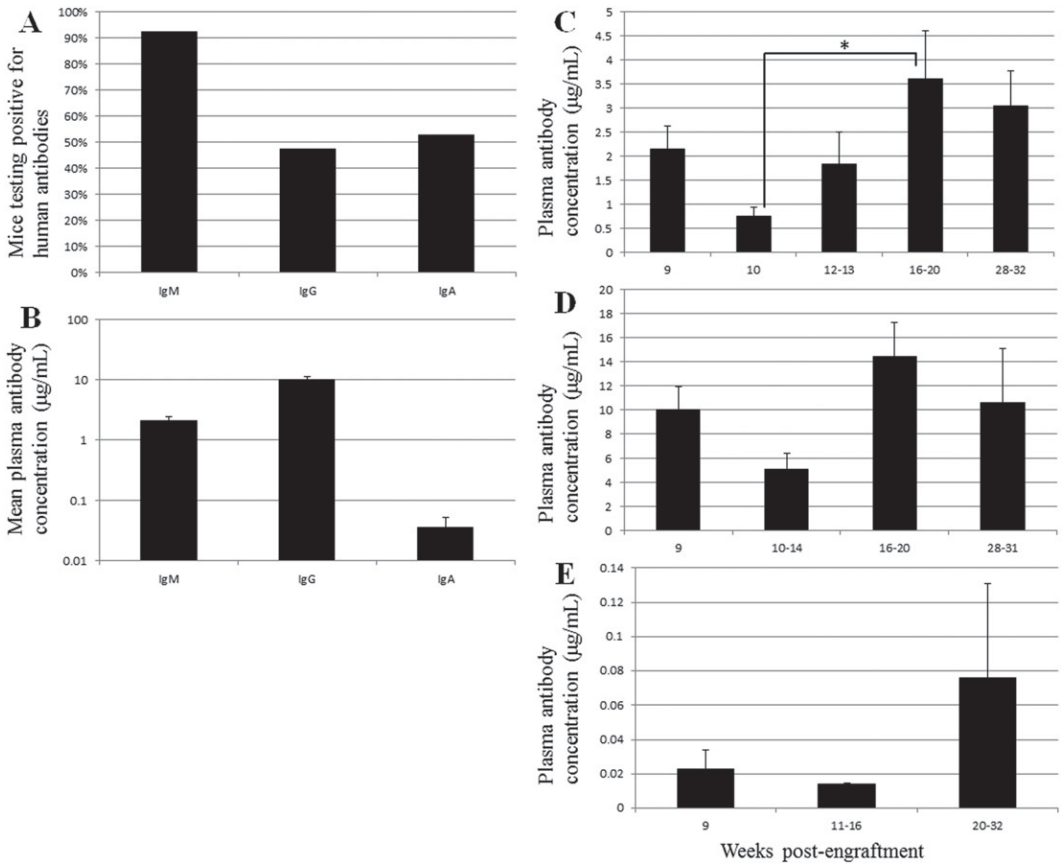

Fig. 5. Total human antibody concentrations in humanized mouse plasma. ELISA was used to measure total human antibody concentrations in plasma. (A) Fraction of animals testing positive for IgM, IgG, or IgA ($n = 53$ animals for each group). (B) Mean antibody concentrations for IgM, IgG, IgA; only including positive animals ($n = 49$, 25, and 28, respectively). A time course of (C) IgM, (D) IgG, and (E) IgA in plasma after human cell engraftment. (* ANOVA $p = .04$ with *post hoc* Tukey–Kramer, $p < .05$). Sample sizes per time point are: C) $n = 10$ (9 w), $n = 6$ (10 w), $n = 3$ (12–13 w), $n = 4$ (16–20 w), and $n = 3$ (28–32 w); D) $n = 4$ for all time points; and E) $n = 4$ (9 w), $n = 3$ (11–16 w), and $n = 3$ (20–32 w).

that lasted up to 32 wpe. All 3 antibody classes (IgM, IgG, IgA) were detectable in plasma by 9 wpe, and only minor differences in antibody concentrations were noted at later time points. No significant differences in total antibody concentrations were detected across the time course for IgG (Welch's ANOVA test, $p = 0.11$) (Fig. 5D) or IgA (Welch's ANOVA test, $p = 0.53$) (Fig. 5E). A single significant difference was detected in IgM from 10 wpe to 16-20 wpe where an increase was detected (ANOVA $p = .04$ with *post hoc* Tukey–Kramer, $p < 0.05$) (Fig. 5C). However, this significant increase was not maintained to the 28–32 wpe time point. Our results show that human antibody production persists through at least 32 wpe, with no significant decreases at late time points.

3.8. No correlation exists between peripheral blood engraftment and plasma antibody concentration

Since only a fraction of humanized mice produce detectable antigen-specific responses to infection or immunization, it would be useful if a marker could be developed which would allow one to predict the likelihood of an animal producing a detectable response. However, such a marker has not yet been reported. We analyzed our data to see if a correlation exists between the percent peripheral blood engraftment (defined as $hCD45^+$ cells divided by the sum of ($hCD45^+$ plus $mCD45^+$ cells)) and the plasma concentrations of various human antibody classes. We failed to detect a correlation between animals with higher peripheral blood engraftment and those with higher levels of IgM, IgG, or IgA (Supplementary Fig. 1). These findings suggest that the level of chimerism in humanized mice is not the most critical aspect involved in antibody responses.

Improvements in human erythrocyte and platelet development have been made by eliminating murine macrophages which may engulf human immune system components [33–35]. In contrast, little research has been conducted to specifically improve B cell development and functionality. One interesting study analyzed the defect in class-switching from IgM to IgG responses in humanized mice. Chen et al. used NOD/SCID gammanull mice engrafted with either fetal liver or cord blood $CD34^+$ cells and found that better human antibody responses and enhanced class-switching were detected following administration of human Interleukin 4 (IL-4) and Granulocyte-Macrophage Colony-Stimulating Factor (GM-CSF) to humanized mice [32]. IgM responses were 42% higher in cytokine-treated animals and IgG responses were over 10.5-fold higher using this protocol. In addition, tetanus toxin-specific IgG went from undetectable to detectable levels in many animals administered IL-4 and GM-CSF. Thus, the production of humanized mice in a background strain that produces human cytokines may also be beneficial to achieve normal human antibody responses.

4. Conclusions

We have shown that RAG-hu mice produce human B cells which are dispersed in blood, bone marrow, and spleen. B cell engraftment in peripheral blood reached a peak in relative numbers of cells at 14 wpe, while T cell levels were stable from 8 to 28 wpe. The vast majority of mice had detectable levels of human IgM in plasma, while only about half had detectable IgG or IgA. The mean antibody concentrations were considerably lower than those seen humans, and in general antibody concentrations did not significantly change over time from 9 to ~30 wpe. We detected relatively few $CD138^+$ plasma cells in the bone marrow, despite the fact that most plasma cells reside in this site in humans. Taken together, our results indicate that in the RAG-hu model there are defects in class-switching from IgM to IgG or IgA production, and that naïve B cells are not effectively matured to become plasma B cells. Further work can now be done to test the hypothesis that improvements in T cell levels may enhance the reproducibility of human antibody responses in humanized mice.

Supplementary data to this article can be found online at http://dx.doi.org/10.1016/j.trim.2015.03.002.

Abbreviations

FACS	Fluorescence activated cell sorting
Rag2	Recombinase activating gene 2
γc	Common gamma chain receptor
Wpe	Weeks post-engraftment
Ig	Immunoglobulin
NOD	Non-obese diabetic
SCID	Severe combined immunodeficiency
ELISA	Enzyme-linked immunosorbent assay
HSC	Hematopoietic stem cell
MHC	Major histocompability complex
BLT	Bone marrow/liver/thymus humanized mice
GM-CSF	Granulocyte macrophage colony stimulating factor

Acknowledgments

The authors declare no conflict of interests. We thank Stephen Taylor, Eakachai Prompetchara, Sterling Adams, Jacob Hatch, Greg Low, and Mary Ann Taylor for assistance in extracting cord blood samples, and for engrafting and screening humanized mice. This work was supported by a Brigham Young University Mentoring Environment Grant to BB (award 2012-09016). SH, GC, and SN were recipients of the Office of Research and Creative Activities grant awards from Brigham Young University.

References

[1] Tanner A, Taylor SE, Decottignies W, Berges BK. Humanized mice as a model to study human hematopoietic stem cell transplantation. Stem Cells Dev 2014;23:76–82.
[2] Traggiai E, Chicha L, Mazzucchelli L, Bronz L, Piffaretti JC, Lanzavecchia A, et al. Development of a human adaptive immune system in cord blood cell-transplanted mice. Science 2004;304:104–7.
[3] Berges BK, Rowan MR. The utility of the new generation of humanized mice to study HIV-1 infection: transmission, prevention, pathogenesis, and treatment. Retrovirology 2011;8:65.
[4] Berges BK, Tanner A. Modeling of human herpesvirus infections in humanized mice. J Gen Virol 2014;95:2106–17.
[5] Kuruvilla JG, Troyer RM, Devi S, Akkina R. Dengue virus infection and immune response in humanized $Rag2^{-/-}\gamma c^{-/-}$ (RAG-hu) mice. Virology 2007;369:143–52.
[6] Baenziger S, Tussiwand R, Schlaepfer E, Mazzucchelli L, Heikenwalder M, Kurrer MO, et al. Disseminated and sustained HIV infection in CD34+ cord blood cell-transplanted Rag2−/−{gamma}c−/− mice. Proc Natl Acad Sci U S A 2006;103:15951–6.
[7] Kwant-Mitchell A, Ashkar AA, Rosenthal KL. Mucosal innate and adaptive immune responses against HSV-2 in a humanized mouse model. J Virol 2009;83:10664–76.
[8] Brainard DM, Seung E, Frahm N, Cariappa A, Bailey CC, Hart WK, et al. Induction of robust cellular and humoral virus-specific adaptive immune responses in HIV-infected humanized BLT mice. J Virol 2009;83:7305–21.
[9] Parsons CH, Adang LA, Overdevest J, O'Connor CM, Taylor JRJ, Camerini D, et al. KSHV targets multiple leukocyte lineages during long-term productive infection in NOD/SCID mice. J Clin Invest 2006;116:1963–73.
[10] Yajima M, Imadome K, Nakagawa A, Watanabe S, Terashima K, Nakamura H, et al. A new humanized mouse model of Epstein–Barr virus infection that reproduces persistent infection, lymphoproliferative disorder, and cell-mediated and humoral immune responses. J Infect Dis 2008;198:673–82.
[11] Watanabe S, Terashima K, Ohta S, Horibata S, Yajima M, Shiozawa Y, et al. Hematopoietic stem cell-engrafted NOD/SCID/IL2R{gamma}null mice develop human lymphoid system and induce long-lasting HIV-1 infection with specific humoral immune responses. Blood 2007;109:212–8.
[12] Sato K, Nie C, Misawa N, Tanaka Y, Ito M, Koyanagi Y. Dynamics of memory and naïve CD8(+) T lymphocytes in humanized NOD/SCID/IL-2Rgamma(null) mice infected with CCR5-tropic HIV-1. Vaccine 2010;28S2:B32–7.
[13] Akkina R, Berges BK, Palmer BE, Remling L, Neff CP, Kuruvilla J, et al. Humanized Rag1 −/− gamma-chain −/− mice support multilineage hematopoiesis and are susceptible to HIV-1 infection via systemic and vaginal routes. PLoS ONE 2011;6:e20169.
[14] Becker PD, Legrand N, van Geelen CM, Noerder M, Huntington ND, Lim A, et al. Generation of human antigen-specific monoclonal IgM antibodies using vaccinated "human immune system" mice. PLoS ONE 2010;5:e13137.
[15] Sanchez FM, Cuadra GI, Nielsen SJ, Tanner A, Berges BK. Production and characterization of humanized Rag2(−/−)γc (−/−) mice. Methods Mol Biol 2013;1031:19–26.
[16] Berges BK, Wheat WH, Palmer BE, Connick E, Akkina R. HIV-1 infection and CD4 T cell depletion in the humanized Rag2 −/− gc −/− (RAG-hu) mouse model. Retrovirology 2006;3:76.
[17] Harris DT, Badowski M. Long term human reconstitution and immune aging in NOD-Rag (−)-γ chain (−) mice. Immunobiology 2014;219:131–7.
[18] Nagasawa T. Microenvironmental niches in the bone marrow required for B-cell development. Nat Rev Immunol 2006;6:107–16.
[19] Bladé J, Samson D, Reece D, Apperley J, Björkstrand B, Gahrton G, et al. Criteria for evaluating disease response and progression in patients with multiple myeloma treated by high-dose therapy and haemopoietic stem cell transplantation. Myeloma Subcommittee of the EBMT. European Group for Blood and Marrow Transplant. Br J Haematol 1998;102:1115–23.
[20] Durie BG, Harousseau JL, Miguel JS, Bladé J, Barlogie B, Anderson K, et al. International uniform response criteria for multiple myeloma. Leukemia 2006;20:1467–73.
[21] Melkus MW, Estes JD, Padgett-Thomas A, Gatlin J, Denton PW, Othieno FA, et al. Humanized mice mount specific adaptive and innate immune responses to EBV and TSST-1. Nat Med 2006;12:1316–22.
[22] Biswas S, Chang H, Sarkis PT, Fikrig E, Zhu Q, Marasco WA. Humoral immune responses in humanized BLT mice immunized with West Nile virus and HIV-1

envelope proteins are largely mediated via human CD5(+) B cells. Immunology 2011;134:419–33.
[23] Wang X, Qi Z, Wei H, Tian Z, Sun R. Characterization of human B cells in umbilical cord blood-transplanted NOD/SCID mice. Transpl Immunol 2012;26:156–62.
[24] Baumgarth N, Tung J, Herzenberg L. Inherent specificities in natural 689 antibodies: a key to immune defense against pathogen invasion. Springer Semin Immunopathol 2005;26:347.
[25] Akkina R. New generation humanized mice for virus research: comparative aspects and future prospects. Virology 2013;435:14–28.
[26] Serra-Hassoun M, Bourgine M, Boniotto M, Berges J, Langa F, Michel ML, et al. Human hematopoietic reconstitution and HLA-restricted responses in nonpermissive alymphoid mice. J Immunol 2014;193:1504–11.
[27] Shultz LD, Saito Y, Najima Y, Tanaka S, Ochi T, Tomizawa M, et al. Generation of functional human T-cell subsets with HLA-restricted immune responses in HLA class I expressing NOD/SCID/IL2r{gamma}null humanized mice. Proc Natl Acad Sci U S A 2010;107:13022–7.
[28] Takahashi M, Tsujimura N, Otsuka K, Yoshino T, Mori T, Matsunaga T, et al. Comprehensive evaluation of leukocyte lineage derived from human hematopoietic cells in humanized mice. J Biosci Bioeng 2012;113:529–35.
[29] Lang J, Kelly M, Freed BM, McCarter MD, Kedl RM, Torres RM, et al. Studies of lymphocyte reconstitution in a humanized mouse model reveal a requirement of T cells for human B cell maturation. J Immunol 2013;190:2090–101.
[30] Berges BK, Akkina SR, Folkvord JM, Connick E, Akkina R. Mucosal transmission of R5 and X4 tropic HIV-1 via vaginal and rectal routes in humanized Rag2−/−gc−/− (RAG-hu) mice. Virology 2008;373:342–51.
[31] Tew JG, Phipps RP, Mandel TE. The maintenance and regulation of the humoral immune response: persisting antigen and the role of follicular antigen-binding dendritic cells as accessory cells. Immunol Rev 1980;53:175–201.
[32] Chen Q, He F, Kwang J, Chan JK, Chen J. GM-CSF and IL-4 stimulate antibody responses in humanized mice by promoting T, B, and dendritic cell maturation. J Immunol 2012;189:5223–9.
[33] Pek EA, Chan T, Reid S, Ashkar AA. Characterization and IL-15 dependence of NK cells in humanized mice. Immunobiology 2011;216:218–24.
[34] Chen Q, Khoury M, Chen J. Expression of human cytokines dramatically improves reconstitution of specific human-blood lineage cells in humanized mice. Proc Natl Acad Sci U S A 2010;106:21783–8.
[35] Huntington ND, Legrand N, Alves NL, Jaron B, Weijer K, Plet A, et al. IL-15 trans-presentation promotes human NK cell development and differentiation in vivo. J Exp Med 2009;206:25–34.

Journal of General Virology (2014), **95**, 2106–2117 DOI 10.1099/vir.0.067793-0

Review

Modelling of human herpesvirus infections in humanized mice

Bradford K. Berges and Anne Tanner

Department of Microbiology and Molecular Biology, Brigham Young University, Provo, UT 84602, USA

Correspondence
Bradford K. Berges
brad.berges@gmail.com

The human herpesviruses (HHVs) are remarkably successful human pathogens, with some members of the family successfully establishing infection in the vast majority of humans worldwide. Although many HHV infections result in asymptomatic infection or mild disease, there are rare cases of severe disease and death found with nearly every HHV. Many of the pathogenic mechanisms of these viruses are poorly understood, and in many cases, effective antiviral drugs are lacking. Only a single vaccine exists for the HHVs and researchers have been unable to develop treatments to cure the persistent infections associated with HHVs. A major hindrance to HHV research has been the lack of suitable animal models, with the notable exception of the herpes simplex viruses. One promising area for HHV research is the use of humanized mouse models, in which human cells or tissues are transplanted into immunodeficient mice. Current humanized mouse models mostly transplant human haematopoietic stem cells (HSCs), resulting in the production of a variety of human immune cells. Although all HHVs are thought to infect human immune cells, the beta- and gammaherpesviruses extensively infect and establish latency in these cells. Thus, mice humanized with HSCs hold great promise to study these herpesviruses. In this review, we provide a historical perspective on the use of both older and newer humanized mouse models to study HHV infections. The focus is on current developments in using humanized mice to study mechanisms of HHV-induced pathogenesis, human immune responses to HHVs and effectiveness of antiviral drugs.

Received 9 May 2014
Accepted 18 July 2014

Human herpesviruses

Human herpesviruses (HHVs) are nearly ubiquitous infectious agents that contribute substantially to human morbidity and mortality. Nine HHVs have been discovered to date, including herpes simplex virus types 1 and 2 (HSV-1 and HSV-2), varicella zoster virus (VZV; HHV-3), Epstein–Barr virus (EBV; HHV-4), human cytomegalovirus (hCMV; HHV-5), HHV-6A and HHV-6B, HHV-7, and Kaposi's sarcoma-associated herpesvirus (KSHV; HHV-8). Within the family *Herpesviridae*, there are three subfamilies with natural human pathogens listed: the *Alphaherpesvirinae* (HSV-1, HSV-2, VZV), the *Betaherpesvirinae* (hCMV, HHV-6A, HHV-6B, HHV-7) and the *Gammaherpesvirinae* (EBV, KSHV) (McGeoch *et al.*, 2006). The HHVs are considered to be some of the most successful pathogens of humans due to the high rate of seroconversion and the ability to establish lifelong latent infections.

HHV infections are linked to a wide spectrum of human diseases, ranging from skin lesions to encephalitis, from immune deficiency to autoimmune disease, from blindness to deafness, from organ transplant rejection to post-transplant proliferative disorders, and from epilepsy to several types of cancer. Despite the burden of infection and disease caused by the HHVs, a preventative vaccine is available only for VZV (Takahashi *et al.*, 2008). Further, our ability to control infections and disease is in many cases limited due to the lack of available antiviral drugs. All HHVs are able to form a persistent infection, which typically involves a latent phase characterized by minimal viral gene expression and inability to detect infectious virus, followed by reactivation where many viral genes are expressed, viral particles are produced and virus is shed from the host. Although persistent HHV infections are required for many types of pathogenesis, research efforts have thus far been unable to eliminate persistent HHV infections in humans.

Animal models for HHVs are needed

Part of the reason for our lack of understanding of HHV pathogenesis is due to the lack of appropriate animal models that faithfully recapitulate infection and disease. In the case of HSV-1 and HSV-2, the availability of small-animal models has contributed substantially to our understanding of these viruses; as a result, they are the best understood of the HHVs and serve as prototypes for the family. However, the alphaherpesviruses (HSV-1, HSV-2, VZV) are fundamentally different from the beta and

gammaherpesviruses in that the alphaherpesviruses principally establish latency in neuronal cells *in vivo* and are transmitted predominantly via skin contact or inhalation. The beta and gammaherpesviruses predominantly establish latency in immune cells (also endothelial cells in the case of KSHV) *in vivo*. These viruses can be transmitted by saliva, sexual contact or through breast milk.

Despite the inability to adequately study the HHVs directly in humans due to ethical constraints and the general lack of good animal models for the HHVs, there are several homologues of the HHVs that infect animals and that have been useful towards achieving a better understanding of the human pathogens. For example, animal homologues of hCMV have been well-studied in their native hosts, including murine CMV, rat CMV, guinea pig CMV and rhesus CMV (McGregor, 2010). Murid herpesvirus 68 (MHV-68) (Stevenson & Efstathiou, 2005) and murid herpesvirus 4 (Nash *et al.*, 2001) in mice and rhesus rhadinovirus (macacine herpesvirus 5) in monkeys (Orzechowska *et al.*, 2008) serve as models of KSHV infection in humans. EBV can infect some types of New World primates, including the common marmoset and the cottontop tamarin (Shope *et al.*, 1973; Wedderburn *et al.*, 1984). These animal models have been very useful and will continue to yield valuable data, but they have several limitations. (i) Animal homologues of HHVs are genetically divergent from their HHV counterparts and thus encode different genes. Hence, any information gained on mechanisms of pathogenesis, development of antiviral drugs and vaccines may not be directly applicable to HHVs in a human host. (ii) Non-human primate research is expensive and can only be performed in specialized facilities that are not available to many researchers. For these reasons, the availability of new animal models to study mechanisms of viral pathogenesis *in vivo* would be greatly beneficial to the development of vaccines and new treatment strategies.

Humanized mice

One such model is humanized mice, which are immunodeficient mice engrafted with human cells or tissues. The original humanized mouse models, first reported in 1988, involved SCID (severe combined immunodeficiency) mice engrafted with either human peripheral blood leucocytes (SCID-hu-PBL model) (Mosier *et al.*, 1988) or with human foetal thymic and liver tissues as a model of a human thymus (SCID-hu Thy/Liv model) (McCune *et al.*, 1988). Although both models exhibited human immune cell engraftment, there were several limitations noted in these models: lack of long-term human cell engraftment (PBL model), low diversity in types of cells engrafted (PBL and Thy/Liv models), lack of distribution of human cells in the mouse (Thy/Liv model) and inability to generate primary human immune responses (PBL and Thy/Liv models) (Macchiarini *et al.*, 2005; Shultz *et al.*, 2007). Both of these models were explored extensively for studies of human immunodeficiency virus type 1 (HIV-1) (Mosier, 1996) and limited work was also done with HHVs (see below).

Over the past decade, new humanized mouse models have emerged based upon greater mouse immunodeficiency and transplantation of human haematopoietic stem cells (HSCs). A recent review of the mouse strains used and the types of cells used for transplantation is available (Tanner *et al.*, 2014). Briefly, most mouse strains currently in use are double-knockouts that prevent maturation of T-lymphocytes via the inability to produce enzymes involved in the process of DNA recombination required to produce T/B-cell receptors, including mutations in the recombinase activating genes (*rag1* or *rag2*) or *prkdc* gene (SCID) (Shultz *et al.*, 2007). Natural killer (NK)-cells are also effective in eliminating xenografts and mutations in the common γ-chain receptor (IL2Rγ or γ_c) or the NOD (non-obese diabetic) mutation prevent NK-cell development (Shultz *et al.*, 2007). The use of human HSCs for transplantation has resulted in a more broad diversity of human cell types engrafted and the cells are distributed throughout many organs of the mouse (Traggiai *et al.*, 2004). Human HSCs can be obtained from umbilical cord blood, foetal liver or mobilized peripheral blood.

As a result of these advances in humanized mouse technology, humanized mouse engraftment is long-lived and primary human adaptive immune responses are detected against many types of pathogens (Macchiarini *et al.*, 2005; Shultz *et al.*, 2007). Of note, the predominant human cell types present in these new models are human B- and T-lymphocytes, although other cell types (principally monocytes/macrophages and dendritic cells) are readily detectable (Traggiai *et al.*, 2004). Human NK-cells, granulocytes, erythrocytes and platelets are typically found in low abundance, although newer research is allowing more efficient production of some of these immune components (Chen *et al.*, 2009; Hu *et al.*, 2011; Hu & Yang, 2012; Huntington *et al.*, 2009; Pek *et al.*, 2011). Human lymphocytes, myeloid cells and HSCs are important targets and reservoirs of human beta and gammaherpesvirus infections and latency *in vivo*. A variety of HHV pathogens have begun to be explored in these new models in order to determine their suitability for studies of HHV pathogenesis, drug testing, exploration of mechanisms of latency and reactivation, and vaccines.

Although human T- and B-cell responses are commonly detected in humanized mice following exposure to HHVs and other antigens, many experiments have shown sporadic detection of these responses and the amplitude of responses also varies. Although the reasons for these findings are not well understood, it has been hypothesized that as T-cell maturation occurs in a thymus that expresses both murine and human MHC-I molecules, this unusual selection mechanism may play a role in relatively weak adaptive immune responses (Shultz *et al.*, 2012). The very high frequency of EBV-induced cancers in humanized mice (see below) is possibly promoted by weak adaptive immunity and hence a lack of immunological control of EBV. Efforts to improve human adaptive immunity in these models revolve around the introduction of human

MHC-I expression into the thymus by two main mechanisms: (i) transplantation of human thymic stromal cells, referred to as a BLT (bone marrow, liver, thymus) humanized mouse (Melkus *et al.*, 2006), or (ii) a genetic knock-in of human MHC-I into the mouse genome (Shultz *et al.*, 2010). These improvements will be critical for future vaccine studies because weak adaptive immunity will not allow for effective challenge studies to determine vaccine efficacy.

Other mechanisms to humanize mice also exist, built upon the same platform that requires an immunodeficient host. Human liver cells have successfully been transplanted into mice (Azuma *et al.*, 2007), as has human skin, human retinal tissues and human aortic tissues (see below). As the lack of a human receptor molecule is a main obstacle to viral infection, some efforts have been made to produce knock-in mice that express a human viral receptor molecule as another way to confer susceptibility to viral infection to a mouse (Reynaud *et al.*, 2014).

Gammaherpesvirus studies in humanized mice

Of the HHVs, the gammaherpesviruses have been most extensively studied in humanized mice, especially EBV. A number of human EBV-associated diseases have been recapitulated in humanized mice in recent years, thus illustrating the utility of this model to study HHV pathogenesis.

EBV

The main target cells of EBV *in vivo* are epithelial cells and B-lymphocytes, although there is also evidence for infection of T-lymphocytes and NK-cells. Latency is established in B-lymphocytes or epithelial cells (Rickinson & Kieff, 2007). EBV infection is correlated strongly with a number of human diseases, such as infectious mononucleosis and cancers (including Burkitt's lymphoma, nasopharyngeal carcinoma, Hodgkin's lymphoma and gastric carcinoma); in addition, EBV infection is associated with autoimmune diseases, such as multiple sclerosis, systemic lupus erythematosus and rheumatoid arthritis (Longnecker *et al.*, 2013).

Most of the early work on EBV in humanized mice used the SCID-hu-PBL model and, as human blood donors have a high frequency of persistent EBV infection, researchers were able to characterize the effects of transplantation of EBV-positive blood into immunodeficient mice (Fuzzati-Armentero & Duchosal, 1998; Mosier *et al.*, 1989) and lymphoproliferation was noted in many cases. As these reports constitute transfer of virus-infected cells rather than *in vivo* transmission of cell-free virus, we will focus on the latter. Humanized mice can be infected successfully with EBV by several injection mechanisms, including intrasplenic (Islas-Ohlmayer *et al.*, 2004; Wahl *et al.*, 2013), intraperitoneal (Cocco *et al.*, 2008; Heuts *et al.*, 2014; Strowig *et al.*, 2009) and intravenous inoculation (Kuwana *et al.*, 2011; Sato *et al.*, 2011; Yajima *et al.*, 2008). Exposure of HSC-humanized mice to EBV results in detectable viral DNA by 2–4 weeks post-inoculation in the spleen, blood, bone marrow, liver, kidney, adrenal gland, lung and lymph nodes (Islas-Ohlmayer *et al.*, 2004; Traggiai *et al.*, 2004; Yajima *et al.*, 2008). Blood viral load typically peaked in the range of 10^4–10^5 genome copies (Islas-Ohlmayer *et al.*, 2004).

EBV-associated cancers. Development of lymphoproliferative disease and tumours in humanized mice is dependent upon exposure to higher doses of virus (Traggiai *et al.*, 2004; Yajima *et al.*, 2008), although persistence of viral DNA occurs with even a low dose (Yajima *et al.*, 2008). Animals infected with a low dose exhibited persistent viral DNA in various organs, but virus appeared to have been controlled because no cancer was detected (Yajima *et al.*, 2008). Exposure to higher doses leads to tumours in multiple organs, followed by death at 5–10 weeks post-infection (Yajima *et al.*, 2008). Tissues without tumours, but harbouring persistent EBV (bone marrow and spleen), were analysed for viral gene expression patterns, and showed expression of Epstein–Barr nuclear antigen (EBNA) 1, EBNA2, latent membrane protein (LMP1) and LMP2a, indicative of a type III latency program (Yajima *et al.*, 2008).

EBV-positive tumours have been detected in the spleen, liver, kidney and lymph node (Traggiai *et al.*, 2004; Yajima *et al.*, 2008), and as early as 4–7 weeks post-infection in spleen (Heuts *et al.*, 2014; Islas-Ohlmayer *et al.*, 2004). Tumours had a B-cell phenotype ($CD20^+$) and were negative for the pan-T-cell marker CD3 (Islas-Ohlmayer *et al.*, 2004; Yajima *et al.*, 2008). Tumours have been evaluated for viral gene expression patterns, and have been found to express EBNA1, EBV-encoded small RNAs (EBERs), LMP1 and LMP2a, but not EBNA2 (Islas-Ohlmayer *et al.*, 2004; Traggiai *et al.*, 2004; Yajima *et al.*, 2008). This pattern is consistent with a type II latency profile (Islas-Ohlmayer *et al.*, 2004). This characterization of latency is interesting because only a type III expression profile is correlated with cellular proliferation *in vitro*, but it is type II (and not type III) latency that correlates with tumour development *in vivo* in humanized mice. Further analysis has shown that type I and type IIa latency types are found more abundantly in CD8 T-cell-depleted humanized mice and are not found in CD4 T-cell-depleted animals, indicating that T-cell help is required for proliferation (Heuts *et al.*, 2014). *Ex vivo* culture of cells from blood, bone marrow and spleen resulted in production of lymphoblastoid cell lines (Islas-Ohlmayer *et al.*, 2004). Although most reports have focused on B-cell tumours, another study analysed transplantation of peripheral blood mononuclear cells (PBMCs) from patients suffering from chronic active EBV, and found that T-cells and NK-cells continued to proliferate in the context of a humanized mouse model, including clonal expansion of T-cells (Imadome *et al.*, 2011).

Human immune responses to EBV. One of the exciting achievements with human HSC-transplanted mice is the

ability to detect and characterize *de novo* human adaptive immune responses in response to viral antigens. Both T-cell and antibody responses have been detected in humanized mice towards EBV antigens, and it is thought that the inability of the virus to cause tumours after low-dose exposure may be due to control of the virus by the human immune response (Traggiai *et al.*, 2004). T-cell expansion and an inversion of the normal CD4/CD8 ratio have been reported (Traggiai *et al.*, 2004; Yajima *et al.*, 2008), along with EBV-specific T-cell responses that are commonly measured by ELISPOT assay to detect IFN-γ production after exposure to EBV antigen or by a cell-killing assay (Ma *et al.*, 2011; Traggiai *et al.*, 2004; Yajima *et al.*, 2008, 2009). Further evidence of the protective effects of human T-cell responses was gained by depleting either all human T-cells or just the $CD8^+$ fraction; these experiments showed a higher viral load and a reduced lifespan in EBV-infected humanized mice (Strowig *et al.*, 2009; Yajima *et al.*, 2009). Lytic antigens are targeted more frequently by T-cells than latent antigens and the response is also stronger to these antigens (Strowig *et al.*, 2009). Human antibody responses to EBV have also been detected in these models (Yajima *et al.*, 2008). As human lymphocytes develop in the mouse, they are exposed to both murine and human antigens and MHC molecules. In order to determine if human MHC molecules are used to select for T-cell receptors, antibodies specific to human MHC-I and MHC-II were used to block T-cell recognition and detectable T-cell responses were lost, thus showing that at least some selection takes place via human MHC (Melkus *et al.*, 2006; Strowig *et al.*, 2009). One study reported on the development of immunodeficient mice that were additionally engineered to express human HLA-A2 molecules in order to determine if human T-cell responses would be stronger due to selection of T-cell receptors on human MHC. Following human HSC engraftment, they infected these humanized mice with EBV and detected robust HLA-restricted T-cell responses (Shultz *et al.*, 2010).

EBV genetics and relation to cancer. Several studies have been designed to analyse EBV genes that contribute to carcinogenesis in humanized mice in the hope that new targets might be identified to allow for prevention and treatment of EBV-associated cancers. An EBV strain with a mutated BZLF1 gene is defective for lytic replication, but is still able to establish latency in humanized mice. Animals infected with the BZLF1 mutant developed cancers at a lower frequency compared with WT virus, but it is still unclear if this was due to the BZLF1 mutation itself or due to diminished levels of virus due to the inability to replicate (Ma *et al.*, 2011). The same group published a later study with a strain with increased BZLF1 expression as compared with WT virus as a 'super-lytic' virus in order to see if the reverse effect had an impact on lymphomagenesis. They found that the super-lytic virus tended to form abortive lytic infections, but that latency could still develop and the frequency of tumour development was not different compared with WT virus (Ma *et al.*, 2012). These results are interesting, because it has been difficult to achieve HHV mutants that are unable to establish latency to date and a virus with enhanced lytic properties is one way to accomplish that goal; such results would be highly beneficial to HHV vaccine research.

Whilst cell culture research has been very informative in virology, there are many examples of research that differs from the *in vitro* to the *in vivo* environments. An example of this is a study that examined the EBV-encoded BHRF1 microRNA (miRNA) cluster, and found that deletion of these miRNAs prevented B-cell expansion and reduced latent gene expression when studying B-cell transformation *in vitro*. These results suggested that the BHFR1 miRNAs might contribute to cancer development (Feederle *et al.*, 2011). However, when humanized mice were infected with a BHRF1 miRNA mutant, no difference in the ability to develop cancer *in vivo* was noted, although they did find that the miRNAs assist in the development of an acute systemic infection (Wahl *et al.*, 2013). These findings illustrate the utility of humanized mouse research to examine the relevance of *in vitro* research.

EBNA3B is not required for B-cell transformation by EBV *in vitro*. The role of EBNA3B in lymphomagenesis was investigated *in vivo* in humanized mice. Interestingly, infection with EBNA3B-deficient EBV leads to production of aggressive diffuse large B-cell-lymphoma-like cancer in humanized mice, but T-cells are less apt to infiltrate the tumours and to kill tumour cells as compared with WT virus. The authors concluded that EBNA3B is a virus-encoded tumour suppressor that normally assists in immune recognition of tumour cells and slows down tumour progression. After noting these results, the authors analysed human samples and also discovered EBNA3B mutations that had a similar effect on human tumour progression (White *et al.*, 2012). These results indicate that EBV has evolved a fine balance of promoting B-cell proliferation, whilst also acquiring mechanisms to prevent cancer development that would compromise the host.

Other EBV-associated diseases. EBV infection is associated with rheumatoid arthritis and this disease can also be reproduced in humanized mice (Kuwana *et al.*, 2011). Synovial cells were greatly expanded and a variety of human inflammatory cells infiltrated the synovium, including both helper and cytotoxic T-cells, B-cells, and macrophages. Few EBV-positive cells were detected (by EBER expression) in the synovial membrane of arthritic joints, whilst many EBV-positive cells were found in the bone marrow near affected joints. Around 65 % of mice developed these symptoms and the phenomenon was not dose-dependent, as seen in the above cancer studies.

Haemophagocytic lymphohistiocytosis (HLH) is an auto-immune disease that is associated with EBV infection (acquired HLH), and is characterized by leucocytosis, anaemia and thrombocytopenia, plus very high levels of inflammatory cytokines, such as IFN-γ and TNF-α.

Humanized mice were shown to exhibit symptoms similar to those seen in humans after 10 weeks of EBV infection, with two-thirds of mice showing this disease and also showing high/persistent viraemia (Sato *et al.*, 2011). Engulfment of erythrocytes was detected in bone marrow, spleen and liver, and higher viral loads were correlated with higher CD8 T-cell activation frequency and increased IFN-γ secretion.

Summary and future directions. An impressive array of human EBV-associated diseases has been recapitulated in humanized mice. Lymphomagenesis has been detected across all of the new humanized mouse models (Cocco *et al.*, 2008; Islas-Ohlmayer *et al.*, 2004; Ma *et al.*, 2011, 2012; Traggiai *et al.*, 2004; Wahl *et al.*, 2013; White *et al.*, 2012; Yajima *et al.*, 2008) and human T-cell responses to EBV infection have similarly been detected in various models (Melkus *et al.*, 2006; Shultz *et al.*, 2010; Strowig *et al.*, 2009; Traggiai *et al.*, 2004; Yajima *et al.*, 2008, 2009). Not all EBV-associated diseases are expected to be recapitulated in current humanized mouse models, e.g. nasopharyngeal carcinoma involves human cell types not present in current humanized mouse models and the murine equivalent cells cannot be infected with EBV. It has yet to be determined if the humanized mouse model used in a particular report has an impact upon pathogenesis or immunity because of a lack of studies designed to answer this question. Future studies will most likely focus on discovering mechanisms of EBV pathogenesis and the development of new treatments for EBV-associated cancers.

KSHV

KSHV principally infects human B-cells, but is also able to infect endothelial cells, fibroblasts, keratinocytes, monocytes/macrophages and HSCs. Latency is mostly detected in B-cells. The main diseases associated with KSHV in humans are cancers, including Kaposi's sarcoma (KS), pleural effusion lymphoma and multicentric Castleman's disease (Lebbé & Francès, 2009). KS is an endothelial cell cancer and thus it is unlikely to be recapitulated in HSC-engrafted mice because human endothelial cells do not arise from HSCs. As mentioned above, other human tissues and cells have been transplanted to immunodeficient mice besides blood cells. Human skin transplants in SCID mice were injected with KSHV and showed viral replication, with the formation of KS-like lesions (Foreman *et al.*, 2001).

SCID-hu-PBL mice were found to not support transmission of KSHV *in vivo* (Picchio *et al.*, 1997). The lack of infection in SCID-hu-PBL mice was likely due to a lack of the appropriate type of human B-cells as only mature cells are engrafted. The thymic organoid of SCID-hu Thy/Liv mice was directly injected with KSHV and supported lytic replication in rare human B-cells in the thymic graft (Dittmer *et al.*, 1999). However, this model has not been pursued further, possibly due to the rarity of infected cell types and/or lack of pathogenesis. KSHV-transformed cell lines readily produce KSHV-positive tumours in SCID mice and these studies have been useful to gain an understanding of tumorigenesis and angiogenesis, and to test novel antiviral strategies (Boshoff *et al.*, 1998; D'Agostino *et al.*, 1999; Lan *et al.*, 2009; Picchio *et al.*, 1997; Staudt *et al.*, 2004; Wu *et al.*, 2005).

Only a few reports exist on KSHV infection in HSC-engrafted mice. Wu *et al.* (2006) showed that KSHV infection of human HSCs prior to engraftment leads to persistent infection in the transplanted mice. KSHV-positive human B-cells and macrophages in the spleen and bone marrow were detectable by flow cytometry for GFP expressed from recombinant KSHV. Quantitative real-time (qRT)-PCR analysis further showed maintenance of viral DNA in spleen, bone marrow and blood for up to 29 weeks post-infection. Parsons *et al.* (2006) provided evidence for KSHV replication in immunodeficient NOD/SCID mice with no human immune cells. Although published in 2006, to our knowledge that model has not been examined further. The same study also examined animals humanized with human HSCs and demonstrated successful KSHV infection following intravenous injection, accompanied by increases in splenic viral DNA detection over 3 months. They also demonstrated detection of human IgG specific to KSHV.

A recent report describes for the first time KSHV infection of mice previously humanized with HSCs (Wang *et al.*, 2014). The authors demonstrated that humanized mice can be infected via intraperitoneal injection, but also that transmission through mucosal (oral or vaginal) exposure is a better representation of the normal infection pathways in humans. Viral DNA could be detected after infection in the skin, spleen, lung, lymph node, liver, kidney and intestines. Recombinant KSHV expressing GFP was used in the study, thus allowing for detection and characterization of infected cells by flow cytometry. GFP-expressing human cells were detected in the spleen and were found to be mostly human B-cells, with some evidence for macrophage infection. Antigens representing both latent and lytic infection were detected in spleen and in skin. No symptoms of cancer (KS or lymphomas) were noted in this study. It is currently unclear if EBV infection or HIV/AIDS might be co-factors necessary for KSHV cancers to occur (Carbone *et al.*, 2009; da Silva & de Oliveira, 2011), which may explain the lack of disease in this study.

Summary and future directions. There are relatively few studies of KSHV in humanized mice and none have recapitulated any KSHV-associated diseases to date. It is possible that co-infections with EBV and/or HIV may be necessary to reproduce KSHV-associated cancers, because KSHV disease is often associated with these other pathogens. As mentioned above, an engraftment model using human skin supported KSHV infection and induction of KS-like lesions, but that study was published in 2001 and little follow-up work has been performed in that area. Once

disease models are established, a greater understanding of carcinogenic mechanisms can hopefully be achieved, possibly leading to new treatments for KSHV-induced cancers.

Betaherpesvirus studies in humanized mice

hCMV

hCMV has an *in vivo* tropism for human macrophages, dendritic cells, endothelial cells and epithelial cells. Primary hCMV infection is typically asymptomatic, although it can be accompanied by fever and mononucleosis. Transmission can occur through contact with a variety of bodily secretions, such as saliva, breast milk and urine; transplacental transmission also occurs and is associated with serious birth defects. Transplantation of blood or solid organs is also associated with hCMV transmission, although leucodepletion is practiced on blood to prevent transmission of this and other viruses. hCMV disease is most common in immunocompromised hosts, such as AIDS patients and organ transplant recipients (Mocarski *et al.*, 2007).

hCMV infection of HSC-humanized mice. hCMV is thought to be transmitted principally by cell-associated infection; accordingly, cell-free virus did not yield successful transmission, whilst injection of hCMV-infected human fibroblasts via the intraperitoneal route was successful for transmission to humanized mice (Smith *et al.*, 2010). Infection resulted in detectable viral DNA in bone marrow, spleen and kidney, whilst no viral DNA was detected in PBMCs, liver, lung, salivary gland or bladder. After showing evidence of persistent infection, the authors then analysed the effects of human granulocyte colony-stimulating factor (G-CSF) treatment on hCMV-infected animals. G-CSF is commonly used to mobilize human HSCs from bone marrow for later transplantation, and Smith *et al.* (2010) hypothesized that this cytokine could also induce hCMV reactivation and replication *in vivo*. Following G-CSF treatment, viral DNA was detected at higher levels and in new organs in humanized mice, supporting the idea that G-CSF promotes viral replication *in vivo*. Early and late gene expression was detected in G-CSF-treated animals, but not in untreated animals, indicating that G-CSF treatment resulted in reactivation of latent virus. Human liver monocytes/macrophages expressed viral late glycoproteins. Thus, a model has been created that allows for studies of hCMV latency and mechanisms of reactivation, including the potential to study ways to stimulate or block viral reactivation.

A follow-up study examined the possibility of increased probability of hCMV transmission during peripheral blood stem cell transplantation. In this study, the authors took G-CSF mobilized peripheral blood stem cells from hCMV-positive human donors and transplanted them to hCMV-negative humanized mice. Viral DNA was detected in bone marrow, liver and spleen following transplantation, indicating that transmission and dissemination took place (Hakki *et al.*, 2014). These findings indicate that the use of G-CSF stimulates hCMV reactivation and may result in increased probability of viral transmission during blood stem cell transplantation.

This same HSC-engrafted model was also used to study the function of the hCMV UL133–UL138 gene locus *in vivo* (Umashankar *et al.*, 2011). Humanized mice were infected with either WT or UL133–UL138-deleted strains and then virus was stimulated to reactivate using a similar protocol to that mentioned above. Both viruses were able to establish infection in the bone marrow of humanized mice and viral DNA levels were not significantly different either with or without G-CSF treatment. Following G-CSF treatment, both viruses exhibited higher DNA levels in the spleen, but the UL133–UL138 mutant showed higher genome copy numbers in this organ than the WT virus, indicating that these genes may play an important role in viral replication, latency or dissemination.

SCID-hu Thy/Liv and retinal transplant models have also been used to study viral genetics, as the retinal transplant humanized mouse model supports hCMV replication in glial cells of the graft (Bidanset *et al.*, 2001). hCMV UL27 mutants were inoculated into these tissues in order to determine if the UL27 gene is necessary for *in vivo* replication and it was determined to be non-essential (Prichard *et al.*, 2006). A 15 kb region of the hCMV genome that is present in virulent hCMV strains, but missing from attenuated strains, was deleted and then studied for replicative ability in SCID-hu Thy/Liv mice. Although the mutant only had a minor growth defect in human foreskin fibroblast cells, it was unable to replicate in the thymic graft (Wang *et al.*, 2005).

hCMV drug testing in humanized mice. In the early 1990s, it was discovered that hCMV can replicate in thymic epithelial cells of SCID-hu Thy/Liv mice (Mocarski *et al.*, 1993) and in implanted human retinal tissue in immunodeficient mice (Epstein *et al.*, 1994). These experimental systems were used to test new antiviral drugs for efficacy against hCMV and this topic has been reviewed previously (Kern, 2006). Some additional studies have taken place since that review was published (Quenelle *et al.*, 2008), including a report that human hepatocytes can be transplanted to immunodeficient mice, that they can be infected with hCMV and that this model is useful to study antiviral drug testing (Kawahara *et al.*, 2013). In addition, human skin grafts can be achieved, infected with hCMV and controlled by gancyclovir (Bravo *et al.*, 2007).

hCMV pathogenesis in humanized mice. hCMV infection has been associated with a variety of diseases, including transplant coronary arteriosclerosis. An immunodeficient mouse model with transplanted human artery tissue was developed and examined for the impact of hCMV infection upon immune rejection of the graft (Abele-Ohl *et al.*, 2012). Human internal mammary artery tissue was obtained and infected with hCMV, then transplanted to the

infrarenal artery of immunodeficient mice. One week later, human PBMCs were transferred intraperitoneally into mice and then analysed for graft rejection. hCMV infection was confirmed by DNA detection and immunodetection of viral antigens. Vascular lesions and immune cell infiltrates were more pronounced in animals receiving hCMV-infected arterial grafts compared with uninfected grafts, and intercellular adhesion molecule-1 and platelet-derived growth factor receptor-β expression levels were increased upon hCMV infection, which may explain the immune infiltration and vascular lesions.

Summary and future directions. hCMV studies in humanized mice have mostly been performed in older models and with the goal of testing antiviral drug efficacy. Whilst some studies have been performed to examine hCMV-mediated pathogenesis, there are still many diseases associated with hCMV that warrant further exploration. hCMV can cause hepatitis and this disease could be modelled in a humanized liver mouse model (see above). Neuropathogenesis has not yet been explored for hCMV in humanized mice. Interestingly, HIV-1 is able to penetrate the humanized mouse brain, where it replicates and causes inflammation (Dash *et al.*, 2011; Gorantla *et al.*, 2010). At least some human immune cells traffic to the brain in humanized mice and this is an area that could be explored for hCMV. However, it is not expected that hCMV will be able to replicate in murine brain cells. Congenital transmission of hCMV is a major cause of birth defects, but this form of pathogenesis is not able to be studied in current humanized mouse models because animals are engrafted after birth. Similarly, hCMV-associated pneumonia and gastroenteritis are not like to be detected in current humanized mouse models. *In vivo* drug testing for hCMV has an important history in humanized mice and we expect that other HHVs can similarly be tested for drug efficacy in these models.

HHV-6

Previously, HHV-6A and HHV-6B were classified as subtypes of the same virus, but they have recently been classified as two distinct viruses (Adams & Carstens, 2012). Both viruses have primary tropism for $CD4^+$ T-cells, but HHV-6A is also capable of lytic infection in $CD8^+$ T-cells, $\gamma\delta$ T-cells and NK-cells (Dagna *et al.*, 2013). HHV-6B causes roseola – a childhood fever and rash that usually resolves without complication. We are not aware of any studies attempting to infect HSC-humanized mice with HHV-6B or to recapitulate roseola disease. HHV-6A has not been shown definitively to cause any disease, but it is implicated in diseases, including autoimmune diseases such as multiple sclerosis (Virtanen *et al.*, 2007), immunosuppression (Emery *et al.*, 1999; Gobbi *et al.*, 1999; Lusso & Gallo, 1995) and graft-versus-host disease (Appleton *et al.*, 1995).

SCID-hu Thy/Liv mice can be infected with HHV-6. In one study, the implanted Thy/Liv organ of SCID-hu Thy/Liv mice was surgically exposed and injected with HHV-6A strain GS. Thy/Liv implants were harvested at 4, 7, 11 and 27 days post-inoculation. HHV-6A replication was demonstrated by detection of increasing amounts of viral DNA, which peaked at 14 days post-inoculation. The virus induced severe depletion of thymocytes, especially the intrathymic progenitor T-cells (Gobbi *et al.*, 1999).

In a more recent study, $Rag2^{-/-}\gamma_c^{-/-}$ mice were infected with HHV-6A. Cell-associated or cell-free virus was injected intraperitoneally into the mice and nearly all infected mice had detectable levels of HHV-6A DNA by qRT-PCR in at least one of the samples tested (blood, bone marrow, lymph node and thymus). Cell-free injected mice were sacrificed at 1 week post-infection and cell-associated mice were sacrificed at 6.5–9.5 weeks post-infection. Thymocyte populations were significantly altered in the HHV-6A-infected mice sacrificed at time points later than 1 week post-infection, including a significant decrease in CD3 expression as well as a significant loss of intrathymic T progenitor cells ($CD3^-CD4^+CD8^-$) as was seen in the previously mentioned study in SCID-hu Thy/Liv mice. Increased populations of $CD4^+CD8^+$ T-cells were detected in peripheral blood (Tanner *et al.*, 2013).

CD46 transgenic mice have also been shown to be susceptible to HHV-6 infection (Reynaud *et al.*, 2014). These mice were injected intracranially with HHV-6A and HHV-6B. Although HHV-6B DNA levels decreased rapidly after infections, HHV-6A DNA was detectable in the brain for up to 9 months post-infection. Primary brain glial cultures from the transgenic mice that were infected with HHV-6A showed production of pro-inflammatory cytokines CCL2, CCL5 and CXCL10. This represents the first murine model to study HHV-6A infection in the brain.

Summary and future directions. HHV-6 viruses have been associated with a large number of diseases in humans, but the ubiquitous nature of the viruses has made it difficult to prove causal relationships. Most data gained to date in humanized mice show a role of HHV-6 viruses in immunosuppression, but many other diseases remain to be explored.

HHV-7

HHV-7 is genetically similar to HHV-6 and also infects human T-cells, although no known human diseases are attributed to HHV-7. We are not aware of any attempts to infect humanized mice with HHV-7 to date.

Alphaherpesvirus studies in humanized mice

HSV-1 and HSV-2

HSV-1 and HSV-2 normally replicate in epithelial cells and establish latency in neuronal cells, with only limited evidence for infection of immune cells. As these viruses infect mice, rats, rabbits and other small-animal models, they have not been explored much in humanized mice.

Table 1. Summary of pathological findings in humanized mouse models and future directions for HHV research in humanized mice

Virus	Reported findings	Future directions
EBV	Persistent infection in B-cells	Gain greater understanding of molecular biology of EBV-induced cancers
	Lymphoproliferation; associated with type II latency	
	Symptoms of rheumatoid arthritis	Develop new treatments for EBV-associated cancers
	Symptoms of HLH	
hCMV	Persistent infection in monocytes/macrophages in bone marrow and spleen	Determine mechanisms of latency *in vivo*
	Viral reactivation due to G-CSF has implications for bone marrow transplants	
KSHV	Persistent infection in B-cells and macrophages	Develop a model for KSHV-associated lymphomas
	Mucosal transmission through oral and vaginal exposure	Develop new treatments for KSHV-associated cancers
	KS-like lesions in human skin-transplanted mice	
HHV-6	Persistent infection in blood and lymphoid organs	Model roseola pathogenesis by HHV-6B
	Thymocyte depletion due to HHV-6A/HHV-6B	Determine diseases caused by HHV-6A in humans

Human skin grafts in SCID mice support replication by HSV-1 and VZV, and the SCID-hu Thy/Liv model also can be infected by each virus (Moffat *et al.*, 1998a). HSV-1 only infected epidermal cells in either model; small, superficial lesions were detected in the epidermis of skin grafts and no replication in thymic T-cells was detected. HSV-1 glycoprotein C (gC) is dispensable for replication in culture, but a mutant revealed that gC is an important virulence factor in HSV-1 replication *in vivo* (Moffat *et al.*, 1998a).

HSC-humanized mice can be infected with attenuated HSV-2 (thymidine kinase mutant) by intravaginal inoculation and were used as a model to study protective human immune responses by later giving a lethal challenge with a WT stain (Kwant-Mitchell *et al.*, 2009). Primary infection resulted in human T-cell and NK-cell trafficking to the genital tract and iliac lymph nodes. Human T-cells in spleen, lymph nodes and the vaginal tract produced IFN-γ in response to HSV-2 antigens, thus showing an adaptive cellular response. Human IgG specific to HSV-2 was also detected. Upon challenge with a lethal dose of HSV-2, immunized animals survived significantly better if a human immune system was transplanted; in contrast, none of the non-humanized mice survived.

VZV

VZV shares a tropism for replication in epithelial cells and latency in neurons, although unlike the other alphaherpesviruses it also infects human T-cells, which it uses to traffic to the skin. Humans and some non-human primates are the only hosts infectable by VZV. As VZV replicates in T-cells, it has been studied in the SCID-hu Thy/Liv model as well as in skin graft models. Skin graft studies showed that VZV extensively infected dermal and epidermal cells, whilst HSV-1 only formed small lesions in the epidermis. VZV gC was found to be an important virulence factor in skin, although it is not required for replication *in vitro* (Moffat *et al.*, 1998a). Similar studies were performed to determine the roles of the ORF47 and ORF66 gene products in thymic and skin implants. Although strains with mutations in these genes still allowed for tissue culture replication, ORF47 was found to be required for replication in skin and thymic grafts, and ORF66 was necessary for T-cell infectivity and had a partial effect on skin infectivity (Moffat *et al.*, 1998b). The skin graft model was used to study mechanisms of T-cell transfer of virus to the skin, demonstrating that VZV-infected T-cells move to skin within 24 h of entering the circulation. Memory $CD4^+$ T-cells were the predominant T-cell type recovered from skin grafts. VZV is able to downregulate host IFN-α production in infected skin cells and also blocks the ability of IL-1α to recruit inflammatory cells to sites of virus replication (Ku *et al.*, 2004). Taken together, these studies provide information that could be useful to develop improved VZV vaccines by identifying virulence factors and by gaining an understanding of how VZV traffics in the host.

Summary and future directions. We do not anticipate much further research on the alphaherpesviruses in humanized mice, because of the tropism of the HSVs for standard mouse models, and as VZV replicates principally in epithelial cells and skin models in humanized mice have not been adopted widely. However, one area that has greater potential is for vaccine studies because humanized mice generate human cellular and humoral immune responses to HHVs (see above), and can be challenged with virus after experimental vaccination in order to determine the efficacy of the vaccine. As human genes are used to generate human T- and B-cell receptors, the antigenic targets are expected to be similar to those seen in humans.

Overall summary and future directions

Humanized mice have served as an excellent model to study various aspects of HHV biology including pathogenesis, tropism, establishment of latency, reactivation,

Table 2. Summary of recent reports of HHV pathogenesis in HSC-humanized mice

Virus	Findings	Humanized mouse model	Reference(s)
EBV	Lymphoproliferation	$Rag2^{-/-}\gamma_c^{-/-}$	Traggiai *et al.* (2004)
EBV	Lymphoproliferation	NOD/SCID$\gamma_c^{-/-}$	Heuts *et al.* (2014), Wahl *et al.* (2013), White *et al.* (2012), Yajima *et al.* (2008)
EBV	Lymphoproliferation	NOD/SCID	Islas-Ohlmayer *et al.* (2004)
EBV	Lymphoproliferation	NOD/SCID$\gamma_c^{-/-}$ BLT	Ma *et al.* (2011, 2012)
EBV	Rheumatoid arthritis	NOD/SCID$\gamma_c^{-/-}$	Kuwana *et al.* (2011)
EBV	HLH	NOD/SCID$\gamma_c^{-/-}$	Sato *et al.* (2011)
KSHV	Mucosal transmission; no disease detected	NOD/SCID$\gamma_c^{-/-}$ BLT	Wang *et al.* (2014)
hCMV	G-CSF treatment reactivates latent hCMV	NOD/SCID$\gamma_c^{-/-}$	Smith *et al.* (2010), Umashankar *et al.* (2011)
HHV-6A	Thymocyte depletion	$Rag2^{-/-}\gamma_c^{-/-}$	Tanner *et al.* (2013)
HSV-2	Protective human immune responses	$Rag2^{-/-}\gamma_c^{-/-}$	Kwant-Mitchell *et al.* (2009)

efficacy of antiviral drugs and human immune responses. A summary of the major findings of HHV research in the new generation of humanized mice is given in Table 1, accompanied by areas for future research.

It is currently unclear if one humanized mouse model will be superior to others as it pertains to a particular virus due to a lack of studies designed to compare the various models. However, a number of HHVs infect human cell types that are not produced in the most common and current humanized mouse models (e.g. epithelial cells, endothelial cells and neurons). In order to recapitulate these models, it may be necessary to combine multiple humanized mouse models together in order to have both target cells and human immune cells that may be involved in either infection or pathogenesis. Such a study was achieved with hepatitis C virus infection in a humanized mouse model that combined transplantation of human hepatocytes with transplantation of human HSCs (Washburn *et al.*, 2011), and we envision that similar studies can be planned to better understand immunological control of HHV infection as well as immune-mediated pathologies.

Clearly, the HSVs already have well-established animal models and humanized mice are not as important to the study of those pathogens, although vaccine research of HSVs would be benefitted by studies of the human adaptive immune response in humanized mice due to differences in mouse and human genetics. With the current state of humanized mice focused mostly on human immune cell transplants, the beta and gammaherpesvirus fields stand to gain the most from humanized mouse models. The contributions of EBV to cancer development in humanized mice have been explored more than any other area of HHV biology to date, but further work is needed to find new treatments that will target specifically EBV-positive cancer cells. We expect that further work in EBV genetics will yield new targets for chemotherapy of EBV cancers. In general, the humanized mouse platform has been underutilized for HHV drug development. Although EBV and hCMV have been studied the most in these models, only a few studies on KSHV and HHV-6 have been performed. A summary of HHV-induced pathogenesis in humanized mice with accompanying references is provided in Table 2. With the recent development of new models for these infections, we anticipate further elucidation of their pathogenic mechanisms and validation of antiviral drugs *in vivo*. We believe that humanized mouse models will be a useful tool to study the contributions of particular HHV genes to latency and persistence, and anticipate that this area of research will be helpful to create HHV vaccines with no capacity for persistence in the host.

References

Abele-Ohl, S., Leis, M., Wollin, M., Mahmoudian, S., Hoffmann, J., Müller, R., Heim, C., Spriewald, B. M., Weyand, M. & other authors (2012). Human cytomegalovirus infection leads to elevated levels of transplant arteriosclerosis in a humanized mouse aortic xenograft model. *Am J Transplant* **12**, 1720–1729.

Adams, M. J. & Carstens, E. B. (2012). Ratification vote on taxonomic proposals to the International Committee on Taxonomy of Viruses (2012). *Arch Virol* **157**, 1411–1422.

Appleton, A. L., Sviland, L., Peiris, J. S., Taylor, C. E., Wilkes, J., Green, M. A., Pearson, A. D., Kelly, P. J., Malcolm, A. J. & other authors (1995). Human herpes virus-6 infection in marrow graft recipients: role in pathogenesis of graft-versus-host disease. Newcastle upon Tyne Bone Marrow Transport Group. *Bone Marrow Transplant* **16**, 777–782.

Azuma, H., Paulk, N., Ranade, A., Dorrell, C., Al-Dhalimy, M., Ellis, E., Strom, S., Kay, M. A., Finegold, M. & Grompe, M. (2007). Robust expansion of human hepatocytes in $Fah^{-/-}/Rag2^{-/-}/Il2rg^{-/-}$ mice. *Nat Biotechnol* **25**, 903–910.

Bidanset, D. J., Rybak, R. J., Hartline, C. B. & Kern, E. R. (2001). Replication of human cytomegalovirus in severe combined immunodeficient mice implanted with human retinal tissue. *J Infect Dis* **184**, 192–195.

Boshoff, C., Gao, S. J., Healy, L. E., Matthews, S., Thomas, A. J., Coignet, L., Warnke, R. A., Strauchen, J. A., Matutes, E. & other authors (1998). Establishing a $KSHV^+$ cell line (BCP-1) from peripheral blood and characterizing its growth in Nod/SCID mice. *Blood* **91**, 1671–1679.

Bravo, F. J., Cardin, R. D. & Bernstein, D. I. (2007). A model of human cytomegalovirus infection in severe combined immunodeficient mice. *Antiviral Res* **76**, 104–110.

Carbone, A., Cesarman, E., Spina, M., Gloghini, A. & Schulz, T. F. (2009). HIV-associated lymphomas and gamma-herpesviruses. *Blood* **113**, 1213–1224.

Chen, Q., Khoury, M. & Chen, J. (2009). Expression of human cytokines dramatically improves reconstitution of specific human-blood lineage cells in humanized mice. *Proc Natl Acad Sci U S A* **106**, 21783–21788.

Cocco, M., Bellan, C., Tussiwand, R., Corti, D., Traggiai, E., Lazzi, S., Mannucci, S., Bronz, L., Palummo, N. & other authors (2008). $CD34^+$ cord blood cell-transplanted $Rag2^{-/-}$ $\gamma_c^{-/-}$ mice as a model for Epstein–Barr virus infection. *Am J Pathol* **173**, 1369–1378.

D'Agostino, G., Aricò, E., Santodonato, L., Venditti, M., Sestili, P., Masuelli, L., Coletti, A., Modesti, A., Picchio, G. & other authors (1999). Type I consensus IFN (IFN-con1) gene transfer into KSHV/HHV-8-infected BCBL-1 cells causes inhibition of viral lytic cycle activation via induction of apoptosis and abrogates tumorigenicity in sCID mice. *J Interferon Cytokine Res* **19**, 1305–1316.

da Silva, S. R. & de Oliveira, D. E. (2011). HIV, EBV and KSHV: viral cooperation in the pathogenesis of human malignancies. *Cancer Lett* **305**, 175–185.

Dagna, L., Pritchett, J. C. & Lusso, P. (2013). Immunomodulation and immunosuppression by human herpesvirus 6A and 6B. *Future Virol* **8**, 273–287.

Dash, P. K., Gorantla, S., Gendelman, H. E., Knibbe, J., Casale, G. P., Makarov, E., Epstein, A. A., Gelbard, H. A., Boska, M. D. & Poluektova, L. Y. (2011). Loss of neuronal integrity during progressive HIV-1 infection of humanized mice. *J Neurosci* **31**, 3148–3157.

Dittmer, D., Stoddart, C., Renne, R., Linquist-Stepps, V., Moreno, M. E., Bare, C., McCune, J. M. & Ganem, D. (1999). Experimental transmission of Kaposi's sarcoma-associated herpesvirus (KSHV/HHV-8) to SCID-hu Thy/Liv mice. *J Exp Med* **190**, 1857–1868.

Emery, V. C., Atkins, M. C., Bowen, E. F., Clark, D. A., Johnson, M. A., Kidd, I. M., McLaughlin, J. E., Phillips, A. N., Strappe, P. M. & Griffiths, P. D. (1999). Interactions between beta-herpesviruses and human immunodeficiency virus *in vivo*: evidence for increased human immunodeficiency viral load in the presence of human herpesvirus 6. *J Med Virol* **57**, 278–282.

Epstein, L. G., Cvetkovich, T. A., Lazar, E. S., DiLoreto, D., Saito, Y., James, H., del Cerro, C., Kaneshima, H., McCune, J. M. & other authors (1994). Human neural xenografts: progress in developing an in-vivo model to study human immunodeficiency virus (HIV) and human cytomegalovirus (HCMV) infection. *Adv Neuroimmunol* **4**, 257–260.

Feederle, R., Haar, J., Bernhardt, K., Linnstaedt, S. D., Bannert, H., Lips, H., Cullen, B. R. & Delecluse, H. J. (2011). The members of an Epstein–Barr virus microRNA cluster cooperate to transform B lymphocytes. *J Virol* **85**, 9801–9810.

Foreman, K. E., Friborg, J., Chandran, B., Katano, H., Sata, T., Mercader, M., Nabel, G. J. & Nickoloff, B. J. (2001). Injection of human herpesvirus-8 in human skin engrafted on SCID mice induces Kaposi's sarcoma-like lesions. *J Dermatol Sci* **26**, 182–193.

Fuzzati-Armentero, M. T. & Duchosal, M. A. (1998). hu-PBL-SCID mice: an *in vivo* model of Epstein–Barr virus-dependent lymphoproliferative disease. *Histol Histopathol* **13**, 155–168.

Gobbi, A., Stoddart, C. A., Malnati, M. S., Locatelli, G., Santoro, F., Abbey, N. W., Bare, C., Linquist-Stepps, V., Moreno, M. B. & other authors (1999). Human herpesvirus 6 (HHV-6) causes severe thymocyte depletion in SCID-hu Thy/Liv mice. *J Exp Med* **189**, 1953–1960.

Gorantla, S., Makarov, E., Finke-Dwyer, J., Castanedo, A., Holguin, A., Gebhart, C. L., Gendelman, H. E. & Poluektova, L. (2010). Links between progressive HIV-1 infection of humanized mice and viral neuropathogenesis. *Am J Pathol* **177**, 2938–2949.

Hakki, M., Goldman, D. C., Streblow, D. N., Hamlin, K. L., Krekylwich, C. N., Fleming, W. H. & Nelson, J. A. (2014). HCMV infection of humanized mice after transplantation of G-CSF-mobilized peripheral blood stem cells from HCMV-seropositive donors. *Biol Blood Marrow Transplant* **20**, 132–135.

Heuts, F., Rottenberg, M. E., Salamon, D., Rasul, E., Adori, M., Klein, G., Klein, E. & Nagy, N. (2014). T cells modulate Epstein–Barr virus latency phenotypes during infection of humanized mice. *J Virol* **88**, 3235–3245.

Hu, Z. & Yang, Y. G. (2012). Full reconstitution of human platelets in humanized mice after macrophage depletion. *Blood* **120**, 1713–1716.

Hu, Z., Van Rooijen, N. & Yang, Y. G. (2011). Macrophages prevent human red blood cell reconstitution in immunodeficient mice. *Blood* **118**, 5938–5946.

Huntington, N. D., Legrand, N., Alves, N. L., Jaron, B., Weijer, K., Plet, A., Corcuff, E., Mortier, E., Jacques, Y. & other authors (2009). IL-15 trans-presentation promotes human NK cell development and differentiation *in vivo*. *J Exp Med* **206**, 25–34.

Imadome, K., Yajima, M., Arai, A., Nakazawa, A., Kawano, F., Ichikawa, S., Shimizu, N., Yamamoto, N., Morio, T. & other authors (2011). Novel mouse xenograft models reveal a critical role of $CD4^+$ T cells in the proliferation of EBV-infected T and NK cells. *PLoS Pathog* **7**, e1002326.

Islas-Ohlmayer, M., Padgett-Thomas, A., Domiati-Saad, R., Melkus, M. W., Cravens, P. D., Martin, M. P., Netto, G. & Garcia, J. V. (2004). Experimental infection of NOD/SCID mice reconstituted with human $CD34^+$ cells with Epstein–Barr virus. *J Virol* **78**, 13891–13900.

Kawahara, T., Lisboa, L. F., Cader, S., Douglas, D. N., Nourbakhsh, M., Pu, C. H., Lewis, J. T., Churchill, T. A., Humar, A. & Kneteman, N. M. (2013). Human cytomegalovirus infection in humanized liver chimeric mice. *Hepatol Res* **43**, 679–684.

Kern, E. R. (2006). Pivotal role of animal models in the development of new therapies for cytomegalovirus infections. *Antiviral Res* **71**, 164–171.

Ku, C. C., Zerboni, L., Ito, H., Graham, B. S., Wallace, M. & Arvin, A. M. (2004). Varicella-zoster virus transfer to skin by T cells and modulation of viral replication by epidermal cell interferon-alpha. *J Exp Med* **200**, 917–925.

Kuwana, Y., Takei, M., Yajima, M., Imadome, K., Inomata, H., Shiozaki, M., Ikumi, N., Nozaki, T., Shiraiwa, H. & other authors (2011). Epstein–Barr virus induces erosive arthritis in humanized mice. *PLoS ONE* **6**, e26630.

Kwant-Mitchell, A., Ashkar, A. A. & Rosenthal, K. L. (2009). Mucosal innate and adaptive immune responses against herpes simplex virus type 2 in a humanized mouse model. *J Virol* **83**, 10664–10676.

Lan, K., Murakami, M., Bajaj, B., Kaul, R., He, Z., Gan, R., Feldman, M. & Robertson, E. S. (2009). Inhibition of KSHV-infected primary effusion lymphomas in NOD/SCID mice by gamma-secretase inhibitor. *Cancer Biol Ther* **8**, 2136–2143.

Lebbé, C. & Francès, C. (2009). Human herpesvirus 8. *Cancer Treat Res* **146**, 169–188.

Longnecker, R. M., Kieff, E. & Cohen, J. I. (2013). Epstein–Barr virus. In *Fields Virology*, 6th edn, pp. 1898–1959. Edited by D. M. Knipe & P. M. Howley. Philadelphia, PA: Lippincott Williams & Wilkins.

Lusso, P. & Gallo, R. C. (1995). Human herpesvirus 6 in AIDS. *Immunol Today* **16**, 67–71.

Ma, S. D., Hegde, S., Young, K. H., Sullivan, R., Rajesh, D., Zhou, Y., Jankowska-Gan, E., Burlingham, W. J., Sun, X. & other authors (2011). A new model of Epstein–Barr virus infection reveals an

important role for early lytic viral protein expression in the development of lymphomas. *J Virol* **85**, 165–177.

Ma, S. D., Yu, X., Mertz, J. E., Gumperz, J. E., Reinheim, E., Zhou, Y., Tang, W., Burlingham, W. J., Gulley, M. L. & Kenney, S. C. (2012). An Epstein–Barr virus (EBV) mutant with enhanced BZLF1 expression causes lymphomas with abortive lytic EBV infection in a humanized mouse model. *J Virol* **86**, 7976–7987.

Macchiarini, F., Manz, M. G., Palucka, A. K. & Shultz, L. D. (2005). Humanized mice: are we there yet? *J Exp Med* **202**, 1307–1311.

McCune, J. M., Namikawa, R., Kaneshima, H., Shultz, L. D., Lieberman, M. & Weissman, I. L. (1988). The SCID-hu mouse: murine model for the analysis of human hematolymphoid differentiation and function. *Science* **241**, 1632–1639.

McGeoch, D. J., Rixon, F. J. & Davison, A. J. (2006). Topics in herpesvirus genomics and evolution. *Virus Res* **117**, 90–104.

McGregor, A. (2010). Current and new cytomegalovirus antivirals and novel animal model strategies. *Inflamm Allergy Drug Targets* **9**, 286–299.

Melkus, M. W., Estes, J. D., Padgett-Thomas, A., Gatlin, J., Denton, P. W., Othieno, F. A., Wege, A. K., Haase, A. T. & Garcia, J. V. (2006). Humanized mice mount specific adaptive and innate immune responses to EBV and TSST-1. *Nat Med* **12**, 1316–1322.

Mocarski, E. S., Bonyhadi, M., Salimi, S., McCune, J. M. & Kaneshima, H. (1993). Human cytomegalovirus in a SCID-hu mouse: thymic epithelial cells are prominent targets of viral replication. *Proc Natl Acad Sci U S A* **90**, 104–108.

Mocarski, E. S., Shenk, T. & Pass, R. F. (2007). Cytomegaloviruses. In *Fields Virology*, 5th edn, pp. 2701–2772. Edited by D. M. Knipe & P. M. Howley. Philadelphia, PA: Lippincott Williams & Wilkins.

Moffat, J. F., Zerboni, L., Kinchington, P. R., Grose, C., Kaneshima, H. & Arvin, A. M. (1998a). Attenuation of the vaccine Oka strain of varicella-zoster virus and role of glycoprotein C in alphaherpesvirus virulence demonstrated in the SCID-hu mouse. *J Virol* **72**, 965–974.

Moffat, J. F., Zerboni, L., Sommer, M. H., Heineman, T. C., Cohen, J. I., Kaneshima, H. & Arvin, A. M. (1998b). The ORF47 and ORF66 putative protein kinases of varicella-zoster virus determine tropism for human T cells and skin in the SCID-hu mouse. *Proc Natl Acad Sci U S A* **95**, 11969–11974.

Mosier, D. E. (1996). Human immunodeficiency virus infection of human cells transplanted to severe combined immunodeficient mice. *Adv Immunol* **63**, 79–125.

Mosier, D. E., Gulizia, R. J., Baird, S. M. & Wilson, D. B. (1988). Transfer of a functional human immune system to mice with severe combined immunodeficiency. *Nature* **335**, 256–259.

Mosier, D. E., Gulizia, R. J., Baird, S. M., Spector, S., Spector, D., Kipps, T. J., Fox, R. I., Carson, D. A., Cooper, N. & other authors (1989). Studies of HIV infection and the development of Epstein–Barr virus-related B cell lymphomas following transfer of human lymphocytes to mice with severe combined immunodeficiency. *Curr Top Microbiol Immunol* **152**, 195–199.

Nash, A. A., Dutia, B. M., Stewart, J. P. & Davison, A. J. (2001). Natural history of murine γ-herpesvirus infection. *Philos Trans R Soc Lond B Biol Sci* **356**, 569–579.

Orzechowska, B. U., Powers, M. F., Sprague, J., Li, H., Yen, B., Searles, R. P., Axthelm, M. K. & Wong, S. W. (2008). Rhesus macaque rhadinovirus-associated non-Hodgkin lymphoma: animal model for KSHV-associated malignancies. *Blood* **112**, 4227–4234.

Parsons, C. H., Adang, L. A., Overdevest, J., O'Connor, C. M., Taylor, J. R. J., Jr, Camerini, D. & Kedes, D. H. (2006). KSHV targets multiple leukocyte lineages during long-term productive infection in NOD/SCID mice. *J Clin Invest* **116**, 1963–1973.

Pek, E. A., Chan, T., Reid, S. & Ashkar, A. A. (2011). Characterization and IL-15 dependence of NK cells in humanized mice. *Immunobiology* **216**, 218–224.

Picchio, G. R., Sabbe, R. E., Gulizia, R. J., McGrath, M., Herndier, B. G. & Mosier, D. E. (1997). The KSHV/HHV8-infected BCBL-1 lymphoma line causes tumors in SCID mice but fails to transmit virus to a human peripheral blood mononuclear cell graft. *Virology* **238**, 22–29.

Prichard, M. N., Quenelle, D. C., Bidanset, D. J., Komazin, G., Chou, S., Drach, J. C. & Kern, E. R. (2006). Human cytomegalovirus UL27 is not required for viral replication in human tissue implanted in SCID mice. *Virol J* **3**, 18.

Quenelle, D. C., Collins, D. J., Pettway, L. R., Hartline, C. B., Beadle, J. R., Wan, W. B., Hostetler, K. Y. & Kern, E. R. (2008). Effect of oral treatment with (*S*)-HPMPA, HDP-(*S*)-HPMPA or ODE-(*S*)-HPMPA on replication of murine cytomegalovirus (MCMV) or human cytomegalovirus (HCMV) in animal models. *Antiviral Res* **79**, 133–135.

Reynaud, J. M., Jégou, J. F., Welsch, J. C. & Horvat, B. (2014). Human herpesvirus 6A infection in CD46 transgenic mice: viral persistence in the brain and increased production of proinflammatory chemokines via Toll-like receptor 9. *J Virol* **88**, 5421–5436.

Rickinson, A. B. & Kieff, E. (2007). Epstein–Barr virus. In *Fields Virology*, 5th edn, pp. 2655–2700. Edited by D. M. Knipe & P. M. Howley. Philadelphia, PA: Lippincott Williams & Wilkins.

Sato, K., Misawa, N., Nie, C., Satou, Y., Iwakiri, D., Matsuoka, M., Takahashi, R., Kuzushima, K., Ito, M. & other authors (2011). A novel animal model of Epstein–Barr virus-associated hemophagocytic lymphohistiocytosis in humanized mice. *Blood* **117**, 5663–5673.

Shope, T., Dechairo, D. & Miller, G. (1973). Malignant lymphoma in cottontop marmosets after inoculation with Epstein–Barr virus. *Proc Natl Acad Sci U S A* **70**, 2487–2491.

Shultz, L. D., Ishikawa, F. & Greiner, D. L. (2007). Humanized mice in translational biomedical research. *Nat Rev Immunol* **7**, 118–130.

Shultz, L. D., Saito, Y., Najima, Y., Tanaka, S., Ochi, T., Tomizawa, M., Doi, T., Sone, A., Suzuki, N. & other authors (2010). Generation of functional human T-cell subsets with HLA-restricted immune responses in HLA class I expressing NOD/SCID/IL2rγ^{null} humanized mice. *Proc Natl Acad Sci U S A* **107**, 13022–13027.

Shultz, L. D., Brehm, M. A., Garcia-Martinez, J. V. & Greiner, D. L. (2012). Humanized mice for immune system investigation: progress, promise and challenges. *Nat Rev Immunol* **12**, 786–798.

Smith, M. S., Goldman, D. C., Bailey, A. S., Pfaffle, D. L., Kreklywich, C. N., Spencer, D. B., Othieno, F. A., Streblow, D. N., Garcia, J. V. & other authors (2010). Granulocyte-colony stimulating factor reactivates human cytomegalovirus in a latently infected humanized mouse model. *Cell Host Microbe* **8**, 284–291.

Staudt, M. R., Kanan, Y., Jeong, J. H., Papin, J. F., Hines-Boykin, R. & Dittmer, D. P. (2004). The tumor microenvironment controls primary effusion lymphoma growth *in vivo*. *Cancer Res* **64**, 4790–4799.

Stevenson, P. G. & Efstathiou, S. (2005). Immune mechanisms in murine gammaherpesvirus-68 infection. *Viral Immunol* **18**, 445–456.

Strowig, T., Gurer, C., Ploss, A., Liu, Y. F., Arrey, F., Sashihara, J., Koo, G., Rice, C. M., Young, J. W. & other authors (2009). Priming of protective T cell responses against virus-induced tumors in mice with human immune system components. *J Exp Med* **206**, 1423–1434.

Takahashi, M., Asano, Y., Kamiya, H., Baba, K., Ozaki, T., Otsuka, T. & Yamanishi, K. (2008). Development of varicella vaccine. *J Infect Dis* **197** (Suppl 2), S41–S44.

Tanner, A., Carlson, S. A., Nukui, M., Murphy, E. A. & Berges, B. K. (2013). Human herpesvirus 6A infection and immunopathogenesis in humanized Rag2$^{-/-}$ γc$^{-/-}$ mice. *J Virol* **87**, 12020–12028.

Tanner, A., Taylor, S. E., Decottignies, W. & Berges, B. K. (2014). Humanized mice as a model to study human hematopoietic stem cell transplantation. *Stem Cells Dev* **23**, 76–82.

Traggiai, E., Chicha, L., Mazzucchelli, L., Bronz, L., Piffaretti, J. C., Lanzavecchia, A. & Manz, M. G. (2004). Development of a human adaptive immune system in cord blood cell-transplanted mice. *Science* **304**, 104–107.

Umashankar, M., Petrucelli, A., Cicchini, L., Caposio, P., Kreklywich, C. N., Rak, M., Bughio, F., Goldman, D. C., Hamlin, K. L. & other authors (2011). A novel human cytomegalovirus locus modulates cell type-specific outcomes of infection. *PLoS Pathog* **7**, e1002444.

Virtanen, J. O., Färkkilä, M., Multanen, J., Uotila, L., Jääskeläinen, A. J., Vaheri, A. & Koskiniemi, M. (2007). Evidence for human herpesvirus 6 variant A antibodies in multiple sclerosis: diagnostic and therapeutic implications. *J Neurovirol* **13**, 347–352.

Wahl, A., Linnstaedt, S. D., Esoda, C., Krisko, J. F., Martinez-Torres, F., Delecluse, H. J., Cullen, B. R. & Garcia, J. V. (2013). A cluster of virus-encoded microRNAs accelerates acute systemic Epstein–Barr virus infection but does not significantly enhance virus-induced oncogenesis *in vivo*. *J Virol* **87**, 5437–5446.

Wang, W., Taylor, S. L., Leisenfelder, S. A., Morton, R., Moffat, J. F., Smirnov, S. & Zhu, H. (2005). Human cytomegalovirus genes in the 15-kilobase region are required for viral replication in implanted human tissues in SCID mice. *J Virol* **79**, 2115–2123.

Wang, L. X., Kang, G., Kumar, P., Lu, W., Li, Y., Zhou, Y., Li, Q. & Wood, C. (2014). Humanized-BLT mouse model of Kaposi's sarcoma-associated herpesvirus infection. *Proc Natl Acad Sci U S A* **111**, 3146–3151.

Washburn, M. L., Bility, M. T., Zhang, L., Kovalev, G. I., Buntzman, A., Frelinger, J. A., Barry, W., Ploss, A., Rice, C. M. & Su, L. (2011). A humanized mouse model to study hepatitis C virus infection, immune response, and liver disease. *Gastroenterology* **140**, 1334–1344.

Wedderburn, N., Edwards, J. M., Desgranges, C., Fontaine, C., Cohen, B. & de Thé, G. (1984). Infectious mononucleosis-like response in common marmosets infected with Epstein–Barr virus. *J Infect Dis* **150**, 878–882.

White, R. E., Rämer, P. C., Naresh, K. N., Meixlsperger, S., Pinaud, L., Rooney, C., Savoldo, B., Coutinho, R., Bödör, C. & other authors (2012). EBNA3B-deficient EBV promotes B cell lymphomagenesis in humanized mice and is found in human tumors. *J Clin Invest* **122**, 1487–1502.

Wu, W., Rochford, R., Toomey, L., Harrington, W. J., Jr & Feuer, G. (2005). Inhibition of HHV-8/KSHV infected primary effusion lymphomas in NOD/SCID mice by azidothymidine and interferon-alpha. *Leuk Res* **29**, 545–555.

Wu, W., Vieira, J., Fiore, N., Banerjee, P., Sieburg, M., Rochford, R., Harrington, W. J., Jr & Feuer, G. (2006). KSHV/HHV-8 infection of human hematopoietic progenitor ($CD34^+$) cells: persistence of infection during hematopoiesis *in vitro* and *in vivo*. *Blood* **108**, 141–151.

Yajima, M., Imadome, K., Nakagawa, A., Watanabe, S., Terashima, K., Nakamura, H., Ito, M., Shimizu, N., Honda, M. & other authors (2008). A new humanized mouse model of Epstein–Barr virus infection that reproduces persistent infection, lymphoproliferative disorder, and cell-mediated and humoral immune responses. *J Infect Dis* **198**, 673–682.

Yajima, M., Imadome, K. I., Nakagawa, A., Watanabe, S., Terashima, K., Nakamura, H., Ito, M., Shimizu, N., Yamamoto, N. & Fujiwara, S. (2009). T cell-mediated control of Epstein–Barr virus infection in humanized mice. *J Infect Dis* **200**, 1611–1615.

JVI Journals.ASM.org

Human Herpesvirus 6A Infection and Immunopathogenesis in Humanized Rag2$^{-/-}\gamma c^{-/-}$ Mice

Anne Tanner,[a] Stephanie A. Carlson,[a] Masatoshi Nukui,[b] Eain A. Murphy,[b] Bradford K. Berges[a]

Department of Microbiology and Molecular Biology, Brigham Young University, Provo, Utah, USA[a]; Department of Molecular Genetics, Lerner Research Institute, Cleveland Clinic, Cleveland, Ohio, USA[b]

Although serious human diseases have been correlated with human herpesvirus 6A (HHV-6A) and HHV-6B, the lack of animal models has prevented studies which would more definitively link these viral infections to disease. HHV-6A and HHV-6B have recently been classified as two distinct viruses, and in this study we focused specifically on developing an *in vivo* model for HHV-6A. Here we show that Rag2$^{-/-}\gamma c^{-/-}$ mice humanized with cord blood-derived human hematopoietic stem cells produce human T cells that express the major HHV-6A receptor, CD46. Both cell-associated and cell-free viral transmission of HHV-6A into the peritoneal cavity resulted in detectable viral DNA in at least one of the samples (blood, bone marrow, etc.) analyzed from nearly all engrafted mice. Organs and cells positive for HHV-6A DNA were the plasma and cellular blood fractions, bone marrow, lymph node, and thymic samples; control mice had undetectable viral DNA. We also noted viral pathogenic effects on certain T cell populations. Specific thymocyte populations, including CD3$^-$ CD4$^+$ CD8$^-$ and CD3$^+$ CD4$^-$ cells, were significantly modified in humanized mice infected by cell-associated transmission. In addition, we detected significantly increased proportions of CD4$^+$ CD8$^+$ cells in the blood of animals infected by cell-free transmission. These findings provide additional evidence that HHV-6A may play a role in human immunodeficiencies. These results indicate that humanized mice can be used to study HHV-6A *in vivo* infection and replication as well as aspects of viral pathogenesis.

Human herpesvirus 6 (HHV-6) is a member of the betaherpesvirus subfamily and was identified in 1986 (1). Recently this virus has been reclassified as two distinct variants, HHV-6A and HHV-6B, based upon differences in tropism, disease, and epidemiology. These two variants have an overall nucleotide identity of 90% (2, 3), and serological assays to differentiate the variants are in development (4). The main cellular receptor for HHV-6A is CD46, which is expressed on all nucleated cells (5). CD134 has recently been identified as a cellular receptor for HHV-6B (6). While HHV-6B infection is ubiquitous in humans and is known to cause roseola infantum (7), the prevalence of HHV-6A and its role in human disease are poorly understood. HHV-6 has been implicated in diseases that include multiple sclerosis (8–10), encephalitis, graft-versus-host disease (11, 12), other clinical complications of solid-organ transplants and hematopoietic stem-cell transplants (13, 14), drug-induced hypersensitivity syndrome (15, 16), malignancies, myocarditis, and cardiomyopathy (17, 18). HHV-6A has an impact upon human T cell populations (19) and can enhance human immunodeficiency virus type 1 (HIV-1) replication (20). HHV-6A infects helper T cells, as does HIV-1, and HHV-6A has been suggested as a potential cofactor in AIDS progression (18, 20–22).

A variety of animal models have been explored for HHV-6 studies but with limited success. Early reports indicated that HHV-6A was able to replicate in T cells isolated from chimpanzees (23) and pigtailed macaques (24). More recent reports have shown that nonhuman primate (NHP) models exhibit signs of disease following infection with HHV-6. Leibovitch et al. recently showed that common marmosets can be infected with HHV-6A and that infection is accompanied by neurological symptoms (25). Lusso et al. demonstrated that HHV-6A replicates *in vivo* in pigtailed macaques and that coinfection of macaques with HHV-6A and simian immunodeficiency virus (SIV) resulted in faster depletion of CD4$^+$ T cells (22). The requirement for specialized facilities and the expenses involved in NHP research have been detrimental to further studies.

A small-animal model of HHV-6 infection would allow for further investigation of viral pathogenesis without the costs and facilities required for NHP research. The viral target cells in humanized mice are human immune cells; hence, viral infection in humanized mice may be more reflective of human infection than infection in NHP due to differences in human and NHP genetics. Additionally, humanized mice can be infected with HIV-1, as opposed to the genetically distinct SIV isolates used in NHP models. Humanized mice infected with HIV-1 manifest symptoms of AIDS (26) for studies of HHV-6A as a cofactor in AIDS progression.

Here we report on the use of a newer generation of humanized mice to study HHV-6A replication and pathogenesis *in vivo*. Rag2$^{-/-}\gamma c^{-/-}$ mice (RAG-hu mice) are engrafted with human hematopoietic stem cells (HSCs) and undergo multilineage hematopoiesis to produce a variety of human blood cell types which are dispersed throughout the lymphoid and nonlymphoid organs. These mice (and other similar HSC-humanized mouse models) have been shown to support replication and viral pathogenesis after challenge with the herpesviruses Epstein-Barr virus (EBV) (27–30), Kaposi's sarcoma-associated herpesvirus (KSHV) (31, 32), and human cytomegalovirus (hCMV) (33). Here RAG-hu mice were challenged with recombinant HHV-6A expressing green fluorescent protein (GFP) via either cell-free or cell-associ-

Received 7 June 2013 **Accepted** 29 August 2013
Published ahead of print 4 September 2013
Address correspondence to Bradford K. Berges, brad.berges@gmail.com.

doi:10.1128/JVI.01556-13

ated transmission. Our findings show that viral DNA is detectable in blood and lymphoid organs for up to 8 weeks after infection. Viral DNA was detected in the plasma, blood cells, thymus, lymph nodes, and bone marrow; although no single mouse tested positive for viral DNA in all of these compartments, 11 of 12 mice were positive in at least one. Specific thymocyte populations were found to be significantly modified in animals infected for longer periods (and via cell-associated transmission), while animals infected via cell-free transmission showed a significant increase in $CD4^+$ $CD8^+$ cells in blood. These findings suggest that humanized mice represent a new *in vivo* model to study HHV-6A replication and immunopathogenesis.

MATERIALS AND METHODS

Cells. Human cord blood samples were obtained with permission from the University of Colorado Cord Blood Bank. The Institutional Review Board does not require a protocol for human cord blood because samples are shipped without patient identifiers. HSCs were purified from human cord blood based upon the CD34 marker, using an EasySep human cord blood CD34-positive selection kit (StemCell Technologies). Cells were cultured for 2 days in Iscove's modified Dulbecco's medium (IMDM; Invitrogen) supplemented with 10% fetal calf serum (FCS) and 10 ng/ml each of human interleukin-3 (IL-3), IL-6, and stem cell factor (SCF) (R&D Systems).

Virus propagation. Bacterial artificial chromosome (BAC)-derived HHV-6A, strain U1102, was previously engineered to express GFP (34). BAC-derived HHV-6A DNA was isolated from overnight *Escherichia coli* cultures grown at 32°C in LB containing chloramphenicol (15 μg/ml) and purified using NucleoBond PC 100 columns (Clontech) per the manufacturer's protocols. HHV-6A BAC DNA (5 μg) and 1 μg of the human cytomegalovirus pp71-expressing plasmid pCGN1-pp71 (35) were transfected into 5×10^6 Jjhan cells with transfection reagent "V," utilizing a Nucleofector instrument (Lonza AG) per the manufacturer's protocols. After transfection, the cells were maintained in 3 ml RPMI medium containing 8% fetal bovine serum (Sigma) and supplemented with 100 U/ml each of penicillin and streptomycin. After 5 to 7 days, the medium was changed and supplemented with 20 ng/ml tetradecanoyl phorbol acetate (TPA; Sigma) and 3 mM sodium butyrate (Sigma) for 24 h. Cells were washed 3 times with phosphate-buffered saline (PBS) to remove the TPA and sodium butyrate and cocultured with an equal number of HSB-2 cells that were prestimulated for 24 h with 2 pg/ml IL-2 (Sigma) and 5 ng/ml phytohemagglutinin (PHA; Sigma). Fresh prestimulated HSB2 cells were added every 4 to 6 days to allow accumulation of the virus by cell-to-cell spread.

To isolate virus, we pelleted the cultures by low-speed centrifugation and reserved the supernatants. Infected cells were resuspended in 10 ml of medium and sonicated to release virus from infected cells. The medium was then cleared of cellular debris, and the supernatant was added to the reserved medium. Virus was then purified by ultracentrifugation through a 20% sorbitol cushion in a SW 28 rotor for 90 min at 53,000 × *g*. The resulting pellet was resuspended in medium supplemented with 1.5% bovine serum albumin (BSA), and aliquots were stored at −80°C following snap-freezing in liquid nitrogen.

Determination of virus titers. Titers of HHV-6A were calculated using standard 50% tissue culture infective dose ($TCID_{50}$) assays (36). Briefly, Jjhan cells were plated onto a 96-well plate at 1×10^5 cells per well and incubated overnight at 37°C. Aliquots of HHV-6A were thawed at 37°C and briefly sonicated. The stock was serially diluted in 10-fold increments and used to inoculate Jjhan cells. The cultures were incubated in a 37°C incubator with 5% CO_2 for 10 to 14 days. GFP-positive (GFP^+) wells were scored to determine the titers of the stock.

Animals. BALB/c-$Rag2^{-/-}\gamma c^{-/-}$ mice were humanized by engraftment with $CD34^+$ human HSCs purified from human umbilical cord blood as described previously (37). Mice were maintained in a specific-pathogen-free room at the Brigham Young University Central Animal Care Facility. These studies have been reviewed and approved by the Institutional Animal Use and Care Committee (protocol 120101). Briefly, 1- to 5-day-old mice were conditioned by irradiation with 350 rads and then injected intrahepatically with 2×10^5 to 5×10^5 human $CD34^+$ cells. Mice were screened for human cell engraftment at 8 weeks postengraftment. Peripheral blood was collected by tail bleed and stained with antibodies specific to either human or mouse CD45. Fluorescence-activated cell sorter (FACS) analysis was performed to determine percent peripheral blood engraftment of human cells (38, 39).

Preparation of carrier cells for viral transmission to humanized mice. Fresh CD34-depleted cord blood mononuclear cells (1×10^6) were cultured in basal medium (RPMI 1640 plus 10% FCS plus 1× penicillin-streptomycin) and stimulated with PHA (20 μg/ml) for 48 h followed by IL-2 (100 units/ml) for 10 days. We chose to use these cells because (i) they are routinely used for HHV-6A infections and (ii) they are readily available in our lab. DNA extraction and quantitative PCR (Q-PCR) were performed on a portion of the cells to verify lack of endogenous HHV-6A. Cells (1.7×10^6) were infected with 3.3×10^5 infectious units (i.u.) of a recombinant strain of HHV-6A expressing GFP under the CMV immediate early (IE) promoter and in the U1102 strain background (34) (hereafter referred to as HHV-6A) plus 5 μg/ml Polybrene (Sigma), and mock-infected cells were resuspended in basal medium with Polybrene. Samples were infected for 2 h and shaken every 30 min. The final multiplicity of infection (MOI) was 0.02. After incubation, cells were resuspended in 3 ml basal medium and plated on a 6-well plate. IL-2 was added, and cells were incubated for 48 h. FACS analysis was performed on infected and mock-infected cells to detect and quantify HHV-6A-infected cells prior to mouse infection. GFP was used to identify infected cells, and samples were stained with anti-human CD3, CD4, and CD8 antibodies (see below) to characterize infected cell types.

HHV-6A transmission to humanized mice. In the cell-associated viral-transmission study, 1×10^5 cells (of which ~20% were GFP^+) in 100 μl serum-free RPMI 1640 were injected intraperitoneally (i.p.) into mice. Uninfected mice were injected similarly with uninfected cells in the same medium as that for infected mice. In the cell-free viral-transmission study, cell-free HHV-6A was thawed and immediately diluted in RPMI 1640 (no serum or antibiotics). One hundred microliters of cell-free virus (4.3×10^5 i.u./mouse) was injected i.p. into mice.

Measurement of blood viral load. Blood was collected by tail bleed for 6 weeks. Seventy microliters of whole blood was collected per time point, and the blood was usually centrifuged to separate cellular and plasma fractions. DNA was then extracted with a QIAamp DNA blood minikit (Qiagen). Q-PCR was performed using an Applied Biosystems StepOne machine to detect and quantify the presence of viral genomes using a published assay (40). Serial dilutions (10-fold) of a plasmid containing the target HHV-6A sequence were used as copy number standards; the sensitivity of the assay was previously reported to be 10 DNA copies (40). The limit of detection of the assay was 1,000 normalized copies in plasma/ml and 400 copies in bone marrow, lymph node, thymus, and spleen (see below).

Organ collection and measurement of viral load in organs. In the cell-associated study, mice were sacrificed at time points ranging from 6.5 to 9.5 weeks postinfection (p.i.) (Table 1), and lymphoid organs (thymus, bone marrow, lymph nodes, and spleen) were collected. Bone marrow was extracted from both femurs. The thymus was divided in half for Q-PCR or FACS analysis in one infected and one mock-infected animal. Subsequently, single-cell suspensions were made and divided in half in order to perform both FACS and Q-PCR analyses. For Q-PCR, DNA was extracted using a QIAamp DNA blood minikit and analyzed by Q-PCR as described above. Similar methods were used for organ collection in the cell-free viral-transmission study except that mice were sacrificed at 1 week p.i.

FACS analysis. Anti-human CD45 (eBioscience) and anti-mouse CD45 (eBioscience) were used for screening mice preinfection to deter-

TABLE 1 Characteristics of humanized mice used for HHV-6A infections[a]

Mouse no.	Injected with HHV-6A	Age (mo)	Engraftment (%)	Irradiated	Sacrificed (wk)
33	+, CA	2	0	−	9.5
34	+, CA	2	0	−	6.5
35	+, CA	2	0	−	9.5
36	+, CA	2	0	−	9.5
685	+, CA	3	0	+	9.5
686	+, CA	3	0	+	9.5
687	+, CA	3	0	+	9.5
688	+, CA	3	0	+	6.5
708	+, CA	5	29	+	8
3089	+, CA	4	58	+	8
3090	+, CA	4	56	+	8
3092	+, CA	4	71	+	6.5
3099	+, CA	5	36	+	8
3100	+, CA	5	49	+	8
698	−, M	3	41	+	8
3095	−, M	4	42	+	6.5
3096	−, M	4	32	+	8
3098	−, M	4	39	+	8
759	−, U	6	18	+	NA
767	−, U	6	43	+	NA
769	−, U	6	68	+	NA
37	+, CF	2	0	−	1
38	+, CF	2	0	−	1
39	+, CF	2	0	−	1
40	+, CF	2	0	−	1
711	+, CF	7	38	+	1
715	+, CF	7	75	+	1
755	+, CF	4	46	+	1
756	+, CF	4	36	+	1
778	+, CF	5	48	+	1
781	+, CF	5	35	+	1

[a] CA, cell-associated virus; M, mock-infected cells; U, uninfected; CF, cell-free virus; NA, not applicable.

mine percent engraftment. Anti-human CD3 (BioLegend), anti-human CD4 (eBioscience), anti-human CD8 (eBioscience), and anti-human CD46 (eBioscience) were used in FACS analyses of regular tail bleeds and on the harvested organs. Samples were run on a BD FACSCanto flow cytometer and analyzed with Summit version 4.3 software.

RESULTS

RAG-hu mice produce cells that express the HHV-6A receptor. RAG-hu mice were engrafted with human $CD34^+$ hematopoietic stem cells isolated from cord blood as described previously (37) and as outlined in Materials and Methods. Mice were screened for human cell engraftment at 8 weeks postreconstitution by FACS analysis of peripheral blood for the panleukocyte markers human CD45 (hCD45) and mouse CD45 (mCD45).

CD46 is a known receptor involved in HHV-6A entry (5) and serves as an inhibitor of complement-mediated cell lysis. CD46 is thought to be expressed in all nucleated human cells but in mice is expressed only in testis (41), which may explain murine resistance to HHV-6A infection. Thus, we stained cells from RAG-hu mice for the presence of CD46 in order to determine if this animal model might be useful for HHV-6A research. We found that RAG-hu mice produce human $CD46^+$ cells in the blood, thymus, and bone marrow (Fig. 1). $CD3^+$ T cells were $CD46^+$ as well as some $CD3^-$ cells that were not characterized further.

Infection of RAG-hu mice with HHV-6A. Initial attempts at HHV-6A infection used cell-associated virus because HHV-6 is known to be a highly cell-associated virus (42) and because a recent study using the related hCMV in humanized mice was unable to achieve infection with cell-free virus but was successful using infected fibroblasts as carrier cells (33). We also attempted cell-free viral transmission with a high-titer stock of HHV-6A to determine if this mechanism would also be viable for inoculation of humanized mice. Detection of cell-free transmission provides additional evidence for the permissiveness of *in vivo* infection because in cell-associated transmission the input virus may subsequently be detected whether transmission to the graft takes place or not.

In the cell-associated transmission study, mice were divided into 5 groups: (i) nonhumanized $Rag2^{-/-}\gamma c^{-/-}$ mice, never irradiated, inoculated with infected cells, (ii) 0%-engrafted $Rag2^{-/-}\gamma c^{-/-}$ mice, irradiated, inoculated with infected cells, (iii) >30%-engrafted $Rag2^{-/-}\gamma c^{-/-}$ mice inoculated with infected cells, (iv) >30%-engrafted $Rag2^{-/-}\gamma c^{-/-}$ mice inoculated with uninfected cells, and (v) engrafted $Rag2^{-/-}\gamma c^{-/-}$ mice, not inoculated, uninfected (Table 1). Animals with >30% peripheral blood engraftment [defined as ($hCD45^+$ cells)/($hCD45^+$ cells + $mCD45^+$ cells)] were used in order to ensure that the human immune system was sufficient to support viral infection. Group 1 served as a control for determining if HHV-6A could infect and/or persist in nonhumanized immunocompromised mice. Group 2 served as a control for determining if HHV-6A could infect mice that had been sublethally irradiated (thus becoming further immunocompromised) and reconstituted but had undetectable engraftment. Group 3 was the experimental group to determine if HHV-6A could infect engrafted RAG-hu mice. Groups 4 and 5 served as uninfected controls. Cells used for viral transmission were not donor matched with cell samples used to engraft, similar to a previous study where successful hCMV transmission was accomplished with allogeneic human fibroblasts in a related humanized-mouse model (33). In the cell-free transmission study, mice were divided into 2 groups: (i) nonhumanized, never irradiated, inoculated with cell-free virus and (ii) >30% engrafted, inoculated with cell-free virus. Engraftment of mice in the >30% groups in both studies ranged from 30 to 75% (Table 1).

All RAG-hu mice were tested for the presence of HHV-6A DNA by Q-PCR prior to experimental infection. This verification was necessary because a low percentage of human cord blood samples (which are used to initially engraft the humanized mice) are contaminated with HHV-6A (43). All mice tested negative for HHV-6A DNA in whole-blood samples analyzed prior to cell-associated HHV-6A inoculation as did PHA-plus-IL-2-stimulated cord blood cells prior to HHV-6A infection (used as carrier cells for transmission).

Generation of infected cells for use in cell-associated transmission study. PHA- and IL-2-stimulated CD34-depleted cord blood mononuclear cells were infected with HHV-6A or uninfected for 2 h as described previously in Materials and Methods. Cells were cultured for 48 h p.i. (with green cells present upon visual inspection by fluorescence microscopy at 20 h p.i. in infected samples; data not shown). We observed an increase in cell size in the infected group compared to cell size in the uninfected group, which is a common cytopathic effect of HHV-6A (data not shown). We also observed a $CD3^{low}$ $CD4^+$ subgroup in the infected sample (Fig. 2D) that was not present in the uninfected

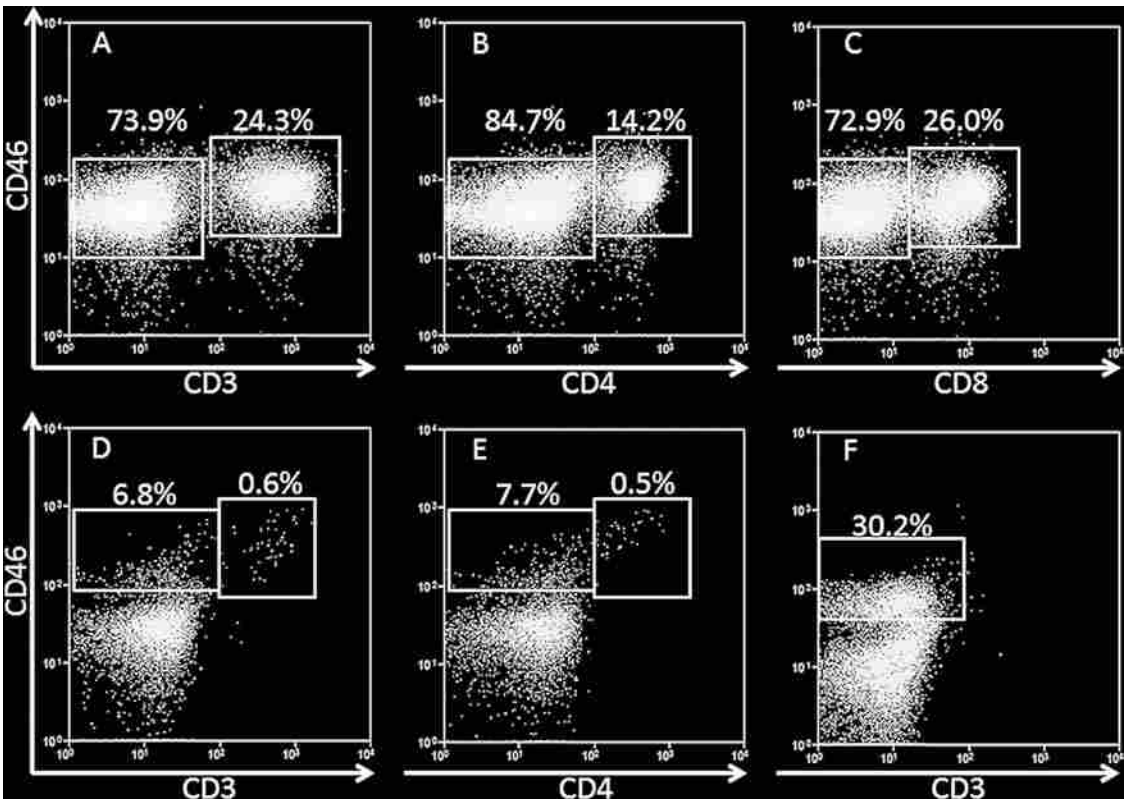

FIG 1 Humanized mice harbor human cells that express the HHV-6A receptor. (A to C) RAG-hu thymocytes are $CD46^+$, including $CD3^+$ T cells and the two major subsets of T cells (A), $CD4^+$ helper T cells (B), and $CD8^+$ cytotoxic T cells (C). (D and E) RAG-hu blood also contains $CD46^+$ cells, some of which are also $CD3^+$ (D) and $CD4^+$ (E). (F) The bone marrow also harbors $CD46^+$ cells, but only a minimal number of T cells were detected in this organ.

sample (Fig. 2C); downregulation of CD3 is also common upon HHV-6A infection of T cells (44). Approximately 20% of lymphocytes were GFP^+ in the infected sample (Fig. 2B) immediately prior to injection into RAG-hu mice, and there was a low background of GFP expression in the uninfected sample (Fig. 2A).

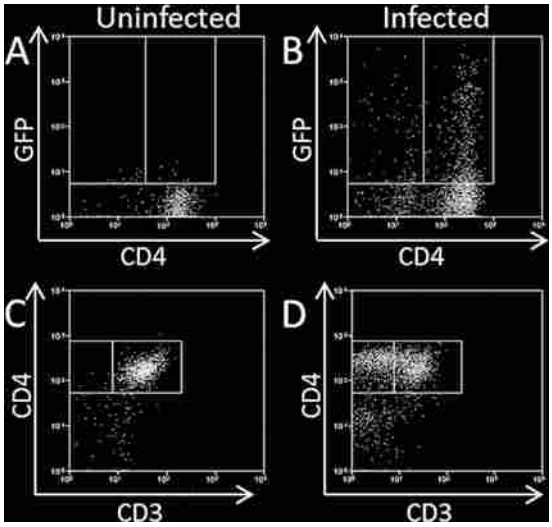

FIG 2 HHV-6A-infected carrier cells used in cell-associated transmission to humanized mice. (A to D) Flow cytometry of uninfected (A and C) and HHV-6A-infected (B and D) cells prior to injection into RAG-hu mice. (A and B) Detection of GFP expression. (C and D) Analysis of CD3 and CD4 expression.

HHV-6A DNA detection in blood and lymphoid organs. All animals were bled regularly, and DNA was extracted for Q-PCR analysis of the viral genome from different blood fractions (plasma, blood cell, or whole blood, as indicated in Tables 2 and 3). In addition, animals were sacrificed at various time points (Table 1) in order to examine various organs for viral genome detection and/or to analyze cellular populations for GFP expression and for depletion or enrichment of specific T cell populations. Viral DNA was detected by Q-PCR in nearly all animals at at least one time point in the >30%-engrafted, HHV-6A-inoculated

TABLE 2 Viral DNA detected in blood and lymphoid organs 1 week after cell-free infection[a]

Mouse no.	Mouse group	Blood (PF, BC)	BM	Thy	Spl
37–40	NH, I	−	−	NT	−
711	H, I	14,000 (BC)	110,000	−	−
715	H, I	13,000 (PF)	3,600	NT	−
755	H, I	−	42,000	−	−
756	H, I	−	6,200	−	−
778	H, I	−	1,400	NT	−
781	H, I	−	650	NT	−

[a] NH, nonhumanized; H, humanized; I, infected; PF, plasma fraction; BC, blood cell fraction; BM, bone marrow; Thy, thymus; Spl, spleen; −, below limit of detection; NT, not tested. Results for plasma and blood cell fractions are reported in DNA copies/ml, for BM in DNA copies per femur, for Thy in DNA copies per half thymus, and for Spl in DNA copies per one-third spleen. Blood fractions analyzed are indicated in the column headings.

TABLE 3 Viral DNA detected in blood after cell-associated infection[a]

Mouse no.	Mouse group	1 wk (PF)	2 wk (WB)	3 wk (PF)	4 wk (PF, BC)	5 wk (PF)	6 wk (PF, BC)
33–36	NH, I	−	−	−	−	−	−
685–688	NH, I	−	−	−	−	−	−
698, 3095, 3096, 3098	H, M	−	−	−	−	−	−
708	H, I	−	−	−	−	−	−
3089	H, I	3,200	5,200	68,000	−	−	1,900, −
3090	H, I	−	−	−	−	−	−, 46,000
3092	H, I	−	−	33,000	130,000, 290,000	2,100	−, 77,000
3099	H, I	−	−	−	15,000, −	1,200	−
3100	H, I	−	−	−	−, 36,000	1,200	−, 9,700

[a] NH, nonhumanized; H, humanized; I, infected; M, mock-infected; PF, plasma fraction; BC, blood cell fraction; WB, whole blood; −, below limit of detection. Results for plasma and blood cell fractions are reported in DNA copies/ml. Not all samples were analyzed by Q-PCR each week. Blood fractions analyzed are indicated in the column headings.

groups (both cell-free transmission and cell-associated transmission) (Tables 2, 3, and 4).

In the cell-free transmission study, viral DNA was detected in the bone marrow of all 6 >30%-engrafted, HHV-6A-inoculated mice, while no viral DNA was detectable in the nonhumanized mice ($n = 4$) (Table 2). Two of the >30%-engrafted, HHV-6A-inoculated mice had detectable viral DNA present in the blood, whereas no viral DNA was detected in the blood of infected, unengrafted mice. No viral DNA was detected in analyzed thymic ($n = 3$) or splenic ($n = 6$) tissues from RAG-hu mice infected by cell-free transmission. All samples in the cell-free transmission study were analyzed at the time of sacrifice (1 week postinfection).

In the cell-associated transmission study, HHV-6A DNA was detected by Q-PCR in plasma and cellular fractions of blood (Table 3) and in the bone marrow, lymph node, and thymus but not in spleen (Table 4). In the >30%-engrafted, HHV-6A-inoculated group, viral DNA was detected in the plasma fraction in 4 of 6 mice, in the blood cell fraction in 3 of 6 mice tested, and in 1 of 6 whole-blood samples tested. In addition, 2 of 6 mice in this group had detectable viral DNA in the bone marrow, and the thymic and lymph node samples from the lone mouse tested from this group had detectable viral DNA (Table 4). We noted that viral DNA was detected mostly in the plasma from weeks 1 to 5 and that plasma viral load decreased in copy number after week 4 and in frequency of detection after week 5. Four of 18 samples collected from engrafted, humanized infected mice during the first 3 weeks of the cell-associated transmission experiment were positive for viral DNA, while 15 of 38 samples tested from week 4 onward were positive and had generally higher levels of viral DNA. In total, 5 of 6 mice in the >30%-engrafted, HHV-6A-inoculated group had viral DNA present in blood or organs. Mouse 708 had undetectable viral DNA in blood and lymphoid organs, but this animal was inadvertently inoculated with about half of the volume of infected carrier cells into the subcutaneous space and the other half into the intended intraperitoneal cavity. No viral DNA was detected in any of the three control groups in the cell-associated transmission study.

TABLE 4 Viral DNA detected in lymphoid organs from mice sacrificed 6 1/2 to 9 1/2 weeks after cell-associated infection

Mouse no.	Mouse group	Bone marrow	Thymus	Lymph node	Spleen
33–36	NH, I	−	NT	NT	−
685–688	NH, I	−	NT	NT	−
698	H, M	−	NT	NT	−
3095	H, M	−	−	−	−
3096	H, M	−	NT	NT	−
3098	H, M	−	NT	NT	−
708	H, I	−	NT	NT	−
3089	H, I	9,200	NT	NT	−
3090	H, I	−	NT	NT	−
3092	H, I	−	8,100	2,800	−
3099	H, I	−	NT	NT	−
3100	H, I	2,700	NT	NT	−

NH, nonhumanized; H, humanized; I, infected; M, mock-infected; −, below limit of detection; NT, not tested. Results for bone marrow are reported in DNA copies per femur, for thymus in DNA copies per half thymus, for lymph node in DNA copies per node, and for spleen in DNA copies per one-third spleen.

Detection of HHV-6A-infected cells *in vivo* via GFP expression. We attempted to detect GFP^+ cells as an additional way to verify successful infection in both the cell-associated transmission and cell-free transmission studies. However, no GFP^+ cells were detected in the cell-associated study in blood samples collected weeks 1 and 3 postinfection and analyzed by flow cytometry. Additionally, no GFP^+ cells were detected when lymphoid organs were collected at the time of sacrifice. A single mesenteric lymph node sample (mouse 715) from the cell-free transmission study was found to harbor GFP^+ cells when animals were sacrificed and analyzed at 1 week postinfection (data not shown). $CD4^+$ cells (0.04%) in the lymph node were GFP^+, while 0.28% of $CD8^+$ cells were GFP^+. Of the $CD4^+$ GFP^+ cells, most were $CD3^-$ (95%). Of the GFP^+ cells detected in this sample, 4% were $CD3^+$, 55% were $CD4^+$, and 7% were $CD8^+$.

Thymocyte populations are significantly changed in HHV-6A-infected RAG-hu mice. Previous work with humanized mice (SCID-hu *thy/liv* model) infected with HHV-6A or HHV-6B indicated that these viruses are capable of modifying thymic populations after direct viral inoculation into the thymic graft (19). We thus analyzed thymic populations taken from RAG-hu mice infected by either cell-associated or cell-free transmission. Animals infected by cell-free transmission had undetectable levels of viral DNA in the thymus at 1 week postinfection (3 of 3 tested) (Table 2), and their thymocyte populations were similar to those of uninfected animals (data not shown). Thus, we focused our thymocyte analysis on animals infected by the cell-associated transmission route, noting that these animals were also infected for a longer duration. RAG-hu mice infected by cell-associated transmission did exhibit significant shifts in thymic populations (Fig. 3). We noted a significant decrease ($P = 0.05$) in CD3 expression on $CD4^+$ thymocytes, with means of 3.9% and 17.9% of thymocytes that were $CD3^+$ $CD4^-$ in infected ($n = 4$) and uninfected

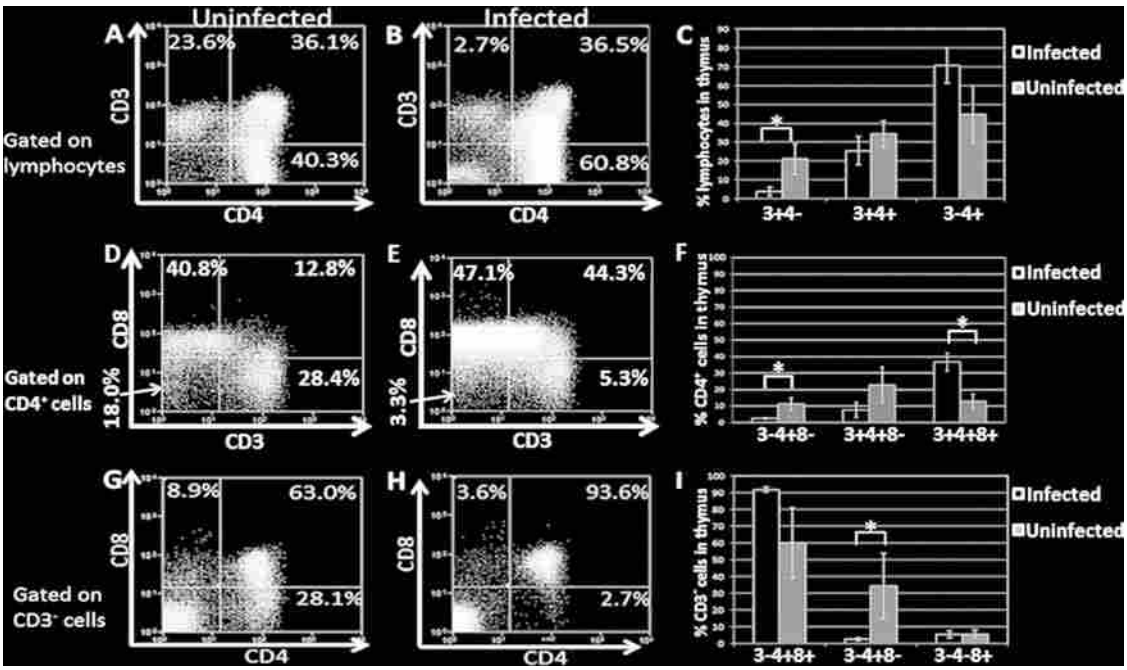

FIG 3 Depletion of specific thymocyte populations in HHV-6A-infected mice. RAG-hu mice infected with HHV-6A by cell-associated viral transmission showed modulation of specific thymocyte populations. (A to C) The $CD3^+$ $CD4^-$ population was depleted, while the $CD3^-$ $CD4^+$ population was increased in infected animals. Mouse 3095 (uninfected) is shown in panel A and mouse 3099 (infected) is shown in panel B. Samples were gated on a lymphocyte gate. n = 4 infected; n = 6 uninfected. (D to F) The $CD3^-$ $CD4^+$ $CD8^-$ and $CD3^+$ $CD4^+$ $CD8^-$ populations were depleted and the $CD3^+$ $CD4^+$ $CD8^+$ population was increased when analysis was gated upon $CD4^+$ cells. Mouse 3098 (uninfected) is shown in panel D and mouse 3099 (infected) is shown in panel E. n = 3 infected; n = 5 uninfected. (G to I) The $CD3^-$ $CD4^+$ $CD8^+$ population expanded and the $CD3^-$ $CD4^+$ $CD8^-$ population was reduced when analysis was gated on the $CD3^-$ population. Mouse 3098 (uninfected) is shown in panel G and mouse 3089 (infected) is shown in panel H. n = 3 infected; n = 5 uninfected. When data analysis was performed, the two single-positive and the double-positive cell populations were normalized to 100%. Mouse 708 was excluded from these analyses because no viral DNA was detected in that mouse at any time point and we concluded that the mouse likely was not successfully infected. Standard errors are indicated; Student's t test was used for statistical analysis. *, $P \leq 0.05$.

(n = 6) groups, respectively. This is similar to a previous report indicating that HHV-6 can downregulate CD3 expression (45). We also detected a significant loss (P = 0.04) of intrathymic T progenitor cells ($CD3^-$ $CD4^+$ $CD8^-$), with means of 2.5% for infected mice (n = 3) and 11.3% for uninfected mice (n = 5) when gating on the $CD4^+$ population. When analyzing this same population on a $CD3^-$ gate, we again found a significant depletion (P = 0.03), with means of 2.7% for infected mice (n = 3) and 32.2% for uninfected mice (n = 5). We also detected a significant (P = 0.02) increase in the number of $CD3^+$ $CD4^+$ $CD8^+$ thymocytes, with means of 36.6% for infected mice (n = 3) and 12.8% for uninfected mice (n = 5). The $CD3^-$ $CD4^+$ $CD8^+$ population appeared to increase in infected animals, but the difference was not significant (P = 0.08), and the $CD3^+$ $CD4^+$ $CD8^-$ population appeared to decrease in infected animals, but the difference was not significant (P = 0.25).

Detection of $CD4^+$ $CD8^+$ T cells in HHV-6A-infected RAG-hu blood. Previous studies have indicated that HHV-6A infection can induce CD4 expression on primary human CD8 T cells *in vitro* (46). Thus, we analyzed samples by FACS for the presence of $CD4^+$ $CD8^+$ T cells. We detected significantly increased ratios (P = 0.04) of $CD3^+$ $CD4^+$ $CD8^+$ cells in the blood of RAG-hu mice infected by the cell-free transmission route (Fig. 4). This population represented a mean of 8.8% of $CD3^+$ T cells, while in uninfected humanized mice these cells were 3.1% of all T cells. $CD4^+$ $CD8^+$ cells are normally rare in human blood, with one report showing an average of 2.91% of $CD4^+$ $CD8^+$ cells in normal human blood (n = 10) (47), which is similar to our results for uninfected humanized mouse blood. Other blood T cell populations, including $CD3^+$ $CD4^-$ $CD8^+$, $CD3^+$ $CD4^+$ $CD8^-$, $CD3^-$ $CD4^+$ $CD8^+$, $CD3^-$ $CD4^+$ $CD8^-$, and $CD3^-$ $CD4^-$ $CD8^+$ populations, were not significantly altered in infected samples.

DISCUSSION

Here we have shown that RAG-hu mice are susceptible to infection with HHV-6A by either cell-associated or cell-free transmission. Viral DNA was detected in blood (cellular and plasma fractions), bone marrow, lymph node, and thymic tissues (Tables 2, 3, and 4), although no single mouse tested positive for viral DNA in all of these compartments, as mentioned previously. Following cell-associated transmission, viral DNA was detectable for up to 8 weeks postinfection, indicating a persistent infection. No viral DNA was detected in any of the three control groups in the cell-associated study, indicating that viral transmission from the infected carrier cells to the originally engrafted cells and subsequent replication were successful because no viral DNA was detectable in either blood or lymphoid organs in control mice without an HSC graft. Irradiated but nonengrafted animals were included as a control because of the higher level of murine immunodeficiency of irradiated mice, and they also had undetectable viral DNA after transmission. Some animals in the cell-associated transmission study had detectable viral DNA at early time points and not later,

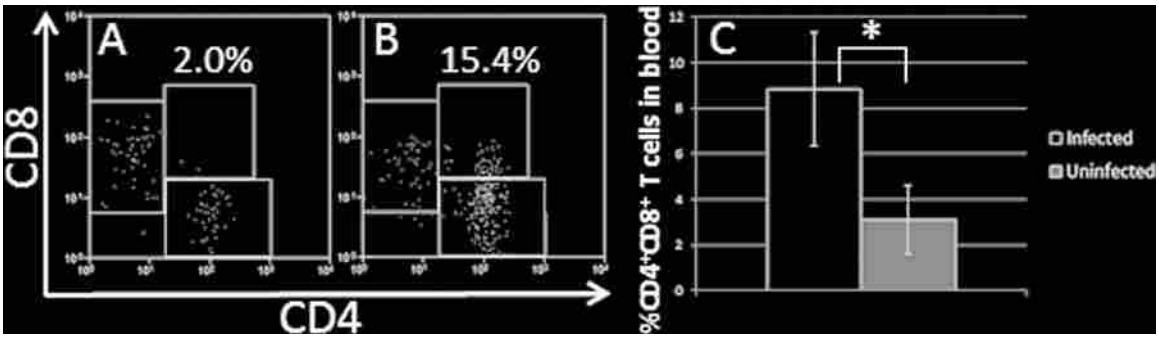

FIG 4 Detection of $CD4^+$ $CD8^+$ T cells in blood of HHV-6A-infected mice. (A to C) Levels of $CD4^+$ $CD8^+$ T cells in blood were quantified by flow cytometry. (A) Uninfected mouse. (B) HHV-6A-infected mouse 715 (cell-free transmission and highest amount of $CD4^+$ $CD8^+$ cells). All samples were first gated on CD3. (C) Mean levels of $CD4^+$ $CD8^+$ cells were quantified in cell-free-infected mice ($n = 6$) and uninfected mice ($n = 4$). Standard errors are indicated; Student's t test was used for statistical analysis. *, $P \leq 0.05$.

and some animals had no detectable DNA at early time points but detectable DNA at later time points. We attribute this to a relatively high limit of detection in the assay, because only small blood samples can be obtained from mice. We noted that plasma viral DNA levels peaked at 3 to 4 weeks postinfection, but levels decreased to near the level of detection in plasma by 5 weeks and only a single animal had detectable viral DNA in the plasma at 6 weeks. Viral DNA was still detected in the cellular fraction of blood at 6 weeks in three animals, while plasma viral DNA was found in a single mouse at that time point, potentially indicating a shift from lytic infection (extracellular DNA) to latency (intracellular DNA).

Cell-associated transmission was attempted because a similar previous experiment with hCMV was successful only with this method (33). However, cell-free transmission was successful in all 6 animals in our study. We also noted a greater tendency to detect viral DNA in the bone marrow of animals infected by cell-free transmission, but it is not clear if that finding is due to a different mode of transmission or to different sacrificial time points (1 week for cell-free transmission and 6.5 to 9.5 weeks for cell-associated transmission). We also detected a significant increase in $CD4^+$ $CD8^+$ cells in the blood of mice infected by cell-free transmission (Fig. 4). This was possibly due to CD4 upregulation in CD8 T cells, which was previously shown *in vitro* in HHV-6A-infected cells (46). When we correlated Q-PCR results for blood cells and plasma with detection of these $CD4^+$ $CD8^+$ cells, there was not a clear trend because one animal (715) had high proportions of these cells and detectable viral DNA in plasma, while other animals also had high proportions of the cells but undetectable viral DNA in either blood fraction. Another animal (711) had low proportions of the cells with only intracellular blood viral DNA. The frequent detection of this effect combined with the relatively rare detection of viral DNA in either blood fraction indicates that these cells may be uninfected by HHV-6A. These cells largely maintained CD3 expression, which also indicates a lack of infection. It is possible that HHV-6A infection promotes the release of these cells from the thymus because $CD4^+$ $CD8^+$ cells are rare outside of the thymus. However, we failed to detect viral DNA in the thymus of 3 animals tested, so if infection promotes a release of these cells from the thymus then it must occur from a distal site. There is evidence that the presence of $CD4^+$ $CD8^+$ cells in human blood is upregulated following viral infection, including after infection with persistent viruses such as the herpesvirus EBV (47).

We attempted to use GFP expression from a recombinant virus to further demonstrate successful infection. However, the only animal with detectable GFP^+ cells was mouse 715 from the cell-free transmission group, and those cells were from the mesenteric lymph node. FACS analysis of GFP^+ cells indicated that they were mostly $CD3^-$ $CD4^+$, which is in accordance with our *in vitro* results shown in Fig. 2D and previously published data showing a tropism for $CD4^+$ T cells and a downregulation of CD3 after infection (45, 48). We later determined that the GFP cassette in this virus is driven by the CMV IE promoter (Y. Mori, personal communication). Since the cell-associated mice were sacrificed at 6.5 to 9.5 weeks p.i., it is possible that the virus was in a latent state at the time of organ collection; this hypothesis is supported by the shift from extracellular to intracellular DNA seen in blood. The activity of the CMV IE promoter in the context of a latent HHV-6A infection is currently unknown, and if that promoter is inactive during latency it may explain a lack of GFP^+ cells in any of the mice infected by cell-associated transmission.

We made the interesting observation that several thymocyte populations were altered in HHV-6A-infected animals versus those in uninfected animals (Fig. 3). These observations further support that successful viral transmission occurred, because similar findings have been reported for *in vitro* studies and for another humanized-mouse study. In those studies, CD3 depletion occurred only in infected (not in bystander) cells (19, 46, 48). Thymocyte depletion was detected only in animals infected by the cell-associated pathway, but these animals were also infected for a longer period. It is possible that virus had not trafficked to the thymus in mice infected by cell-free transmission, a finding supported by our Q-PCR data, where 0 of 3 of these thymic samples harbored viral DNA (Table 2). We noted significant depletion of the $CD3^+$ $CD4^-$ and $CD3^-$ $CD4^+$ $CD8^-$ populations in HHV-6A-infected animals. We also noted a significant increase in the $CD3^+$ $CD4^+$ $CD8^+$ subset, with a marginally significant increase in the $CD3^-$ $CD4^+$ $CD8^+$ population. The significant loss of $CD3^-$ $CD4^+$ $CD8^-$ thymocytes was similarly reported by Gobbi et al. when HHV-6A was directly inoculated into the thymic organoid of SCID-hu *thy/liv* mice (19). In contrast to that report, our results show a significant increase in the $CD3^+$ $CD4^+$ $CD8^+$ subset. These discrepancies may be explained by the use of different virus isolates, with strain GS used in that report and a recombinant isolate based upon strain U1102 used here. In addition, we have used a newer generation of humanized mice with a wider scope of human cell types and a much broader distribution in the

mouse, and we inoculated at a site distant from the thymus. Several of these thymocyte populations that were modified by infection *in vivo* can be explained by a tropism and cytopathogenicity of the virus for $CD4^+$ T cells. Additionally, the tendency of the virus to downregulate CD3 and/or to upregulate CD4 expression can also explain shifting populations (e.g., $CD3^+$ $CD4^-$ and $CD3^+$ $CD4^+$ $CD8^-$ populations expected to decrease and $CD3^-$ $CD4^+$ $CD8^+$ population expected to increase). The $CD3^+$ $CD4^+$ $CD8^-$ population was previously shown to be more infectible with HHV-6A than other thymocyte populations (19). We have proposed that in the cell-associated study the virus was predominantly latent at the time points at which the thymic samples were collected. We are not aware of any studies documenting CD3 downregulation or CD4 upregulation in latently infected primary cells, so it is currently not clear if lytic replication is required for these effects upon host cell gene expression.

We and others have previously shown that RAG-hu mice are also highly susceptible to HIV-1 infection (26, 38, 49, 50). Our current findings indicate higher proportions of $CD4^+$ cells in HHV-6A-infected animals, similar to those shown by Lusso et al. *in vitro*, where they showed that HHV-6A-infected $CD8^+$ T cells began to express CD4 and were able to replicate HIV-1 (46). If HHV-6A is able to convert $CD8^+$ T cells to become infectible by HIV-1 *in vivo*, then those cells may be depleted by HIV-1 and/or by HHV-6A. Downregulation of CD3, as our results herein have indicated, is expected to cause immunosuppression because CD3 serves as the signaling subunit of the T cell receptor. Hence, T cells could engage the T cell receptor but not be able to respond effectively. Either of these two effects would support the hypothesis that HHV-6A is a cofactor in AIDS progression (21, 22). Our future directions include plans to perform coinfection studies of HHV-6A and HIV-1 in humanized mice in order to determine if there is a synergistic effect between the two viruses in the progression to AIDS as well as to determine if RAG-hu mice can be infected with HHV-6B.

ACKNOWLEDGMENTS

We are grateful to Yasuko Mori (National Institute of Biomedical Innovation, Osaka, Japan) for giving permission to use a recombinant strain of HHV-6A produced in her laboratory. BALB/c-Rag2$^{-/-}\gamma c^{-/-}$ mice were generously provided by Ramesh Akkina at Colorado State University.

This work was funded by a Pilot Grant award from the HHV-6 Foundation to B.K.B. This work was partially supported by National Institutes of Health grant U54 AI057160 to the Midwest Regional Center of Excellence for Biodefense and Emerging Infectious Diseases Research (MRCE) to E.A.M. A.T. was supported by the Brigham Young University Cancer Research Center and the HHV-6 Foundation.

REFERENCES

1. **Salahuddin SZ, Ablashi DV, Markham PD, Josephs SF, Sturzenegger S, Kaplan M, Halligan G, Biberfeld P, Wong-Staal F, Kramarsky B, Gallo RC.** 1986. Isolation of a new virus, HBLV, in patients with lymphoproliferative disorders. Science **234:**596–601.
2. **Dominguez G, Dambaugh TR, Stamey FR, Dewhurst S, Inoue N, Pellett PE.** 1999. Human herpesvirus 6B genome sequence: coding content and comparison with human herpesvirus 6A. J. Virol. **73:**8040–8052.
3. **Emery VC, Clark DA.** 2007. Chapter 49. HHV-6A, 6B, and 7: persistence in the population, epidemiology and transmission. *In* Arvin A, Campadelli-Fiume G, Mocarski E, Moore PS, Roizman B, Whitley R, Yamanishi K (ed), Human herpesviruses: biology, therapy, and immunoprophylaxis. Cambridge University Press, Cambridge, United Kingdom.
4. **Burbelo PD, Bayat A, Wagner J, Nutman TB, Baraniuk JN, Iadarola MJ.** 2012. No serological evidence for a role of HHV-6 infection in chronic fatigue syndrome. Am. J. Transl. Res. **4:**443–451.
5. **Santoro F, Kennedy PE, Locatelli G, Malnati MS, Berger EA, Lusso P.** 1999. CD46 is a cellular receptor for human herpesvirus 6. Cell **99:**817–827.
6. **Tang H, Serada S, Kawabata A, Ota M, Hayashi E, Naka T, Yamanishi K, Mori Y.** 2013. CD134 is a cellular receptor specific for human herpesvirus-6B entry. Proc. Natl. Acad. Sci. U. S. A. **110:**9096–9099.
7. **Yamanishi K, Okuno T, Shiraki K, Takahashi M, Kondo T, Asano Y, Kurata T.** 1988. Identification of human herpesvirus-6 as a causal agent for exanthem subitum. Lancet **i:**1065–1067.
8. **Virtanen JO, Farkkila M, Multanen J, Uotila L, Jaaskelainen AJ, Vaheri A, Koskiniemi M.** 2007. Evidence for human herpesvirus 6 variant A antibodies in multiple sclerosis: diagnostic and therapeutic implications. J. Neurovirol. **13:**347–352.
9. **Sola P, Merelli E, Marasca R, Poggi M, Luppi M, Montorsi M, Torelli G.** 1993. Human herpesvirus 6 and multiple sclerosis: survey of anti-HHV-6 antibodies by immunofluorescence analysis and of viral sequences by polymerase chain reaction. J. Neurol. Neurosurg. Psychiatry **56:**917–919.
10. **Behzad-Behbahani A, Mikaeili MH, Entezam M, Mojiri A, Pour GY, Arasteh MM, Rahsaz M, Banihashemi M, Khadang B, Moaddeb A, Nematollahi Z, Azarpira N.** 2011. Human herpesvirus-6 viral load and antibody titer in serum samples of patients with multiple sclerosis. J. Microbiol. Immunol. Infect. **44:**247–251.
11. **Appleton AL, Sviland L, Peiris JS, Taylor CE, Wilkes J, Green MA, Pearson AD, Kelly PJ, Malcolm AJ, Proctor SJ.** 1995. Human herpes virus-6 infection in marrow graft recipients: role in pathogenesis of graft-versus-host disease. Newcastle upon Tyne Bone Marrow Transport Group. Bone Marrow Transpl. **16:**777–782.
12. **Agut H.** 2011. Deciphering the clinical impact of acute human herpesvirus 6 (HHV-6) infections. J. Clin. Virol. **52:**164–171.
13. **Le J, Gantt S, AST Infectious Diseases Community of Practice.** 2013. Human herpesvirus 6, 7 and 8 in solid organ transplantation. Am. J. Transplant. **13**(Suppl 4)**:**128–137.
14. **Razonable RR, Zerr DM, AST Infectious Diseases Community of Practice.** 2009. HHV-6, HHV-7 and HHV-8 in solid organ transplant recipients. Am. J. Transplant. **9**(Suppl 4)**:**S97–S100.
15. **Saraya T, Mikoshiba M, Kamiyama H, Yoshizumi M, Tsuchida S, Tsukagoshi H, Ishioka T, Terada M, Tanabe E, Tomioka C, Ishii H, Kimura H, Kozawa K, Shiohara T, Takizawa H, Goto H.** 2013. Evidence for reactivation of human herpesvirus 6 in generalized lymphadenopathy in a patient with drug-induced hypersensitivity syndrome. J. Clin. Microbiol. **51:**1979–1982.
16. **Tohyama M, Hashimoto K, Yasukawa M, Kimura H, Horikawa T, Nakajima K, Urano Y, Matsumoto K, Iijima M, Shear NH.** 2007. Association of human herpesvirus 6 reactivation with the flaring and severity of drug-induced hypersensitivity syndrome. Br. J. Dermatol. **157:**934–940.
17. **Yao K, Crawford JR, Komaroff AL, Ablashi DV, Jacobson S.** 2010. Review part 2: human herpesvirus-6 in central nervous system diseases. J. Med. Virol. **82:**1669–1678.
18. **Ablashi DV, Devin CL, Yoshikawa T, Lautenschlager I, Luppi M, Kühl U, Komaroff AL.** 2010. Review part 3: human herpesvirus-6 in multiple non-neurological diseases. J. Med. Virol. **82:**1903–1910.
19. **Gobbi A, Stoddart CA, Malnati MS, Locatelli G, Santoro F, Abbey NW, Bare C, Linquist-Stepps V, Moreno MB, Herndier BG, Lusso P, McCune JM.** 1999. Human herpesvirus 6 (HHV-6) causes severe thymocyte depletion in SCID-hu Thy/Liv mice. J. Exp. Med. **189:**1953–1960.
20. **Emery VC, Atkins MC, Bowen EF, Clark DA, Johnson MA, Kidd IM, McLaughlin JE, Phillips AN, Strappe PM, Griffiths PD.** 1999. Interactions between beta-herpesviruses and human immunodeficiency virus in vivo: evidence for increased human immunodeficiency viral load in the presence of human herpesvirus 6. J. Med. Virol. **57:**278–282.
21. **Lusso P, Gallo RC.** 1995. Human herpesvirus 6 in AIDS. Immunol. Today **16:**67–71.
22. **Lusso P, Crowley RW, Malnati MS, Di Serio C, Ponzoni M, Biancotto A, Markham PD, Gallo RC.** 2007. Human herpesvirus 6A accelerates AIDS progression in macaques. Proc. Natl. Acad. Sci. U. S. A. **104:**5067–5072.
23. **Lusso P, Markham PD, DeRocco SE, Gallo RC.** 1990. In vitro susceptibility of T lymphocytes from chimpanzees (*Pan troglodytes*) to human herpesvirus 6 (HHV-6): a potential animal model to study the interaction between HHV-6 and human immunodeficiency virus type 1 in vivo. J. Virol. **64:**2751–2758.

24. **Lusso P, Secchiero P, Crowley RW.** 1994. In vitro susceptibility of Macaca nemestrina to human herpesvirus 6: a potential animal model of coinfection with primate immunodeficiency viruses. AIDS Res. Hum. Retroviruses **10:**181–187.
25. **Leibovitch E, Wohler JE, Cummings Macri SM, Motanic K, Harberts E, Gaitán MI, Maggi P, Ellis M, Westmoreland S, Silva A, Reich DS, Jacobson S.** 2013. Novel marmoset (*Callithrix jacchus*) model of human herpesvirus 6A and 6B infections: immunologic, virologic and radiologic characterization. PLoS Pathog. **9:**e1003138. doi:10.1371/journal.ppat.1003138.
26. **Berges BK, Rowan MR.** 2011. The utility of the new generation of humanized mice to study HIV-1 infection: transmission, prevention, pathogenesis, and treatment. Retrovirology **8:**65. doi:10.1186/1742-4690-8-65.
27. **Cocco M, Bellan C, Tussiwand R, Corti D, Traggiai E, Lazzi S, Mannucci S, Bronz L, Palummo N, Ginanneschi C, Tosi P, Lanzavecchia A, Manz MG, Leoncini L.** 2008. $CD34^+$ cord blood cell-transplanted $Rag2^{-/-}\gamma_c^{-/-}$ mice as a model for Epstein-Barr virus infection. Am. J. Pathol. **173:**1369–1378.
28. **Ma SD, Hegde S, Young KH, Sullivan R, Rajesh D, Zhou Y, Jankowska-Gan E, Burlingham WJ, Sun X, Gulley ML, Tang W, Gumperz JE, Kenney SC.** 2011. A new model of Epstein-Barr virus infection reveals an important role for early lytic viral protein expression in the development of lymphomas. J. Virol. **85:**165–177.
29. **Strowig T, Gurer C, Ploss A, Liu YF, Arrey F, Sashihara J, Koo G, Rice CM, Young JW, Chadburn A, Cohen JI, Münz C.** 2009. Priming of protective T cell responses against virus-induced tumors in mice with human immune system components. J. Exp. Med. **206:**1423–1434.
30. **Yajima M, Imadome K, Nakagawa A, Watanabe S, Terashima K, Nakamura H, Ito M, Shimizu N, Honda M, Yamamoto N, Fujiwara S.** 2008. A new humanized mouse model of Epstein-Barr virus infection that reproduces persistent infection, lymphoproliferative disorder, and cell-mediated and humoral immune responses. J. Infect. Dis. **198:**673–682.
31. **Wu W, Vieira J, Fiore N, Banerjee P, Sieburg M, Rochford R, Harrington WJ, Feuer G.** 2006. KSHV/HHV-8 infection of human hematopoietic progenitor ($CD34^+$) cells: persistence of infection during hematopoiesis in vitro and in vivo. Blood **108:**141–151.
32. **Parsons CH, Adang LA, Overdevest J, O'Connor CM, Taylor JRJ, Camerini D, Kedes DH.** 2006. KSHV targets multiple leukocyte lineages during long-term productive infection in NOD/SCID mice. J. Clin. Invest. **116:**1963–1973.
33. **Smith MS, Goldman DC, Bailey AS, Pfaffle DL, Kreklywich CN, Spencer DB, Othieno FA, Streblow DN, Garcia JV, Fleming WH, Nelson JA.** 2010. Granulocyte-colony stimulating factor reactivates human cytomegalovirus in a latently infected humanized mouse model. Cell Host Microbe **8:**284–291.
34. **Tang H, Kawabata A, Yoshida M, Oyaizu H, Maeki T, Yamanishi K, Mori Y.** 2010. Human herpesvirus 6 encoded glycoprotein Q1 gene is essential for virus growth. Virology **407:**360–367.
35. **Kalejta RF, Bechtel JT, Shenk T.** 2003. Human cytomegalovirus pp71 stimulates cell cycle progression by inducing the proteasome-dependent degradation of the retinoblastoma family of tumor suppressors. Mol. Cell. Biol. **23:**1885–1895.
36. **Reed LJ, Muench H.** 1938. A simple method of estimating fifty per cent endpoints. Am. J. Hyg. (Lond.) **27:**493–497.
37. **Traggiai E, Chicha L, Mazzucchelli L, Bronz L, Piffaretti JC, Lanzavecchia A, Manz MG.** 2004. Development of a human adaptive immune system in cord blood cell-transplanted mice. Science **304:**104–107.
38. **Berges BK, Wheat WH, Palmer BE, Connick E, Akkina R.** 2006. HIV-1 infection and CD4 T cell depletion in the humanized $Rag2^{-/-}\gamma c^{-/-}$ (RAG-hu) mouse model. Retrovirology **3:**76. doi:10.1186/1742-4690-3-76.
39. **Akkina R, Berges BK, Palmer BE, Remling L, Neff CP, Kuruvilla J, Connick E, Folkvord J, Gagliardi K, Kassu A, Akkina SR.** 2011. Humanized $Rag1^{-/-}\gamma c^{-/-}$ mice support multilineage hematopoiesis and are susceptible to HIV-1 infection via systemic and vaginal routes. PLoS One **6:**e20169. doi:10.1371/journal.pone.0020169.
40. **Gautheret-Dejean A, Manichanh C, Thien-Ah-Koon F, Fillet AM, Mangeney N, Vidaud M, Dhedin N, Vernant JP, Agut H.** 2002. Development of a real-time polymerase chain reaction assay for the diagnosis of human herpesvirus-6 infection and application to bone marrow transplant patients. J. Virol. Methods **100:**27–35.
41. **Tsujimura A, Shida K, Kitamura M, Nomura M, Takeda J, Tanaka H, Matsumoto M, Matsumiya K, Okuyama A, Nishimune Y, Okabe M, Seya T.** 1998. Molecular cloning of a murine homologue of membrane cofactor protein (CD46): preferential expression in testicular germ cells. Biochem. J. **330:**163–168.
42. **Zhen Z, Bradel-Tretheway B, Sumagin S, Bidlack JM, Dewhurst S.** 2005. The human herpesvirus 6 G protein-coupled receptor homolog U51 positively regulates virus replication and enhances cell-cell fusion in vitro. J. Virol. **79:**11914–11924.
43. **Adams O, Krempe C, Kögler G, Wernet P, Scheid A.** 1998. Congenital infections with human herpesvirus 6. J. Infect. Dis. **178:**544–546.
44. **Braun DK, Dominguez G, Pellett PE.** 1997. Human herpesvirus 6. Clin. Microbiol. Rev. **10:**521–567.
45. **Lusso P, Malnati M, De Maria A, Balotta C, DeRocco SE, Markham PD, Gallo RC.** 1991. Productive infection of CD4+ and CD8+ mature human T cell populations and clones by human herpesvirus 6. Transcriptional down-regulation of CD3. J. Immun. **147:**685–691.
46. **Lusso P, De Maria A, Malnati M, Lori F, DeRocco SE, Baseler M, Gallo RC.** 1991. Induction of CD4 and susceptibility to HIV-1 infection in human $CD8^+$ T lymphocytes by human herpesvirus 6. Nature **349:**533–535.
47. **Nascimbeni M, Shin EC, Chiriboga L, Kleiner DE, Rehermann B.** 2004. Peripheral $CD4^+CD8^+$ T cells are differentiated effector memory cells with antiviral functions. Blood **104:**478–486.
48. **Grivel JC, Santoro F, Chen S, Fagá G, Malnati MS, Ito Y, Margolis L, Lusso P.** 2003. Pathogenic effects of human herpesvirus 6 in human lymphoid tissue ex vivo. J. Virol. **77:**8280–8289.
49. **Baenziger S, Tussiwand R, Schlaepfer E, Mazzucchelli L, Heikenwalder M, Kurrer MO, Behnke S, Frey J, Oxenius A, Joller H, Aguzzi A, Manz MG, Speck RF.** 2006. Disseminated and sustained HIV infection in $CD34^+$ cord blood cell-transplanted $Rag2^{-/-}\gamma_c^{-/-}$ mice. Proc. Natl. Acad. Sci. U. S. A. **103:**15951–15956.
50. **Zhang L, Kovalev GI, Su L.** 2007. HIV-1 infection and pathogenesis in a novel humanized mouse model. Blood **109:**2978–2981.

STEM CELLS AND DEVELOPMENT
Volume 23, Number 1, 2014

DOI: 10.1089/scd.2013.0265

COMPREHENSIVE REVIEW

Humanized Mice as a Model to Study Human Hematopoietic Stem Cell Transplantation

Anne Tanner, Stephen E. Taylor, Wittnee Decottignies, and Bradford K. Berges

Hematopoietic stem cell (HSC) transplantation has the potential to treat a variety of human diseases, including genetic deficiencies, immune disorders, and to restore immunity following cancer treatment. However, there are several obstacles that prevent effective HSC transplantation in humans. These include finding a matched donor, having a sufficient number of cells for the transplant, and the potency of the cells in the transplant. Ethical issues prevent effective research in humans that could provide insight into ways to overcome these obstacles. Highly immunodeficient mice can be transplanted with human HSCs and this process is accompanied by HSC homing to the murine bone marrow. This is followed by stem cell expansion, multilineage hematopoiesis, long-term engraftment, and functional human antibody and cellular immune responses. As such, humanized mice serve as a model for human HSC transplantation. A variety of conditions have been analyzed for their impact on HSC transplantation to produce humanized mice, including the type and source of cells used in the transplant, the number of cells transplanted, the expansion of cells with various protocols, and the route of introduction of cells into the mouse. In this review, we summarize what has been learned about HSC transplantation using humanized mice as a recipient model and we comment on how these models may be useful to future preclinical research to determine more effective ways to expand HSCs and to determine their repopulating potential in vivo.

Human hematopoietic stem cell transplantation (HSCT) is used to treat a variety of human diseases, including genetic disorders that affect the immune system, rescue following irradiation or chemoablation as a cancer treatment, autoimmune disorders, and chronic infectious diseases [1]. Gene therapies are also currently under evaluation in conjunction with cellular therapies, thus greatly expanding the diseases that could be potentially treated by HSCT. Human HSCs used for transplantation can be obtained from several sources, including umbilical cord blood (UCB), mobilized peripheral blood (MPB), or direct extraction from bone marrow. Advantages of the various sources of HSCs are reviewed elsewhere [2]. Although UCB is the most readily available source of HSCs, these samples typically have insufficient numbers of HSCs for successful transplantation in adult humans [3] although they may still be useful for pediatric patients.

HSCT in humans has a relatively high mortality rate, which varies depending upon several factors such as the severity of the disease being treated, similarity of donor cells to the recipient, and the carrier status of the donor and recipient for pathogens such as human herpesviruses. Rejection of transplanted cells and graft versus host disease (GVHD) are common outcomes when the major histocompatibility complex (MHC) types differ between the donor and recipient. The availability of experimental models to evaluate these various parameters can provide insight into how to perform HSCT with minimal risk to patients.

Immunodeficient mice can be engrafted with various types of human cells to produce what are referred to as "humanized mice." Current humanized mouse models are excellent recipients for human HSCT because they exhibit high rates of HSC engraftment and multilineage hematopoiesis, migration of HSCs and their progeny cells to lymphoid and nonlymphoid tissues occurs, and functional human innate and adaptive immune responses are detected in vivo. It is useful to understand the history of how current humanized mouse models were developed to better understand improvements that are still needed or those that are currently under development.

The original humanized mouse models were introduced in 1988 using severe combined immunodeficiency (SCID) mice [4] or *bg/nu/xid* mice [5]. [*Many references are made to mouse strains in this review. See Table 1 for technical names of these strains.*] SCID mice are unable to produce B or T lymphocytes due to a gene mutation that prevents DNA rearrangement steps required to generate the genes encoding B- and T-cell receptors. However, these mice do go on to produce a limited repertoire of mature B and T cells as they age [6], and thus, different/additional genes involved in lymphocyte development are now commonly targeted. *Bg/nu/xid* mice lack the ability to produce a thymus due to the nude

Department of Microbiology and Molecular Biology, Brigham Young University, Provo, Utah.

Table 1. Mouse Strains Commonly Used to Produce Humanized Mice

Common name	*Technical name*	*Comments*
SCID or CB17-*scid*	CB17-*Prkdc*^{scid}	
NOD/SCID	NOD.CB17-*Prkdc*^{scid}	
NOD/SCID$\gamma c^{-/-}$ or NOG	NOD.Shi.Cg-*Prkdc*^{scid}*Il2rg*^{tm1Sug}	Truncation of γc receptor
NOD/SCID$\gamma c^{-/-}$ or NSG	NOD.Cg-*Prkdc*^{scid}*Il2*^{tm1Wjl}	Entire deletion of γc receptor
Balb/c-Rag2$^{-/-}\gamma c^{-/-}$	C.129-*Rag2*^{tm1Fwa}*Il2rg*^{tm1Sug}	See references 38 and 39 for additional similar strains
Rag1$^{-/-}\gamma c^{-/-}$	C.129-*Rag1*^{tm1Mom}*Il2rg*^{tm1Wjl}	

mutation, have a reduced number of natural killer (NK) cells due to the beige mutation, and also harbor the *scid* mutation to prevent lymphocyte maturation [7]. One original humanized mouse model (pioneered by Mosier) uses human peripheral blood leukocytes (PBLs) and is usually referred to as the SCID-hu-PBL model [8]. PBL populations contain very low levels of human HSCs and thus that model was not useful to study human HSC engraftment or multilineage hematopoiesis [9]. A second model uses human fetal thymic and liver tissues, which are transplanted under the kidney capsule to produce a thymic organoid. This model was developed by McCune and is referred to as the SCID-hu *thy/liv* model [10]. A third model used human HSCs originally obtained from unpurified bone marrow and was developed by Dick (human/immune-deficient or HID mice) [5]. Of the original models, the SCID-hu *thy/liv* and HID models resulted in transplantation of a significant number of human HSCs. Although HSCT can be accomplished in the SCID-hu *thy/liv* model, HSC homing to the bone marrow cannot be studied. Human T cells are the major product of hematopoiesis in these mice and these cells also remain largely restricted to the graft [11]. In the original HID model, human bone marrow was injected directly into the murine bone marrow and thus HSC trafficking was largely unnecessary [12].

As our understanding of HSCs has grown, new humanized mouse models have been sought that can recapitulate the human immune system more faithfully. A groundbreaking study was published in 2004 when Traggiai et al. [13] showed that highly immunodeficient Rag2$^{-/-}\gamma c^{-/-}$ mice (C.129-Rag2^{tm1Fwa}Il2rg^{tm1Sug} strain) can be engrafted intrahepatically with human HSCs (CD34$^+$ cells) isolated from UCB. They demonstrated multilineage hematopoiesis, a broad distribution of human immune cells, and functional human antibody and CD8$^+$ T-cell responses [13]. Many other studies have been published using similar protocols, and a wide variety of human hematopoietic cell types have been detected in these models, including strong production of B and T lymphocytes, monocytes/macrophages, dendritic cells, and typically a weak production of granulocytes, erythrocytes, and platelets [13–17]. The precursor cells for production of granulocytes, erythrocytes, and platelets are detectable in the bone marrow of humanized mice, but murine macrophages appear to prevent the proper development of erythrocytes and platelets as evidenced by increased detection following murine macrophage depletion [18,19]. These human cells are in many cases widely dispersed throughout the lymphoid organs (bone marrow, thymus, lymph nodes, and spleen) as well as other organs (brain, lungs, gut mucosa, reproductive tracts, etc.) [13,15,20–23].

A broad diversity of humanized mouse models is currently in use. Models differ based upon many variables, but successful engraftment of human HSCs has been detected under many different experimental conditions. These differing conditions include the mouse strain used as a recipient, the conditioning protocol used to prepare mice for transplantation, the source of human HSCs used for engraftment, the phenotypes of HSCs used for engraftment, the culture and/or expansion of HSCs with various cytokines or no culturing at all, the number of cells used for engraftment, the use of fresh or frozen cells, the use of coinjected non-HSC support cells, and the method or site of inoculation of cells into the host. Although the vast array of conditions used to make humanized mice makes it difficult to directly compare the results of these various studies to determine which method is most effective, they also indicate that a wide variety of engraftment protocols can be successfully carried out in immunodeficient mice. Thus, factors that influence the efficacy of HSCT can be compared to discover methods which are more effective and carry fewer risks. The use of well-controlled experiments to compare single variables and their individual effects on the efficacy of HSCT is an area that is still underdeveloped in the humanized mouse field.

The definition of the phenotype of a true HSC is currently not well defined, but nearly always includes the CD34 marker. A review of the capacity of CD34-negative cells to act as HSCs is available [24]. Interestingly, one common way to define HSC populations is actually in terms of their ability to engraft immunodeficient mice; in this case, the HSCs are referred to as SCID repopulating cells. As mentioned previously, Traggiai et al. showed that intrahepatic (i.h.) injection of UCB CD34$^+$ cells into Rag2$^{-/-}\gamma c^{-/-}$ mice resulted in the development of human B, T, and dendritic cells [13]. Since then, experiments have been performed with various types of cellular populations that revolved around the CD34 marker. Results of these various studies are summarized in Table 2 as a function of the cellular phenotype and the source of HSCs. Notta et al. recently showed that a single purified human HSC is capable of producing detectable engraftment in highly immunodeficient mice, and their work sheds further light on the phenotype of true HSCs [25]. There are several methods of isolating human HSCs to engraft humanized mice, including from UCB, fetal liver, MPB, and from adult human bone marrow. UCB is a common source of HSCs because it is readily available and has a high concentration of HSCs. Mononuclear cells from human UCB are isolated by Ficoll separation and then enriched using CD34$^+$-specific magnetic beads. The cells can either be used immediately for engrafting or they can be cultured. Culturing these cells requires specific cytokines to stimulate growth/expansion without differentiation.

Table 2. Phenotypes and Sources of Hematopoietic Stem Cells Successfully Used to Produce Humanized Mice

Phenotype	*Source of cells*	*References*
$CD34^+$	UCB	[9,38,41,47,48,61,62]
$CD34^+CD7^{++}$	UCB	[47]
$CD34^+CD38^-$ $CD90^+$	UCB	[44]
$CD34^+CD38^-$	UCB	[12,63,64]
$CD34^+CD133^+$	UCB	[43,65]
$CD34^+$	Fetal liver	[11,14,25,32,37,66–69]
$CD34^+CD38^-$	Fetal liver	[70–73]
$CD34^+$	Derived from human embryonic stem cells	[24]
$CD34^+$	Mobilized peripheral blood	[19,20,62]
$CD34^+CD38^-$	Adult bone marrow	[64]
$CD34^+$	Adult bone marrow	[18,62]

UCB, umbilical cord blood.

Fetal liver is another source of the HSCs for engraftment. Tissues are minced and a single-cell suspension is created, then $CD34^+$ cells are isolated as above. These samples are more difficult to obtain, but contain much higher numbers of $CD34^+$ cells as compared to UCB [15]. HSCs can also be obtained by direct extraction from bone marrow, followed by similar methods to obtain the $CD34^+$ fraction [26].

Murine engraftment can also be accomplished using human MPB as a source of cells. A human patient is injected with cytokines such as the granulocyte-colony stimulating factor (G-CSF), which increases the number of circulating HSCs. A blood sample is drawn and leukapheresis is performed. $CD34^+$ cells are then purified out of the sample [27]. It has been reported that 50-fold more cells are required to achieve the same level of mouse engraftment when comparing hMPB cells to UCB cells [28], but it is unclear why these cells require a higher dose.

Human embryonic stem cells (hESCs) or induced pluripotent stem cells can also be used to obtain $CD34^+$ cells for engraftment and multiple types of human blood cells have successfully been produced from these sources [29,30]. One way to do this is to culture the hESCs with irradiated murine cell lines. This coculture allows hESCs to differentiate into HSCs without additional cytokines [31]. These differentiated cells are injected into irradiated mice to produce human immune cell engraftment. Since samples containing primary HSCs can be difficult to obtain due to scarcity, the ability to derive HSCs from a replenishable source is highly desirable. In addition, cells from a replenishable source can be better characterized as compared to those obtained from cord blood or fetal liver where each donor is unique. hESCs can be maintained in their undifferentiated state indefinitely if they are passaged regularly [31] and this suggests their utility as a HSC source. Human HSCs themselves cannot currently be expanded indefinitely in culture without losing their potency for long-term engraftment and multilineage hematopoiesis. Tian et al. demonstrated successful murine engraftment when hESC-derived HSCs were injected into the bone marrow or intravenously [32].

Highly immunodeficient mice are critical for success in the engraftment of human HSCs, and many such mouse strains are currently in use. Common strains include nonobese diabetic/SCID mice (NOD-SCID), NOD-SCID $\gamma c^{-/-}$ (NSG or NOG; see Table 1), $Rag2^{-/-}\gamma c^{-/-}$, $Rag1^{-/-}\gamma c^{-/-}$, among others and have all been used to make humanized mice and study HSC transplantation [15,33–36]. These mutations impair the ability to produce functional T and B lymphocytes (*SCID, Rag1,* and *Rag2*) or mature NK cells (γc). γc is the signaling subunit of both the interleukin-2 (IL-2) and IL-15 receptors, thus preventing expansion/maturation of T cells and NK cells, respectively. When the HSC donor and the recipient MHCs do not match, then myeloablative conditioning and use of highly immunodeficient mice are required for effective engraftment [37]. For the above mouse strains, conditioning is always required to achieve human engraftment levels higher than a low fraction (1%–5%) of chimerism in peripheral blood. Waskow et al. [37] created a mouse model that they termed a "universal" HSC recipient because it can accept allogeneic grafts without earlier conditioning. The mouse strain used ($Rag2^{-/-}\gamma c^{-/-}Kit^{W/Wv}$) was generated in a $Rag2^{-/-}\gamma c^{-/-}$ background and additionally has a *Kit* knockout, which prevents sustained self-renewal of HSCs [37]. Excellent reviews of the types of immunodeficient mouse strains currently in use to make humanized mice are available [38–40].

There is another type of humanized mouse model, referred to as the bone marrow, liver, thymus (BLT) mouse, which utilizes these immunodeficient mouse strains to make an effective model of HSC engraftment. In this model, immunodeficient mice (NOD/SCID, NSG, or $Rag2^{-/-}\gamma c^{-/-}$) are sublethally irradiated and the following day 1 mm^3 human fetal liver and thymus tissue fragments are inserted under the kidney capsule of the mouse. These tissues develop into a human thymic organoid. After the thymic organoid develops, the mice are then injected intravenously with autologous human fetal liver-derived $CD34^+$ cells to create the BLT model. This model also shows good engraftment and has the added advantage of the selection of human T cells on human MHC-I-expressing stromal cells in the thymic graft, which leads to better human T-cell responses in vivo [41–43].

HSC homing to the bone marrow in humanized mice occurs rapidly and engraftment can be a long-lasting and stable phenomenon. Human HSC homing to the murine bone marrow has been seen in as little as 20 h following intravenous (i.v.) injection of $CD34^+$ HSCs into NOD/SCID mice [44,45]. Humanized $Rag2^{-/-}\gamma c^{-/-}$ mice injected with human fetal liver $CD34^+$ cells showed evidence of human cell engraftment up to 63 weeks later [46]. Various other studies have shown engraftment lasting for at least 6 months [15,35,47–49]. Takahashi et al. showed that $CD34^+$ cells were present in NOG mice at a statistically constant level over 4 months [45].

The two most common methods for engraftment of human HSCs into immunodeficient mice are i.h. injection and i.v. injection. Other methods of injection include intraperitoneal, intracardial, intrasplenic, or directly into the bone marrow. It is currently unknown if one of these methods is significantly better than the others because of multiple variables across the various studies. However, a comparison of i.h. and i.v. injection showed an insignificant difference in the effectiveness of human HSC engraftment [50]. I.h. injection of cells is commonly used in newborn mice; this method may be effective because HSCs are primarily located in the liver of newborn mice and traffic to the bone marrow within the first

weeks after birth. It is possible that human HSCs respond to the same trafficking signals as murine HSCs, thus explaining the effectiveness of this method. However, i.v. injection is also successfully used in newborn mice, and it is clear that a variety of injection routes are successful in both newborn and adult mice. In the literature, Rag2$^{-/-}\gamma c^{-/-}$ mice are commonly engrafted as newborns [15,50,51], while mice on the NOD/SCID background are commonly engrafted as adults [44,45], although animals with the NOD/SCID background can be engrafted as newborns as well [16,52].

Secondary transplantation can be accomplished in immunodeficient mice, thus providing additional evidence for true HSC engraftment. Human CD34$^+$ cells can be taken from the bone marrow of engrafted mice and serially transplanted to other immunodeficient mice. Eighteen weeks after initial engraftment of NOD/SCID/$\gamma c^{-/-}$ mice, cells obtained from the bone marrow were successfully transplanted into secondary recipients to achieve engraftment. This is another demonstration that human CD34$^+$ cells do home to the engrafted mouse bone marrow [53]. CD34$^+$CD133$^+$ cells have also been proven effective for secondary transplantation and this population appears to also have long-term repopulating HSCs [54]. Furthermore, NSG mice are able to undergo serial transplants of bone marrow with as few as 10 HSCs [55]. Genetically modified human CD34$^+$ cells were also capable of secondary transplantation [56].

One of the problems of engrafting human patients with UCB-derived HSCs is that it usually takes 6 months or more to detect donor-derived immune cells (B and T lymphocytes) in the recipient [53]. A way to induce a quicker recovery and repopulation of immune cells would be valuable in increasing the effectiveness of UCB transplantation. The dose of progenitor cells given in a transplant is correlated with the successful outcome of the graft in humanized mice, with the mice receiving the highest amount of transplanted cells showing detectable levels of HSCs in the peripheral blood just 4 weeks postengraftment [53]. These findings suggest that higher UCB HSC doses may be more effective in terms of the kinetics of reconstitution in humans.

The dose of HSCs required for stable engraftment in humans is not well defined, although 2×10^8 bone marrow cells/kg is considered adequate [2]. Use of at least 3×10^6 CD34$^+$ cells/kg showed a higher efficacy than lower doses [57]. Similarly, the number of HSCs required to achieve engraftment in an immunodeficient mouse is not entirely understood, although a broad range of cell doses has been used. Since a 2–3-day-old mouse (age at time of engraftment) weighs about 0.002 kg, a similar dose of CD34$^+$ HSCs for mice (using the 3×10^6 CD34$^+$ cells/kg amount cited above) would be only 6,000 cells per animal. Whereas a dose this low has not been reported in humanized mice, it is not clear if it has been attempted. Traggiai et al. [13] reported human nucleated cells in the bone marrow and spleen of the mice engrafted with as few as $3.8–12\times10^4$ CD34$^+$ cells from human UCB. The peripheral blood engraftment ranged from ~5% to ~85% at time periods of 4–26 weeks [13]. Human leukocytes have also been found in the thymus of mice engrafted with $2.5–5.0\times10^5$ CD34$^+$CD7^{++} cells and $1.5–2.5\times10^5$ CD34$^+$ cells harvested from human UCB [58]. Lang et al. reported successful engraftment after injecting mice with a range of human CD34$^+$ UCB cells from 5×10^4 to 2×10^6 [50].

Although the current generation of humanized mice is superior in many ways to the original models, there are still improvements in development. One such improvement is in seeking ways to increase the number and/or potency of HSCs available for engraftment. Since UCB samples typically do not contain sufficient cells for human adult HSCT, these findings are highly relevant to methods that can improve human HSCT outcomes. Some mouse humanization protocols call for the CD34$^+$ cells to be expanded in vitro before engraftment, whereas others use the cells for engraftment shortly after purification, without expansion. Expansion of HSCs in vitro increases the number of mice that can be engrafted by increasing the total number of CD34$^+$ cells. Cytokines are commonly used to culture CD34$^+$ cells in an effort to increase the number of HSCs and also to prevent HSC differentiation in vitro and a variety of cytokine cocktails have been shown to be effective [15,41,50,59]. Following are examples that illustrate some specific experimental protocols and their effects on engraftment levels.

In one study, human fetal liver-derived CD34$^+$ cells were cultured for 7 days with stem cell factor (SCF), thrombopoietin (TPO), Flk2/Flk3 ligand, and IL-3. This combination of cytokines for HSC culture led to higher peripheral blood engraftment levels in Rag2$^{-/-}\gamma c^{-/-}$ mice as compared to other cytokine growth cocktails examined [41]. Another group reported that CD34$^+$CD133$^+$ cells purified from UCB and supplemented with fibroblast growth factor 1, SCF, TPO, insulin-like growth factor binding protein 2, angiopoietin-like 5, and heparin were cultured for 10 days and then used to engraft NOD/SCID$\gamma c^{-/-}$ mice. These mice showed ~21-fold increase in SCID repopulating activity as opposed to the untreated cells and showed good reconstitution in both neonates and adults that received the transplant, providing the option of engraftment in older mice. This method of ex vivo expansion minimizes the number of cells needed for injection and thus provides a way to maximize the amount of mice engrafted from a single cord blood sample [54].

When CD34$^+$ cells from UCB were cultured short term (1–8 days) in IL-6, SCF, and Flt3-Ligand, and T cell-depleted CD34$^-$ support cells were engrafted into Rag2$^{-/-}\gamma c^{-/-}$ mice, these samples showed higher levels of human IgM and IgG as compared to mice that received fresh/uncultured CD34$^+$ cells or long-term cultured cells (9–28 days). Human leukocyte levels were significantly higher in peripheral blood as well as lymphoid tissue in mice receiving these short-term cultured cells, indicating that culturing cells short term in the presence of appropriate cytokines and support cells is beneficial to successful humanization of mice [50]. Further, engraftment with autologous T cells promotes more effective B-cell maturation in HSC-humanized mice [60]. It has also been shown that clearing the space for human donor HSCs to populate by eliminating the recipient mouse's own HSCs using ACK2, an antibody that blocks c-kit function, can provide much higher engraftment in treated mice [61].

Sangeetha et al. observed that UCB-derived CD34$^+$ cells show increased levels of apoptosis in vitro when treated with cytokines to promote expansion [59]. Treatment of expanding CD34$^+$ cells with apoptotic inhibitors resulted in increased expansion of the cells. Additionally, higher engraftment levels in mice were detected in animals that received cells treated with apoptotic inhibitors during expansion in vitro. In a recent study, a screen was carried out for novel agents that induce

effective expansion of UCB-derived $CD34^+$ cells followed by successful engraftment into immunodeficient mice. The screen was carried out with SCF and TPO, accompanied by other chemicals. They found that the chemokine CCL28 both enhanced cellular proliferation and decreased rates of apoptosis, and these findings were replicated in the fetal liver and bone marrow-derived cells [62]. Such findings illustrate the utility of humanized mice as a model to study methods to produce larger numbers of potent HSCs.

As mentioned above, culturing cells in the presence of cytokines and chemokines can lead to enhanced engraftment. Several research groups have also shown that supplementing humanized mice with human cytokines in vivo results in enhanced engraftment. Use of a lentiviral vector to stably produce human IL-7 (hIL-7) resulted in enhanced levels of human T cells in humanized mice [63]. Similarly, enhanced levels of hIL-15 resulted in the production of NK cells in humanized mice [17,64,65]; NK cells are very rare without introduction of hIL-15. Administration of other human cytokines leads to enhanced reconstitution of T and B lymphocytes, dendritic cells, erythrocytes, and monocytes/macrophages [17], and improved T- and B-lymphocyte production and dendritic cell maturation lead to better human antibody responses [66].

A recent article demonstrates the utility of humanized mice to study complications associated with HSCT. They showed recapitulation of human GVHD in humanized mice, indicating that this common complication of HSCT can be studied in a mouse system. They also demonstrated that $CD8^{hi}$ regulatory T cells were able to control GVHD by reducing proliferation of alloreactive T cells and by decreasing production of inflammatory cytokines and chemokines [67]. It should be noted that HSCs were not used to engraft these animals. Rather, they used mature human peripheral blood mononuclear cells (PBMCs) for the initial graft, followed by a second graft of allogeneic PBMCs.

Viral infections are common risk factors for complications associated with HSCT, and humanized mice have been shown to support viral replication and associated pathogenesis for a variety of human viruses of blood cells, including the human cytomegalovirus (hCMV) and the Epstein-Barr virus [68–71]. One such study showed that G-CSF treatment of humanized mice latently infected with hCMV induced reactivation of the virus, indicating that the use of G-CSF to mobilize HSCs from humans may also reactivate the virus and potentially lead to hCMV-associated disease in donors and/or recipients [68]. However, relatively few studies have been performed to examine complications associated with HSCT, and this area warrants further investigation in humanized mouse models.

In summary, humanized mice are a useful tool to perform preclinical studies aimed at increasing our understanding of the mechanisms of HSC expansion, homing, and engraftment. These models can be effectively engrafted with human HSCs under a large variety of experimental parameters, and have proven to be a useful preclinical testing ground for the repopulating potential of human HSCs expanded by novel methodologies. Whereas strides have been made to discover the phenotype of a true human HSC and new techniques to expand human HSCs without differentiation are being reported regularly, there is still much to learn in these areas. We expect that HSCT engraftment of immunodeficient mice will continue to be an important tool as we seek to improve the efficacy of HSCT in humans.

Acknowledgments

This work was supported by a mentoring environment grant by the Brigham Young University. All authors read and approved the final manuscript.

Author Disclosure Statement

No competing financial interests exist.

References

1. Copelan EA. (2006). Hematopoietic stem-cell transplantation. N Engl J Med 354:1813–1826.
2. Hatzimichael E and M Tuthill. (2010). *Hematopoietic Stem Cell Transplantation*. Dovepress, Princeton, NJ.
3. Barker JN. (2007). Umbilical Cord Blood (UCB) transplantation: an alternative to the use of unrelated volunteer donors? Hematology Am Soc Hematol Educ Program 55–61.
4. Bosma GC, RP Custer and MJ Bosma. (1983). A severe combined immunodeficiency mutation in the mouse. Nature 301:527–530.
5. Kamel-Reid S and JE Dick. (1988). Engraftment of immune-deficient mice with human hematopoietic stem cells. Science 242:1706–1709.
6. Greiner DL, RA Hesselton and LD Shultz. (1998). SCID mouse models of human stem cell engraftment. Stem Cells 16:166–177.
7. Andriole GL, JJ Mulé, CT Hansen, WM Linehan and SA Rosenberg. (1985). Evidence that lymphokine-activated killer cells and natural killer cells are distinct based on an analysis of congenitally immunodeficient mice. J Immunol 135:2911–2913.
8. Mosier DE, RJ Gulizia, SM Baird and DB Wilson. (1988). Transfer of a functional human immune system to mice with severe combined immunodeficiency. Nature 335:256–259.
9. Mosier DE. (1991). Adoptive transfer of human lymphoid cells to severely immunodeficient mice: models for normal human immune function, autoimmunity, lymphomagenesis, and AIDS. Adv Immunol 50:303–325.
10. McCune JM, R Namikawa, H Kaneshima, LD Shultz, M Lieberman and IL Weissman. (1988). The SCID-hu mouse: murine model for the analysis of human hematolymphoid differentiation and function. Science 241:1632–1639.
11. Mosier DE. (1996). Human immunodeficiency virus infection of human cells transplanted to severe combined immunodeficient mice. Adv Immunol 63:79–125.
12. Lapidot T, F Pflumio, M Doedens, B Murdoch, DE Williams and JE Dick. (1992). Cytokine stimulation of multilineage hematopoiesis from immature human cells engrafted in SCID mice. Science 255:1137–1141.
13. Traggiai E, L Chicha, L Mazzucchelli, L Bronz, JC Piffaretti, A Lanzavecchia and MG Manz. (2004). Development of a human adaptive immune system in cord blood cell-transplanted mice. Science 304:104–107.
14. Kuruvilla JG, RM Troyer, S Devi and R Akkina. (2007). Dengue virus infection and immune response in humanized $Rag2^{-/-}\gamma c^{-/-}$ (RAG-hu) mice. Virol 369:143–152.
15. Berges BK, WH Wheat, BE Palmer, E Connick and R Akkina. (2006). HIV-1 infection and CD4 T cell depletion in the humanized Rag2-/-gc-/- (RAG-hu) mouse model. Retrovirology 3:76.
16. Ishikawa F, M Yasukawa, B Lyons, S Yoshida, T Miyamoto, G Yoshimoto, T Watanabe, K Akashi, LD Shultz and M

Harada. (2005). Development of functional human blood and immune systems in NOD/SCID/IL2 receptor {gamma} chain(null) mice. Blood 106:1565–1573.
17. Chen Q, M Khoury and J Chen. (2010). Expression of human cytokines dramatically improves reconstitution of specific human-blood lineage cells in humanized mice. Proc Natl Acad Sci U S A 106:21783–21788.
18. Hu Z, N Van Rooijen and YG Yang. (2011). Macrophages prevent human red blood cell reconstitution in immunodeficient mice. Blood 118:5938–5946.
19. Hu Z and YG Yang. (2012). Full reconstitution of human platelets in humanized mice after macrophage depletion. Blood 120:1713–1716.
20. Berges BK, SR Akkina, JM Folkvord, E Connick and R Akkina. (2008). Mucosal transmission of R5 and ×4 tropic HIV-1 via vaginal and rectal routes in humanized Rag2-/- gc-/- (RAG-hu) mice. Virology 373:342–351.
21. Sun Z, PW Denton, JD Estes, FA Othieno, BL Wei, AK Wege, MW Melkus, A Padgett-Thomas, M Zupancic, AT Haase and JV Garcia. (2007). Intrarectal transmission, systemic infection, and CD4+ T cell depletion in humanized mice infected with HIV-1. J Exp Med 204:705–714.
22. Dash PK, S Gorantla, HE Gendelman, J Knibbe, GP Casale, E Makarov, AA Epstein, HA Gelbard, MD Boska and LY Poluektova. (2011). Loss of neuronal integrity during progressive HIV-1 infection of humanized mice. J Neurosci 31:3148–3157.
23. Gorantla S, E Makarov, J Finke-Dwyer, A Castanedo, A Holguin, CL Gebhart, HE Gendelman and L Poluektova. (2010). Links between progressive HIV-1 infection of humanized mice and viral neuropathogenesis. Am J Pathol 177:2938–2949.
24. Bonnet D. (2001). Normal and leukemic CD34-negative human hematopoietic stem cells. Rev Clin Exp Hematol 5:42–61.
25. Notta F, S Doulatov, E Laurenti, A Poeppl, I Jurisica and JE Dick. (2011). Isolation of single human hematopoietic stem cells capable of long-term multilineage engraftment. Science 333:218–221.
26. Kalscheuer H, N Danzl, T Onoe, T Faust, R Winchester, R Goland, E Greenberg, TR Spitzer, DG Savage, et al. (2012). A model for personalized *in vivo* analysis of human immune responsiveness. Sci Transl Med 4:125ra30.
27. Shultz LD, BL Lyons, LM Burzenski, B Gott, X Chen, S Chaleff, M Kotb, SD Gillies, M King, et al. (2005). Human lymphoid and myeloid cell development in NOD/LtSz-scid IL2R gamma null mice engrafted with mobilized human hemopoietic stem cells. J Immunol 174:6477–6489.
28. van der Loo JC, H Hanenberg, RJ Cooper, FY Luo, EN Lazaridis and DA Williams. (1998). Nonobese diabetic/severe combined immunodeficiency (NOD/SCID) mouse as a model system to study the engraftment and mobilization of human peripheral blood stem cells. Blood 92:2556–2570.
29. Anderson JS, S Bandi, DS Kaufman and R Akkina. (2006). Derivation of normal macrophages from human embryonic stem (hES) cells for applications in HIV gene therapy. Retrovirology 3:24.
30. Choi KD, J Yu, K Smuga-Otto, G Salvagiotto, W Rehrauer, M Vodyanik, J Thomson and I Slukvin. (2009). Hematopoietic and endothelial differentiation of human induced pluripotent stem cells. Stem Cells 27:559–567.
31. Kaufman DS, ET Hanson, RL Lewis, R Auerbach and JA Thomson. (2001). Hematopoietic colony-forming cells derived from human embryonic stem cells. Proc Natl Acad Sci U S A 98:10716–10721.
32. Tian X, PS Woll, JK Morris, JL Linehan and DS Kaufman. (2006). Hematopoietic engraftment of human embryonic stem cell-derived cells is regulated by recipient innate immunity. Stem Cells 24:1370–1380.
33. Akkina R, BK Berges, BE Palmer, L Remling, CP Neff, J Kuruvilla, E Connick, J Folkvord, K Gagliardi, A Kassu and SR Akkina. (2011). Humanized Rag1-/-gamma-chain-/- mice support multilineage hematopoiesis and are susceptible to HIV-1 infection via systemic and vaginal routes. PLos ONE 6:e20169.
34. Bente DA, MW Melkus, JV Garcia and R Rico-Hesse. (2005). Dengue fever in humanized NOD/SCID mice. J Virol 79:13797–13799.
35. Watanabe S, K Terashima, S Ohta, S Horibata, M Yajima, Y Shiozawa, MZ Dewan, Z Yu, M Ito, et al. (2007). Hematopoietic stem cell-engrafted NOD/SCID/IL2R{gamma}null mice develop human lymphoid system and induce long-lasting HIV-1 infection with specific humoral immune responses. Blood 109:212–218.
36. Brehm MA, A Cuthbert, C Yang, DM Miller, P DiIorio, J Laning, L Burzenski, B Gott, O Foreman, et al. (2010). Parameters for establishing humanized mouse models to study human immunity: analysis of human hematopoietic stem cell engraftment in three immunodeficient strains of mice bearing the IL2rgamma(null) mutation. Clin Immunol 135:84–98.
37. Waskow C, V Madan, S Bartels, C Costa, R Blasig and HR Rodewald. (2009). Hematopoietic stem cell transplantation without irradiation. Nat Methods 6:267–269.
38. Shultz LD, MA Brehm, JV Garcia-Martinez and DL Greiner. (2012). Humanized mice for immune system investigation: progress, promise and challenges. Nat Rev Immunol 12:786–798.
39. Shultz LD, F Ishikawa and DL Greiner. (2007). Humanized mice in translational biomedical research. Nat Rev Immunol 7:118–130.
40. Zhang B, Z Duan and Y Zhao. (2009). Mouse models with human immunity and their application in biomedical research. J Cell Mol Med 13:1043–1058.
41. Joo SY, BK Choi, MJ Kang, DY Jung, KS Park, JB Park, GS Choi, J Joh, CH Kwon, et al. (2009). Development of functional human immune system with the transplantations of human fetal liver/thymus tissues and expanded hematopoietic stem cells in RAG2(-/-)gamma(c)(-/-) mice. Transplant Proc 41:1885–1890.
42. Denton PW and JV García. (2011). Humanized mouse models of HIV infection. AIDS Rev 13:135–148.
43. Stoddart CA, E Maidji, SA Galkina, G Kosikova, JM Rivera, ME Moreno, B Sloan, P Joshi and BR Long. (2011). Superior human leukocyte reconstitution and susceptibility to vaginal HIV transmission in humanized NOD-scid IL-2Rγ(-/-) (NSG) BLT mice. Virol 417:154–160.
44. Hall KM, TL Horvath, R Abonour, K Cornetta and EF Srour. (2006). Decreased homing of retrovirally transduced human bone marrow CD34+ cells in the NOD/SCID mouse model. Exp Hematol 34:433–442.
45. Takahashi M, N Tsujimura, K Otsuka, T Yoshino, T Mori, T Matsunaga and S Nakasono. (2012). Comprehensive evaluation of leukocyte lineage derived from human hematopoietic cells in humanized mice. J Biosci Bioeng 113:529–535.
46. Berges BK, SR Akkina, L Remling and R Akkina. (2010). Humanized Rag2(-/-)gammac(-/-) (RAG-hu) mice can sustain long-term chronic HIV-1 infection lasting more than a year. Virol 397:100–103.
47. Baenziger S, R Tussiwand, E Schlaepfer, L Mazzucchelli, M Heikenwalder, MO Kurrer, S Behnke, J Frey, A Oxenius, et al. (2006). Disseminated and sustained HIV infection in

CD34+ cord blood cell-transplanted Rag2-/-{gamma}c-/- mice. Proc Natl Acad Sci U S A 103:15951–15956.
48. Sato K, C Nie, N Misawa, Y Tanaka, M Ito and Y Koyanagi. (2010). Dynamics of memory and naïve CD8(+) T lymphocytes in humanized NOD/SCID/IL-2Rgamma(null) mice infected with CCR5-tropic HIV-1. Vaccine 28S2:B32–B37.
49. Gorantla S, H Sneller, L Walters, JG Sharp, SJ Pirruccello, JT West, C Wood, S Dewhurst, HE Gendelman and L Poluektova. (2007). Human immunodeficiency virus type 1 pathobiology studied in humanized Balb/c-Rag2-/-{gamma}c-/- mice. J Virol 81:2700–2712.
50. Lang J, N Weiss, BM Freed, RM Torres and R Pelanda. (2011). Generation of hematopoietic humanized mice in the newborn BALB/c-Rag2(null)Il2rγ(null) mouse model: a multivariable optimization approach. Clin Immunol 140:102–116.
51. Zhang L, GI Kovalev and L Su. (2006). HIV-1 infection and pathogenesis in a novel humanized mouse model. Blood 109:2978–2981.
52. Ishikawa F, AG Livingston, JR Wingard, S Nishikawa and M Ogawa. (2002). An assay for long-term engrafting human hematopoietic cells based on newborn NOD/SCID/beta2-microglobulin(null) mice. Exp Hematol 30:488–494.
53. Liu C, BJ Chen, D Deoliveira, GD Sempowski, NJ Chao and RW Storms. (2010). Progenitor cell dose determines the pace and completeness of engraftment in a xenograft model for cord blood transplantation. Blood 116:5518–5527.
54. Drake AC, M Khoury, I Leskov, BP Iliopoulou, M Fragoso, H Lodish and J Chen. (2011). Human CD34 CD133 hematopoietic stem cells cultured with growth factors including Angptl5 efficiently engraft adult NOD-SCID Il2rγ (NSG) mice. PLoS ONE 6:e18382.
55. Park CY, R Majeti and IL Weissman. (2008). *In vivo* evaluation of human hematopoiesis through xenotransplantation of purified hematopoietic stem cells from umbilical cord blood. Nat Protoc 3:1932–1940.
56. Holt N, J Wang, K Kim, G Friedman, X Wang, V Taupin, GM Crooks, DB Kohn, PD Gregory, MC Holmes and PM Cannon. (2010). Human hematopoietic stem/progenitor cells modified by zinc-finger nucleases targeted to CCR5 control HIV-1 *in vivo*. Nat Biotechnol 28:839–847.
57. Bahçeci E, EJ Read, S Leitman, R Childs, C Dunbar, NS Young and AJ Barrett. (2000). CD34+ cell dose predicts relapse and survival after T-cell-depleted HLA-identical haematopoietic stem cell transplantation (HSCT) for haematological malignancies. Br J Haematol 108:408–414.
58. Awong G, E Herer, CD Surh, JE Dick, RN La Motte-Mohs and JC Zúñiga-Pflücker. (2009). Characterization *in vitro* and engraftment potential *in vivo* of human progenitor T cells generated from hematopoietic stem cells. Blood 114:972–982.
59. Sangeetha VM, VP Kale and LS Limaye. (2010). Expansion of cord blood CD34 cells in presence of zVADfmk and zLLYfmk improved their in vitro functionality and in vivo engraftment in NOD/SCID mouse. PLoS One 5:e12221.
60. Lang J, M Kelly, BM Freed, MD McCarter, RM Kedl, RM Torres and R Pelanda. (2013). Studies of lymphocyte reconstitution in a humanized mouse model reveal a requirement of T cells for human B cell maturation. J Immunol 190:2090–2101.
61. Czechowicz A, D Kraft, IL Weissman and D Bhattacharya. (2007). Efficient transplantation via antibody-based clearance of hematopoietic stem cell niches. Science 318:1296–1299.
62. Karlsson C, A Baudet, N Miharada, S Soneji, R Gupta, M Magnusson, T Enver, G Karlsson and J Larsson. (2013). Identification of the chemokine CCL28 as a growth and survival factor for human hematopoietic stem and progenitor cells. Blood 121:3838–3842.
63. O'Connell RM, AB Balazs, DS Rao, C Kivork, L Yang and D Baltimore. (2010). Lentiviral vector delivery of human interleukin-7 (hIL-7) to human immune system (HIS) mice expands T lymphocyte populations. PLoS One 5:e12009.
64. Huntington ND, N Legrand, NL Alves, B Jaron, K Weijer, A Plet, E Corcuff, E Mortier, Y Jacques, H Spits and JP Di Santo. (2009). IL-15 trans-presentation promotes human NK cell development and differentiation *in vivo*. J Exp Med 206:25–34.
65. Pek EA, T Chan, S Reid and AA Ashkar. (2011). Characterization and IL-15 dependence of NK cells in humanized mice. Immunobiology 216:218–224.
66. Chen Q, F He, J Kwang, JK Chan and J Chen. (2012). GM-CSF and IL-4 stimulate antibody responses in humanized mice by promoting T, B, and dendritic cell maturation. J Immunol 189:5223–5229.
67. Zheng J, Y Liu, Y Liu, M Liu, Z Xiang, KT Lam, DB Lewis, YL Lau and W Tu. (2013). Human CD8+ regulatory T cells inhibit GVHD and preserve general immunity in humanized mice. Sci Transl Med 5:168ra9.
68. Smith MS, DC Goldman, AS Bailey, DL Pfaffle, CN Kreklywich, DB Spencer, FA Othieno, DN Streblow, JV Garcia, WH Fleming and JA Nelson. (2011). Granulocyte-colony stimulating factor reactivates human cytomegalovirus in a latently infected humanized mouse model. Cell Host Microbe 8:284–291.
69. Sato K, N Misawa, C Nie, Y Satou, D Iwakiri, M Matsuoka, R Takahashi, K Kuzushima, M Ito, K Takada and Y Koyanagi. (2011). A novel animal model of Epstein-Barr virus-associated hemophagocytic lymphohistiocytosis in humanized mice. Blood 117:5663–5673.
70. Yajima M, K Imadome, A Nakagawa, S Watanabe, K Terashima, H Nakamura, M Ito, N Shimizu, M Honda, N Yamamoto and S Fujiwara. (2008). A new humanized mouse model of Epstein-Barr virus infection that reproduces persistent infection, lymphoproliferative disorder, and cell-mediated and humoral immune responses. J Infect Dis 198:673–682.
71. Strowig T, C Gurer, A Ploss, YF Liu, F Arrey, J Sashihara, G Koo, CM Rice, JW Young, et al. (2009). Priming of protective T cell responses against virus-induced tumors in mice with human immune system components. J Exp Med 206:1423–1434.
72. van Lent, AU, W Dontje, M Nagasawa, R Siamari, AQ Bakker, SM Pouw, KA Maijoor, K Weijer, JJ Cornelissen, et al. (2009). IL-7 enhances thymic human T cell development in "human immune system" Rag2-/-IL-2Rc-/- mice without affecting peripheral T cell homeostasis. J Immunol 183:7645–7655.
73. Bonnet, D, M Bhatia, JC Wang, U Kapp, and JE Dick. (1999). Cytokine treatment or accessory cells are required to initiate engraftment of purified primitive human hematopoietic cells transplanted at limiting doses into NOD/SCID mice. Bone Marrow Transplant 23:203–209.

Address correspondence to:
Dr. Bradford K. Berges
Department of Microbiology and Molecular Biology
Brigham Young University
Provo, UT 84602

E-mail: brad.berges@gmail.com

Received for publication June 11, 2013
Accepted after revision August 19, 2013
Prepublished on Liebert Instant Online August 20, 2013

Chapter 2

Production and Characterization of Humanized Rag2$^{-/-}\gamma c^{-/-}$ Mice

Freddy M. Sanchez, German I. Cuadra, Stanton J. Nielsen, Anne Tanner, and Bradford K. Berges

Abstract

Mice reconstituted with human immune cells represent a model to study the development and functionality of the human immune system. Recent improvements in humanized mice have resulted in multi-lineage hematopoiesis, prolonged human cell engraftment that is detectable in many mouse organs, and the ability to generate de novo human innate and adaptive immune responses. Here, we describe the methods used to produce and characterize humanized Rag2$^{-/-}\gamma c^{-/-}$ mice.

Key words Humanized mice, Animal disease models, Hematopoietic stem cells, Stem cell transplantation, RAG-hu mice, SCID-hu mice, BLT mice

1 Introduction

The preclinical evaluation of therapeutics for a variety of human diseases has relied mainly on the use of small animals and nonhuman primates. Despite the genetic traits conserved between some of these animals and humans, species-specific differences exist. Among these differences are the susceptibility to infection by microbial pathogens, and the host immune response to those infections. The discovery of the severe combined immunodeficiency mutation (*Prkdc*^{scid}) in mice (C.B-17 SCID mice) led to the first attempts to use these animals for the development of effective in vivo models that more accurately resemble the complexity of human biology [1]. One such development has been the "humanization" of mice.

Humanized mice are described as immunocompetent mice capable of transgenically expressing human genes, or immunodeficient mice capable of being engrafted with cells of human origin (typically hematopoietic stem cells, HSCs, or peripheral blood mononuclear cells, PBMCs). These models have provided important findings relevant to various fundamental aspects of human

Irving C. Allen (ed.), *Mouse Models of Innate Immunity: Methods and Protocols*, Methods in Molecular Biology, vol. 1031, DOI 10.1007/978-1-62703-481-4_2,

biology and immunology, including human hemato-lymphopoiesis, innate and adaptive immune responses, autoimmune diseases, infectious diseases, and cancer [2, 3]. The introduction of additional genetic modifications capable of overcoming the limitations (e.g., engraftment barriers) present in the earlier models of humanized mice has permitted a gradual optimization in the generation of such mouse models. Thus, in the past two decades various improved humanized mouse models have been developed [4, 5].

A more recent innovation in the humanization of mice was achieved by crossing mice homozygous for a deletion in the recombination activating gene 2 (Rag2) with mice homozygous for a deletion in the common gamma chain receptor (γc) [6, 7]. $Rag2^{-/-}\gamma c^{-/-}$ mice are incapable of producing mature T, B, and NK cells because Rag2 is required to generate B and T cell receptors and γc is required for cytokine signaling via IL-2 and IL-15 [8, 9]. Since T cells and NK cells play a major role in identification and elimination of foreign cells, this mouse strain is ideal for humanization experiments. Transplantation of human HSCs into $Rag2^{-/-}\gamma c^{-/-}$ mice leads to human multi-lineage hematopoiesis and the development of the major functional components of the human adaptive immune system. Human B and T cells, monocytes/macrophages, and dendritic cells are readily detected in lymphoid organs and in the periphery. Humanized mice have been useful in the study of viral pathogenesis and new treatment strategies for human viruses such as HIV-1, human T-lymphotropic virus, Epstein–Barr virus, human cytomegalovirus, and dengue virus [8, 10–15]. In addition, these mice are capable of producing primary human adaptive immune responses such as human antibody and T cell responses against a variety of viral, bacterial, and other antigenic targets [6, 7, 16].

In this chapter we describe the generation of humanized mice through purification of human HSCs, intrahepatic transplantation into newborn BALB/c $Rag2^{-/-}\gamma c^{-/-}$ mice, and verification of successful engraftment through FACS analysis of peripheral blood samples.

2 Materials

2.1 Purification and Culture of Human Hematopoietic Stem Cells

1. Human $CD34^+$ Selection Kit (Miltenyi Biotec, Auburn, CA, USA, or Stem Cell Technologies, Vancouver, BC, Canada). We have successfully used both kits.
2. Iscove's Modified Dulbecco's Medium supplemented with 10 % fetal calf serum, 2 % penicillin–streptomycin, and 10 ng/ml each of SCF, IL-3, and IL-6. Filter-sterilize the medium and store at 4 °C.

2.2 Transplantation of BALB/c Rag2$^{-/-}$ $\gamma c^{-/-}$ Mice with Human HSCs

1. BALB/c Rag2$^{-/-}$ $\gamma c^{-/-}$ mice (*see* **Note 1**).
2. 28 gauge insulin syringes.
3. Cultured human HSCs.
4. Iscove's Modified Dulbecco's Medium.

2.3 Bleeding Mice to Screen for Human Cell Engraftment

1. Heating pad.
2. Mouse restraint apparatus (Model TV-150; Braintree scientific Inc., Braintree, MA, USA). This device has a groove across the top. A plunger prevents the mouse from escaping.
3. Scalpel blade (surgical blade stainless steel No. 11).
4. Gauze pads.
5. Styptic powder (Kwik-Stop Styptic Powder with Benzocaine; ARC Laboratories).
6. Heparinized microcapillary tubes (Heparinized Micro-hematocrit capillary tubes; Thermo Fisher Scientific Inc., Waltham, MA, USA).
7. Micropipettor with tips.

2.4 FACS Analysis to Detect and Quantify Human Cell Engraftment

1. Antibodies: hCD45-PE-Cy7 and mCD45-PE (eBioscience, San Diego, CA, USA).
2. 10× ammonium chloride erythrocyte lysing solution: Dissolve 89.9 g NH_4Cl, 10.0 g $KHCO_3$, and 370.0 mg tetrasodium EDTA in 1 liter of ddH_2O. Adjust pH to 7.3. Store at 4 °C in full, tightly closed 50 ml tubes. Dilute to 1× with ddH_2O and use immediately.
3. FACS stain buffer: 1× PBS, 0.1 % BSA, and 0.1 % sodium azide. Store at 4 °C.
4. Fc blocking buffer: Human Gamma Globulin (Jackson Immunoresearch Labs, West Grove, PA, USA), Normal Mouse Serum (Jackson Immunoresearch Labs), 2.4G2 monoclonal antibody to murine CD16/CD32 (BD, Franklin Lakes, NJ, USA). Reconstitute Normal Mouse Serum with 5.0 ml of ddH20. Add 2 ml of Human Gamma Globulin. Add 200 μl of 2.4G2 anti-mouse CD16/CD32. Store at 4 °C.
5. 1 % paraformaldehyde in 1× PBS: Paraformaldehyde does not dissolve effectively in PBS. Prepare a stock of 2 % paraformaldehyde in ddH_2O and a stock of 2× PBS in ddH_2O. Mix these solutions together in equal parts and store at 4 °C.
6. Flow cytometer.
7. FACS tubes.

3 Methods

3.1 Preparation of Human HSCs for Transplantation

1. $CD34^+$ human HSCs are purified from human umbilical cord blood or other sources (*see* **Note 2**) using magnetically labeled antibodies according to the manufacturer's protocol. $CD34^+$ cells are cultured for 40–48 h (*see* **Note 3**) post extraction in IMDM supplemented with 10 % FCS, 1× penicillin/streptomycin, and 10 ng/ml each of IL-3, IL-6, and SCF.
2. Resuspend cells by repeated pipetting, since many cells will be semi-adherent. Count cells using a hemocytometer. Samples used for engrafting mice may be divided to engraft multiple mice.
3. Centrifuge samples for 3 min at 900 × *g* and discard the supernatant. Resuspend the cell pellet in serum-free IMDM. Approximately 30–50 μl of re-suspended cells is best for an individual mouse injection. Divide the solution into different samples equal to the number of pups that will be engrafted. We use a minimal dose of 250,000 cells per mouse in order to achieve consistent, high-level engraftment (*see* **Note 4**).

3.2 Conditioning Pups for Transplantation

1. 1- to 5-day-old pups (*see* **Note 5**) are conditioned by gamma irradiation at a dose of 350 rads. Wait at least 1 h between irradiation and cell injection. Care must be taken to prevent animals from being exposed to mouse pathogens during transportation and cell injection (*see* **Note 6**).

3.3 Transplantation of Pups with Human HSCs

1. Add 30–50 μl of $CD34^+$ cells in solution into each syringe. The exact volume depends upon the age and size of the pups (*see* **Note 7**). 30 μl is best for 1-day-old pups. Since some volume is retained in the needle after injection, larger volumes are preferable for older pups in order to prevent loss of cells due to retention of liquid in the syringe.
2. Place pups on their backs and stretch out their bodies to allow visualization of the liver. Since pups are albino, the liver is readily visible. Pups are injected with cells in the liver at a depth of 1–2 mm. Greater depths can result in bleeding from the injection site. Following injection keep the syringe inserted for 20 s to prevent cells from being expelled after needle withdrawal. Upon completion of the injection, place the pups back with their mother.

3.4 Bleeding Mice for FACS Analysis

1. Eight weeks post reconstitution, mice should be screened for human cell engraftment. Warm up the mice by placing them in an empty plastic cage on top of a heating pad. Allow at least 5 min for the mice to sufficiently heat up. The mice are warm enough when their movements are rapid and they are breathing quickly.

2. Remove a mouse from the heating cage and place it in the restraint apparatus. Holding the mouse by the tail, gently pull the mouse (tail first) into the apparatus. Pull the tail along the groove in the top of the apparatus, thus pulling the mouse into the apparatus. Push the plunger into the front of the apparatus so that the mouse is held inside (*see* **Note 8**).
3. Locate the veins on the tail and choose one for tail nick bleeding. Using the scalpel, make a small transverse cut across the selected vein. After the mouse begins to bleed, hold the capillary tube horizontally (to avoid forming air bubbles that can lead to clotting) at the cut site and begin collecting blood. When the capillary is full withdraw it (keeping it horizontal) and place the blood sample into an appropriately labeled microfuge tube.
4. Pinch the tail above the cut site to stop the blood flow and wipe away any excess blood. Scoop out a small amount of styptic powder and apply it to the cut site. Allow enough time for clotting to occur. Place the mouse back into its original cage.
5. Eject the blood from the capillary tube using the micropipettor and draw the capillary tube up and out of the microfuge tube as you eject the blood. This technique will prevent the blood from entering back into the capillary.

3.5 Preparing Blood Samples for FACS Analysis

1. Lyse red blood cells by adding 1.4 ml of erythrocyte lysing solution per 100 μl of blood. Incubate at room temperature for 5–10 min. Centrifuge samples at 900 × *g* for 3 min. Discard the supernatant and resuspend the cell pellet in 100 μl of FACS stain buffer.
2. Add 3 μl of Fc blocking buffer and place samples at 4 °C for 15 min (*see* **Note 9**). Add 3 μl of both mCD45-PE and hCD45-PE-Cy7 to each sample and incubate at 4 °C for 30 min. Keep light exposure to a minimum.
3. Add 900 μl of 1 % paraformaldehyde in 1× PBS to each sample. Spin samples at 900 g for 3 min. Dispose of the supernatant and resuspend the pellet in 150 μl of 1× PBS solution. Transfer samples into FACS tubes and analyze by FACS.

4 Notes

1. There are multiple types of immunodeficient mouse strains that support engraftment of human HSCs and multi-lineage hematopoiesis. The original SCID mouse retains natural killer (NK) cell activity and the SCID mutation can result in leaky production of lymphocytes in older mice; both NK cells and T lymphocytes recognize and reject foreign cells. As a result, strains with greater defects in NK and T cell development are now typically used, including Rag2$^{-/-}\gamma c^{-/-}$ mice, NOD/SCID mice,

NOD/SCID $\gamma c^{-/-}$ mice, and $Rag1^{-/-}$ $\gamma c^{-/-}$ mice. $Rag2^{-/-}$ $\gamma c^{-/-}$ mice are commercially available on a C57BL/6 background, but for unknown reasons these animals cannot be effectively engrafted (BALB/c $Rag2^{-/-}$ $\gamma c^{-/-}$ mice work effectively). Excellent reviews are available that explain the phenotype of each mutation, as well as the history of using these strains to produce humanized mice [3, 17].

2. Three main sources are currently employed to obtain HSCs: umbilical cord blood, fetal liver, and mobilized peripheral blood. Magnetic separation techniques are commonly employed to purify $CD34^+$ cells. Umbilical cord blood is most readily available, but this source yields a low number of cells, at most 1×10^6. Relatively fewer mice can be engrafted per sample due to lower yields. Fetal liver samples have ethical constraints and few suppliers exist, but these samples yield more cells. Fetal liver samples commonly yield greater than 20×10^6 cells. We have no experience using mobilized peripheral blood and this source is rarely used to produce humanized mice [18, 19].
3. $CD34^+$ cells are cultured for 40–48 h in order to obtain maximum expansion of the hematopoietic stem cell population while preventing differentiation of the stem cells. There is no method currently available to culture HSCs without eventual differentiation and loss of potency for engraftment. Density of cells is critical for expansion during culture. Denser cell cultures grow more efficiently than cultures that are less dense. We culture cells in 48-well plates since that provides the appropriate cell density for most umbilical cord blood-derived samples.
4. The number of $CD34^+$ HSCs to inject varies considerably in the literature. In the original paper by Traggiai et al. showing HSC engraftment in $Rag2^{-/-}$ $\gamma c^{-/-}$ mice, they found engraftment with as few as 3.8×10^4 $CD34^+$ HSCs [8]. We typically use at least 2.5×10^5 cells per mouse to achieve consistent, high-level engraftment. Some researchers use up to $1–2 \times 10^6$ cells per mouse [20].
5. Several experiments have shown that age of mice at the time of engraftment has an impact on the level of engraftment achieved. We have found that engraftment levels are superior when $Rag2^{-/-}$ $\gamma c^{-/-}$ pups are less than 5 days of age at the time of irradiation and transplantation. Attempts to engraft older $Rag2^{-/-}$ $\gamma c^{-/-}$ mice result in lower levels of engraftment. Different mouse strains can show effective engraftment with older mice (e.g., NOD/SCID $\gamma c^{-/-}$), but in some cases different conditioning techniques were used [19, 21–23].
6. Immunodeficient mice are housed in specific pathogen-free facilities because they are unable to defend against various types of infections. They are often given antibiotics in their

drinking water in order to prevent bacterial infection. When preparing mice for irradiation, they often have to leave the animal facility; therefore, great care must be taken to keep the animals pathogen-free while in transit so as to avoid contaminating the colony.

7. Intrahepatic injection into newborn mice can be technically challenging. BALB/c mice are albino and hence the liver is readily visible. We typically inject a volume of 30–50 µl of cells per mouse. However, we find that the volume used for cell injection must be smaller for 1-day-old pups; if not the inoculated cells can exit the injection site after withdrawing the needle due to pressure accumulated during injection. For smaller pups, we use an injection volume of 30 µl. Allow the needle to remain in place for 20 s to ensure that the cells will not be expelled from the mouse.
8. Be careful not to catch the mouse's feet between the plunger and the wall of the apparatus. Do not let go of the tail or the mouse may pull the tail inside. Animals can sometimes bury their heads underneath their bodies and suffocate, so make sure that the head stays up for access to fresh air.
9. FACS analysis using cells from chimeric animals is more complicated than using cells from a single organism due to the requirement to block nonspecific antibody binding to both human and mouse cells. We perform initial workup experiments with FACS antibodies on pure mouse blood or pure human blood to verify the accuracy of the staining. We block nonspecific staining by using a combination mouse/human Fc block consisting of anti-mouse CD16/CD32, human gamma globulin, and normal mouse serum (*see* Subheading 2). We typically use mouse monoclonal antibodies for FACS staining and we rarely detect background or cross-species staining.

Acknowledgments

This work was supported by a Mentoring Environment Grant from Brigham Young University.

References

1. Bosma GC, Custer RP, Bosma MJ (1983) A severe combined immunodeficiency mutation in the mouse. Nature 301(5900):527–530
2. Brehm MA, Shultz LD, Greiner DL (2010) Humanized mouse models to study human diseases. Curr Opin Endocrinol Diabetes Obes 17(2):120–125
3. Shultz LD, Ishikawa F, Greiner DL (2007) Humanized mice in translational biomedical research. Nat Rev Immunol 7:118–130
4. Pearson T, Greiner DL, Shultz LD (2008) Humanized SCID mouse models for biomedical research. Curr Top Microbiol Immunol 324:25–51

5. Goldstein H (2008) Summary of presentations at the NIH/NIAID New Humanized Rodent Models 2007 Workshop. AIDS Res Ther 5:3
6. Goldman JP, Blundell MP, Lopes L, Kinnon C, Di Santo JP, Thrasher AJ (1998) Enhanced human cell engraftment in mice deficient in RAG2 and the common cytokine receptor gamma chain. Br J Haematol 103(2):335–342
7. Mazurier F, Gan OI, McKenzie JL, Doedens M, Dick JE (1999) A novel immunodeficient mouse model–RAG2 x common cytokine receptor gamma chain double mutants–requiring exogenous cytokine administration for human hematopoietic stem cell engraftment. J Interferon Cytokine Res 19(5):533–541
8. Traggiai E, Chicha L, Mazzucchelli L, Bronz L, Piffaretti JC, Lanzavecchia A, Manz MG (2004) Development of a human adaptive immune system in cord blood cell-transplanted mice. Science 304:104–107
9. Baenziger S, Tussiwand R, Schlaepfer E, Mazzucchelli L, Heikenwalder M, Kurrer MO, Behnke S, Frey J, Oxenius A, Joller H, Aguzzi A, Manz MG, Speck RF (2006) Disseminated and sustained HIV infection in CD34+ cord blood cell-transplanted Rag2−/−gc−/− mice. Proc Natl Acad Sci U S A 103:15951–15956
10. Berges BK, Wheat WH, Palmer B, Connick E, Akkina R (2006) HIV-1 infection and CD4 T cell depletion in the humanized Rag2−/−gc−/− (RAG-hu) mouse model. Retrovirology 3:76
11. Berges BK, Rowan MR (2011) The utility of the new generation of humanized mice to study HIV-1 infection: transmission, prevention, pathogenesis, and treatment. Retrovirology 8:65
12. Kuruvilla JG, Troyer RM, Devi S, Akkina R (2007) Dengue virus infection and immune response in humanized Rag2$^{-/-}$gc$^{-/-}$ (RAG-hu) mice. Virol 369:143–152
13. Smith MS, Goldman DC, Bailey AS, Pfaffle DL, Kreklywich CN, Spencer DB, Othieno FA, Streblow DN, Garcia JV, Fleming WH, Nelson JA, Smith MS (2012) Granulocyte-colony stimulating factor reactivates human cytomegalovirus in a latently infected humanized mouse model. Cell Host Microbe 8:284–291
14. Banerjee P, Tripp A, Lairmore MD, Crawford L, Sieburg M, Ramos J, Harrington W Jr, Beilke MA, Feuer G (2010) Adult T cell leukemia/lymphoma development in HTLV-1-infected humanized SCID mice. Blood 115:2640–2648
15. Berges BK, Akkina SR, Remling L, Akkina R (2010) Humanized Rag2(−/−)gammac(−/−) (RAG-hu) mice can sustain long-term chronic HIV-1 infection lasting more than a year. Virol 397:100–103
16. Chicha L, Tussiwand R, Traggiai E, Mazzucchelli L, Bronz L, Piffaretti JC, Lanzavecchia A, Manz MG (2005) Human adaptive immune system Rag2−/− gamma(c)−/− mice. Ann N Y Acad Sci 1044:236–243
17. Manz MG (2007) Human-hemato-lymphoid-system mice: opportunities and challenges. Immunity 26:537–541
18. Lang J, Weiss N, Freed BM, Torres RM, Pelanda R (2011) Generation of hematopoietic humanized mice in the newborn BALB/c-Rag2(null)Il2rγ(null) mouse model: a multivariable optimization approach. Clin Immunol 140:102–116
19. Shultz LD, Lyons BL, Burzenski LM, Gott B, Chen X, Chaleff S, Kotb M, Gillies SD, King M, Mangada J, Greiner DL, Handgretinger R (2005) Human lymphoid and myeloid cell development in NOD/LtSz-scid IL2R gamma null mice engrafted with mobilized human hemopoietic stem cells. J Immun 174: 6477–6489
20. Kwant-Mitchell A, Ashkar AA, Rosenthal KL (2009) Mucosal innate and adaptive immune responses against HSV-2 in a humanized mouse model. J Virol 83:10664–10676
21. Brehm MA, Cuthbert A, Yang C, Miller DM, DiIorio P, Laning J, Burzenski L, Gott B, Foreman O, Kavirayani A, Herlihy M, Rossini AA, Shultz LD, Greiner DL (2010) Parameters for establishing humanized mouse models to study human immunity: analysis of human hematopoietic stem cell engraftment in three immunodeficient strains of mice bearing the IL2rgamma(null) mutation. Clin Immunol 135:84–98
22. Pearson T, Shultz LD, Miller D, King M, Laning J, Fodor W, Cuthbert A, Burzenski L, Gott B, Lyons B, Foreman O, Rossini AA, Greiner DL (2008) Non-obese diabetic-recombination activating gene-1 (NOD-Rag 1(null)) interleukin (IL)-2 receptor common gamma chain (IL 2 rgamma(null)) null mice: a radioresistant model for human lymphohaematopoietic engraftment. Clin Exp Immunol 154:270–284
23. Rozemuller H, Knaan-Shanzer S, Hagenbeek A, van Bloois L, Storm G, Martens AC (2004) Enhanced engraftment of human cells in RAG2/gammac double-knockout mice after treatment with CL2MDP liposomes. Exp Hematol 32:1118–1125